The Effect of Heavy Metals on Differentiated Neuronal and Glial Cells.

Michelle Lawton

A thesis submitted in partial fulfilment of the requirements of Nottingham Trent University for the degree of Doctor of Philosophy

December 2007

Table of contents

Abstract

Heavy metal poisoning poses a serious health risk among populations worldwide. The symptoms presented by exposure are varied and depend upon the species of the metal, the age of the individual and the exposure dose. All heavy metals have debilitating effects on the CNS. Children are especially sensitive to the neurological effects due to the intense growth and activity of a developing nervous system and inadequately developed defences.
The aims of this study were to determine the effects of sub-lethal concentrations of numerous heavy metals on neuronal and glial cell differentiation. Using established cellular models, the toxicity of zinc, lead, mercury, methylmercury and thimerosal were investigated using assays of cell viability and morphology on differentiating N2a and C6 cells. Initial research revealed thimerosal, methylmercury and cadmium to be the most toxic compounds tested, in terms of their ability to inhibit the outgrowth of neurites in both cell lines at sub-lethal concentrations.

Although cadmium chloride showed similar patterns of toxicity to the mercury compounds, thimerosal and MeHgCl were chosen for further investigation at a molecular level. Methylmercury chloride a common environmental pollutant and thimerosal; a preservative found in many medicines, were chosen for further investigation, as previous work has demonstrated the health risks posed by the two organic mercury compounds but little is known about non-lethal changes that occur in the nervous system, especially with thimerosal.

Both thimerosal and MeHgCl inhibited MTT reduction and neurite outgrowth after 4 and 24 hours exposure at sub-lethal concentrations (0.1 and 1 µM). The inhibition of neurite outgrowth by sub-lethal concentrations of MeHgCl and thimerosal was accompanied by cytoskeletal changes in the cells. At 4 hours in C6 cells there was no change in the levels of tyrosinated α-tubulin, whereas in N2a cells the level of tubulin tyrosination was shown to be reduced compared to the control. Both cell lines exhibited a fall in total α-tubulin, tyrosinated α-tubulin and total β-tubulin after 24 hours of exposure to organic mercury compounds, indicating proteolysis and/or reduced synthesis of the tubulin subunit. N2a cells also showed a decrease in the levels of phosphorylation in the neurofilament heavy chain after 4 hours of exposure to thimerosal and MeHgCl, whereas after 24 hours there appeared to be proteolytic degradation, as the total neurofilament heavy chain levels were reduced compared to the untreated controls. Reduced levels of tubulin and NFH were confirmed by immunofluorescence staining of fixed cell monolayers.

Western blotting analysis also indicated increased ERK activation in glial cells incubated with 0.1 and 1 µM thimerosal for 4 hours, followed by reduced activation after 24 hours exposure, whereas exposure to MeHgCl decreased the levels of ERK activation at both time points. In the neuronal cell line ERK activation was suppressed at both 4 and 24 hours and with both concentrations of the organic mercury compounds. As ERK activation plays a key role in the regulation of neurite outgrowth and NFH phosphorylation, both of which were inhibited by the addition of thimerosal and MeHgCl, the findings are consistent with a role for disrupted ERK signalling in the sub-lethal toxicity of these compounds.

Both thimerosal and MeHgCl caused redistribution of SERCA and ryanodine receptors, both of which are mechanisms by which intracellular Ca^{2+} concentrations are maintained. As the endoplasmic reticulum (ER) houses both SERCA and ryanodine receptors, the reorganisation may indicate that organic mercury compounds cause redistribution of the ER. Such disruption may lead to sustained increases in intracellular Ca^{2+}, causing elevated activity in Ca^{2+} dependant enzymes. Indeed, western blotting analysis and enzyme assays showed that calpain activity (particularly calpain 1) increased in response to sub-lethal concentrations of the organic mercury compounds. As calpains target cytoskeletal proteins, the increased activity may be at least partly responsible for reduced levels of tubulin and NFH.

1.1: Heavy Metals

Heavy metals can be broadly defined as metallic elements that have a molecular weight greater than 50 Daltons and are able to form polyvalent cations. These cations are extremely reactive and many of them have an affinity for sulphydryl groups (Foulkes, 2000). Heavy metals can not be metabolised by the body and if they accumulate in tissues faster than the body can eliminate them, they will gradually reach toxic levels and cause numerous and severe health problems. Heavy metal elements can be assigned to four distinct classes; Class A metals are essential for life in high concentrations (e.g. iron). Class B has no clear biological role and in low concentrations is not toxic, (e.g. strontium). Class C metals are essential in trace amounts for some living systems (e.g. zinc and copper), but can be toxic at higher concentrations. Class D have no recognised biological role and are toxic even at low concentrations (e.g. lead, cadmium and mercury amongst others) (Foulkes, 2000). The metals investigated in this thesis were lead and the transition metals cadmium, mercury and zinc.

In the environment, toxic metals can originate from natural sources and industrialisation. Heavy metals such as mercury, lead, cadmium and zinc are common environmental pollutants and can accumulate in biological systems. The symptoms of heavy metal poisoning vary according to the heavy metal, the age of the individual and whether the dose of the metal was acute or chronic (Redwood, 2001). The toxicity produced by exposure to heavy metals tends to involve neurotoxicity, hepatotoxicity and nephrotoxicity (Stohs & Bagchi, 1995).

1.1.1: Mercury and Methylmercury

Since mercury is present in the environment from the normal degradation of the earths crust, everyone is exposed to tiny amounts of background mercury. However, industrial accidents, consumption of contaminated food and exposure in the workplace can result in individuals and populations being exposed to a higher than normal dose. For example, the earliest recorded use of mercury as a preservative was in Spain 5000 years ago where it was used in embalming (Myers *et al.*, 2000). In the 1800s it was common practice in the hat making industry to use a mercury solution in the process of turning fur into felt. The symptoms of mercury poisoning suffered by

the workers became known as ‘mad hatter’s disease’. Mercury was also widely used as a treatment for syphilis (Baldwin & Marshall, 1999). More recently in Minamata bay in Japan in the 1950s residents ingested seafood that was contaminated with methylmercury from a local industrial plant (Castoldi *et al.*, 2001). Toxic effects including damage to areas of the brain controlling motor function and mental impairment were observed in adults and in infants born after the industrial accident. It was later found that methylmercury was able to induce congenital poisoning via transplacental transfer (Castoldi *et al.*, 2001). In the 1970s another incidence of methylmercury poisoning occurred in Iraq, when grain that had been treated with a methylmercury fungicide was used to make bread (Myers *et al.*, 2000).

There are three forms of mercury (Hg), organic, inorganic and elemental. Elemental mercury occurs naturally, is liquid at room temperature and vaporises when heated. Elemental Hg is released during volcanic eruptions in the form of vapour. Contact with excessive amounts of the metal can also arise from human activities, such as the burning of fossil fuel or exposure to dental amalgams. Mercury tends to be more hazardous as vapour; exposure can cause a variety of symptoms, including pleuritic pain, shortness of breath, fever, tiredness, tremors and delusions (Baldwin & Marshall, 1999). Children and adults show similar symptoms but poisoning of infants is extremely rare in modern society (Counter & Buchanan, 2004).

Exposure to inorganic mercury or mercury salts can come from soaps, skin creams, and traditional Chinese and Indian medicines. There have even been cases of infants presenting with classic signs of mercury poisoning linked to a teething powder containing mercury (Counter & Buchanan, 2004). The symptoms of inorganic Hg exposure are not dissimilar to the symptoms presented with the other forms of Hg poisoning.

The organic form of methylmercury is considered the most dangerous and common source of mercury toxicity (Gopal, 2002). However it is far from clear why organic mercury compounds like methylmercury are much more toxic than the inorganic mercury species. The difference in toxicity of inorganic mercury and organic mercury compounds should be related to alterations in their chemical structure and reactivity. The principal feature of organic mercury is the presence of both the metal centre (Hg) and the organic moieties covalently bonded to the mercury atom in their molecules (Milaeva, 2006). The organic group attached to the mercury makes the compound more lipid soluble, which makes transport into cells easier.

Nowadays, widespread exposure to methylmercury is rare, however methylmercury remains a significant threat, mainly from low dose exposure as a result of the consumption of contaminated sea food (Atchison, 2005). Inorganic mercury deposits are converted to methylmercury in the aquatic environment by microorganisms, which are then ingested by larger species leading to methylmercury accumulation in the food chain (Counter & Buchanan, 2004). In humans 90-100% of methylmercury is absorbed through the gastrointestinal (GI) tract and into the bloodstream, where it is then transported round the body. Methylmercury can cross the blood-brain barrier via the neutral amino acid transport system L as a MeHg-L-cysteine complex. There it is partially demethylated to inorganic mercury (Allen *et al.*, 2002). Once in the brain methylmercury induces loss of neurons and has been shown to accumulate within astrocytes (Allen *et al.*, 2002). In adults, the main symptoms of methylmercury poisoning are the loss of sensory, visual and auditory functions, weakness and damage in areas of the brain controlling motor function. Neurological disturbances have been report in populations with a high consumption of seafood at Hg concentrations as low as 50 μg/g (Zahir *et al.*, 2005). In prenatal exposure, the main symptoms are severely impaired motor and mental development, general paralysis and cerebral palsy (Jacobson, 2001; Sanfeliu *et al.*, 2001). Epidemiological data has correlated Hg concentrations in maternal blood with impaired neurological development of neonates. Mothers with blood concentrations of 24 μg/l reflected in neurological impairment in the child (Grandjean *et al.*, 1994). Treatment for all mercury species involves the use of dimercaprol, oral penicilliamine and the newer chelating agent 2,3-dimercapto-1-propansufonic acid (DMPS) (Baldwin & Marshall, 1999). The minimum risk level for mercury consumption was established by the Agency for Toxic Substances and Disease Registry as 0.3 μg/kg per day in children (Castoldi *et al.*, 2001).

Table 1.1: A comparison of the different forms of mercury

	Elemental Mercury	Inorganic mercury	Organic Mercury (Methylmercury)
Sources of exposure	Dental amalgams, occupational exposure, Caribbean religious ceremonies, fossil fuels, incinerators.	Oxidation of elemental mercury or demethylation of MeHg; exposure to $HgCl_2$.	Fish, marine mammals, crustaceans, animals and poultry fed fish meal.
Biological monitoring	Urine and blood.	Urine and blood.	Hair, blood, cord blood.
Toxicokinetics	Is readily absorbed when inhaled. Absorption via the GI tract is poor. Can also enter the body from skin contact.	Exposure can occur in the form of aerosols, 7-15% of the ingested dose of $HgCl_2$ will be absorbed in the GI tract whilst 2-3% of applied dose can be taken up via the dermal route.	Methylmercury vapours can be inhaled. Poisoning can occur from diet, particularly a diet rich in sea food, where organic mercury is absorbed in the GI tract and can be absorbed via contact with the skin.
Distribution	Rapidly distributed throughout the body since it is lipophilic. Half-life in blood, 45 days (slow phase); half-life appears to increase with increasing dose Readily crosses blood– brain and placental barriers	Highest accumulation in kidney Half-life in blood, 19.7–65.6 days; Does not readily penetrate blood– brain or placental barriers.	Distributed throughout body since lipophilic; approximately 1–10% of absorbed oral dose of MeHg distributed to blood; 90% of blood MeHg in red blood cells Half-life in blood, 50 days; Readily crosses blood–brain and placental barriers.
Biotransformation	Hg in tissue and blood oxidized to Hg^{2+} by catalase and hydrogen peroxide.	Vapor is exhaled following oral administration of mercuric Hg. Mercuric Hg is not methylated in body tissues but GI micro-organisms can form MeHg.	MeHg slowly demethylated to mercuric Hg (Hg^{2+}).Tissue macrophages, intenstinal flora, and foetal liver are sites of tissue demethylation.
Excretion	Excreted as Hg^{o} in exhaled air, sweat and saliva, and as mercuric Hg in faeces and urine Half life elimination: 58 days.	Excreted in urine and faeces; also excreted in saliva, bile, sweat, exhaled air, and breast milk Half life elimination: 1–2 months.	Major route is bile and faeces; 90% excreted in faeces as Hg^{2+}; 10% excreted in urine as Hg^{2+} Half-life elimination: (Whole body) 70– 80 days.
Toxicodynamics	brain and kidney.	Kidney.	Brain, adult and foetal.

Table 1.1 Differences between organic, elemental and inorganic mercury, from sources of exposure to excretion (Counter & Buchanan, 2004).

1.1.2: Thimerosal

The organic ethyl mercury compound Sodium ethylmercuri-thiosalicylate (thimerosal), is the sodium salt of the complex formed between thiosalicylic acid and ethylmercuric ion (Tan & Parkin, 2000). It has both antifungal and antibacterial properties and is widely used as an antiseptic agent and preservative in cleaning solutions for contact lenses, cosmetics, eye drops, topical medicines and vaccines (Elferink, 1999). Part of the physiological response to thimerosal is due to its ability to bind to SH and disulphide groups in various proteins (Nishio, 1996). Whilst not much is known about the metabolism, excretion or toxicity of thimerosal it's use in some infant vaccines as a preservative is of concern.

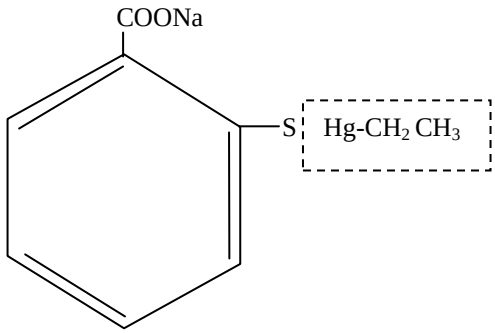

Thimerosal

Figure 1.1. The structure of thimerosal. The ethylmercury radical is highlighted with the dashed line (Van't Veen, 2001).

In 1999, the US Public Health Service and the American Academy of Pediatrics (AAP) called for the reduction or elimination of thimerosal from vaccines due to the amount of mercury that children were exposed to and a potential link to autism (Blaxill *et al.*, 2004). However the World Health Organisation (WHO) in 2002 recommended the continued use of vaccines containing thimerosal, as they stated that the benefits of immunization out way any theoretical risks (Knezevic *et al.*, 2004). At present the connection between autism and mercury toxicity from infant vaccines is controversial since there appears to be little evidence to either confirm or refute these links.

Vaccines containing thimerosal have been reported to cause sensitivity reactions in some recipients, such as dermatitis and conjunctivitis (Van't Veen, 2001).

There is also evidence to suggest that exposure to large amounts (ranging from 3-several hundred mg/kg) of thimerosal causes toxicity and death in humans (Ball *et al.*, 2001; Redwood, 2001). Various studies indicate that thimerosal has similar effects to methylmercury on biological events such as calcium homeostasis (Wiktorek *et al.*, 1996; Elferink, 1999; Ucha-Ishibashi *et al.*, 2004). It is thought that thimerosal is converted in to inorganic mercury *in vivo*, but does not have the same transport mechanism across the blood-brain barrier as methylmercury (Van't Veen, 2001). In addition ethylmercury (of which thimerosal is an example) has a larger molecular weight and faster decomposition rate than methylmercury (Counter & Buchanan, 2004).

1.1.3: Lead

Lead is a potential neurotoxin to which most people are exposed, albeit at differing concentrations (Erdahl *et al.*, 2000). Lead is found in mineral deposits and therefore naturally released into the environment. The toxicity of lead has been known since roman times, when it was common practice to use lead in wine and food because of its sweet taste (Toscano & Guilarte, 2005). Lead is also used in a variety of industrial activities, and was until recently, commonly used in petrol and paint. General marketing of lead in petrol was banned in January 2000 in the UK (Papanikolaou *et al.*, 2005), and the use of leaded paint ceased in 1992 (Toscano & Guilarte, 2005). Lead exposure comes from a variety of sources including cigarette smoke, occupational exposure and old lead water pipes. Lead gains entry to the body via inhalation, through the skin or by direct swallowing and ingestion, after which it is absorbed and transported by the blood stream to various organs and tissues. Lead can accumulate in three areas; blood, soft tissue and bone. Lead excretion is low, with a half life of approximately 10 years. However, the use of chelating agents such as dimercaprol can increase the rate of lead excretion (Papanikolaou *et al.*, 2005).

At low levels lead poisoning does not produce obvious symptoms but can cause long term impairment of cognitive function (Mike *et al.*, 2000). In an adult central nervous system lead crosses the blood-brain barrier rapidly in the form of a $Pb\text{-}OH^{+}$ complex and through cation channels (Mazzolini *et al.*, 2001) The earliest lead induced neurological damage is seen within the endothelial cells of microvessels,

which form the major structural component of the blood-brain barrier (Finkelstein *et al.*, 1998). Once in the brain lead accumulates within astrocytes, which appear to sequester lead away from the mitochondria, thereby protecting their respiration and potentially that of neighbouring neurons (Mazzolini *et al.*, 2001). Lead is thought to initiate apoptosis by depolarising the mitochondrial membrane leading to the opening of the permeability transition pore. This then allows the release of cytochrome c, resulting in the activation of the caspase cascade and cell death (Pulido & Parrish, 2003). Apoptotic cell death is a regulated process that involves a series of molecular events, such as cell shrinkage, chromatin condensation, membrane blebbing, caspase activation and the formation of apoptotic bodies (Wang *et al.*, 2005). Caspases are aspartate-specific cysteine proteases that initiate and ensure the efficacy of apoptosis. The family can be grouped into the initiator caspases, such as caspase 8, 9 and 10. This group initiates and amplifies cellular death signals from receptors such as the tumor necrosis factor receptor (TNFR) and Fas (Wang, 2000). Effector caspases such as caspases 2, 3, 6 and 7 degrade vital cellular components (Wang *et al.*, 2005).

Lead effects numerous biological systems such the reproductive, nervous, gastrointestinal, immune, renal, cardiovascular, skeletal, muscular and hematopoetic (Bouton *et al.*, 2001). The adverse affects of lead can be seen with concentrations as low as 10 μg/dl (Papanikolaou *et al.*, 2005) The symptoms of lead exposure include paralysis, seizures (Dai *et al*, 2001), restlessness, irritability, headaches, muscle tremors abdominal cramps and loss of memory at concentrations of around 100-120 μg/dl (Papanikolaou *et al.*, 2005). Impaired hearing has been reported with blood lead concentrations of around 10-20 μg/dl (Staessen *et al.*, 1994). Lead has been shown to inhibit myelination processes in brain tissue and alter the number of synapses per neuron, thus disrupting signal propagation in the CNS (Crumpton *et al*, 2001). Lead may also have the ability to cause cancers in humans, since epididemeological data indicates that individuals with a blood lead concentration of 20μg/dl and above have an increased risk of cancer and heart disease. The carcinogenic properties of lead have not yet been fully elucidated but it may be by inhibiting DNA repair mechanisms or by replacing zinc in DNA binding proteins (Silbergeld, 2003). In addition it may factor in diseases such as Alzheimer's that effect the aged as during osteoporosis, lead is released from bone storage (Bressler *et al.*, 1999). The Centres for Disease Control and Prevention defined elevated levels of lead as $\geq$ 10 μg/dl and recommended

treatment for concentrations greater than ≥15 μg/dl in adults and ≥10 μg/dl in children (Toscano & Guilarte, 2005).

1.1.4: Cadmium

Cadmium is a significant industrial and environmental toxin and is ranked sixth out the top ten hazardous substances (Hinkle & Osborne, 1994; Lau *et al.*, 2006). Exposure to cadmium can occur via cigarette smoke, contaminated food, drinking water, soil. It is used in various industrial processes, for example in the production of certain pigments in paints and plastics and in the production of nickel-cadmium batteries. The importance of cadmium as a compound detrimental to humans was evident at the Jinzu River in Japan where the out break of a severe disease known as Itai-Itai disease was linked to cadmium contaminated food. The disease caused bone pain, fractures, proteinuria and ostoemalacia (Waisberg *et al.*, 2003).

Cadmium can produce genotoxic and mutagenic events at high concentrations of 10-40 μM (Waisberg *et al.*, 2003). In 1993 cadmium was classified as a human carcinogen by the International Agency for Research on Cancer. The exact mechanism by which cadmium causes malignancies is not yet known. It has been proposed that it may interfere with the expression of early genes like c-jun or the tumour suppressor gene p53 (Waisberg *et al.*, 2003). Cadmium toxicity is thought to occur in numerous ways. Like other heavy metals, cadmium has an affinity for SH groups and is able to bind tightly to proteins. It is also able to replace calcium in calmodulin and a variety of calcium binding enzymes; as well as substituting for zinc in zinc containing enzymes (Hinkle & Osborne, 1994). Cadmium can enter cells via calcium channels and can also block calcium uptake by cells (Hinkle & Osborne, 1994). It can also affect gene expression through metal-responsive upstream regulatory elements (Watjen, 2001). It can also produce reactive oxygen species (ROS) leading to cell death in neurons via the caspase pathway (Lopez *et al.*, 2006). The susceptibility of cells to cadmium mediated apoptosis is however dependent upon levels of metallothionein. This protein binds to cadmium thereby restricting intracellular availability and reducing toxicity (Pulido & Parrish, 2003). The mitochondria are possibly the initial target for cadmium induced apoptosis, studies have shown that the disruption of the mitochondrial membrane causes the release of

cytochrome c and the subsequent activation of caspase 9 (Habeebu *et al.*, 1998). The kidney is the critical target organ for cadmium toxicity (Lermioglu & Bernard, 1998), but exposure to cadmium may result in damage to numerous organs, bone, lungs, reproductive organs and the central nervous system. The neurological symptoms of cadmium poisoning include cerebral bleeding and edema, hyperactivity, aggressiveness and decreased ability to learn (Lopez *et al.*, 2006).

1.1.5: Zinc

Unlike the other heavy metals mentioned earlier, zinc is an essential element. It is the second most prevalent metal in the body (Weiss *et al.*, 2000), and whilst an excess of zinc is toxic, zinc deficiency is also deleterious to health. (Maret & Sandstead, 2006) estimated that over 25% of the world's population is at risk from zinc deficiency. The normal zinc concentration within a healthy adult range from 2-3g throughout the body and daily intake is recommended at 0.25 mg/kg (Sandstead, 1993). Zinc is an important catalytic and structural component of hundreds of enzymes involved in metabolism and gene expression (Turan *et al.*, 1997). It is essential for normal growth and development and is involved in cellular proliferation, differentiation and apoptosis (Ross *et al.*, 1997). The immune system, metabolism, reproduction, vision, taste and behaviour all essentially require zinc (Fraga, 2005). In addition zinc has a role neuronal growth and transmission (Maret & Sandstead, 2006). The brain has the highest zinc content around 10 times higher than the concentration found in plasma. The vast majority of zinc in the brain is bound to zinc metalloproteins, around 10% of zinc is free or loosely bound and is found mostly in certain synaptic vesicles (Mathie *et al.*, 2005). These zinc rich vesicle are only found in glutamatergic neurons (Frederickson & Bush, 2001) at a concentration estimated to be around 300 μM (Takeda *et al.*, 2003). Zinc is present in vesicles within excitatory nerve terminals and when released in a calcium dependent manner, can reach concentrations of 100 μM in the extra cellular space (Gee *et al.*, 2002). Synaptically released zinc can then modify the activity of certain proteins such as glutamate and γ-aminobutyric acid (GABA) receptors (Frederickson & Bush, 2001; Mathie *et al.*, 2005).

However an excess of extra cellular zinc is damaging and is implicated in cell death following an ischemic period or seizure (Park & Koh, 1999; Kim *et al.*,

2000). An excess of zinc during pregnancy can be teratogenic and sometimes lethal. Toxic doses in adults of around 325-650 mg causes nausea, abdominal pain, vomiting and diarrhoea (Maret & Sandstead, 2006). Changes in zinc homeostasis within the brain has been linked to the occurrence of seizures in epileptics, this is part due to the discovery that prior to a seizure zinc concentrations are higher in the brains of epileptic mice than in control mice (Mathie *et al.*, 2005).

1.2: Cellular Responses to Heavy Metals

Once heavy metals have entered the body, the cellular machinery attempts to detoxify and/or remove them from the cell via a combination of processes collectively known as metalloregulation (Castiglioni *et al.*, 2001). This is mediated by metal chelating proteins such as metallothioneins. Other detoxification pathways involve removal of the metal from within the cell via diffusion, or through the action of P-type ATPases. These are energy dependant pumps which extrude cations into or out of the intracellular matrix or intracellular compartments, thereby protecting internal cellular mechanisms from heavy metal damage (Lutsenko & Kaplan, 1995). In addition toxic metals can also be mineralised within mitochondria or lysosomes (Castiglioni *et al*, 2001). Another mechanism of detoxification in marine invertebrate has been speculated and it is the formation of insoluble metal-calcium precipitates (Mason & Nott, 1981). Metallothionein is a highly conserved low molecular weight intracellular protein. It is known to be important in the detoxification of heavy metals and can bind to at least 18 different elements including zinc, cadmium and mercury (Baldwin & Marshall, 1999). Metallothioneins store and release essential metals such as zinc and copper; thus maintaining the low intracellular concentration of free essential metals. Metallothioneins have a regulatory capacity and influence transcription, replication, protein synthesis, metabolism, as well as other zinc-dependent biological processes. Increasing cellular expression of metallothionein protects the cell from heavy metal damage (Yao *et al.*, 1999). Lead and mercury exposure gives rise to insoluble protein bodies in the kidneys, however the precise nature of these protein inclusions remains uncertain, they could be an excretory process or passive shedding of cells (Baldwin & Marshall, 1999). If the exposure of the individual reaches pathological levels heavy metals can be deposited into tissue. An example of this is mercury which can be found

deposited in a wide variety of body tissue, which would account for the variety of symptoms that accompany mercury poisoning.

The central nervous system is extremely susceptible to heavy metal toxicity. The brain already contains significant amounts of zinc, iron, copper and magnesium (Castiglioni *et al*. 2001). Normal copper concentrations in the brain are around 0.2-1.7 µM but can exceed this level at the synaptic cleft; reaching concentrations of 200 µM. Compared to all other organs the brain has the highest concentration of zinc at concentrations of 100-150 µM. Therefore the brain needs effective protective mechanisms in order to allow these metals to exist in the nervous system without causing any damage. One such protective system is glial cell activity. Astroglia have high levels of metallothioneins I, II and type III; which is unique to the CNS. Neuronal cells have been shown to express very low levels of metallothioneins, making them susceptible to heavy metal damage. Glial cells express levels of metallothionein I 10 times greater than that of neuronal cells, 538 pg metallothionein I/µg protein in glial cells compared to just 49 pg/µg protein in neuronal cells (Hidalgo *et al.*, 2000). Metallothioneins are cysteine rich proteins with a high affinity for metal ions, which may allow glial cells to chelate heavy metals. Exposure to heavy metals induces metallothionein synthesis in astrocytes. Zinc exposure of 50 µM increased metallothionein I concentrations by 3.5 fold in neurons and 2.5 in astrocytes (Hidalgo *et al.*, 2000). Astrocytes protect neighbouring cells including neurons from oxidative damage. They are rich in glutathione (GSH), which is a powerful anti-oxidant and in addition they provide GSH precursors to neurons (Takuma *et al.*, 2004). GSH concentration within mature astrocytes is around 2 mM (Castiglioni & Qian, 2001). Glial cells provide protection to neurons against excitotoxicity, caused by an excess of the neurotransmitter glutamate (Glu). Exposure to heavy metals reduces the ability of astrocytes to take up Glu (Aschner, 1996). Since glial cells line the ventricles of the central nervous system they are the first cells that come into contact with metals crossing the blood-brain barrier. Hence, despite their protective roles, the heavy metals may overwhelm the regulatory capacity of the glia (Castiglioni & Qian, 2001).

1.3: The developing nervous system

Children tend to be more susceptible to the toxic effects of heavy metals since their nervous system is still developing (Choi *et al*, 1989, Castoldi *et al*, 2001).

Hence exposure to heavy metals can have a devastating effect on the normal development of an infant. Many studies have reported that even very low doses of 0.1 μM lead and methylmercury can affect growth and development (Crumpton *et al.*, 2001; Moreira *et al.*, 2001). Both metals can cross the placenta. The concentration of heavy metal in foetal blood is assumed to be proportional to that in maternal blood. In adult brain tissue mercury damage tends to be restricted to areas of anatomical importance such as the visual cortex but in a developing CNS the damage is more extensive (Castoldi *et al.*, 2001). The major difference between a mature CNS and a developing one is the intense cellular proliferation that occurs during development. The toxicity of methylmercury, mercury and lead occurs by the compounds interfering with normal biological processes, such as calcium homeostasis, interaction with the cytoskeleton and/or protein SH groups in enzymes. Cytoskeletal proteins like tubulin are important in a developing nervous system since it is subject to intense cellular proliferation and differentiation. Any interference in these processes are liable to damage the CNS. In addition mercury affects microtubule formation during the cell cycle (Miura *et al.*, 1999). It has also been suggested that methylmercury has an inhibitory effect on axon formation and that the inhibition is partly responsible for the resultant developmental problems seen in cases of mercury poisoning (Heidemann *et al.*, 2001).

Lead is known to impair the cytoarchitectural development of the nervous system, particularly an immature CNS (Erdahl *et al.*, 2000), infants have an inadequate blood-brain barrier (Moreira *et al*, 2001). In addition there is evidence that children do not form lead-protein complexes, a protective process that is used to bind lead in adult brain (Moreira *et al*, 2001). The plasma lead concentration of children should remain below 10μg/dl. The Centre for Disease Control (CDC) recommends treatment for levels over 20μg/dl, while 70μg/dl is considered a medical emergency (Kaufman, 2001). Data from a national health and nutrition survey indicated that blood lead levels had an inverse correlation with height, weight and chest circumference in children in the U.S.A (Tonner & Heiman, 1997). It was found that lead exposure reduced the secretion of both the thyroid hormone and growth hormone, which would account for the reduction in height, weight and chest circumference seen in that survey (Huseman *et al.*, 1992). Lead has been shown to alter the expression of various receptors on the cell surface, altering normal signalling

pathways. It can inhibit NMDA receptor-receptor ion channel function which is thought to be involved in learning and memory, which is a classic indication of lead toxicity (Finkelstein *et al.*, 1998). Like mercury, lead is also able to cross the placental barrier. Concentrations in the umbilical cord were found to be 80-100% of that found in maternal blood. During pregnancy bone turnover can increase, which can release the lead taken up by bone potentially leading to chronic lead toxicity in both mother and baby (Papanikolaou *et al.*, 2005).

1.4: Potential mechanisms of heavy metal toxicity

1.4.1: Oxidative stress

Oxidative stress is caused by an imbalance between the production of reactive oxygen species (ROS) and the anti-oxidant defences of the cell. Normal metabolism in a healthy CNS is high and generates large amounts of ROS. This is counteracted by high concentrations of antioxidants, such as reduced glutathione (GSH). The increase in levels of ROS can damage cellular components including proteins, membrane lipids and nucleic acids (Halliwell and Gutteridge, 1989). When the anti-oxidant defences are overwhelmed, ROS can cause catastrophic damage to cellular components leading to necrosis or apoptosis. (Yee & Choi, 1996.) suggested that the mitochondria is one of the earliest sites of heavy metal accumulation. Disruption to the mitochondrial electron transport chain is possibly a major cause of free radical production, which would deplete the cell's energy levels.

Production of free radicals is a common toxic mechanism for many heavy metals including lead, cadmium and mercury. Cadmium does not appear to generate free radicals but lipid peroxidation in an earlier indicator of cadmium exposure (Manca *et al.*, 1991). In the case of cadmium exposure ROS damage could occur via depletion of anti-oxidant systems rather than the creation of the radicals themselves as glutathione levels have been shown to be depleted (Li *et al.*, 1993). In contrast zinc appears to prevent the formation of ROS by protecting sulphydryl groups from oxidation (Bray & Bettger, 1990). Lead, mercury and other heavy metals have high affinities for sulphydryl (SH) groups in proteins. The binding of heavy metals to SH groups in anti-oxidant enzymes, such as superoxide dismutase (SOD) and GSH would seriously affect the ability of cells to cope with the ROS. It would also leave cells

more susceptible to further oxidative damage (Hsu & Guo, 2002). For example methylmercury has high thiol reactivity, which would render GSH ineffective as an anti-oxidant (Gatti *et al.*, 2004).

The generation of ROS may also be one of the mechanisms thorough which heavy metals affect calcium homeostasis.(Burlando *et al.*, 1997b) demonstrated that increased levels of free radicals can lead to a massive release of calcium from the sarcoplasmic reticulum stores via the ryanodine receptor. The evidence for ROS playing a part in metal toxicity is supported by the observation that the addition of certain anti-oxidants like vitamin E, C, B_6 and selenium, can increase the protection for cells that have been exposed to heavy metals (Stohs & Bagchi, 1995; Dare *et al.*, 2000; Gurer & Ercal, 2000).

Numerous studies suggest that oxidative stress is an important mechanism of damage for all of the metals that are of interest to this research. There are however other pathways that are also relevant

1.4.2: Interaction with the cytoskeleton

The neuronal cytoskeleton is a complex and dynamic structure that extends through the cell cytoplasm. The main components of the cytoskeleton within the cells of the central nervous system are microtubules, microfilaments and intermediate filaments. Together these components are responsible for cellular organisation, communication, transport and cell stability. Each component of the neuronal cytoskeleton has different biochemical properties and functions within the cell.

1.4.2.1: Microtubules

Both neuronal and glial cells contain microtubules. Microtubules are hollow cylindrical organelles, approximately 25nm in diameter. They are labile polymers assembled from heterodimeric subunits of α- and β-tubulin, each with a molecular weight of around 50 kDa (Graff *et al.*, 1997). Tubulin is an acidic protein of which there are two main isotypes, α- and β-tubulin. The heterodimeric subunit comprised of these two isotypes is the principle constituent of microtubules. Microtubule formation occurs via the binding of the α/β-subunit to two molecules of GTP. One molecule of

GTP binds to α-tubulin and the other is reversible bound to β-tubulin and is hydrolysed during microtubule formation (Hargreaves, 1997). Tubulin synthesis is regulated by the pool of unpolymerised tubulin, for example when microtubule assembly is high the pool lowers and tubulin synthesis is increased so that the pool of unpolymerised tubulin remains the same and when microtubule assembly is low the opposites occurs (Dhamodharan & Wadsworth, 1995).

Microtubules are made up of 13 longitudinally arranged polar protofilaments (Figure 1.2). The polarity allows the ends of the protofilaments to display differences in subunit addition and loss. Polymerisation occurs via the addition of tubulin subunits to the polar end or plus end of the microtubules until equilibrium is reached, where the gain of tubulin subunits at the plus end is equal to the loss of subunits from the minus end (Hargreaves, 1997). Microtubules are dynamic in most interphase cells. Tubulin subunits are constantly polymerising and depolymerising. However some cell types, like neuronal and glial cells contain microtubules that are able to resist depolymerisation and are termed stable. Stable microtubules have a role in maintaining cell polarity and the complex architecture in a mature brain (Graff *et al.*, 1997). Microtubule stability is achieved via posttranslational modification of the α-tubulin subunit, modification such as detyrosination and acetylation (Gundersen & Bulinski, 1986). The detyrosination of microtubules involves the removal of a tyrosine residue from the C-terminal of the α-tubulin subunit; the subunit can also be acetylated on the lysine side chain. The addition of various microtubule associated proteins (MAPs) such as Tau can further stabilise microtubule networks within cells (Bunker *et al.*, 2004).

The integrity of the microtubule network is vital in neuronal migration. Studies have shown that concentrations ranging from 0-10 μM of MeHg inhibit the migration of external granule cells toward the internal granule layer in a concentration dependant manner (Kunimoto & Suzuki, 1997). Methylmercury can disrupt the cell cycle by interfering with microtubules and, through its interaction with the microtubules, cause the induction of apoptosis (Miura *et al.*, 1999). *In vitro* studies have indicated that MeHg produces this effect by binding to tubulin SH groups, which either depolymerises the microtubules or prevents the polymerisation of tubulin (Vogel *et al*. 1985; Sager, 1988; Graff *et al*. 1997). The sensitivity of neuronal cells to mercury toxicity may be related to the high concentration of tubulin

and microtubules in vertebrate brain, which is primarily due to their high density in axons where they mediate the process of axonal transport.

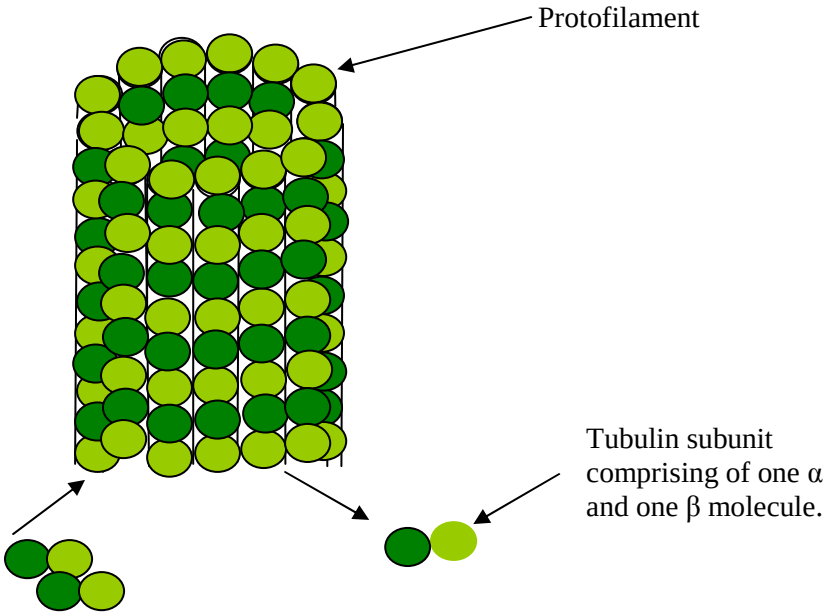

Figure 1.2 Microtubule structure

Microtubules are comprised of 13 longitudinally arranged protofilaments. Each protofilament contains alternate α and β subunits. Subunits are constantly added and removed from the microtubule structure during the steady state. When the microtubule is elongating there is no removal of subunits only additions.

1.4.2.2: Microfilaments

Another important cytoskeletal component is microfilaments, which are composed of the 42 kDa protein actin. Actin has a bi-lobal structure and is arranged helically during polymerisation (Hargreaves, 1997). F-actin is the finished filament; it has an outer diameter of 5-7 nm and appears to be comprised of twisted beads due to the helical arrangement of the actin protein. Actin is abundant in muscle cells where it forms stable thin filaments that enable muscle contraction; it also forms labile microfilament structures in non-muscle cells in the form of stress fibres, lamellipodia and other networks. F-actin formation occurs by a nucleated condensation mechanism in which polymerisation occurs via the addition of monmeric actin subunits, known as

G-actin at the positive end of F-actin filaments (Hargreaves, 1997). Actin is important in the process of axon branching where it forms filopodia and lamellipodia in the axon growth cone (Gitler & Spira, 1998). Actin filament undergo rapid cycles of polymerisation and depolymerisation that enable filopodia to probe the extracellular space (Kornack & Giger, 2005)

1.4.2.3: Neurofilaments

Apart from microtubules and microfilaments, neuronal and glial cells also contain a number of unique intermediate filaments. Glial cells contain glial fibrillary acidic protein (GFAP) and neuronal cells contain neurofilaments, of which there are three main types in mammals, neurofilament light chain (NF-L) with a molecular weight of around 60 kDa, neurofilament medium chain (NF-M), molecular weight of around 102 kDa and neurofilament heavy chain (NF-H) which has a molecular weight of approximately 112 kDa (Ackerley *et al.*, 2003). All NF subunits consist of a globular amino-terminal 'head' domain, an α-helical rod domain and a globular carboxy-terminal 'tail' domain (Figure 1.3). The central rod domain consists of 310 amino acid residues and is consistent between the three main NFs, so the differences in molecular weight are primarily down the differences in the head and tail domains. The central rod domain of the NF subunits is intertwined in order to form dimmers which then form tetramers, the tetramers combine to form protofilaments, which finally assemble to produce the NF (Figure 1.4).

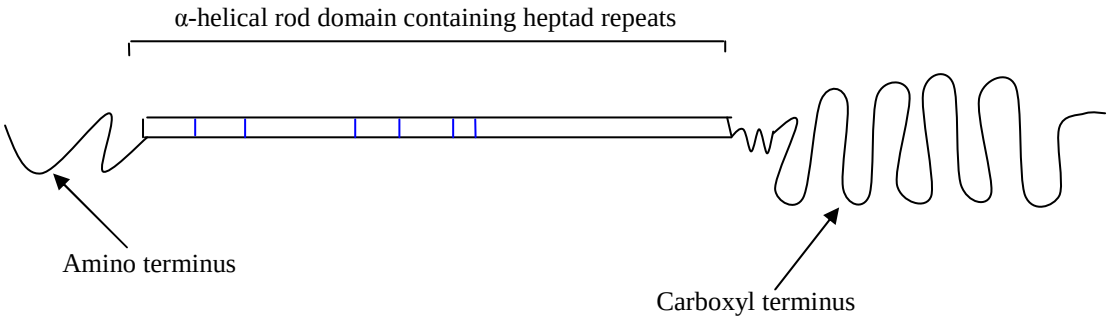

Figure 1.3 Structure of the neurofilament protein

NF-H is one of the most extensively phosphorylated neurofilaments it contains over 50 acceptor serine/threonine sites in the KSP region within the C-terminal (Ackerley *et al.*, 2003). Neurofilament phosphorylation is associated with axonal stability, the neurofilament proteins extend along the axon and are the primary component of its cytoskeleton and in addition to the stabilisation of axons, NF-H also controls axon girth (Williamson, 1996). NFH phosphorylation is also involved with neurofilament transport within the axons (Pant *et al.*, 2000).

Although there is evidence that methylmercury affects axon production (Gopal, 1995) there are very few *in vivo* or *in vitro* studies that have assessed the effects of non-lethal doses of methylmercury on axon outgrowth and the proteins involved in axon stability (Heidemann *et al.*, 2001). Most investigations have simply determined the mechanism by which lethal doses cause cell death. One of the aims of this study is to determine whether sub-lethal concentrations of various heavy metals affect neurite outgrowth in differentiating N2a and C6 cells and the levels of proteins known to be important in the outgrowth and maintenance of axons formed by mouse neuroblastoma (N2a) cells and processes formed by a rat glioma (C6) cells.

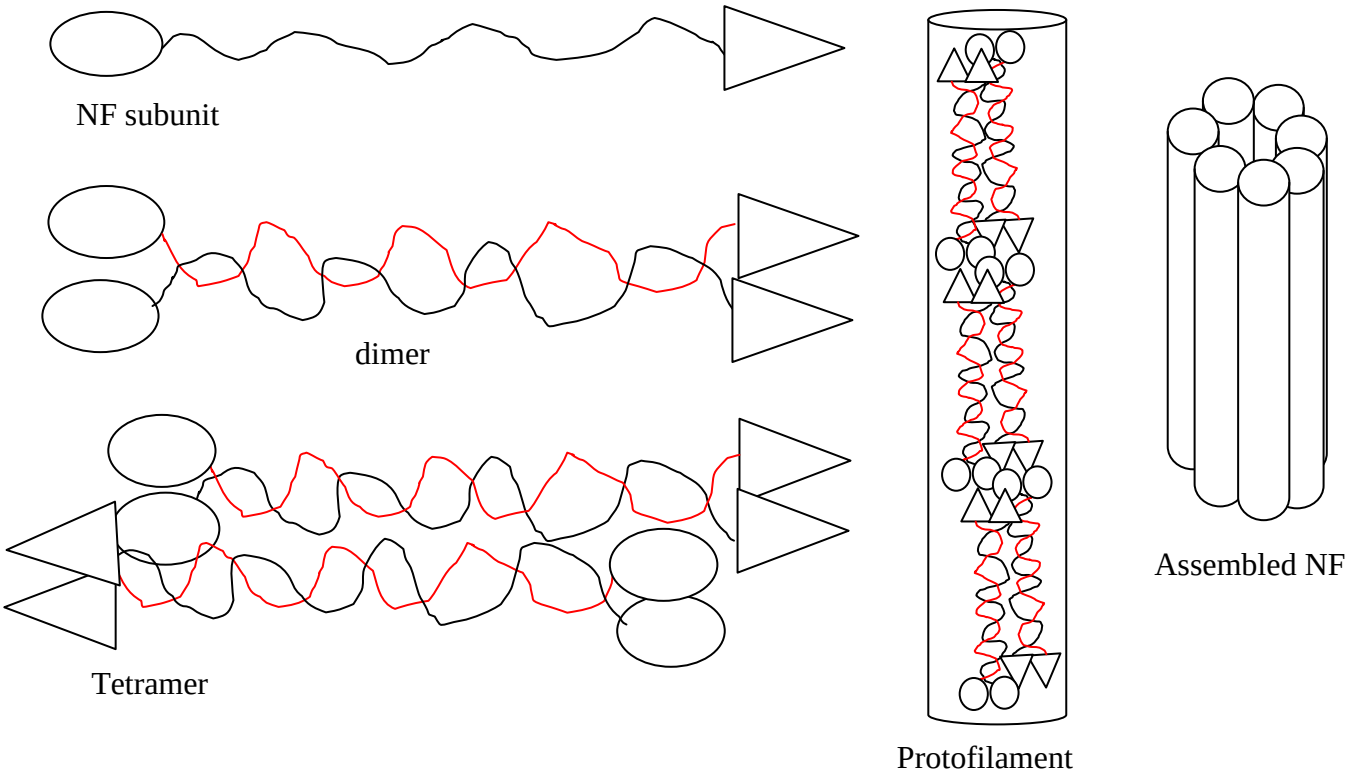

Figure 1.4: Neurofilament Assembly.

The central rod domain of the NF subunits is intertwined in order to form dimers. The dimers are sorted in an anti-parallel fashion and form tetramers. Tetramers combine to form protofilaments, which finally assemble to produce the 10 nm thick NF. Diagram adapted from (Petzold, 2005).

1.5: The Role of Calcium in Heavy Metal Toxicity

Numerous studies have shown that toxic concentrations of heavy metals have an effect on calcium homeostasis (Viarengo *et al*, 1999; Nathenson *et al*, 1995; Szucs *et al*, 1997; Leonhardt *et al*, 1996). These imbalances in calcium can then affect cell signalling mechanisms and impair the activity of calcium dependent enzymes (Panfoli *et al*, 2000; Watjen *et al*, 2001).

Calcium is known to be involved in the regulation of many physiological processes (Saino *et al.*, 2002). It is also widely used as an intracellular signalling molecule. The concentration of free calcium within the cytosol is approximately 0.1μM, whereas the extracellular calcium concentration is around ten thousand fold higher. This difference in calcium concentration creates a chemical gradient greater

than that of any other ions. In addition, the negatively charged interior of the axonal plasma membrane forms an electrical gradient that together creates a large electrochemical force for the entry of calcium into the cell. The electrochemical gradient for calcium entry is opposed by Ca^{2+}ATPases. These are ATP dependant Ca^{2+} pumps that actively remove Ca^{2+} from the cytosol by pumping it into the extra cellular medium or sequester Ca^{2+} into various organelles such as the mitochondria and the endoplasmic or sarcoplasmic reticulum. Thus, when the calcium concentration within the cytosol increases by the entry of Ca^{2+} through voltage gated Ca^{2+} channels, when the cell membrane is depolarised or by the binding of an extra cellular signalling molecule to a cell surface receptor, it generates an intra cellular response such as the activation of inositol triphosphate (see Figure 1.5 for diagram of calcium signalling). With the subsequent stimulation of Ca^{2+} release, Ca^{2+} dependent pathways are then activated within the cell. In the nervous system, Ca^{2+} is involved in the transmission of action potentials across synaptic junctions. When the action potential reaches the pre-synaptic terminal calcium ions enter the depolarised pre-synaptic terminal via voltage gated Ca^{2+} channels and activate the exocytotic pathways resulting in the release of a neurotransmitter into the synaptic cleft (Kostyuk & Verkhrastsky, 1995).

The alteration of calcium homeostasis in cells due to heavy metal exposure has been noted by a number of different studies (Hare *et al.*, 1993; Abramson *et al.*, 1995; Marchi *et al.*, 2000). This rise in intracellular Ca^{2+} is generally caused by the opening of Ca^{2+} channels in the cell membrane (Burlando *et al.*, 1997a; McNulty & Taylor, 1999; Gopal, 2002). The opening of the voltage gated Ca^{2+} channels may be due to the binding of the metals to the SH groups within the channels proteins (Atchison & Hare, 1994). The rise in Ca^{2+} would be further augmented by any interaction between the metals and the SH groups within both the plasma membrane and SERCA Ca^{2+} ATPases (SERCA Ca^{2+} ATPases are calcium pumps that remove calcium ions from the cytoplasm into the ER or SR). The cell would then have a reduced ability to remove Ca^{2+} entering via the open channel (Canesi *et al.*, 2000). Methylmercury has been shown to increase intracellular calcium via an influx from the extracellular medium as well as from intracellular stores. In contrast mercury caused an influx from the extracellular medium alone. Hence although the outcome of increased intracellular calcium was the same, the mechanisms by which it was achieved was different for organic and inorganic mercury (Stohs & Bagchi, 1995). The resultant change in Ca^{2+}

concentrations would affect Ca^{2+} dependent enzymes within the cell. Methylmercury induced rises in $[Ca^{2+}]_i$ can cause the spontaneous release of the neurotransmitter by depolarising the plasma membrane, causing it to become more permeable to calcium ions (Atchison & Hare, 1994). Limited research shows that thimerosal also increases $[Ca^{2+}]_i$ though not as potently as methylmercury (Nishio, 1996; Ucha-Ishibashi *et al.*, 2004).

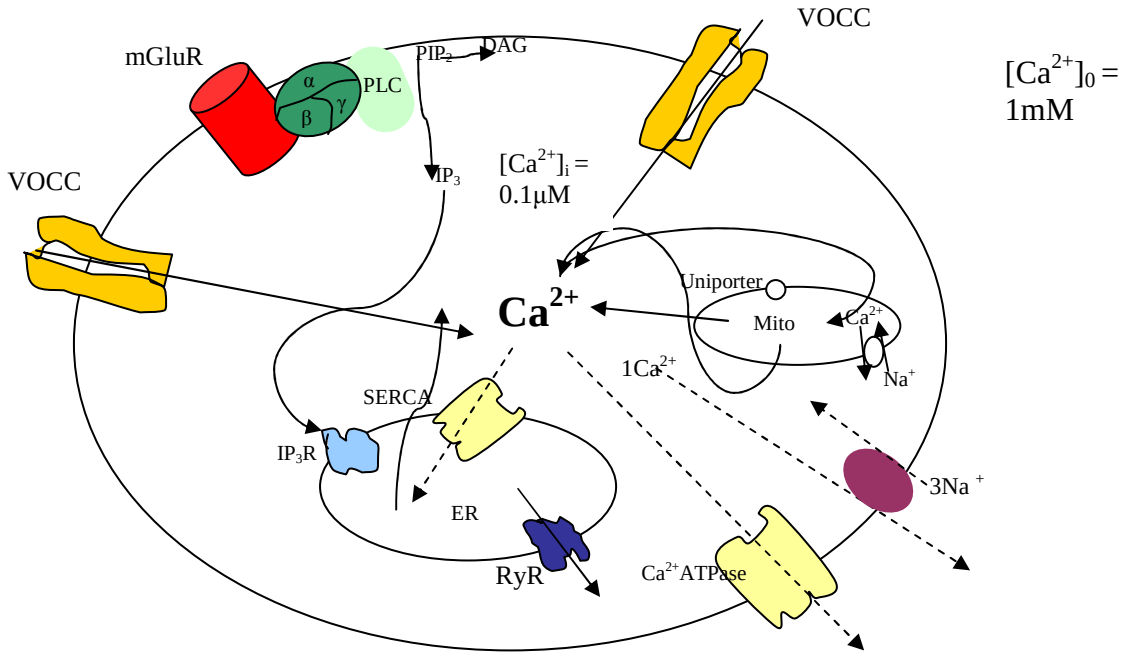

Figure 1.5: Calcium homeostasis

Diagram shows Ca^{2+} homeostasis in a glial cell. Extracellular calcium can enter the cell via voltage activated calcium channels (VOCC). Calcium can also be released from intracellular stores via the binding of an extracellular signalling molecule such as glutamate to a cell surface receptor such as the glutamate receptor (mGluR). This generates the hydrolysis of PI 4, 5-bisphosphate (PIP_2) to inositol triphosphate (IP_3) and diacylglycerol (DAG). IP_3 leaves the cell membrane and diffuses through the cytosol, where it interacts with an inositol triphosphate receptor (IP_3R) on the membrane of the endoplasmic reticulum (ER) causing the release of calcium. Ca^{2+} can be released from the ER via the ryanodine receptor (RyR). RyR are regulated by positive feedback, where the binding of Ca^{2+} to the receptor increases Ca^{2+} release. Stores within the mitochondria (mito) are released via a uniporter; which utilises the large negative potential to translocate calcium, through a Ca^{2+}/Na^{+} exchange and through the calcium permeable 'permeability transition pore' Intracellular extrusion of calcium occurs through Ca^{2+}ATPase pumps in the plasma membrane, through sarcoplasmic and endoplasmic reticulum Ca^{2+}ATPases (SERCA) and through a $1Ca^{2+}/3Na^{+}$ exchange. Diagram adapted from (Deitmer *et al.*, 1998)

Lead can mimic calcium in cells. It enters cells via the calcium channel and can activate protein kinase C (Loikkanen *et al.*, 1998; Raunio & Tahti, 2000). Lead functions as a substitute for calcium in its interaction with other proteins, such as calmodulin and the synaptic vesicle protein synaptotagmin 1. This can lead to an abnormally functioning protein, with potential deleterious effects on cell pathways and gene transcription (Bouton *et al.*, 2001). Lead is so effective as a substitute for calcium, that on most protein targets the affinity of the binding sites is greater for lead than for calcium (Mike *et al.*, 2000).

Alterations in calcium homeostasis, would effect the regulation of calcium dependent enzymes within the cell. Calpains are calcium dependent intracellular cysteine proteases. Since the discovery of the calpain family 14 members have been identified, some of which are tissue specific whilst others are ubiquitously expressed (Nixon, 2003). Calpains are comprised of large 80 kDa catalytic subunit and a small 30 kDa regulatory subunit (Sorimachi *et al.*, 1997). The two most widely distributed isoforms are µ-calpain and m-calpain, sometimes known as calpain 1 and calpain 2. These two forms have virtually identical substrates and are so far only distinguished by their calcium requirements for activation and tissue distribution (Nixon, 2003), calpain 1 requires 5-50 µM and 2 requires 200-1000 µM of calcium (Reverter *et al.*, 2001). Once activated it has been suggested that calpains are modulated by a protein inhibitor called calpastatin (Nixon, 2003).

Calpains exist in an inactive state that requires a conformational change to align the active site residues to form the catalytic centre. Calpain activation is dependent upon the binding of calcium to several areas, translocation to the cell membrane and autoproteolysis, upon activation the regulatory subunit is cleaved (Huang & Wang, 2001).

Calpains act on various cytoskeletal proteins, and are involved in the regulation of cell adhesion, cell spreading or migration and process outgrowth (Khorchid & Ikura, 2002). Calpains interact with various microtubule associated proteins (MAP) such as tau and MAP 2. As MAP's are important in the stabilisation of microtubules, then their degradation by calpain or abnormal phosphorylation by the cdk5-p25 complex would result in disruption of the microtubule network. Calpains are also involved in the processing of p35 to p25. This then forms the cdk5-p25 complex that is involved in the phosphorylation of many proteins including tau and neurofilaments (Sakaue *et al.*, 2005).

Limited research into heavy metal influence on calpain activation indicates that methylmercury exposure increases calpain activation in cell culture systems (Zhang *et al.*, 2003; Sakaue *et al.*, 2005). Abnormal calpain regulation is probably caused by the changes in calcium homeostasis induced by exposure to heavy metals.

A possible pathway for the over activation of calpain is via excessive glutamate build up (see Figure 1.6). Glutamate (Glu) is a common neurotransmitter, but an excess can lead to over stimulation of cells, resulting in cell death. In nerve terminals Glu arises from glucose, through the Krebs cycle and is also secreted by astrocytes. Stimulation of the glutamate receptor (GluR) causes an influx of calcium and depolarisation of the cell. Astrocytes are also responsible for facilitating the removal of Glu from the extracellular matrix. Both mercury and lead affect Glu transmission but in different ways. Mercury causes an increase leading to excitotoxicity. It has been suggested that the increase in Glu is due to the inhibitory effect that mercury has upon astrocytes to clear the extracellular space of Glu. Conversely lead decreases Glu release by acting as a non competitive inhibitor for the receptor.

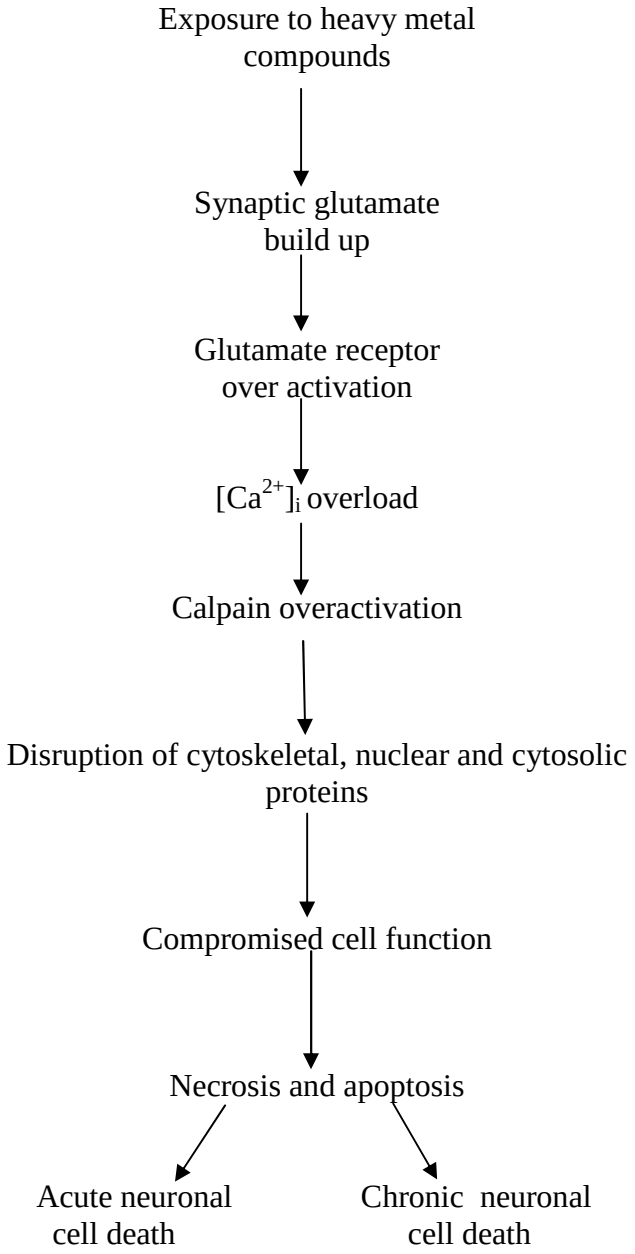

Figure 1.6: Methods by which heavy metals may compromise cell function via calpain activation.

Figure 1.6 shows the mechanism by which exposure to heavy metals may cause cell death via elevations of calcium concentrations and activation of calpains. Exposure to heavy metals such as mercury causes a build up of the neurotransmitter Glu. This leads to over stimulation of the cell, which is known as excitotoxicity. The resultant excessive build up of glutamate over activates ionotropic glutamate in the postsynaptic membrane and causes a sustained influx of Ca^{2+} through these receptors. Because of membrane depolarization, voltage-gated Ca^{2+} channels open, enabling Ca^{2+} to enter, resulting in a massive calcium overload. This then activates several calcium-dependent enzymes, especially calpain 1 and 2. Over activated calpain could lead to uncontrolled degradation of cytoskeletal proteins, cytosolic and nuclear enzymes and, ultimately, neuronal death (Huang & Wang, 2001).

1.6: The Effect of Heavy Metals on the Mitogen Activated Protein Kinase Signalling Pathways

The Mitogen activated protein kinases (MAPKs) are serine/threonine kinases that are ubiquitous enzymes of signalling pathways. They were first discovered in the 1980's in the pheromone-induced mating pathway in yeast (Callaway *et al.*, 2005) and were later found to be involved in cell cycle progression, proliferation and differentiation in all organisms. They are activated via reversible phosphorylation and are vital in connecting cell surface receptors to various targets within the cell (Hirsch & Stork, 1997). Most cell surface receptors involve one or more of the MAPK cascades in signal transduction. MAPKs are under the control of G-protein-coupled, growth factor and cytokine receptors (Werry *et al.*, 2005). The MAPK family consists of three main groups, the extracellular-signal related protein kinases (ERK), the stress-activated protein kinases (SAPK) p38, and the SAPK c-jun N-terminal kinases (JNK) (Chang & Karin, 2001). The signalling cascades for these enzymes are quite complex and are not understood. Each MAPK is activated by a specific Mitogen activated protein kinase kinase (MAPKK), MEK1/2 activates ERK1/2, MKK3/6 activates p38 and MKK4/7 for JNKs. However each MAPKK can be activated by more than 1 MAPKKK (Robinson & Cobb, 1997).

JNK and p38 pathways are involved with cellular responses to stress. The activity of these pathways respond to inflammatory cytokines and stress and have been linked to apoptosis (Wang *et al.*, 1998). ERK activity is controlled by mitogens and growth factors to stimulate cell survival and differentiation, and is suppressed in many events leading to apoptosis (Jin *et al.*, 2002). In recognition of the variety of biological processes that involve the MAPK signalling, a large numbers of studies are being carried out on the potential of the signalling cascades as therapeutic targets.

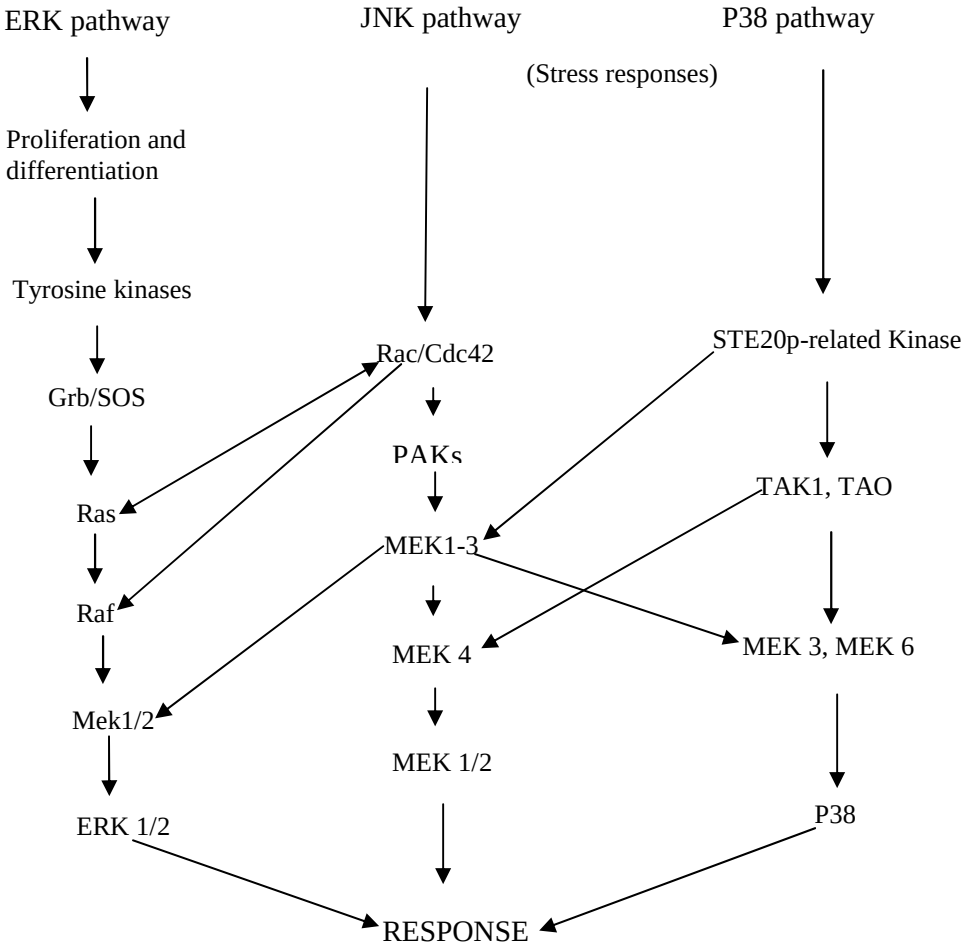

Figure 1.7 schematic diagram of the ERK, JNK and p38 signalling pathways

The diagram shows the complexity of the signalling cascades. Not only can the MAPKs become activated by their traditional pathway, there can also activation via cross talking from other pathways, for example Raf can be activated by Ras in the ERK pathway and Rac/Cdc42 from the JNK pathway. Heavy metals can interfere with ERK1/2 activity, either inhibiting or stimulating the pathway depending on the concentration of the metals. In addition heavy metals have been shown to stimulate the stress activated pathways. Diagram adapted from (Robinson & Cobb, 1997).

Heavy metals affect various signalling pathways including the MAPK signalling cascade shown in figure 1.7. A low exposure to cadmium decreases ERK activity, whilst high concentrations have been shown to increase ERK activity. In contrast p38 is increased by both high and low cadmium concentrations (Pulido & Parrish, 2003). Non toxic concentrations of methylmercury also inhibit ERK activation (Parran *et al.*, 2004). Exposure to zinc and lead caused activation of ERK at concentrations ranging from 1-10 µM (Seo *et al.*, 2001; Cordova *et al.*, 2004). JNK

activation has been found to increase during mercury exposure (Matsuoka *et al.*, 1999; Drzewiecka *et al.*, 2005). However, a separate study found no change in JNK activation (Barnes & Kircher, 2005), indicating that JNK plays an inconsistent or a duel role during exposure to mercury compounds.

1.7: Neuronal and glial cells

Due to the complexities of the kinetics of heavy metals, and the issues of absorption, distribution, metabolism and excretion that occur in a multi organ system, many studies have utilised cellular models. It is therefore of value to outline the rationale and properties of the cells lines used in this project.

Neuronal and glial cells are both generated by neural stem cells that are present in both an adult and developing CNS (Tamm *et al.*, 2006). Neuronal and glial cells have very different functions in the nervous system. Neuronal cells are responsible for the perception of stimuli and the responses to that stimulus. Neurons are argued to be the most polarised cell in the human body, they form two distinct types of processes, axons and dendrites (Barres & Barde, 2000). Glial cells represent the most numerous group within the brain (Bezzi & Volterra, 2001). It includes astrocytes and oligodendrocytes in the CNS (Aschner, 1996). They provide structural, metabolic and trophic support to neurons. It is only recently that the role of glial cells has been uncovered. It was originally believed that neurons were the excitable cells within the CNS, it has now been discovered that glia have active properties and may communicate with neurons during synaptic transmission (Scemes, 2001). Astrocytes respond to neuronal activity by an increase in intracellular calcium concentrations, which trigger the release of chemicals which can then influence neuronal cells (Barres & Barde, 2000). By using both neuronal and glial cells this study will determine the importance of cell specific toxicity.

1.8: Cellular models

Whilst cultured cell lines are useful in the study of heavy metal toxicity, the mechanism of toxicity of such compounds at sub-lethal concentrations is still poorly understood. This study utilised differentiating N2a (mouse neuroblastoma cell line) and C6 cells (a rat glial cell line) in order to investigate the toxic action of heavy

metals on the nervous system. Both N2a and C6 cells are widely used to investigate the cellular mechanisms of neurotoxicity (Castiglioni, 1993; Flaskos *et al.*, 1998; Allen *et al.*, 2001; Fowler *et al.*, 2001; Sachana *et al.*, 2001; Sachana *et al.*, 2003).

1.8.1: Neuroblastoma (N2a) cell line

The N2a cell line was derived from the C1300 neuroblastoma (Klebe & Ruddle, 1967). N2a cell morphology is typically round when in suspension or undifferentiated. However, when attached to a suitable surface N2a cells undergo a striking morphological changes, the most prominent being cellular extrusions. Cells produce one to four processes known as neurites and show an increase in the size of the nucleus and perikaryon (Haffke & Seeds, 1975). These neurites contain large numbers of neurofilaments, which are characteristic of mature neurones. The growth of the neurite can be further augmented by serum withdrawal and the addition of dibutyryl cyclic 3', 5'-monophosphate (dbcAMP). Serum withdrawal causes a reduction in cell division and promotes differentiation and dbcAMP mimics the effect of cAMP to promote differentiation. Together both these processes cause N2a cells to differentiate morphologically and biochemically to mimic a mature phenotype (Prasad & Sinha, 1976).

In addition to the changes in morphology, N2a cells can also develop some other biochemical characteristics of mature neurones. For example they are capable of spontaneous and repetitive depolarisation, as well as the ability to generate action potentials in response to stimulation (Haffke & Seeds, 1975).

Biochemically, N2a cells are classed as an adrenergic neuroblastoma cell line containing high concentrations of tyrosine hydroxylase. This enzyme is involved in the production of catecholamines and shows increased levels when N2a cells are differentiated via the addition of dbcAMP (Waymire *et al.*, 1972). N2a cells have also been shown to express dopamine, norepinephrine and serotonin in low concentrations (Narotzky & Bondareff, 1974).

All heavy metals have been reported to cause neuronal death and N2a cells display characteristics of primary neuronal cells. Methylmercury in particular has been reported to effect cytoskeletal proteins; thus due to the ability of N2a cells to produce neurites, rich in cytoskeletal proteins such as neurofilaments makes them an ideal cell line by which to investigate the toxicity of heavy metals.

1.8.2: C6 Glial cell line

The C6 cell line was cloned from a wistar rat glial tumour. This cell line possesses antigens and enzymes characteristic of astrocytes and oligodendrocytes *in vivo* and in primary cultures; enzymes such as glutamine synthetase, glycerol phosphate hydrogenase and lactate dehydrogenase, that are thought to be involved in myelination and ammonia detoxification (Kumar *et al.*, 1984). The cell line also produces the S-100 protein, which is unique to brain glial tissue in vertebrates, it has also been found in brain tumours of humans and animals. C6 cells have been employed in a variety of studies into neurotoxicology where they have shown similar responses to primary cells (Cookson *et al.*, 1995). Morphologically C6 cells are astroblastic in appearance; they are epitheliod in shape with spherical nuclei. Like N2a cells they can also be induced to differentiate using serum withdrawal and the addition of sodium butyrate which causes reversible changes in morphology, growth and enzyme activities (Kruh, 1982). The compound causes cells to flatten, a process associated with the distribution of the cellular cytoskeleton. The compound induces hyperacetylation of chromatin proteins, which can be associated with gene expression and protein synthesis (Kruh, 1982). When differentiated C6 cells develop short processes and increased expression of a spectrin-like protein related to fodrin which; it has been speculated, is involved in the organisation of the cytoskeleton within these processes (Cookson *et al.*, 1995)

Glial cells are thought to be an important target for heavy metals as research has indicated that the cells accumulate metals and may play a role in the death of neuronal cells, these features taken together make C6 cells a useful investigative tool that have been utilised by previous researchers in their investigation of heavy metals (Cookson & Pentreath, 1996). The use of both cell lines will enable a comparison to be made on their relative susceptibility to metal toxicity.

Putative mechanisms of mercury toxicity

Figure 1.8 is a diagrammatic representation of possible mechanisms of mercury toxicity. It is expected that at non-lethal concentrations the organic mercury compounds selected for further investigation will cause disturbances to the neuronal and glial cytoskeleton, as well as changes to the signalling cascades that control cytoskeletal organisation within the cells. In addition it is thought that the heavy metals will alter calcium homeostasis within the cells causing an increase in the activity of the calcium dependant enzymes, calpain. Calpain activation via increases intracellular calcium may occur through the action of ROS damaging cell membranes allowing the inflow of calcium. An increase in calcium can also occur through a build of glutamate causing over activation of the glutamate receptor and increases in calcium concentrations. Damage to membrane pumps and receptors involved in the control of calcium homeostasis may also contribute to calcium overload within the cell.

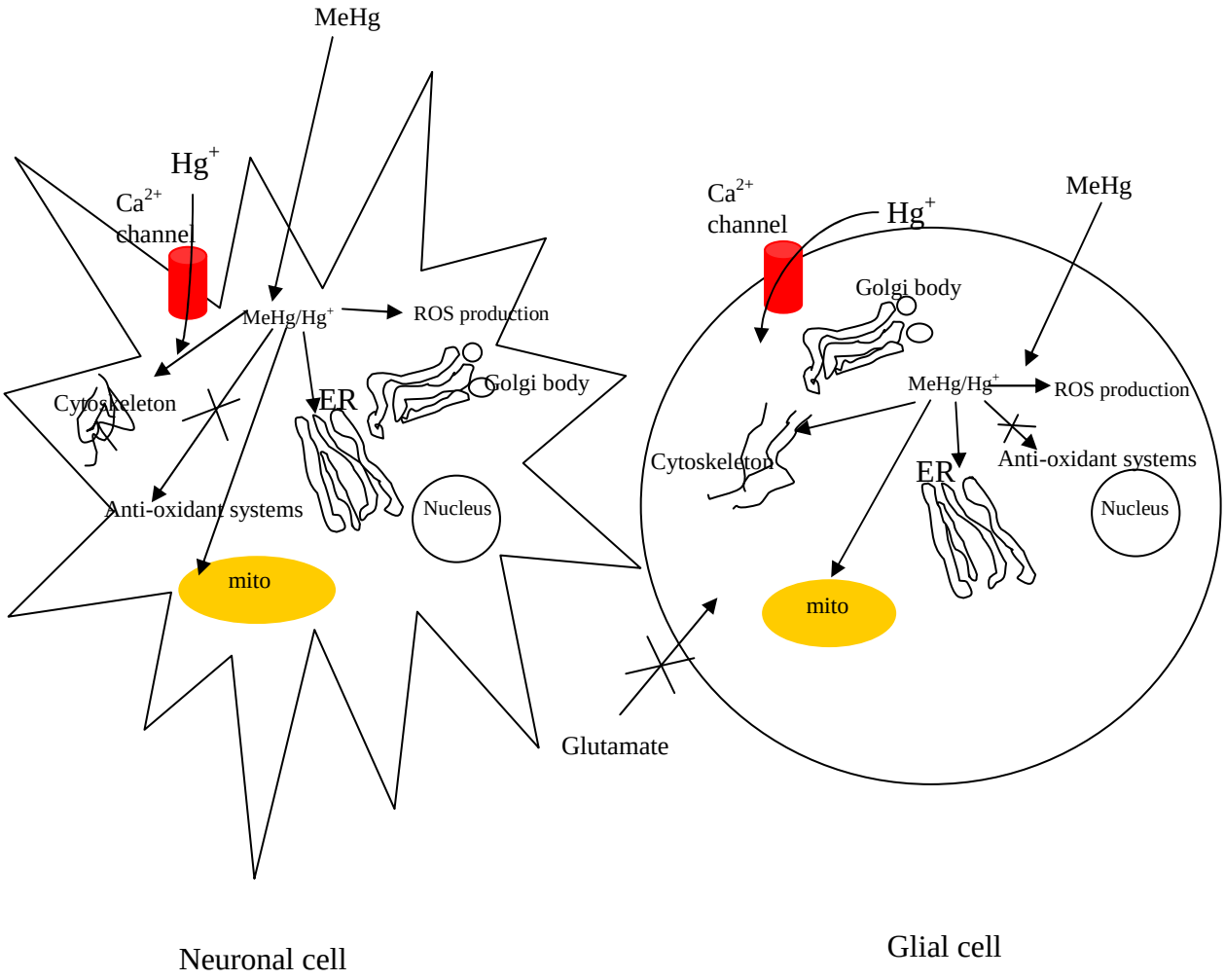

Figure 1.8: Possible mechanisms of Mercury toxicity.

Hg^{+} enters the cell via the Ca^{2+} channel, MeHg diffuses across the cell membrane as does Hg^{0}. Once inside the cell the metal can cause the production of ROS which attacks the mitochondrial membrane (mito) leading to the release of cytochrome c and the initation of the caspase pathway leading to cell death. Mercury exposure has also been shown to interfere with cytoskeletal proteins leading to disruption in the architecture of the cells. This interference may be caused by direct interaction of the metal with protein SH groups or via ROS production. In addition to stimulating ROS production, heavy metals like mercury can also inhibit cellular defences against free radicals, further exacerbating the damage caused by ROS. Exposure to heavy metals has also been shown to disrupt the uptake of glutamate by glial cells, which can lead to the death of neuronal cells by excitotoxicity.

AIMS

To determine the effects of heavy metals on the growth, viability and differentiation of N2a and C6 cells using MTT reduction assays and morphology studies. Using established methods the sub-lethal concentrations of the selected heavy metals will be investigated to enable the selection of compounds for further study in to the sub-lethal effects of the chosen metals.

To establish the molecular changes in the cytoskeleton associated with any sub-lethal changes in morphology that was highlighted by the morphology studies. The sub-lethal effects would be carried out on two compounds selected from the range of heavy metals investigated in the initial studies into cytotoxicity. Western blotting and confocal microscopy will be used to highlight any changes in the levels and distribution of cytoskeletal proteins such as tubulin and neurofilament proteins.

Using western blotting the signalling pathways that control the regulation of the cell cytoskeleton is to be investigated to determine whether any alterations in the levels and distribution of cytoskeletal proteins are preceded by changes to the normal signalling pathways.

Previous studies have shown that treatment with heavy metals impairs the cells ability to regulate intracellular calcium concentrations. Sustained elevations in intracellular calcium concentrations would cause unregulated activation of calcium dependant enzymes such as calpains. Calpains are known to target cytoskeletal proteins for degradation, so the fourth aim of this thesis was to investigate changes in calpain activity, in an attempt to explain the degradation of the cytoskeleton. The distribution of certain proteins essential for calcium homeostasis will also be looked at using confocal microscopy.

2.1: Materials

2.1.1. Specialised Reagents

Dulbecco's modified Eagle's medium (DMEM) and foetal calf serum (BioWhittaker, Wokingham, UK)

Glutamine/penicillin/streptomycin was purchased from Sigma-Aldrich (Poole, UK).

Bodipy thapsigargin, Bodipy ryanodine, calpain substrate and ER tracker were from Invitrogen, (Paisley, UK).

Vectashield mounting medium was supplied by Vectalabs, (Peterborough, UK).

.

2.1.2. Antibodies

Mouse monoclonal antibodies to NF-H (N52), total α-tubulin (B512), tyrosinated α-tubulin (T1A2), β-tubulin (Tub 2.1), anti-phosphorylated serine (PSR-45) and anti-phosphorylated threonine (PTR-8) were supplied by Sigma-Aldrich (Poole, UK)

The mouse hybridoma cell line producing antibody against phosphorylated NF-H (RT97) was originally purchased from The Developmental Hybridoma Bank and culture supernatant produced 'in house'.

Mouse monoclonal anti-phosphorylated NF-H (SMI-34) was from Sternburger Monoclonals, Ltd. (Maryland, USA)

The goat polyclonal anti-calpain 1 antibody (C-20) and mouse monoclonals anti-JNK (D-7) and anti-phosphorylated JNK (G-7) and anti-GRASP 65 were purchased from Autogen Bioclear (Wiltshire, UK)

Alkaline phosphatase-conjugated polyclonal rabbit anti-mouse, TRITC-conjugated polyclonal rabbit anti-mouse and horse radish peroxidase-conjugated goat anti-rabbit were all purchased from DakoCytomation (Ely, UK).

2.1.3. Tissue Culture Plastic-ware

All sterile tissue culture plastics were of the highest quality and purchased from Scientific Laboratory Supplies (Nottingham, UK)

2.1.4. Reagents

All general chemical reagents were purchased from Sigma-Aldrich (Poole, UK) or BDH (Leicester, UK), unless otherwise stated in the text.

2.1.5. Cell Lines

Rat C6 glioma cells and mouse N2a neuroblastoma cell lines were obtained from Flow Laboratories (Irvine, UK)

2.2: Methods

2.2.1: Cell culture and maintenance

N2a cells and C6 cells were both maintained as monolayers in T25 flasks containing DMEM supplemented 10 % foetal bovine serum (FBS) and 2 mM L-glutamine, 100 units/ml penicillin and 100 μg/ml streptomycin (Growth medium). They were incubated at 37 ^{o}C in a humidified atmosphere of 5 % CO_2 / 95 % O_2. Both cell lines were maintained in the logarithmic growth phase and passaged every 3-4 days, when the monolayer was approximately 80 % confluent. The cells were detached gently using a sterile pasture pipette and the cell suspension was centrifuged for 5 minutes at 300 rpm. The supernatant was discarded and the cell pellet was suspended in 1 ml of fresh growth medium. 1-2 drops of the cell suspension were placed in a new T25 flask along with 10 ml of fresh growth medium. Cells were routinely kept and used for approximately 30 passages following revival from liquid nitrogen storage, after which they were discarded and a new batch thawed.

2.2.3: Cryopreservation of cell lines

Cells were detached from the surface of the flask and centrifuged for 5 minutes at 300 rpm. The supernatant was discarded and the pellet of cells was resuspended in 1 ml of freezing medium [69 % (v/v) DMEM, 25 % FBS, 5 % dimethylsulphoxide (DMSO), 2 mM L-glutamine, 100 units /ml penicillin and 100 μg/ml streptomycin]. The cell suspension was transferred to a freezing vial and stored at -70 °C overnight and then into liquid nitrogen for long term storage.

2.2.4: Restoration of cells stored in liquid nitrogen

Cells were removed from liquid nitrogen and thawed as quickly as possible in warm water. The freezing medium containing the cells was immediately diluted in 10 ml of growth medium and centrifuged for 5 minutes at 300 rpm. The supernatant was gently poured off and the pellet was resuspended in 10 ml of fresh growth medium. The cell suspension was centrifuged again and then resuspended in 1 ml of growth medium before being transferred to a sterile T25 flask containing approximately 5 ml of growth medium. The cells were left to recover for 24 hours, after this time the medium was replaced or if the monolayer was 80 % confluent the cells were passaged. Cells were considered fit for experimentation after 1-2 passages.

2.2.5: Seeding of cells for experiments

Both cells lines were used for experimental analysis when they were approximately 60-80 % confluent. The cells were detached using a sterile pasture pipette and growth medium. The cell suspension was transferred to a 'sterilin' tube and centrifuged at 300rpm for 5 minutes. The cell pellet was resuspended in 1 ml of growth medium using a 1000 µl Gilson pipette. A total of 20 µl of the cell suspension was removed and added to 180 µl of growth medium in an Eppendorf tube (1:10 dilution) and a haemocytometer count was carried out to determine cell density. Cells were then plated out at a typical cell density of 50,000 cells/ml. Cells were then incubated at 37 °C in a humidified atmosphere of 95 % O_2 and 5 % CO_2 to allow recovery. Cell viability was determined by the general appearance of the cells and the trypan blue exclusion test. Trypan blue is taken up by dead cells where it stains the cytoplasm, causing the cells to shine blue under a light microscope. A 1:10 dilution of cell suspension was made in trypan blue solution (0.4 % [v/v]) typically 180 µl of trypan blue and 20 µl of cell suspension.

2.2.6: Cell differentiation

Mouse N2a neuroblastoma cells

N2a cells were seeded as described previously. After the recovery incubation overnight, N2a cells were induced to differentiate by serum withdrawal and the addition of dibutyrl cyclicAMP (dbcAMP) at a final concentration of 0.3 mM (Flaskos et al. 1998 etc). For this, the growth medium was carefully removed and replaced with an equal volume of serum-free DMEM supplemented with 2mM L-glutamine, 100 units/ml penicillin and 100 μg/ml streptomycin (serum-free medium) and dbcAMP.

Rat C6 glioma cells

C6 cells were seeded as described previously. After the recovery incubation, C6 cells were induced to differentiate using serum withdrawal and the addition of sodium butyrate at a final concentration of 2 mM. For this, the growth medium was carefully removed and replaced with an equal volume of serum-free DMEM supplemented with 2 mM L-glutamine, 100 units/ml penicillin and 100 μg/ml streptomycin (serum-free medium) and sodium butyrate.

2.2.7: Exposure of cells to heavy metals

All toxins except methylmercury chloride, which was solubilised and diluted in dimethyl sulphoxide (DMSO), were diluted in sterile distilled water to make a master stock concentration of 20 mM, from which working stock solution were prepared by further dilution. Cells were seeded as described previously. The growth medium was removed and replaced with serum free medium containing the compounds to final concentrations of 0.01, 0.1, 1, 10 or 100 μM. The equivalent amount of sterile distilled water or neat DMSO was added to the control cells (final concentration 0.5 % v/v).

2.2.8: Methyl blue tetrazolium (MTT) reduction assays

The MTT assay is based upon the cleavage of a yellow tetrazolium salt to purple formazan crystals which can then be read in a spectrophotometer by lysing the cells with DMSO (Mosmann, 1983). The MTT assay has been shown to be a useful indicator of cell viability when looking at heavy metals (Cookson *et al.*, 1995). Cleavage is thought to be carried out mainly by mitochondrial dehydrogenases. Cells induced to differentiate in the presence and absence of heavy metals, as described earlier, were incubated for the final 30 minutes of the required exposure time in the presence of MTT (50 µl of a stock solution at 5 mg/ml in DMEM). After carefully removing the medium, 1 ml of dimethyl sulphoxide (DMSO) was added to each well to solubilise the reduced dye. The absorbance was read in a spectrophotometer at 570nm.

2.2.9: Quantification of neurite outgrowth

The cells were seeded into 24-well plates and differentiated in the presence and absence of heavy metals. After incubated period was complete the medium was removed and the cells were fixed for 10 minutes at –20 ^{o}C with 0.5 ml of 90 % methanol in TBS (10 mM Tris, 140 mM NaCl, pH 7.4). Cells were stained using 0.5 ml of Coomassie brilliant blue stain (1.25 g Coomassie blue-R250, 10 % (v/v) glacial acetic acid, 40 % (v/v) methanol, 50 % (v/v) distilled water) for approximately 2 min at room temperature. The Coomassie stain was removed and the wells were gently washed with distilled water and then allowed to air dry. Cell counts were carried out on an inverted microscope at x200 magnification. Five fields were counted per well; the counts included total number of cells and number of axons, which were defined as neuronal outgrowths over two cell body diameters in length in the case of N2a cells (Keilbaugh *et al.*, 1991; Flaskos *et al.*, 1998). In the case of C6 cells, all neurites were counted (Flaskos *et al.*, 1998).

2.2.10: Preparation of cell lysates

N2a and C6 cells were differentiated for 4 h or 24 h in the presence and absence of two sub-lethal concentrations of methylmercury chloride or thimerosal (0.1 µM or 1

μM). After the required period of exposure, cells were lysed by the replacement of medium with 0.5 % w/v SDS in TBS, which had been pre-heated in a boiling water bath. The lysate was then transferred to an Eppendorf tube and boiled for 5 min. The protein concentration of cell lysates was determined using the assay of (Lowry *et al.*, 1951) modified to a microtitre plate format.

2.2.11: Mini-Lowry assay to determine protein concentration in cell extracts

Protein estimation was carried out using an assay first described by (Lowry *et al.*, 1951). The mini-Lowry assay has been used routinely in the lab. The typical r^2 for the calibration curve was 0.9883. The protein assay has also been used in previous work using the same cell lines (Sachana *et al.*, 2001). A series of standards were produced in triplicate using bovine serum albumin (BSA). The protein mass in the standard assay tubes was from 0 to 70 μg. In addition to the appropriate BSA amount, standard assay tubes also contained 30 μl of extraction buffer (0.5 % w/v SDS in TBS) and made up to 0.1 ml with distilled water. The unknown samples, which were set up in duplicate, contained 30 μl of cell lysate in extraction buffer and 70 μl of distilled water. Solution A [2 % (w/v) Na_2CO_3, 0.4 % (w/v) NaOH]. Solution B [1 % (w/v) $CuSO_4$. $5H_2O$] and solution C [2.7 % (w/v) sodium potassium tartrate] were combined to make a working solution comprising 50 ml of solution A and 1 ml of solutions B and C. A volume of 1 ml of the Lowry working solution was added to the standards and the cell extracts, vortex mixed and left for 10 minutes at room temperature. Following incubation, 100 μl of Folin-Ciocalteu reagent (freshly diluted 1:1 with distilled water) were added, vortex-mixed and left for a further 30 min. A total of 100 μl of each sample from the Eppendorf tubes was transferred to a 96-well microtitre plate and read the absorbance read at 750nm.

2.2.12: SDS-PAGE and electrotransfer of cell lysates

Lysed cell extracts with an equal protein concentration of 20-60 μg were diluted in an equal volume of x2 concentrated Laemmli electrophoresis sample buffer (10 % w/v SDS, 0.5 M Tris-HCl pH 6.8, 10 % v/v glycerol, 0.04 % w/v bromophenol blue and 10 % v/v β-mercaptoethanol and boiled for 5 min. Samples were then loaded in to

sample wells using gel loading tips. Proteins from cell extracts were separated on a 7.5 % or 10 % w/v polyacrylamide gel, the recipe for which can be seen in table 2.1, overlaid with a 4 % w/v polyacrylamide stacking gel (Laemmli, 1970). The samples were equally loaded on to the gel through electrophoresis running buffer (0.0256 M Tris base, 0.192 M glycine and 0.1 % w/v SDS).

The samples were electrophoresed in parallel with Bio-Rad precision blue pre-stained standards in a mini Protean 3 electrophoresis cell for 10 min at 50 V and then at 200 V until the dye front reached the bottom of the gel (which normally takes about 1 hour). The electrophoresed proteins were then transferred to a nitrocellulose membrane filter using the wet blotting procedure described by (Towbin *et al.*, 1979) with modifications, using a 'tank' buffer system. Following electrophoresis, the gel was immersed in continuous transfer buffer (CTB: 30 mM glycine, 48 mM Tris base, 0.1 % w/v SDS, 20 % v/v methanol in distilled water) to allow partial removal of SDS. Four pieces of blotting paper (3MM Whatman chromatography paper) per gel were soaked in continuous transfer buffer along with a sheet of nitrocellulose (pore size 0.45 mm) all were cut slightly larger than the gel itself. Two pieces of blotting paper were placed on the sponge at the bottom of the wet blotter cassette then the nitrocellulose membrane filter was placed on top of the blotting paper, followed by the gel. The sandwich was completed by a further two sheets of blotting paper and the blotter sponge. Each blotting cassette was carefully assembled to minimised air bubbles between the individual layers. The cassette was placed in the wet blotter tank (nitrocellulose facing towards the positive anode). The transfer was run overnight for approximately 16 hours at 30 V.

2.2.13: Staining of Western blots

The resultant blots were stained using 0.05 % w/v copper pthalocyanine in 12 mM HCl to ensure that the transfer was successful and that the protein loading was indeed equal. Blots showing unequal protein loading were discarded or the differences in protein concentration within the wells were corrected for by densitometric analysis of the bands. Unequal protein loading was standardised against the control by adding or subtracting the differences in absorbance obtained for each band. The nitrocellulose was then destained using 12 mM NaOH, followed by neutralisation in TBS.

Table 2.1 Formulation of SDS-PAGE minigels

Resolving gel (ml)	Volumes for polyacrylamide gel concentrations			
	7.5 %	10 %	12 %	15 %
40 % w/v Acrylamide stock	1.9	2.5	3.0	3.75
1.5 M Tris buffer, pH 8.8	2.5	2.5	2.5	2.5
10 % w/v SDS	100 µl	100 µl	100 µl	100 µl
Millipore water	5.5	4.9	4.4	3.65
TEMED	10 µl	10 µl	10 µl	10 µl
10 % w/v Ammonium persulphate (APS)	100 µl	100 µl	100 µl	100 µl

Formula for stacking gel (10 ml)

	Volume (ml)
40 % w/v Acrylamide stock	1
0.5 M Tris buffer, pH 6.8	2.5
10 % w/v SDS	0.1
Distilled water	6.4
TEMED	40 µl
10 % w/v APS	100 µl

2.2.14: Immunoprobing of nitrocellulose blots

Unoccupied protein binding sites were blocked in 3 % w/v Marvel in TBS (Marvel/TBS) for at least one hour at room temperature. After blocking, the blot was left overnight at 4 ^{o}C in the primary antibody diluted to the appropriate concentration in 3 % w/v BSA or Marvel/TBS. After incubation, any unbound antibody was removed by 6 x 10-minute washes in TBS/Tween (0.05 % Tween-20 in TBS). After washing, the blot was incubated at room temp for at least 2 hours with the appropriate alkaline phosphatase-conjugated secondary antibody, which was used at 1/1000 dilution in Marvel/TBS. The secondary antibody was removed by washing as for the primary antibody. Then the blots were incubated in the substrate buffer for at least 2 min before the addition of developer, containing 20 ml substrate buffer (1.5 M Tris pH 9.5), 33 µl 5-Bromo-4-chloro-3-indolyl-phosphate disodium salt (BCIP – 50 mg/ml in distilled water) and 44 µl nitro blue tetrazolium (NBT – 75 mg/ml in 70 % dimethyl formamide). Once the bands had developed on the probed blot, the reaction was stopped by submerging the blot in distilled water. The blot was then dried with filter paper and a digital image was recorded. With each use of a new antibody a non primary control blot was carried to ensure there was no binding of the secondary antibody to the electrotransfered proteins on the western blot.

Table 2.2 Antibodies

	Working Dilutions	
Antibody	Western blotting	immunofluorescence
Anti-total neurofilament heavy chain (N52)	1:1000	1:200
Anti-phosphorylated neurofilament heavy chain (RT97)	1:10	1:5
Anti-phosphorylated Neurofilament heavy chain (SMI 34)	1:1000	1:200
Anti-calpain 1 (C-20)	1:500	-
Anti-JNK (D-2)	1:500	-
Anti-phosphorylated JNK (G-7)	1:500	-
Anti-ERK	1:500	-
Anti-phosphorylated ERK	1:500	
Anti-phosphorylated serine (PSR-45)	1:500	
Anti-phosphorylated threonine (PTR-8)	1:500	
Anti-β- tubulin (Tub 2.1)	1:500	
Anti-total α-tubulin (B512)	1:1000	1:200
Anti-tyrosinated α-tubulin (T1A2)	1:1000	1:200
Anti-GRASP 65 protein		1:200

2.2.15: Immunofluorescence staining of cells

Antibody staining

Cells were seeded into chamber slides at a density of 50,000 cells per ml and differentiated for 24 hours as before. Cells were then fixed using ice cold 90 % v/v methanol in TBS for 10 minutes at -20 °C. After fixing the cells were rehydrated using TBS for 20 minutes and then blocked in 3 % w/v BSA in TBS overnight at -4 ^{0}C. After the blocking, the appropriate dilution of primary antibody (see table 2.2) was added and incubated overnight at -4 °C. All antibodies were diluted in 3 % w/v BSA or Marvel/TBS. Unbound primary antibody was removed by 3 x 15-minute washes with TBS/Tween using gentle agitation. The TRITC-conjugated secondary antibody was used at a dilution of 1/40 and was incubated for 2-3 hours at room temperature, in the dark. Unbound secondary antibody was removed as for the primary antibody. The slides were then dried and mounted using an anti-fade mountant. Once the cover slips were dry, the slides were viewed using a Leica CLSM confocal laser scanning microscope fitted with epifluorescence optics at a magnification of x 600. FITZ conjugated secondary antibodies were viewed at 488nm excitation and TRITZ conjugated at 532nm.

BODIPY dye staining

Cells were seeded into chamber slides at a density of 50,000 cells per ml and differentiated for 24 hours. Cells were then fixed using ice-cold 90 % v/v methanol for in TBS 10 min at -20 °C. After fixing the cells were rehydrated using TBS for 20 minutes and then blocked in 3 % w/v BSA in TBS overnight at 4 °C. BODIPY-thapsigargin was used at a concentration of 10 µM and BODIPY-ryanodine was used at 1 µM; both were diluted in 3 % w/v BSA in TBS. The BODIPY dye was applied after blocking and incubated with the fixed cells overnight at 4 °C. To prevent the fluorescence from fading, the slides were wrapped in foil at all times. The stain was removed by 3 x 15-minute washes with TBS/Tween, using gentle agitation. The slides were then dried and mounted using an anti-fade mountant. Once the cover slips were

dry, the slides were viewed at a magnification of x 600 using a Leica CLSM confocal laser scanning microscope fitted with epifluorescence optics at 488nm excitation.

2.2.16: Calpain Assay

N2a and C6 cells were seeded into T25 flasks as previously described and differentiated for 4 and 24 hours in the presence and absence of 0.1 and 1 µM thimerosal and methylmercury chloride as before. After the incubation, the medium was gently removed from the monolayer and replaced with the homogenisation buffer (20 mM Tris-HCl pH 7.2, 0.04 % v/v igepal, 2 mM EDTA pH 7.2 and 20 % v/v glycerol). The cells were gently removed using a cell scraper, transferred to an eppendorf and placed on ice. Cells were lysed by sonication, prior to the assay to release the contents. The calpain assay was carried out in black 96 well plate containing 30 µl of sample or 30 µl of homogenisation buffer for control wells, 10 µl of 50 mM CaCl, 40 µl of 120 mM imadizole buffer pH 7.3 and 20 µl substrate. The substrate was added to the wells immediately before the plate was placed in the machine. The assay was carried out over a period of 3 hours with readings obtained every 5 minutes. The fluorescence was read in a FLUOstar OPTIMA at 521nm.

3: Effects of heavy metals on cell growth and differentiation

Introduction

Assays to determine cell viability are a valuable research tool when studying the toxicity of various compounds. Previous researchers have used a variety of cell viability assays in order to determine the toxicity of heavy metals. Numerous cell viability assays exist such as the lactate dehydrogenase (LDH) assay, based upon the detection of the cytosolic enzyme lactate dehydrogenase (Mori *et al.*, 1995). The activity of the enzyme enables conclusions to be made about membrane integrity and thus cytotoxicity. The propidium iodide stain can be used as a marker of dead of dying cells, since it is unable to penetrate the membrane of living cells (Braekman *et al.*, 1997). With the CellTitre blue assay, the non fluorescent resazurin is reduced to resorufin by mitochondrial and cytosolic enzymes and is measured by spectrofluorometry (Bigl *et al.*, 2007). The MTT assay is based upon the cleavage of a yellow tetrazolium salt to purple formazan crystals which can then be read in a spectrophotometer by lysing the cells with DMSO (Edmondson *et al.*, 1988). Cleavage is thought to be carried out mainly by mitochondrial dehydrogenases. All these assays have their technical advantages and disadvantages and comparative experiments show that they may give slightly different results. A study by (Bigl *et al.*, 2007) looked at the LDH, CellTitre blue and MTT assay, all assays gave different toxicity results. This does not render these assays invalid as a research tool as long as the variable is controlled by the use of the same assay throughout the experiments. It does however make the comparison of research using different assays problematic. The MTT assay was used in this work as it is safer than the use of radioactive isotopes and gives less background. The MTT assay is also reproducible and the absorbance correlates strongly with cell number. It is also sensitive enough to detect low cell numbers. In addition the assay is also relatively quick and simple to carry out. The MTT assay has also been used by previous research groups to investigate the toxicity of heavy metals (Cookson *et al.*, 1995; Sanfeliu *et al.*, 2001; Crespo-López *et al.*, 2006).

Changes in cell morphology have been reported by numerous researchers in both neuronal and non-neuronal cells lines during exposure to heavy metals (Schwartz *et al.*, 2000; Bonacker *et al.*, 2004). The process of neurite formation in neuronal cells

is essential in axonal plasticity that accompanies normal development of the CNS (Andrieux *et al.*, 2002; Wall, 2005). Symptoms of neurological impairment seen with cases of poisoning with most heavy metals may in part by down to the effect on axon production, especially with developing children. Methods of looking at cell morphology mainly involve some form of microscopy with cell permeable stain or immunofluorescence.

Methods

The initial aim of the research was to study the effects of the chosen heavy metal compounds on viability, and to establish whether sub-lethal concentrations affected the morphology of N2a and C6 cells. This was achieved using the established methods of MTT reduction assays (Mosmann, 1983; Cookson *et al.*, 1995) and quantification of neurite outgrowth (Flaskos *et al.*, 1998; Sachana *et al.*, 2003). Cells were differentiated via serum withdrawal for 4, 24 and 48 hours for the viability assay in the presence and absence of 6 heavy metals as described in methods section. The concentrations of heavy metals used were 0.01, 0.1, 1, 10 and 100 µM, produced by serial dilution of a stock concentration of 10 mM. Each individual experiment was carried out in a 24 well plate containing the 4 wells of control cells and the range of heavy metal concentrations with 4 wells for each and each experiment was repeated 4 times (see Methods for a detailed description).

Due to the inability of the cell lines used to maintain neurite stability beyond 24 hours, the quantification of neurite outgrowth was measured at 4 and 24 hours. To compare early and late events that occurred with the exposure of the toxins. The cells were fixed using ice cold methanol and stained using Coomassie blue (see Methods). Quantification of neurite outgrowth used the same range of concentrations as the MTT assays in order to establish whether non-toxic concentrations had any effect upon neurite number. In N2a cells, axons were classed as processes over two cell body diameters in length. All processes of the qualifying length and over were counted and the numbers were normalised against the control cell numbers. In the case of C6 cells, all processes were counted and again normalised against the control cell number. Five fields per well were counted and there were 4 wells for each experimental condition. Each experiment was repeated at least 3 times. Data was expressed as % of control for each time point, which was calculated for each well,

then for each separate experiment. All data in this section are shown as mean ± SEM. The results were analysed statistically using 2 way ANOVA to compare differences in data sets followed by post hoc Bonferroni's correction for pair wise multiple comparisons. In the results n = x refers to the number of times the experiment was carried out using cells seeded on different days.

3.0: C6 and N2a cell morphology

Figure 3.0.1 shows typical images of healthy C6 (a) and N2a (b) cells differentiated for 24 hours with no heavy metals present in the media. The C6 cell line produces on average 2-4 processes of varying length per cell indicated by the blue arrows in image a. N2a cells (b) typically produce 2 to 5 processes. Not all of the processes produced by the N2a cells were counted; the shorter processes as indicated by the green arrow were not classed as axons and were excluded from the neurite counts.

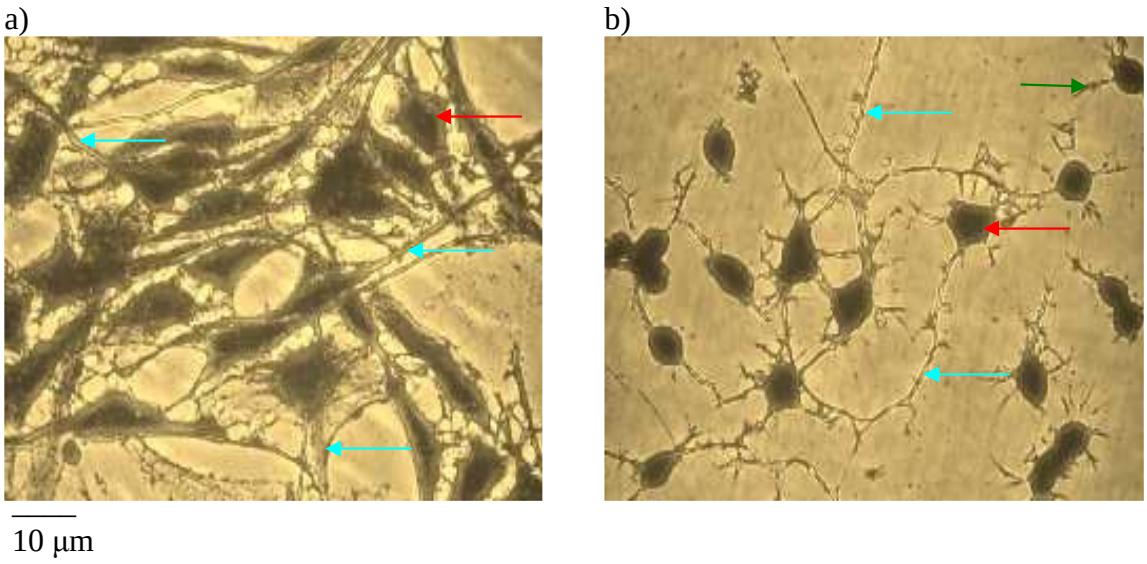

Figure 3.0.1: C6 and N2a control cell morphology

C6 (a) and N2a (b) cells were induced to differentiate for 24 hours as described in Methods. The cells were fixed and stained with Coomassie Brilliant Blue. Blue arrows indicate cellular processes and the red arrows point to the cell body. Images were taken at x 400 magnification.

3.1: The effect of zinc chloride on MTT reduction and neurite outgrowth

Zinc chloride up to 100 µM had no effect on the ability of either C6 or N2a cells to reduce MTT to a coloured product measurable by a spectrophotometer (Figure 3.1.1) when compared to the control, differentiated under the same conditions as the cells exposed to zinc chloride but in the absence of heavy metal. The data was normalised against the control value for the corresponding time points, with typical control absorbance between 0.708 and 0.932, absorbance readings for cells exposed to 1 µM zinc chloride ranged from 0.766 to 0.850. A 2 way ANOVA test confirmed that there were no significant differences in either the 4 or 24 hour data sets (p value 0.94). The presence of zinc chloride in 1 ml of DMSO alone did not alter the absorbance of the spectrophotometer from that of a DMSO blank.

Control cells differentiated for 4 and 24 hours (Figure 3.1.2 a & b) appear flattened as they are attached to the surface of the well with short processes. Treatment with up to 100 µM of zinc chloride for 4 and 24 hours did not cause any reduction in neurite number or changes in cell morphology. The images shown are representative of 5 separate experiments and reflect the effects seen in each.

Similarly exposure of C6 cells to up to 100 µM zinc chloride (Figure 3.1.3) caused no statistically significant alterations in neurite outgrowth at any concentration or time point. In untreated or control cells the number of neurites was between 19 and 30 per 100 cells and 16-18 in cells exposed to 100 µM zinc chloride. Statistics confirmed that there were no significant changes from the controls (p value 0.39). Statistical analysis of time differences was also insignificant the p value for the comparison of 4 and 24 hours was 0.75.

N2a cells differentiated in the absence of zinc chloride (Figure 3.1.4 a-b). The cells appeared round in shape with long axon-like processes extending outwards from the cell body. Treatment with 100 µM zinc chloride did not appear to cause any significant reduction in neurite number or changes in cell morphology. The images shown are representative of 4 separate experiments and reflect the effects seen in each.

a)

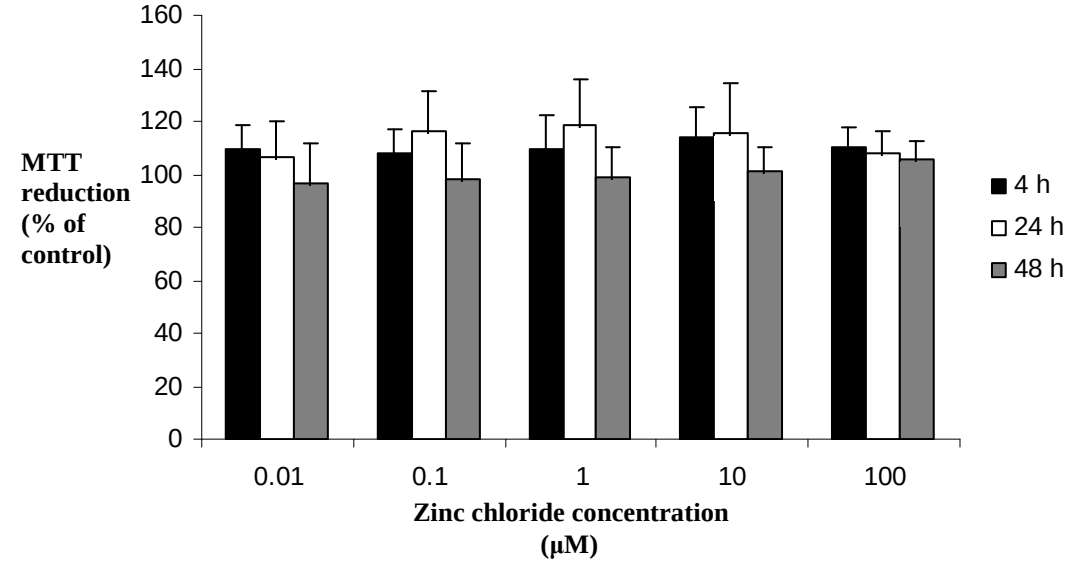

b)

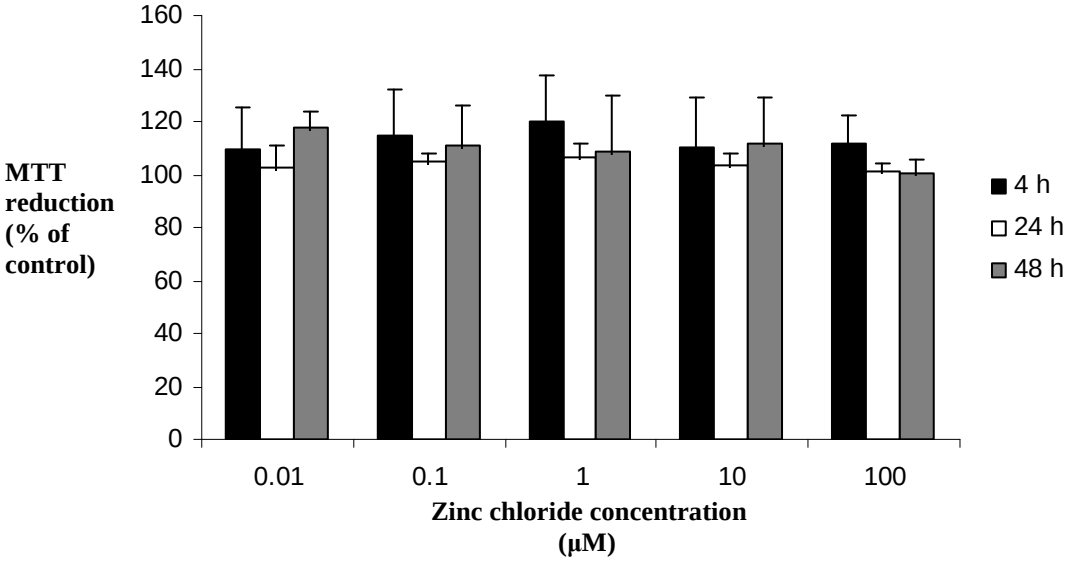

Figure 3.1.1: Effects of zinc chloride on MTT reduction in differentiating C6 and N2a cells

C6 (a) and N2a (b) cells were induced to differentiate for 4, 24 and 48 hours in the presence and absence of zinc chloride as described in Methods. The Data is expressed as mean percentage of the corresponding control $\pm$ SEM (n = 5). Data was analysed using a 2 way ANOVA.

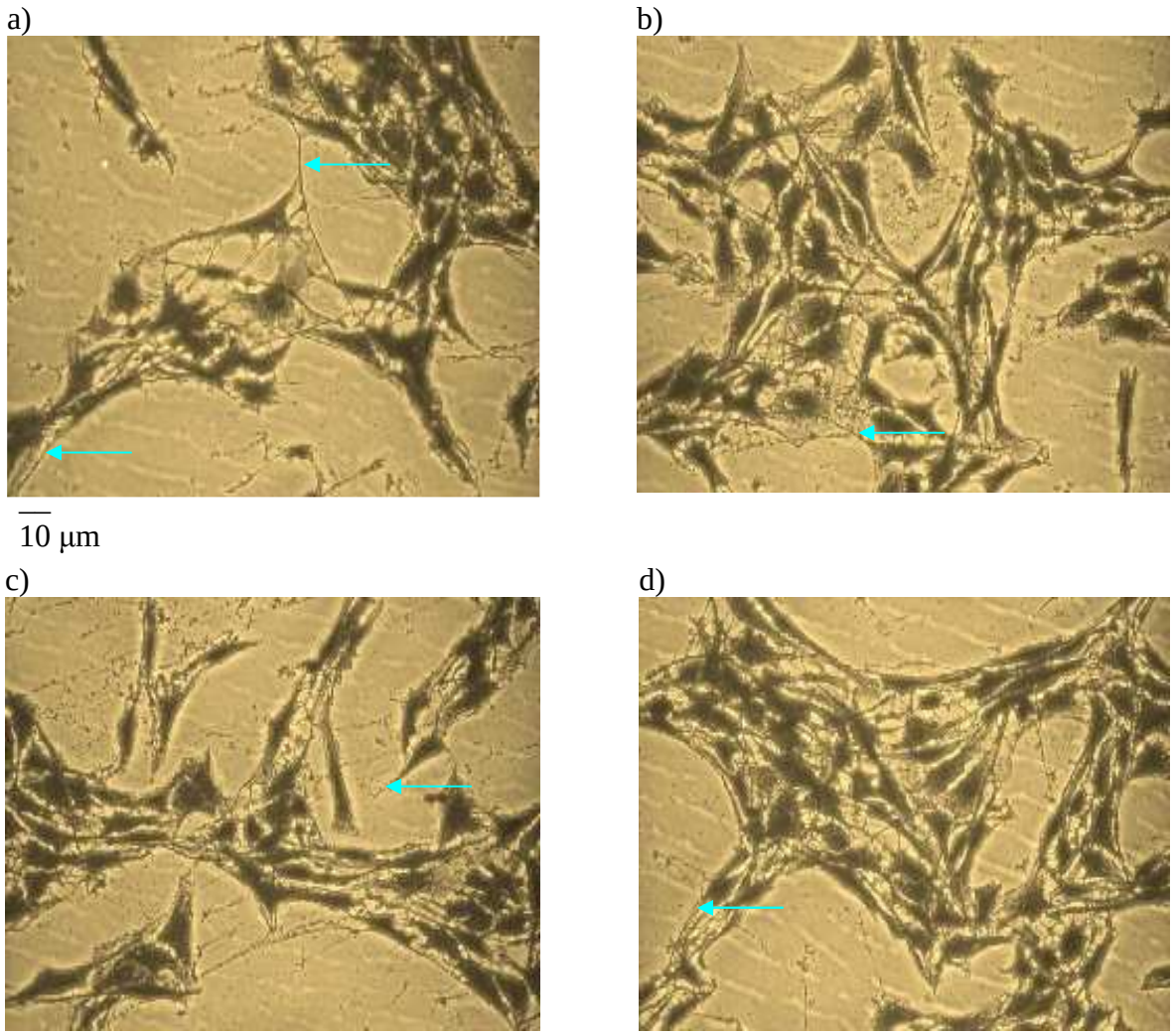

Figure 3.1.2: Effects of zinc chloride on differentiated C6 cell morphology

C6 cells were induced to differentiate for 4 (a, c) and 24 (b, d) hours in the presence (c, d) and absence (a, b) of zinc chloride. The cells were fixed and stained with Coomassie Brilliant Blue as described in Methods. Images of typical C6 cells were taken at x 200 magnification (n = 4).

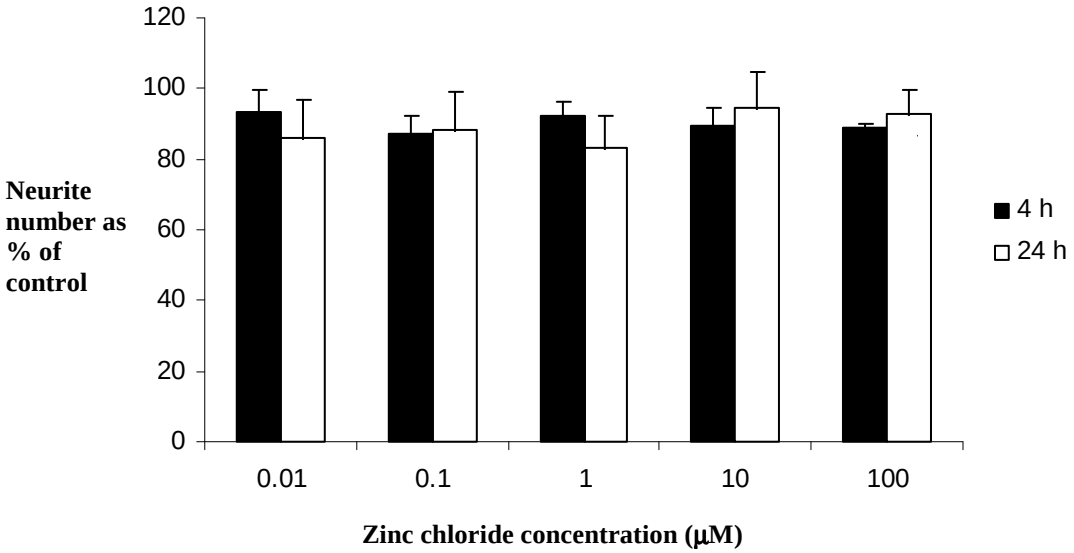

Figure 3.1.3: Effect of zinc chloride on neurite outgrowth in differentiated C6 cells

C6 cells were induced to differentiate for 4 and 24 hours in the presence and absence of zinc chloride as described in Methods. The Data represent is expressed as mean percentage of the corresponding control ± SEM (n = 5). Statistical analysis was carried out using 2 way ANOVA.

Zinc chloride up to 100 µM caused no statistically significant alterations in neurite outgrowth at any concentration or time point (Figure 3.1.3). Typical neurite numbers for control cells differentiated for 24 hours were between 21 and 37 per 100 cells. Exposure to 100 µM zinc chloride caused no significant change in neurite number with neurites produced numbering between 26 and 46 neurite per 100 cells. Statistical analysis of the different time points was also insignificant with a p value of 0.25 when comparing neurite number at 4 and 24 hours.

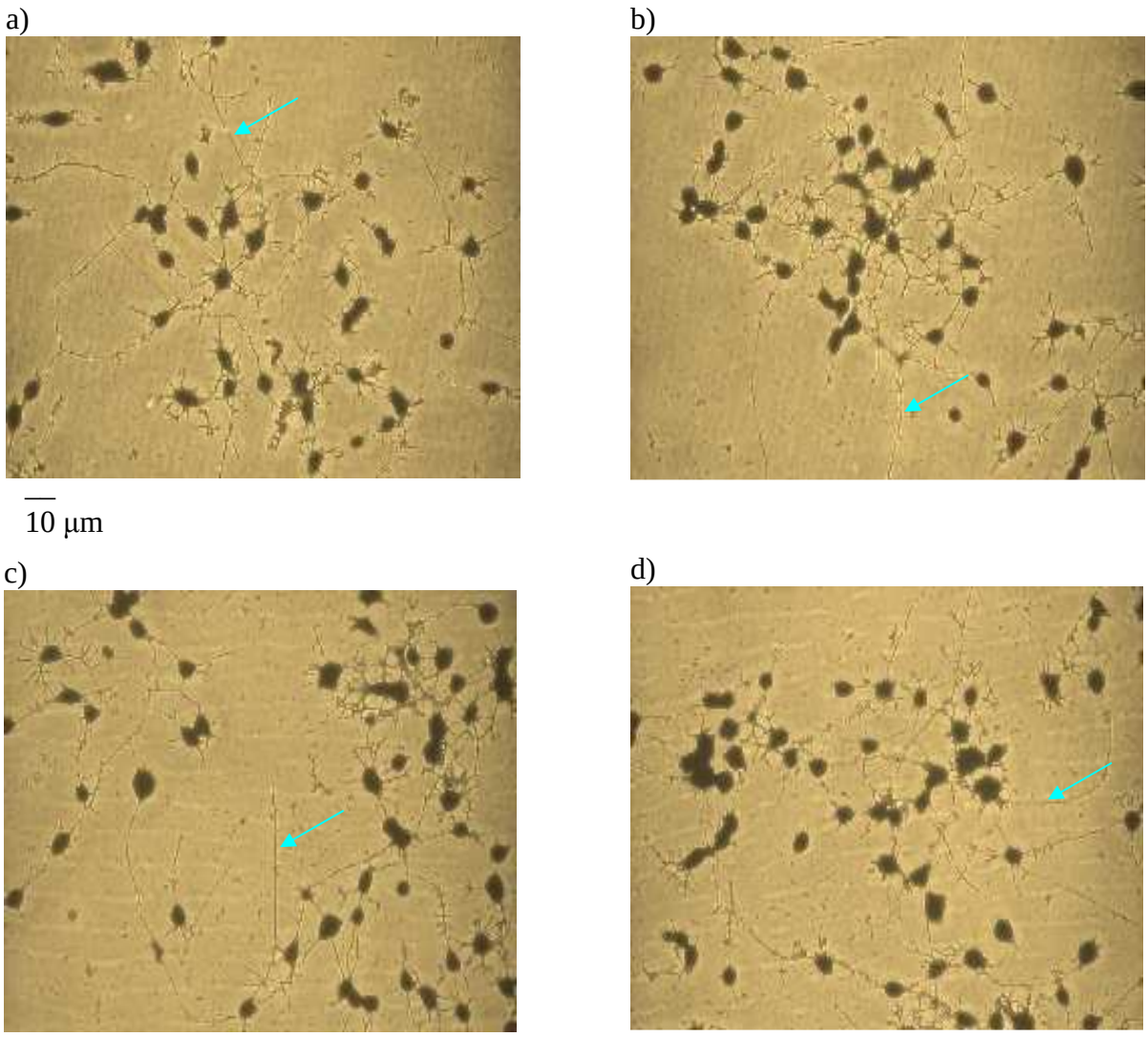

Figure 3.1.4: Effect of zinc chloride on differentiated N2a cell morphology

N2a cells were induced to differentiate for 4 (a, c) and 24 (b, d) hours in the presence(c, d) and absence (a, b) of zinc chloride. The cells were fixed and stained with Coomassie Brilliant Blue as described in Methods. Blue arrows indicate cellular processes. Images of typical N2a cells were taken at x 200 magnification (n = 4).

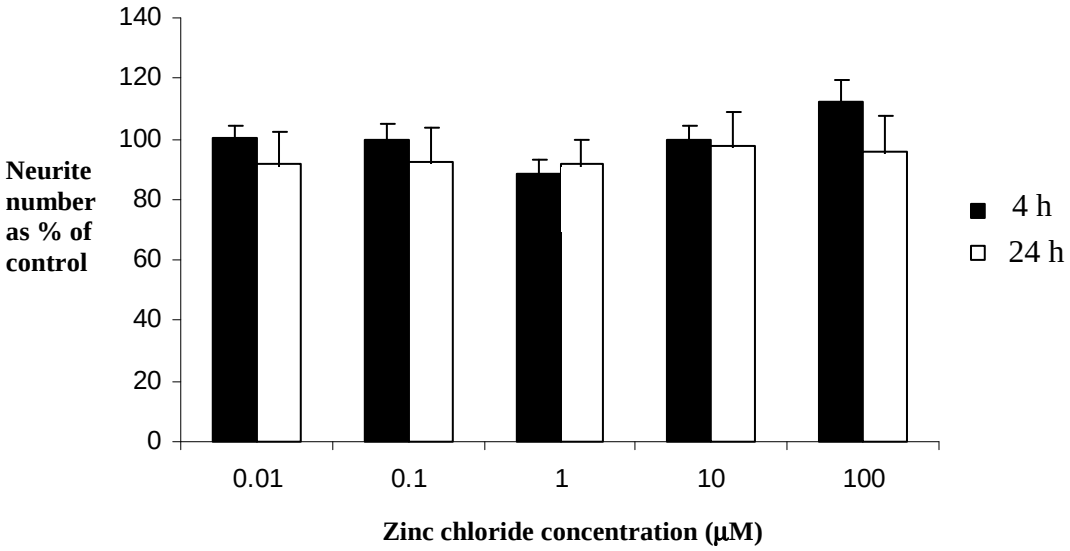

Figure 3.1.5: Effect of zinc chloride on neurite outgrowth in differentiated N2a cells.

N2a cells were induced to differentiate for 4 and 24 hours in the presence and absence of zinc chloride as described in Methods. The Data is expressed as mean percentage of the corresponding control ± SEM (n = 4). Statistical analysis was carried out using 2 way ANOVA.

3.2: The effect of lead chloride on MTT reduction and neurite outgrowth

Figure 3.2.1 shows the effect of lead chloride on the ability of C6 and N2a cells to reduce MTT. Data is expressed as % difference from corresponding control. The typical absorbance obtained for controls was between 0.574 and 0.967. Lead chloride caused a significant increase of around 35-65 % in MTT reduction at 100 µM in both C6 and N2a cells at all time points ($p<0.05$). Actual p values were between 0.03674 and 0.04571. Concentrations below 100 µM had no significant effect on MTT reduction. There was no significant difference between the values obtained for the different time points a comparison of the time points at gave a p value of 0.78. The presence of lead chloride in 1 ml of DMSO alone did not alter the absorbance of the spectrophotometer from that of a DMSO blank.

a)

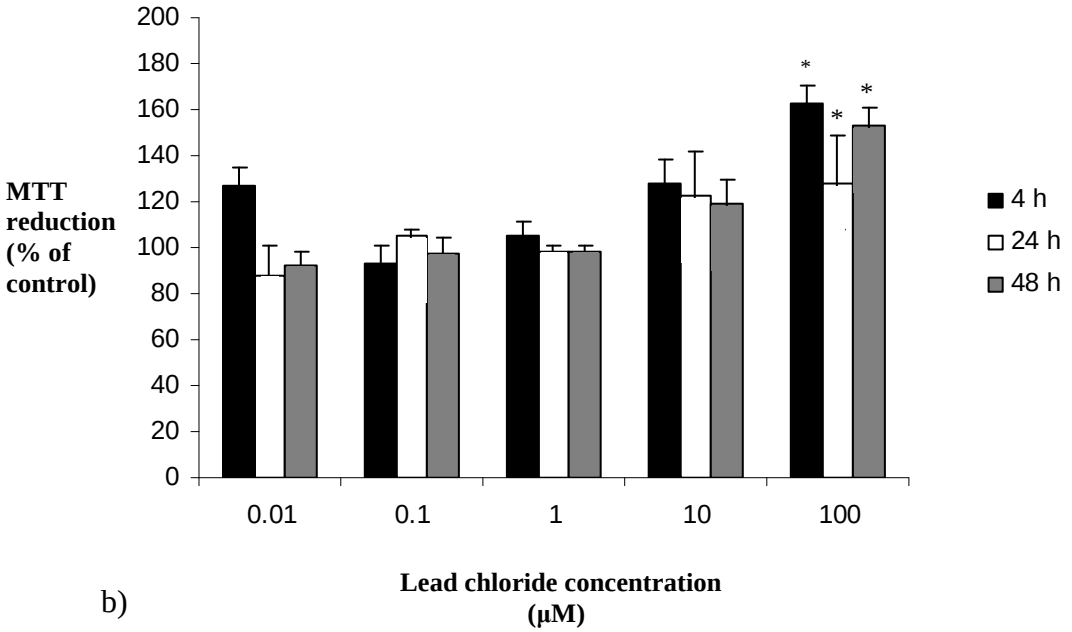

b)

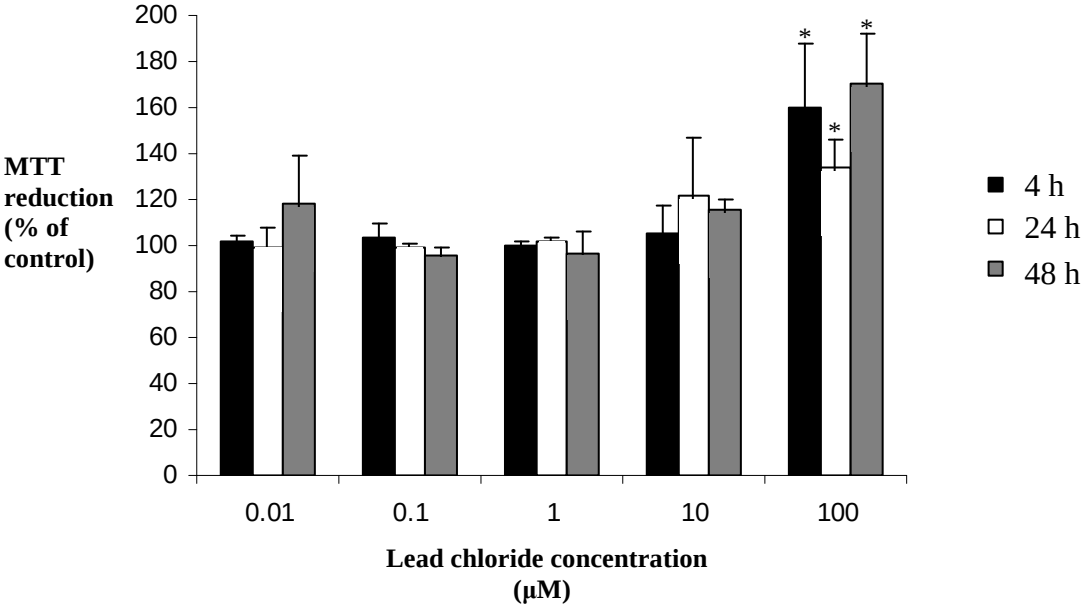

Figure 3.2.1: Effect of lead chloride on MTT reduction in differentiating C6 and N2a cells.

C6 (a) and N2a (b) cells were induced to differentiate for 4, 24 and 48 hours in the presence and absence of zinc chloride as described in Methods. The Data is expressed as mean percentage of the corresponding control $\pm$ SEM (n = 5). Data was analysed using a 2 way ANOVA. * indicates significant differences from the control, * $p < 0.5$, ** $p < 0.1$

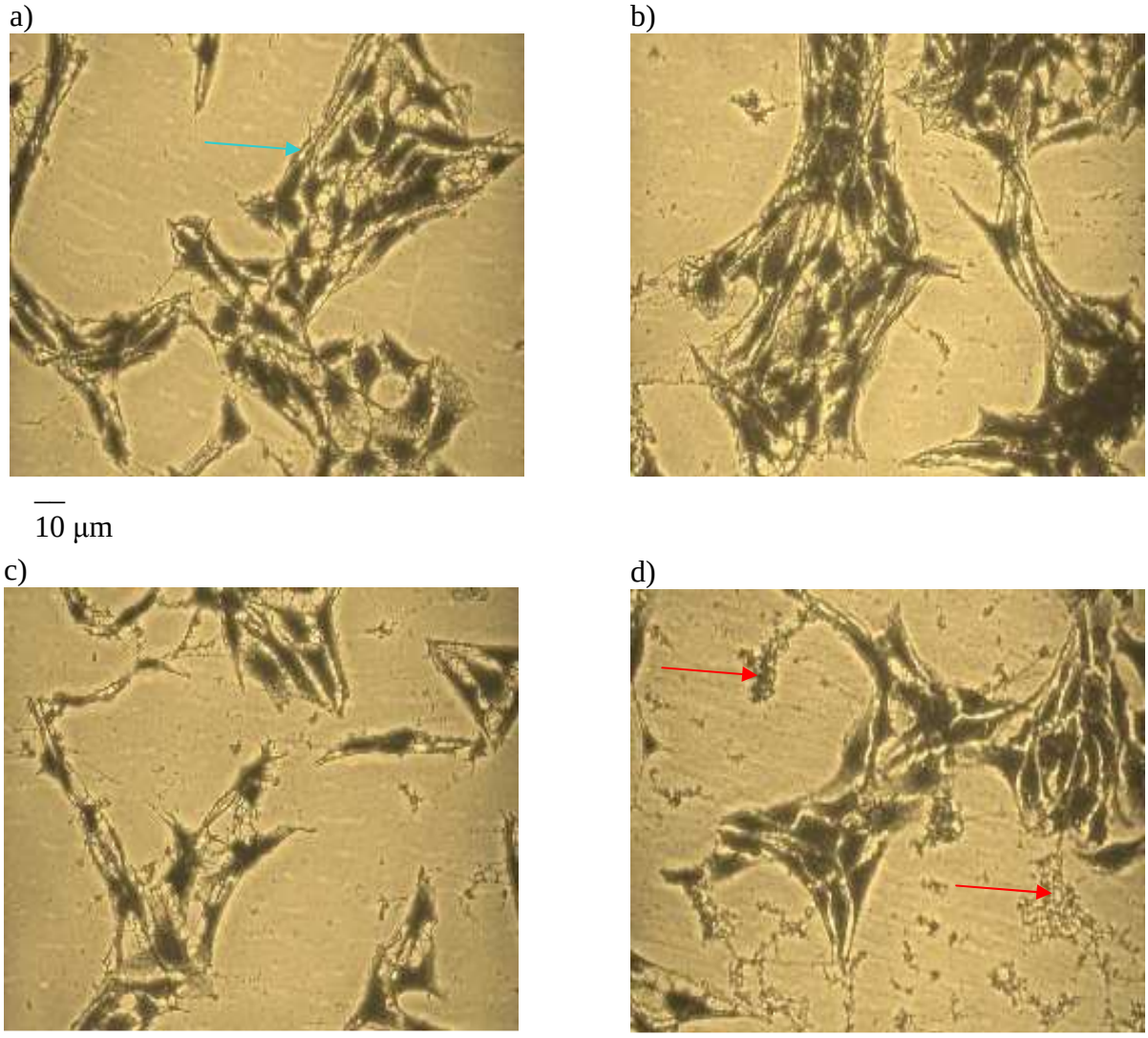

Figure 3.2.2: Effect of lead chloride on differentiated C6 cell morphology

C6 cells were induced to differentiate for 4 (a , c) and 24 (b, d) hours in the presence (c, d) and absence (a, b) of lead chloride. The cells were fixed and stained with Coomassie Brilliant Blue as described in Methods. Blue arrows indicate cellular processes. Images of typical C6 cells were taken at x 200 magnification (n = 4).

Control cells differentiated for 4 and 24 hours have formed numerous processes and have differentiated together in clusters (Figure 3.2.2 a-b). Exposure to 100 µM lead chloride did not appear to have reduced the number of processes formed between the cells when compared to the control cells of the 4 hour incubation time (Figure 3.2.2 c). In Figure 3.2.2 d the cells have been exposed to 100 µM lead chloride for 24 hours, it appeared that the numbers of processes were reduced when compared to the control. There was also evidence of cell debris (red arrows) that was not visible in Figures a-c.

The images are representative of 4 separate experiments and reflect the trends that were seen in each one.

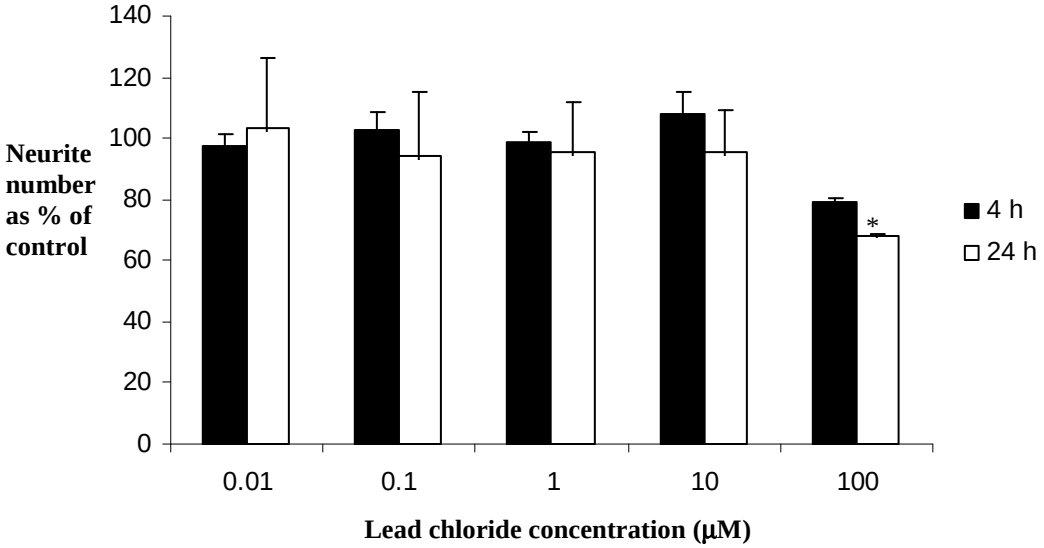

Figure 3.2.3: Effect of lead chloride on neurite outgrowth in C6 cells.

C6 cells were induced to differentiate for 4 and 24 hours in the presence and absence of lead chloride as described in Methods. The Data is expressed as mean percentage of the corresponding control $\pm$ SEM (n = 4). Statistical analysis was carried out using 2 way ANOVA. * indicates significant differences from the control, * $p < 0.5$, ** $p < 0.1$.

In Figure 3.2.3 neurite number is expressed as a percentage of the corresponding control which was calculated per well and then per experiment. Incubation with lead chloride had no significant effect ($p < 0.05$) on C6 cell morphology up to concentrations of 100 µM (Figure 3.2.2 c). Statistical analysis of the data obtained from cells exposed to 100 µM gave a p value of 0.73611. Typical neurite number in control cells were in the range of 13-34 processes per 100 cells. Exposure to 100 µM lead chloride for 24 hours caused a significant reduction of 25 % ($p = 0.03429$), with a corresponding range of neurite number of between 6 and 20 neurites per 100 cells. However there were no significant differences between 4 and 24 hours ($p = 0.09862$).

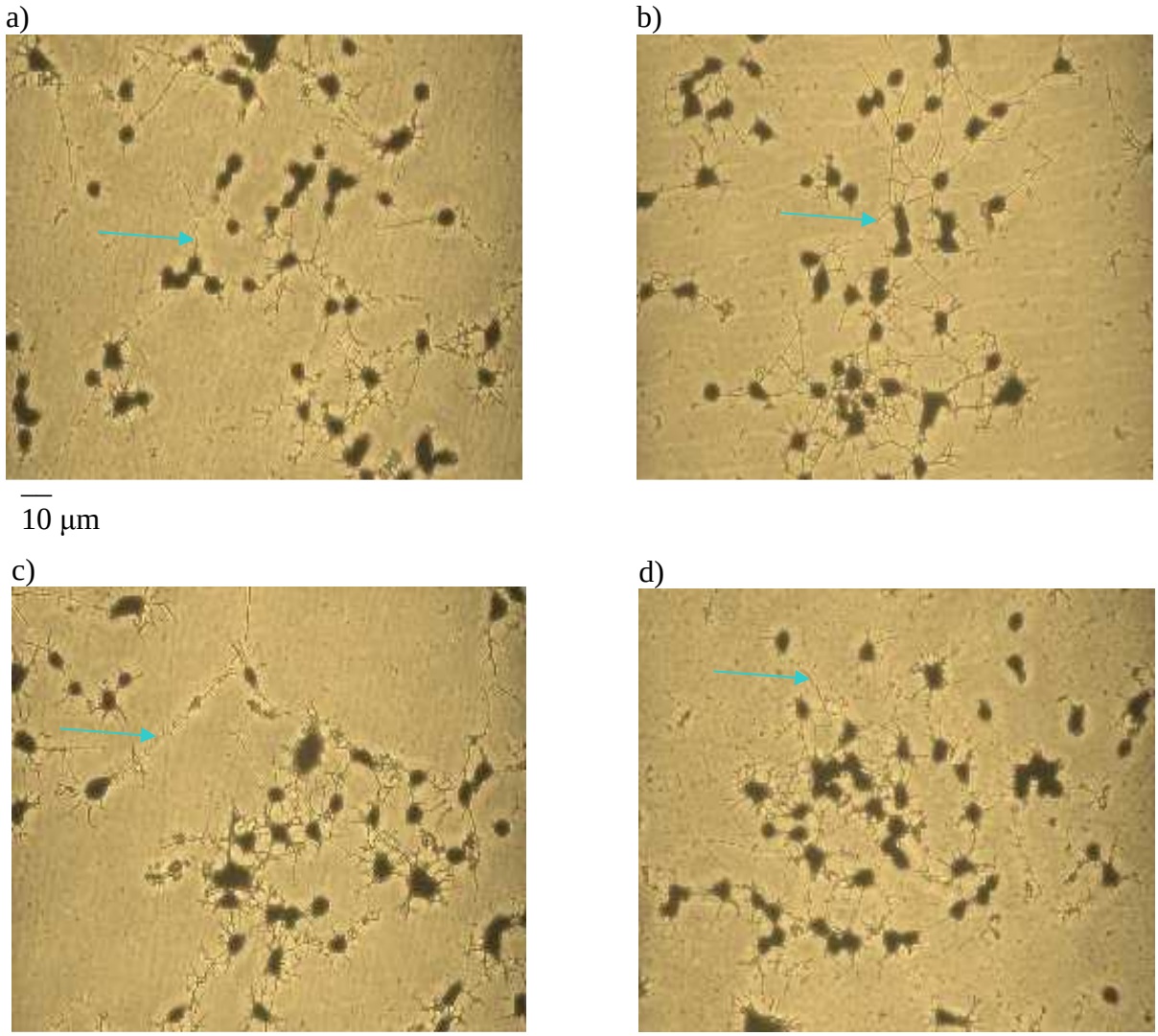

Figure 3.2.4: Effect of lead chloride on differentiated N2a cell morphology.

N2a cells were induced to differentiate for 4 (a , c) and 24 (b, d) hours in the presence (c, d) and absence (a, b) of lead chloride. The cells were fixed and stained with Coomassie Brilliant Blue as described in Methods. Blue arrows indicate cellular processes. Images of typical N2a cells were taken at x 200 magnification (n = 4).

Control cells differentiated for 4 and 24 hours in the absence of lead chloride were spherical in shape with long axon-like processes extending out from the cell body (Figure 3.2.4 a-b). The neurites were not continuous they had shorter branches along their length. When exposed to 100 µM lead chloride, the number of the neurites appeared reduced when compared to the control cells. There appeared to be no obvious changes in the morphology of the cell after toxin exposure. The images were

representative of 4 separate experiments and reflect the major trends seen in each separate one.

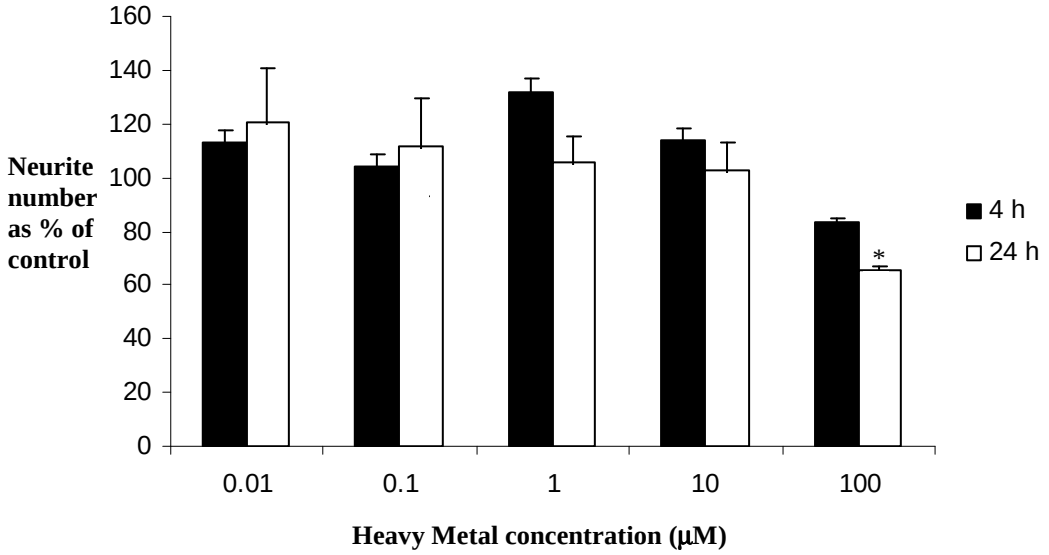

Figure 3.2.5: Effect of lead chloride on neurite outgrowth in N2a cells.

N2a cells were induced to differentiate for 4 and 24 hours in the presence and absence of lead chloride as described in Methods. The Data is expressed as mean percentage of the corresponding control ± SEM (n = 4). Statistical analysis was carried out using 2 way ANOVA. * indicates significant differences from the control, * $p < 0.5$, ** $p < 0.1$.

Neurite number in the control cells at 4 and 24 hours was between 16 and 28 neurites per 100 cells. When exposed to 100 µM lead chloride for 24 hours, axon number was reduced in N2a cells (Figure 3.2.5). Statistical analysis using a 2 way ANOVA and Bonferroni's post hoc test gave a p value of 0.023, confirming that there was a significant change from the control values. The actual number of neurites was between 10 and 17 neurites per 100 cells. There was a significant difference between the 4 and 24 hour time points ($p = 0.026$) but only in cells exposed to 100 µM lead chloride. After 4 hours of treatment, there were no statistically significant ($p<0.05$) events with concentrations of lead chloride up to 100 µM ($p = 0.78$).

3.3: The effect of cadmium chloride on MTT reduction and neurite outgrowth

The typical absorbance for the controls was 0.879. However, exposure to 10 and 100 µM for 4, 24 and 48 hours (Figure 3.3.1) caused a significant decrease in MTT reduction ($p<0.01$) in both C6 and N2a cells. Cadmium chloride, at concentrations below 10 µM for up to 48 hours had no effect on MTT reduction in either cell line. There were significant differences between the 4 and 24 hours data obtained from the exposure of the C6 cells to 10 and 100 µM cadmium chloride ($p = 0.013$ and 0.028 respectively). There were no significant time differences with N2a cells ($p = 0.67$). The presence of cadmium chloride in DMSO did not alter the absorbance from a DMSO blank in the spectrophotometer.

Control C6 cells differentiated for 4 and 24 hours respectively were flattened due to the attachment on the surface of the well. The cells differentiated in close proximity and appeared in clusters (Figure 3.3.2 a-b). When exposed to 1 µM cadmium chloride, processes formed by the cells appeared to be reduced when compared to the control cells of the same incubation time (Figure 3.3.2 c- d). Staining highlighted cell debris (red arrow) which was not evident in control cells (Figure 3.3.2 c). The images are representative of 4 separate experiments and reflect the trends seen in all experiments.

a)

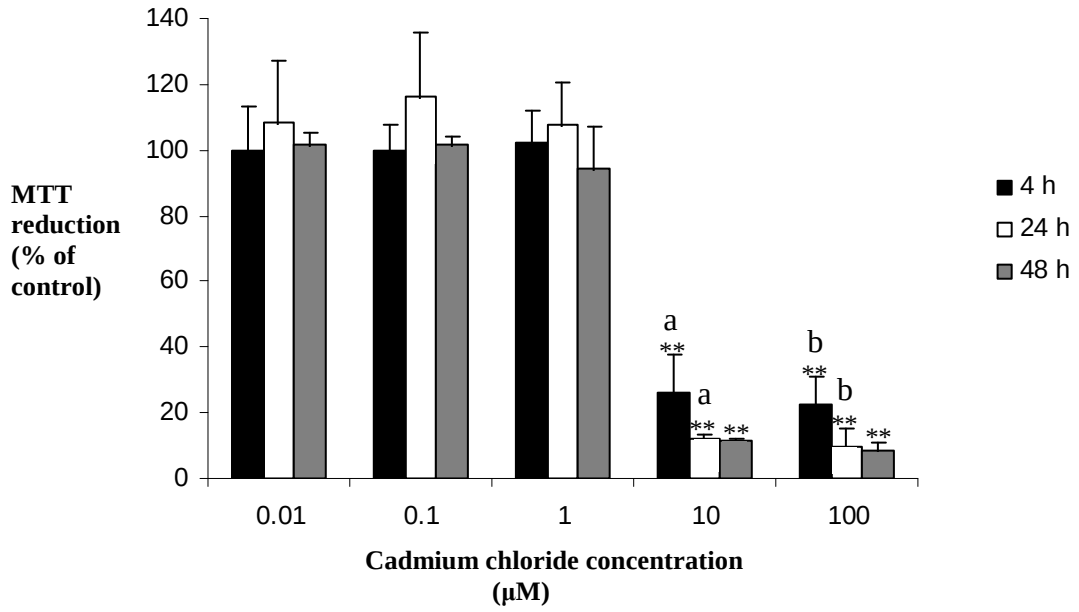

b)

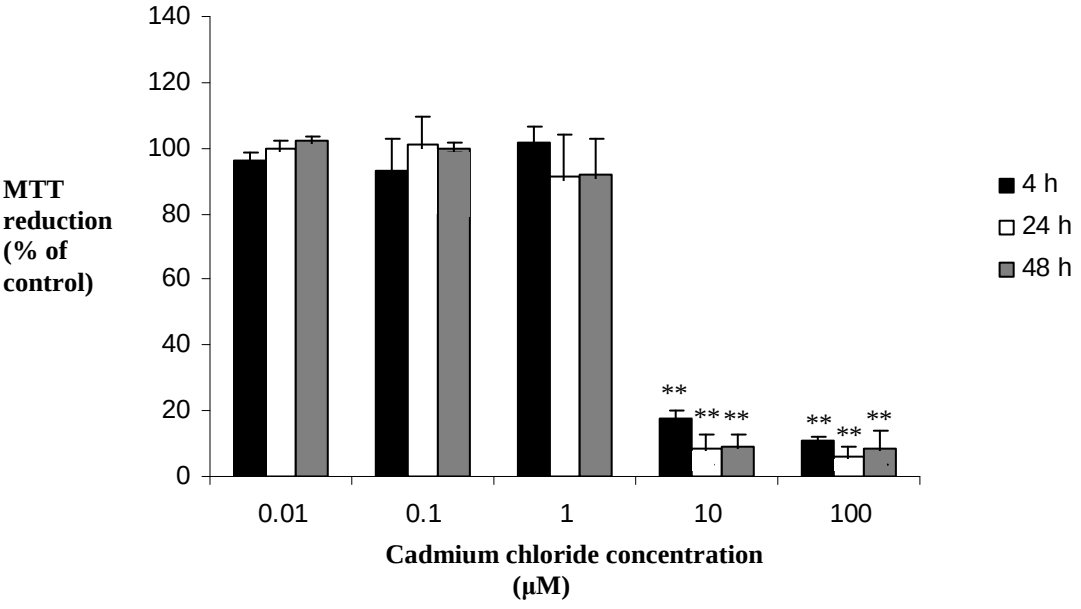

Figure 3.3.1: Effect of cadmium chloride on MTT reduction in differentiating C6 and N2a cells

C6 (a) and N2a (b) cells were induced to differentiate for 4, 24 and 48 hours in the presence and absence of zinc chloride as described in Methods. The Data is expressed as mean percentage of the corresponding control $\pm$ SEM (n = 5). Data was analysed using a 2 way ANOVA. * indicates significant differences from the control, * $p < 0.5$, ** $p < 0.1$.

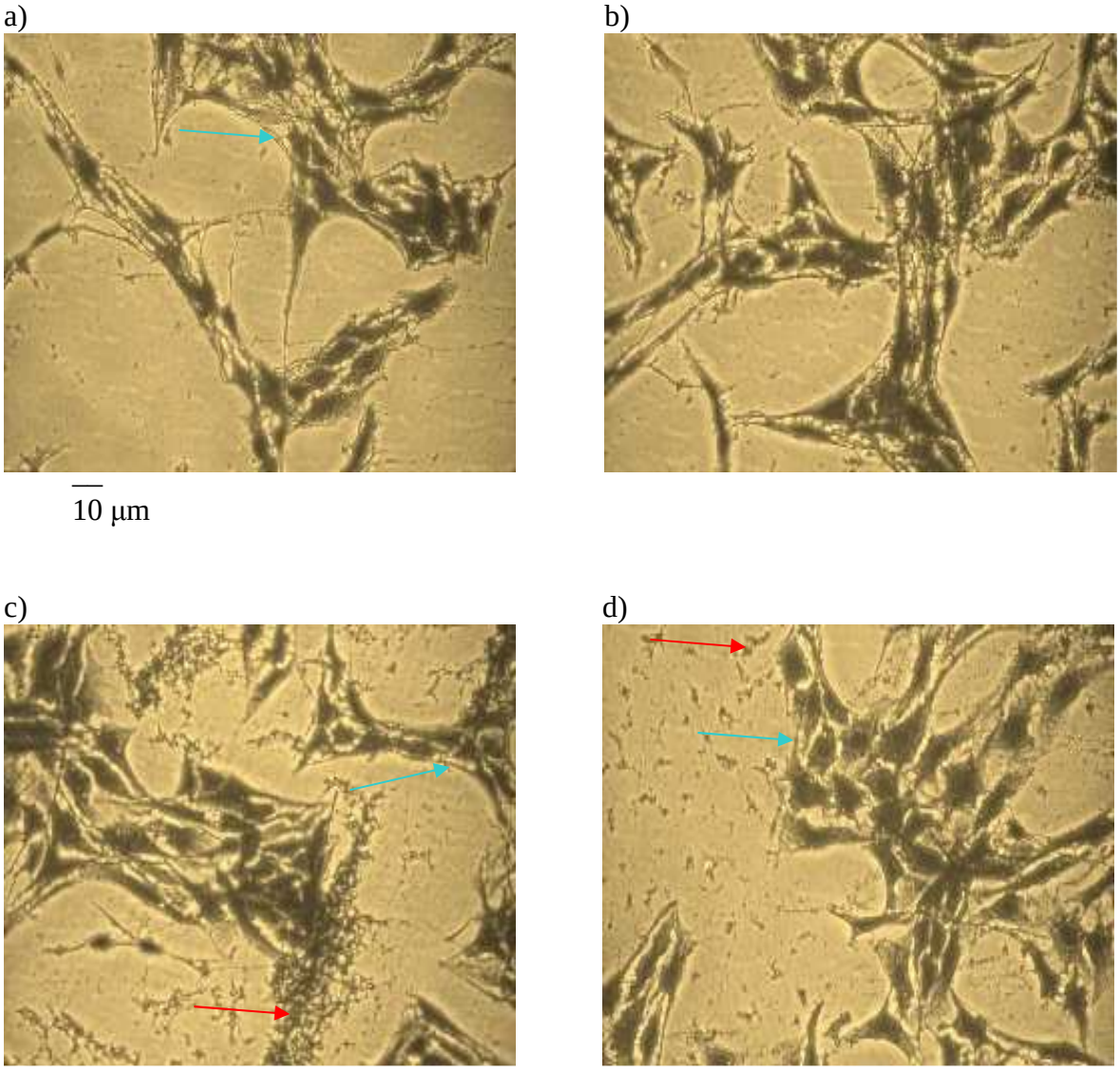

Figure 3.3.2: Effect of cadmium chloride on differentiated C6 cell morphology

C6 cells were induced to differentiate for 4 (a , c) and 24 (b, d) hours in the presence (c, d) and absence (a, b) of cadmium chloride. The cells were fixed and stained with Coomassie Brilliant Blue as described in Methods. Blue arrows indicate cellular processes. Images of typical C6 cells were taken at x 200 magnification (n = 4).

Exposure to cadmium chloride caused a concentration and time dependent reduction in neurite outgrowth in C6 cells (Figure 3.3.3). The average number of neurites for the control cells was 26 after 4 hours of differentiation and 31 after 24 hours. Concentrations of cadmium chloride below 1 µM had no significant effect on neurite number when compared to the control (p = 0.0456-0.97). Exposure to 1 µM cadmium chloride caused a 25 % - 55 % reduction in neurite number at 4 and 24 hours (p =

0.032 and 0.005 respectively). The higher concentrations of 10 and 100 µM reduced the number of neurites by 55-90 % at both time points. Analysis of the data using a 2 way ANOVA test and post hoc test confirmed statistical significance; p values were between 0.0001 and 0.008. The 2 way ANOVA test also highlighted significant difference between the different time points; post hoc Bonferroni's test confirmed that there were significant differences with exposure to 1-100 µM cadmium chloride ($p = 0.034$ for a comparison of the 10 µM data).

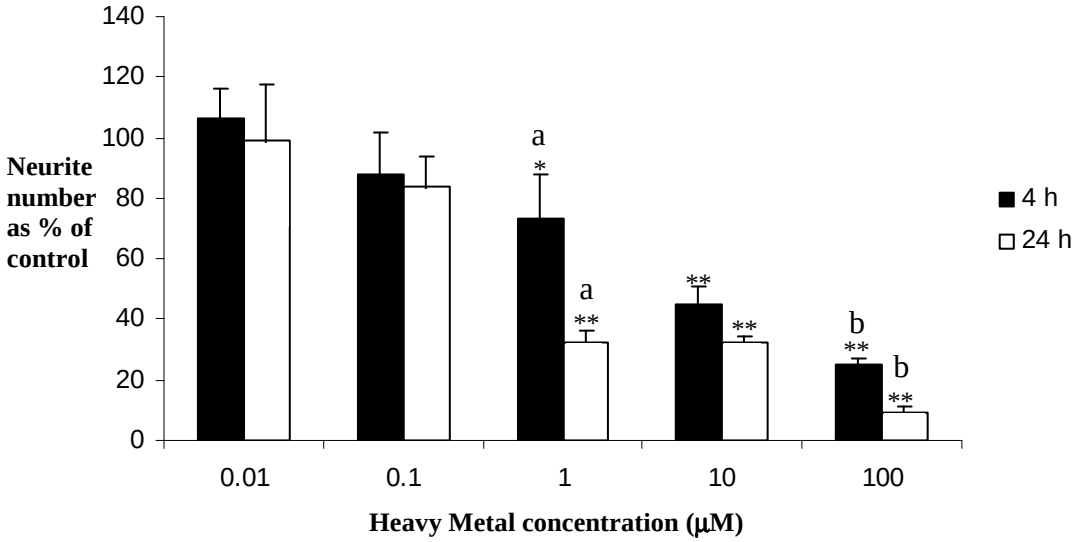

Figure 3.3.3: Effect of cadmium chloride on neurite outgrowth in C6 cells.

C6 cells were induced to differentiate for 4 and 24 hours in the presence and absence of cadmium chloride as described in Methods. The Data is expressed as mean percentage of the corresponding control ± SEM (n = 4). Statistical analysis was carried out using 2 way ANOVA. * indicates significant differences from the control, * $p < 0.5$, ** $p < 0.1$, a and b indicates significant differences between the 4 and 24 hour time points.

Control cells differentiated for 4 and 24 hours in the absence of cadmium chloride were spherical in shape with long axon-like processes extending out from the cell body (Figure 3.3.4 a- b). When exposed to 0.1 µM cadmium chloride the number of the axons appeared reduced when compared to the control cells (Figure 3.3.4 c-d). The images are representative of 4 separate experiments and reflect the trends seen in each one.

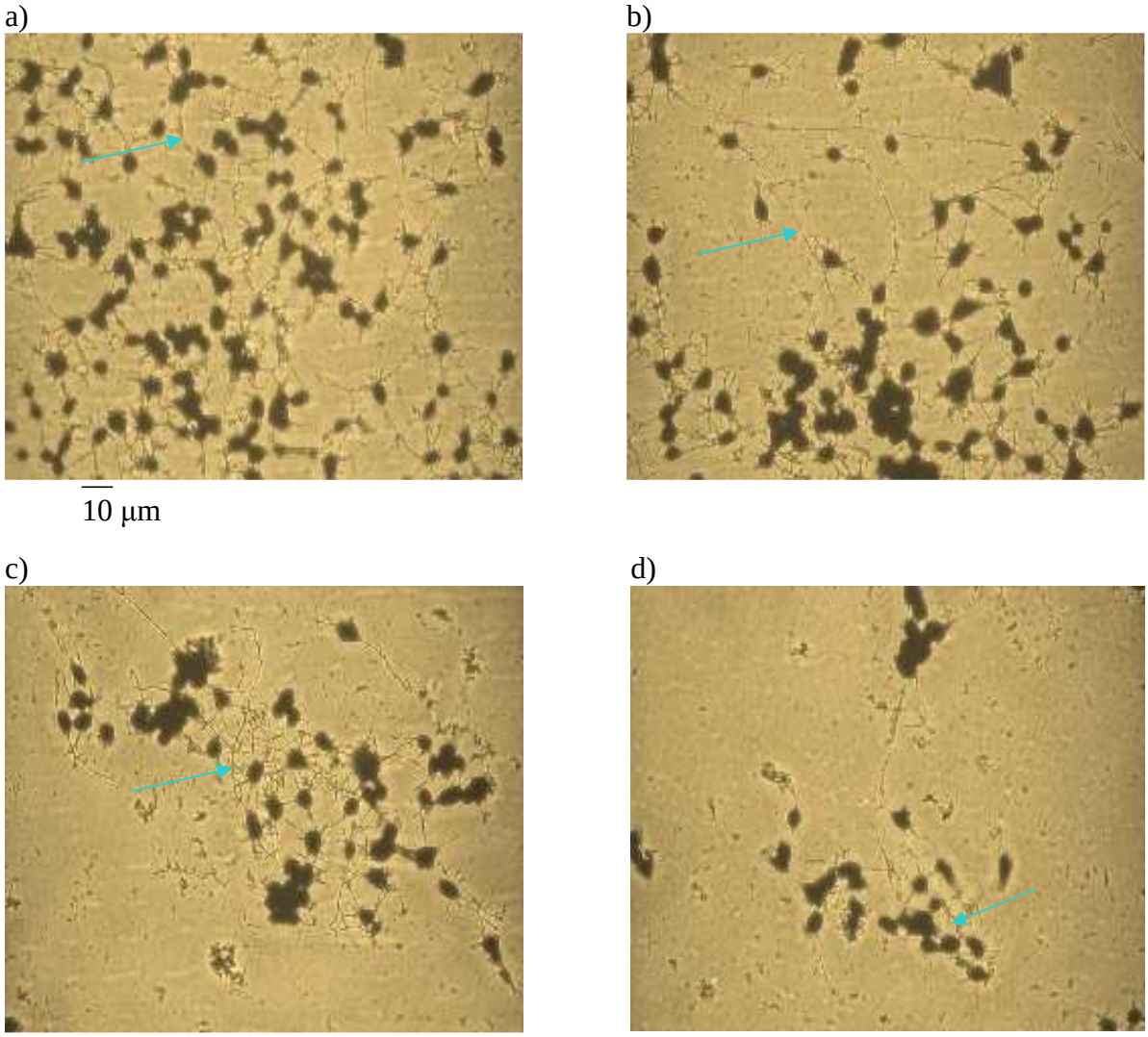

Figure 3.3.4: Effect of cadmium chloride on differentiated N2a cell morphology

N2a cells were induced to differentiate for 4 (a , c) and 24 (b, d) hours in the presence (c, d) and absence (a, b) of cadmium chloride. The cells were fixed and stained with Coomassie Brilliant Blue as described in Methods. Blue arrows indicate cellular processes. Images of typical N2a cells were taken at x 200 magnification (n = 4).

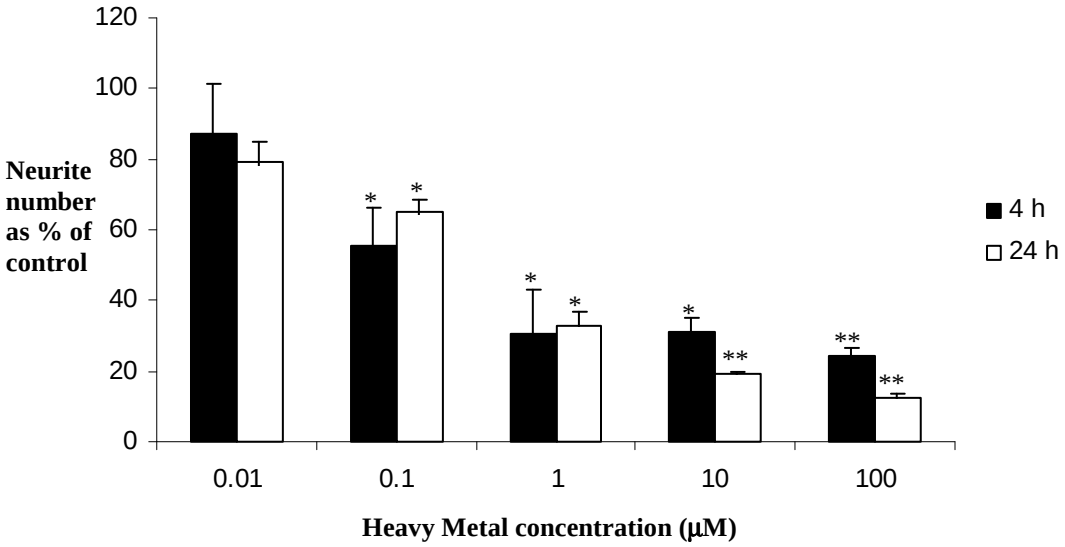

Figure 3.3.5: Effect of cadmium chloride on neurite outgrowth in N2a cells.

N2a cells were induced to differentiate for 4 and 24 hours in the presence and absence of cadmium chloride as described in Methods. The Data is expressed as mean percentage of the corresponding control $\pm$ SEM (n = 4). Statistical analysis was carried out using 2 way ANOVA. * indicates significant differences from the control, * $p < 0.5$, ** $p < 0.1$.

Incubation with cadmium chloride caused a concentration dependent reduction in axon outgrowth in N2a cells (Figure 3.3.5). The average number of neurites for the controls cells was 17 after 4 hours of differentiation and 26 after 24 hours. The lowest concentration that had a statistically significant effect ($p<0.05$) on neurite number was 0.1 µM. After 4 and 24 hours exposure 0.1 µM cadmium chloride caused approximately a 38-40 % decrease in neurite number ($p = 0.072$ and 0.055 respectively). Exposure to 1 µM cadmium chloride caused a 68-70 % decrease ($p = 0.044$ and 0.047 for 4 and 24 hours). Treatment with 10 µM, cadmium chloride reduced neurite outgrowth by 70 – 80 % at 4 and 24 hours ($p = 0.00031$ and 0.00056 respectively). Concentrations of 100 µM cadmium chloride caused a 74-88 % reduction at 4 hours and 24 hours. Concentrations of cadmium chloride below 0.1 µM had no significant effect on N2a morphology ($p = 0.91$). A comparison of the two time points showed that the data obtained at 10 and 100 µM was significantly different ($p = 0.049$).

3.4: The effect of mercury chloride on MTT reduction and neurite outgrowth

There was a significant decrease in MTT reduction of around 55-67 % with exposure to 10 µM mercury chloride ($p = 0.034$, 0.046 and 0.019 for the 4, 24 and 48 hour time points respectively) and 70-85 % with exposure to 100 µM in C6 cells at 4, 24 and 48 hours (Figure 3.4.1 a). Concentrations below 10 µM had no effect on MTT reduction ($p = 0.45$, 0.78 and 0.43 for the 1 µM concentrations of mercury chloride at the 4, 24 and 48 time points). The average absorbance for the C6 control wells was 0.354 and for the N2a 0.475. In N2a cells (Figure 3.4.1 b), MTT reduction was significantly decreased by 43-55 % with exposure to 10 µM ($p = 0.046$, 0.033 and 0.022 for the 4, 24 and 48 hours respectively). Exposure to 100 µM mercury chloride significantly decreased MTT reduction by 57-75 %. A 2 way ANOVA test highlighted significant differences between the 4 and 24 hour time points in both cell lines with a p value of 0.045 at 100 µM in N2a cells and 0.030 in C6 cells. The presence of mercury chloride alone in DMSO did not alter the absorbance from a DMSO blank.

C6 cells differentiated for 4 and 24 hours without the presence of mercury chloride appeared flattened due to attachment to the well and differentiated in close proximity to each other (Figure 3.4.2 a – b). Cells treated with 10 µM mercury chloride for 4 and 24 hours (Figure 3.4.2 c-d) appeared similar morphologically to the control cells but with less processes. In Figure 3.4.2 c there appears to cell debris that is not evident in the images showing the control cells.

a)

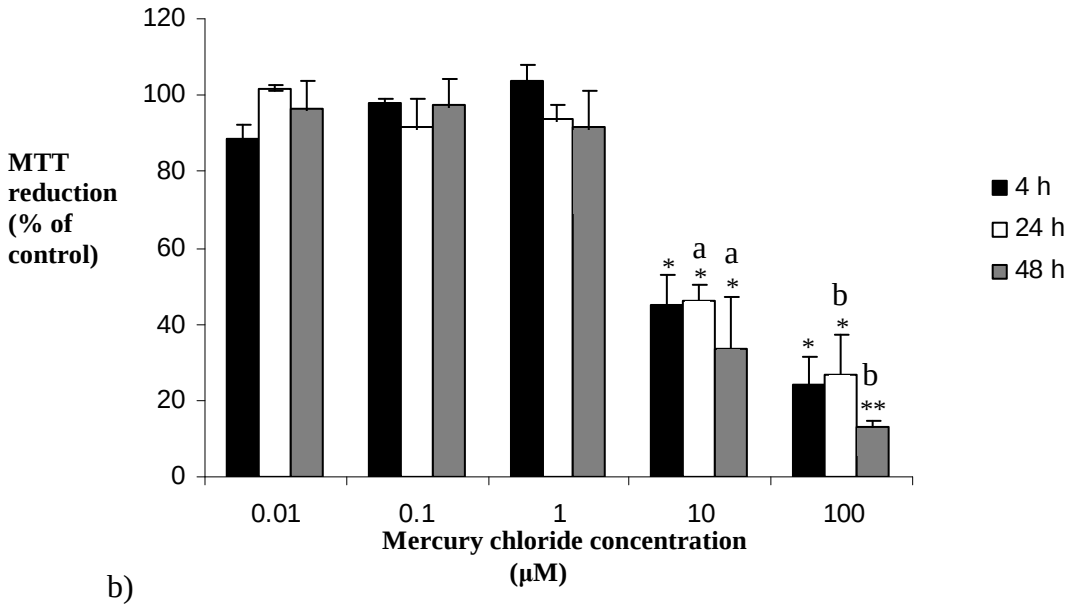

b)

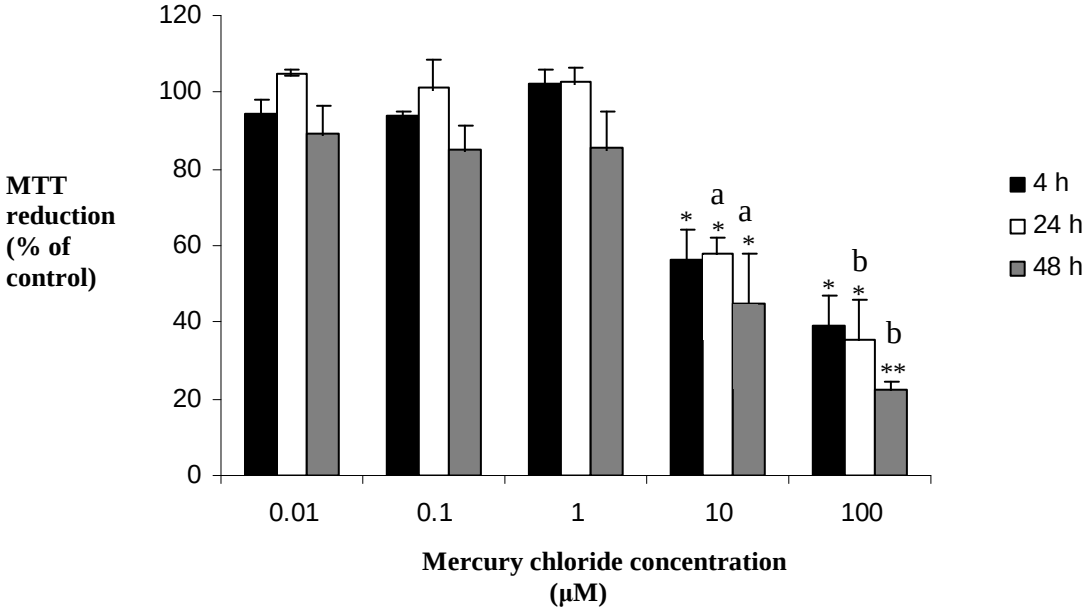

Figure 3.4.1: Effect of mercury chloride on MTT reduction in differentiating C6 and N2a cells

C6 (a) and N2a (b) cells were induced to differentiate for 4, 24 and 48 hours in the presence and absence of zinc chloride as described in Methods. The Data is expressed as mean percentage of the corresponding control $\pm$ SEM (n = 5). Data was analysed using a 2 way ANOVA. * indicates significant differences from the control, * $p < 0.5$, ** $p < 0.1$, a and b indicates significant differences between the time points.

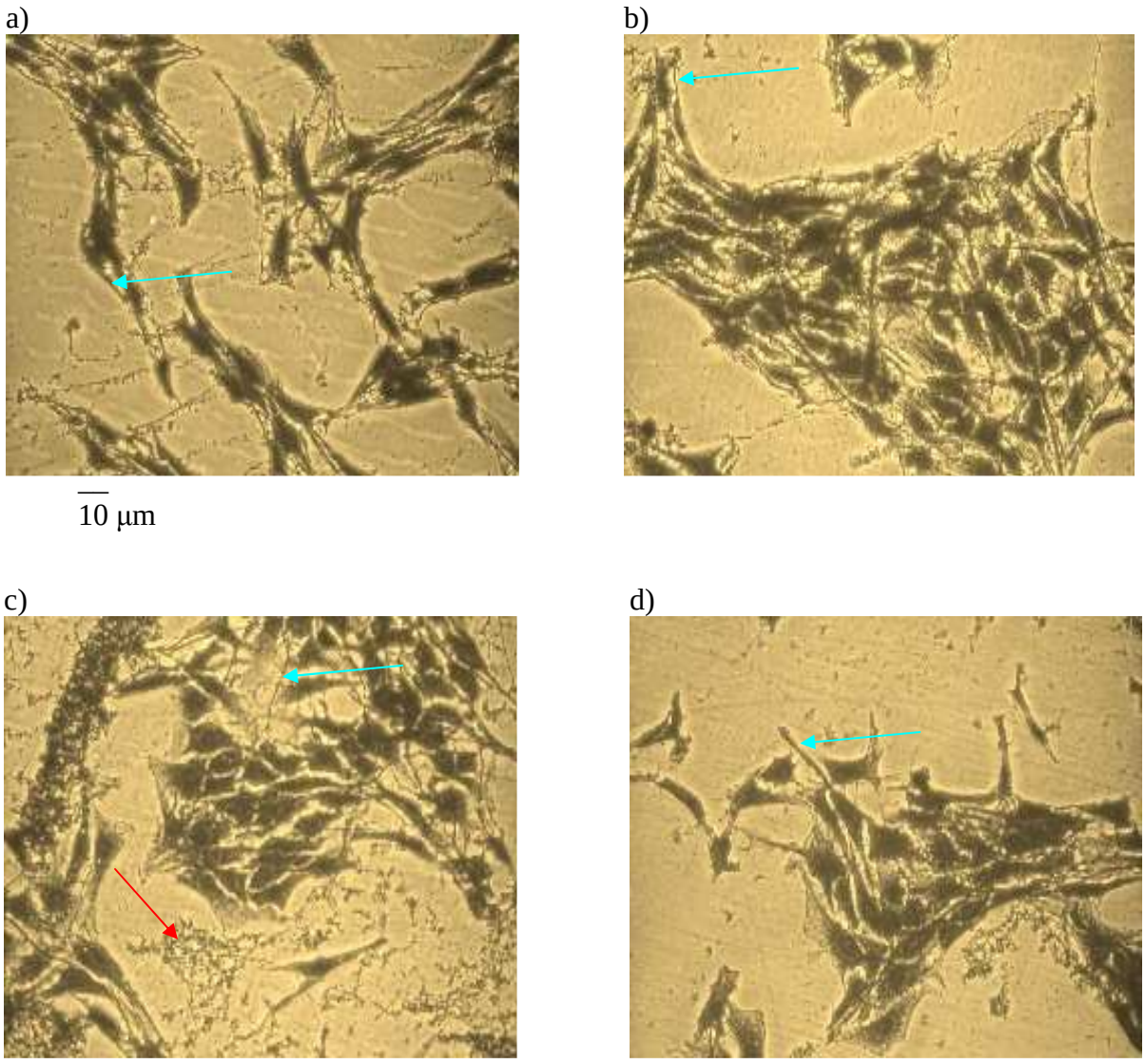

Figure 3.4.2: Effect of mercury chloride on differentiated C6 cell morphology

C6 cells were induced to differentiate for 4 (a, c) and 24 (b, d) hours in the presence (c, d) and absence (a, b) of mercury chloride. The cells were fixed and stained with Coomassie Brilliant Blue as described in Methods. Blue arrows indicate cellular processes. Images of typical C6 cells were taken at x 200 magnification (n = 4).

a)

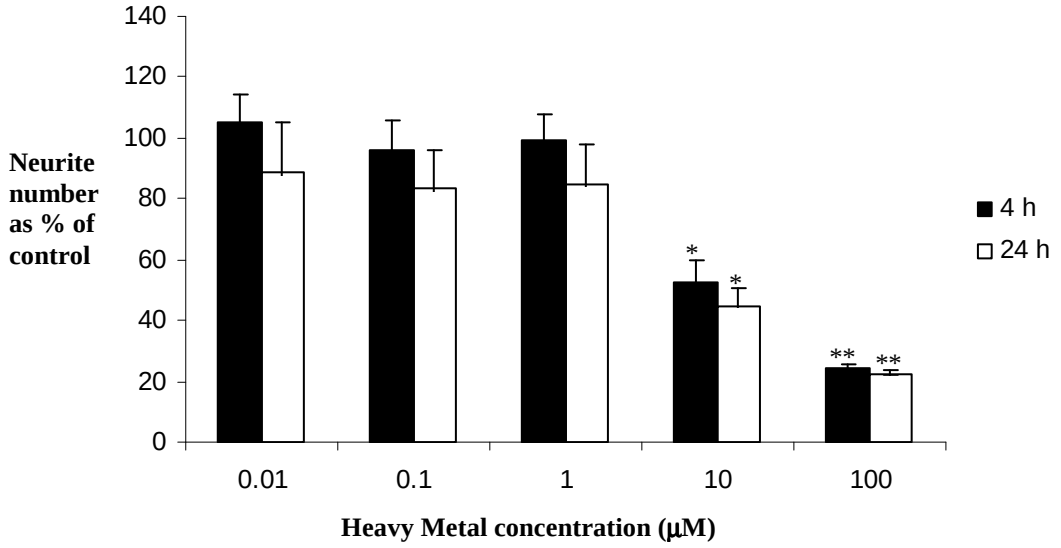

Figure 3.4.3: Effect of mercury chloride on neurite outgrowth in C6 cells.

C6 cells were induced to differentiate for 4 and 24 hours in the presence and absence of mercury chloride as described in Methods. The Data is expressed as mean percentage of the corresponding control $\pm$ SEM (n = 4). Statistical analysis was carried out using 2 way ANOVA. * indicates significant differences from the control, * $p < 0.5$, ** $p < 0.1$.

Exposure to mercury chloride induced a statistically significant ($p<0.05$) reduction in neurite number in C6 cells at concentrations of 10 µM and above (Figure 3.4.3). The actual numbers of neurite ranged between 12 and 23 per 100 cells in control cells and in cells treated with 10 µM mercury chloride the numbers were reduced to the range of 5 to 12 neurites per 100 cells. Incubation with 10 µM mercury chloride caused a reduction in neurite number of approximately 55 % after 4 hours ($p = 0.042$) and 49 % after 24 hours ($p = 0.022$). Exposure to 100 µM mercury chloride significantly reduced neurite outgrowth by around 25 % at 4 and 24 hours. Statistical analysis confirmed that concentrations of 0.01, 0.1 and 1 µM mercury chloride had no significant effect on neurite outgrowth after either 4 or 24 hours exposure time ($p = 0.98$ and 0.56 for the 4 and 24 hour incubation with 1 µM). The 2 way ANOVA test also confirmed that there were no significant differences between the 2 time points at any concentration ($p = 0.33$ for a comparison of 100 µM).

N2a cells differentiated for 4 and 24 hours in the absence of mercury chloride were spherical in shape with long neurites extending out from the cell body (Figure 3.4.4 a - b). When exposed to 10 µM mercury chloride (Figure 3.1.19 c - d), the number of the long (axon-like) neurites appeared reduced when compared to the control cells.

Exposure of N2a cells to mercury chloride induced a statistically significant ($p<0.05$) reduction in neurite number at concentrations of 10 µM and above (Figure 3.4.5). The average numbers of neurites in control cells was 23 neurites per 100 cells. Exposure to 10 µM mercury chloride caused a reduction in neurite outgrowth of 50 % after 4 hours ($p = 0.043$) and 52 % after 24 hours ($p = 0.033$). Exposure of N2a cells to 100 µM mercury chloride reduced neurite outgrowth by 64 % at 4 hours and 70 % at 24 hours. Statistical analysis confirmed that concentrations of 0.01, 0.1 and 1 µM mercury chloride had no significant effect on neurite outgrowth after either 4 or 24 hours exposure time ($p = 0.87$ for 1 µM). Analysis of the 4 and 24 hour data using the 2 way ANOVA test confirmed that there were no significant differences in the toxicity of mercury chloride with the different incubation times.

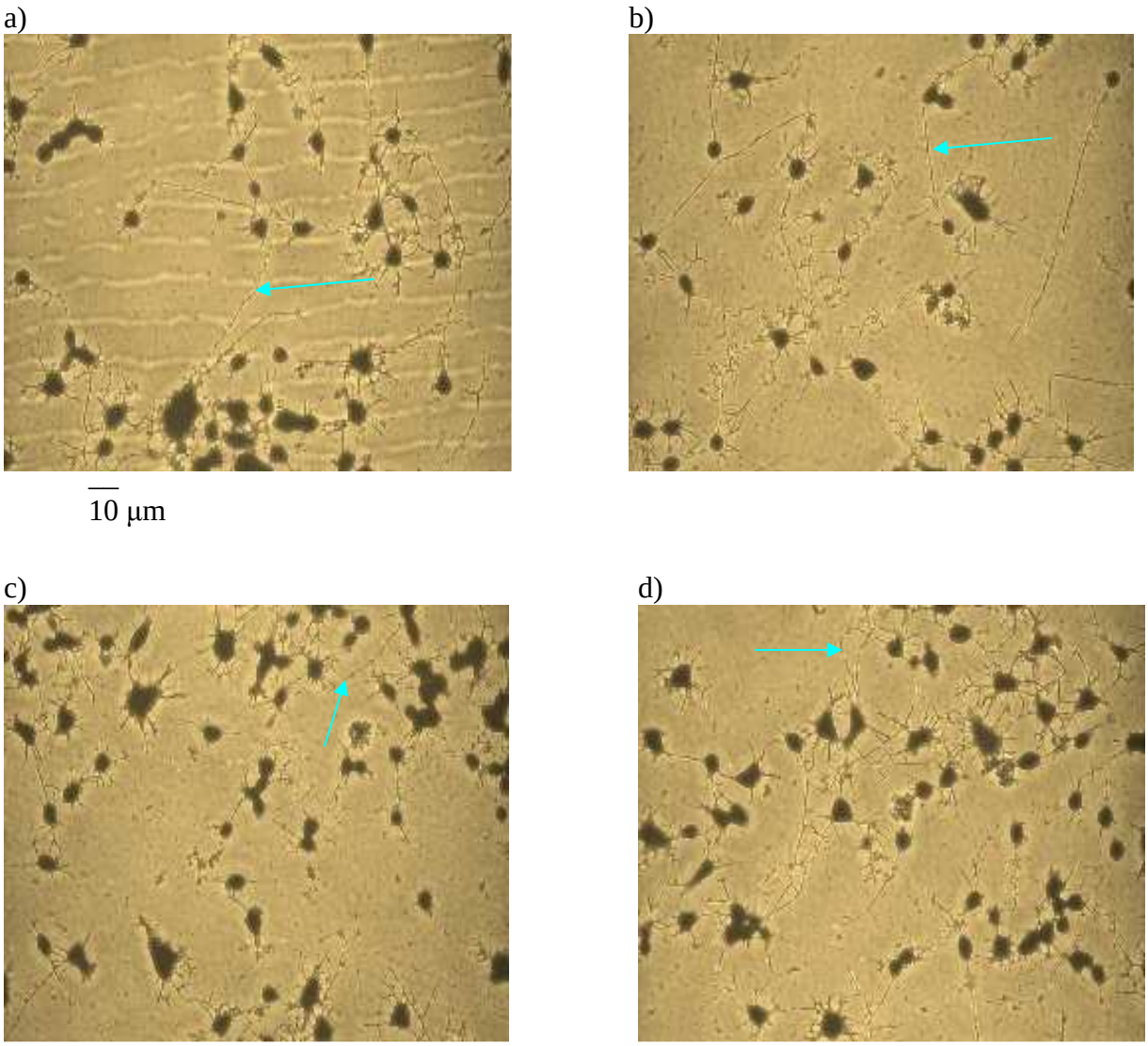

3.4.4: Effect of mercury chloride on differentiated N2a cell morphology

N2a cells were induced to differentiate for 4 (a, c) and 24 (b, d) hours in the presence (c, d) and absence (a, b) of mercury chloride. The cells were fixed and stained with Coomassie Brilliant Blue as described in Methods. Blue arrows indicate cellular processes. Images of typical N2a cells were taken at x 200 magnification (n = 4).

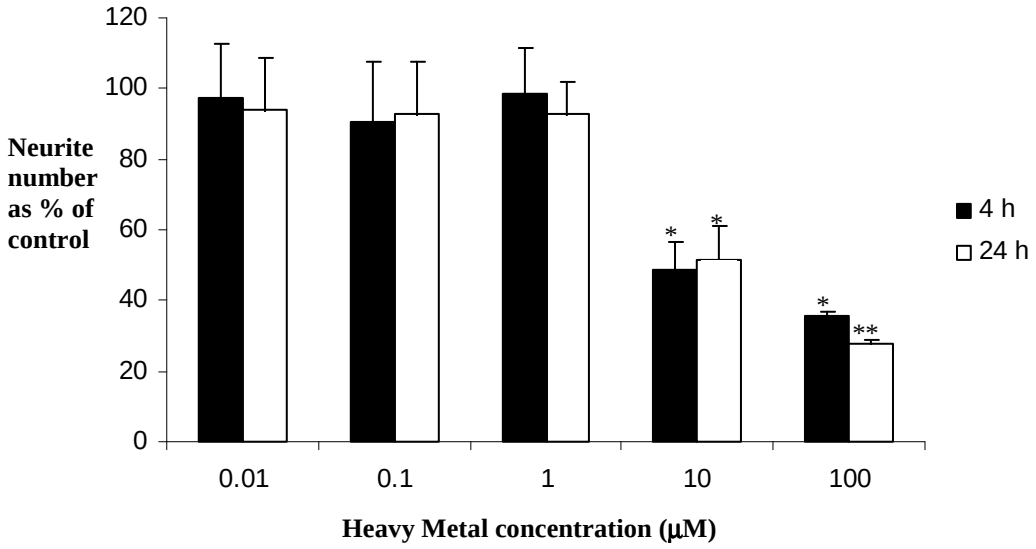

Figure 3.4.5: Effect of mercury chloride on neurite outgrowth in N2a cells

N2a cells were induced to differentiate for 4 and 24 hours in the presence and absence of mercury chloride as described in Methods. The Data is expressed as mean percentage of the corresponding control $\pm$ SEM (n = 4). Statistical analysis was carried out using 2 way ANOVA. * indicates significant differences from the control, * $p < 0.5$, ** $p < 0.1$.

3.5: The effect of thimerosal on MTT reduction and neurite outgrowth

Exposing C6 cells to thimerosal caused a concentration dependent decrease in MTT reduction after 4, 24 and 48 hours incubation (Figure 3.5.1.a). The average absorbance obtained for cells untreated with thimerosal was 0.645. Exposure to 10 µM thimerosal caused a significant reduction of 78 – 90 % after 4, 24 and 48 hours of exposure ($p<0.01$). Exposure to 100 µM thimerosal caused significant reductions at all time points of 80-95 %. A 2 way ANOVA test confirmed that exposure to 0.01, 0.1 and 1 µM thimerosal had no significant effect on MTT reduction ($p = 0.98$ for 1 µM). Statistical analysis also confirmed that there was a significant difference between MTT reduction at 4 and 24 hours with exposure to 10 µM thimerosal ($p = 0.032$) which was not seen with any other concentration. In N2a cells, (Figure 3.5.1.b.), exposure to 10 µM thimerosal caused a significant decrease of 79 - 92 % after 4, 24 and 48 hours ($p = 0.0034$, 0.0089 and 0.0044 for 4, 24 and 48 hours respectively). There were no significant differences from the controls with exposure to 0.01, 0.1 and 1 µM thimerosal after 4 for 24 hours ($p = 0.67$-0.94). However, after 48 hours incubation, 1 µM thimerosal caused a significant decrease of 34 % in N2a cells' ability to reduce MTT ($p = 0.043$). Statistical analysis showed significant differences between the data obtained at 24 and 48 hours during exposure to 1 - 100 µM thimerosal ($p = 0.033$ for 1 µM).

C6 cells differentiated for 4 and 24 hours in the absence of thimerosal are flattened and have formed short processes connecting individual cells in a network (Figure 3.5.2 a-b). In Figure 3.5.2 c and d it appeared that the processes formed between the cells were reduced in number when compared to the control cells of the same incubation time.

a)

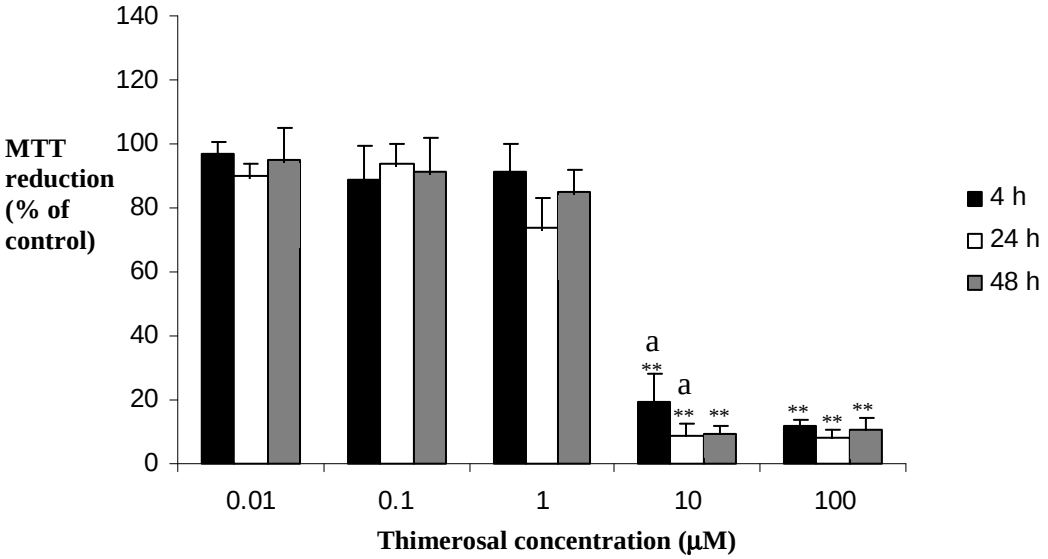

b)

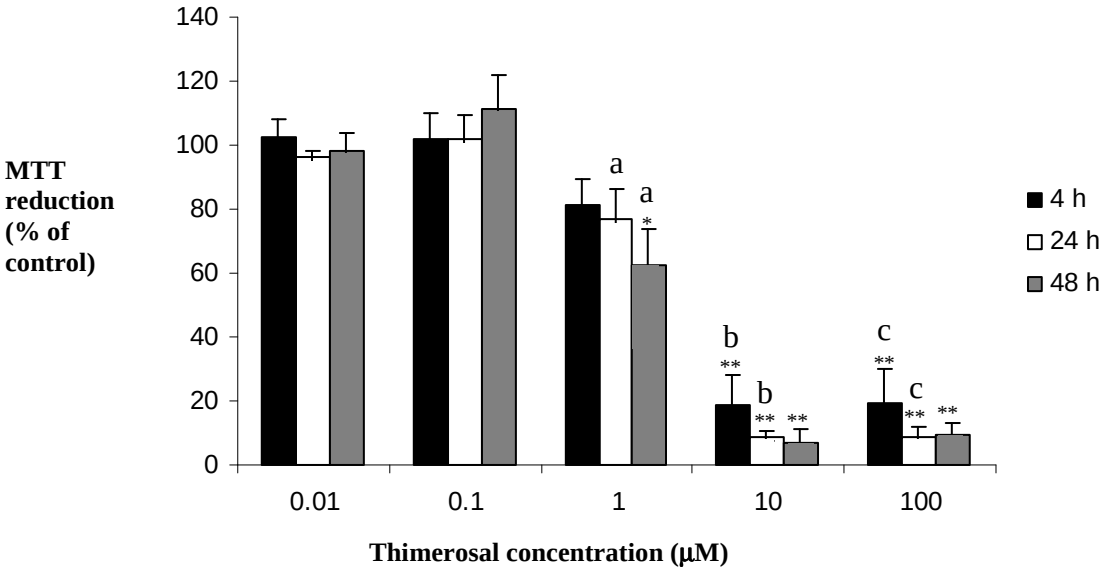

Figure 3.5.1: Effects of thimerosal on MTT reduction in differentiating C6 and N2a cells

C6 (a) and N2a (b) cells were induced to differentiate for 4, 24 and 48 hours in the presence and absence of thimerosal as described in Methods. The Data is expressed as mean percentage of the corresponding control $\pm$ SEM (n = 5). Data was analysed using a 2 way ANOVA. * indicates significant differences from the control, * $p < 0.5$, ** $p < 0.1$, a, b and c indicates significant differences between the time points.

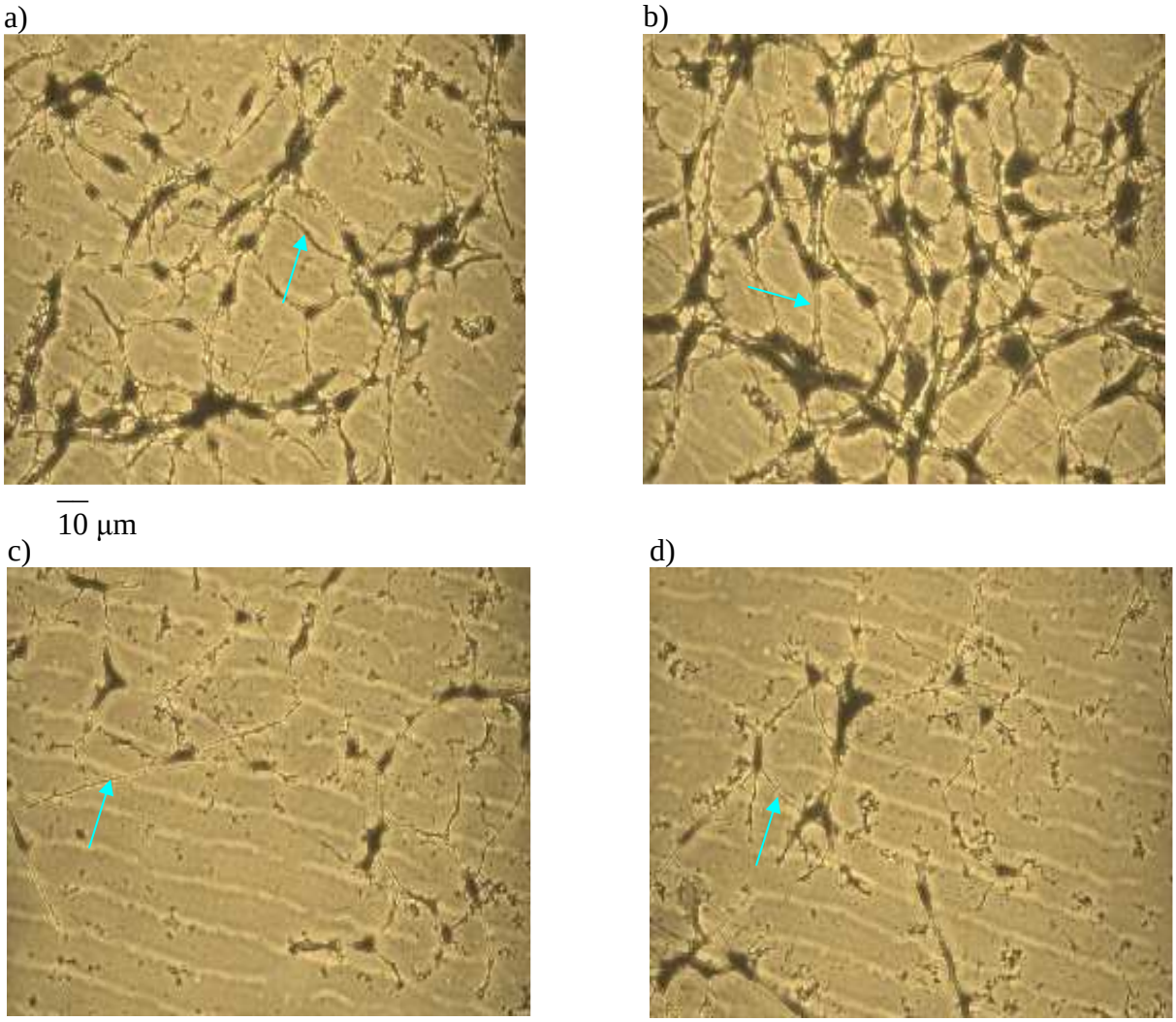

Figure 3.5.2: Effect of thimerosal on C6 cell morphology

C6 cells were induced to differentiate for 4 (a, c) and 24 (b, d) hours in the presence (c, d) and absence (a, b) of thimerosal. The cells were fixed and stained with Coomassie Brilliant Blue as described in Methods. Blue arrows indicate cellular processes. Images of typical C6 cells were taken at x 200 magnification (n = 4).

Thimerosal caused a dose dependent effect upon neurite outgrowth in C6 cells untreated with thimerosal. Cells produced an average of 46 neurites per 100 cells. The lowest concentration that produced a significant effect on the neurite outgrowth was 1 µM which caused a 60 % reduction in processes at both exposure times ($p = 0.036$ and 0.027 for 4 and 24 hours respectively). Exposure to 10 and 100 µM thimerosal significantly reduced neurite numbers by approximately 95 % at both 4 and 24 hours.

Statistical analysis confirmed that there were no significant differences between the 4 and 24 hour time points ($p = 0.57$).

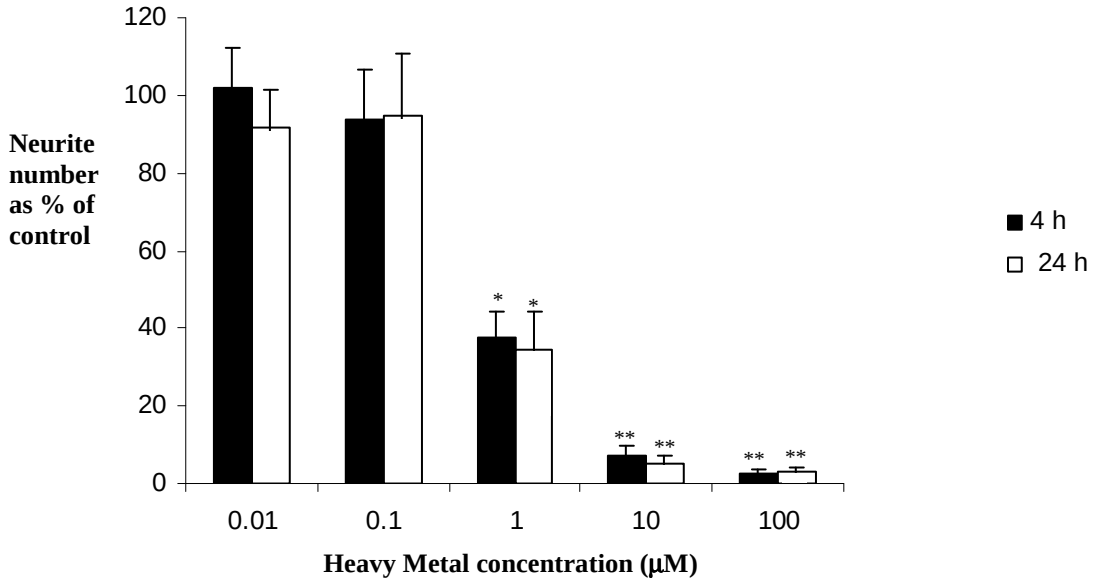

Figure 3.5.3: Effect of thimerosal on neurite outgrowth in differentiated C6 cells

C6 cells were induced to differentiate for 4 and 24 hours in the presence and absence of thimerosal as described in Methods. The Data is expressed as mean percentage of the corresponding control $\pm$ SEM (n = 4). Statistical analysis was carried out using 2 way ANOVA. * indicates significant differences from the control, * $p < 0.5$, ** $p < 0.1$.

N2a cells differentiated for 4 and 24 hours in the absence of thimerosal were spherical in shape with long axon-like processes extending out from the cell body (Figure 3.5.4 a-b). When exposed to 1 µM thimerosal, the number and length of the neurites appeared reduced when compared to the control cells (Figure 3.5.4 c-d).

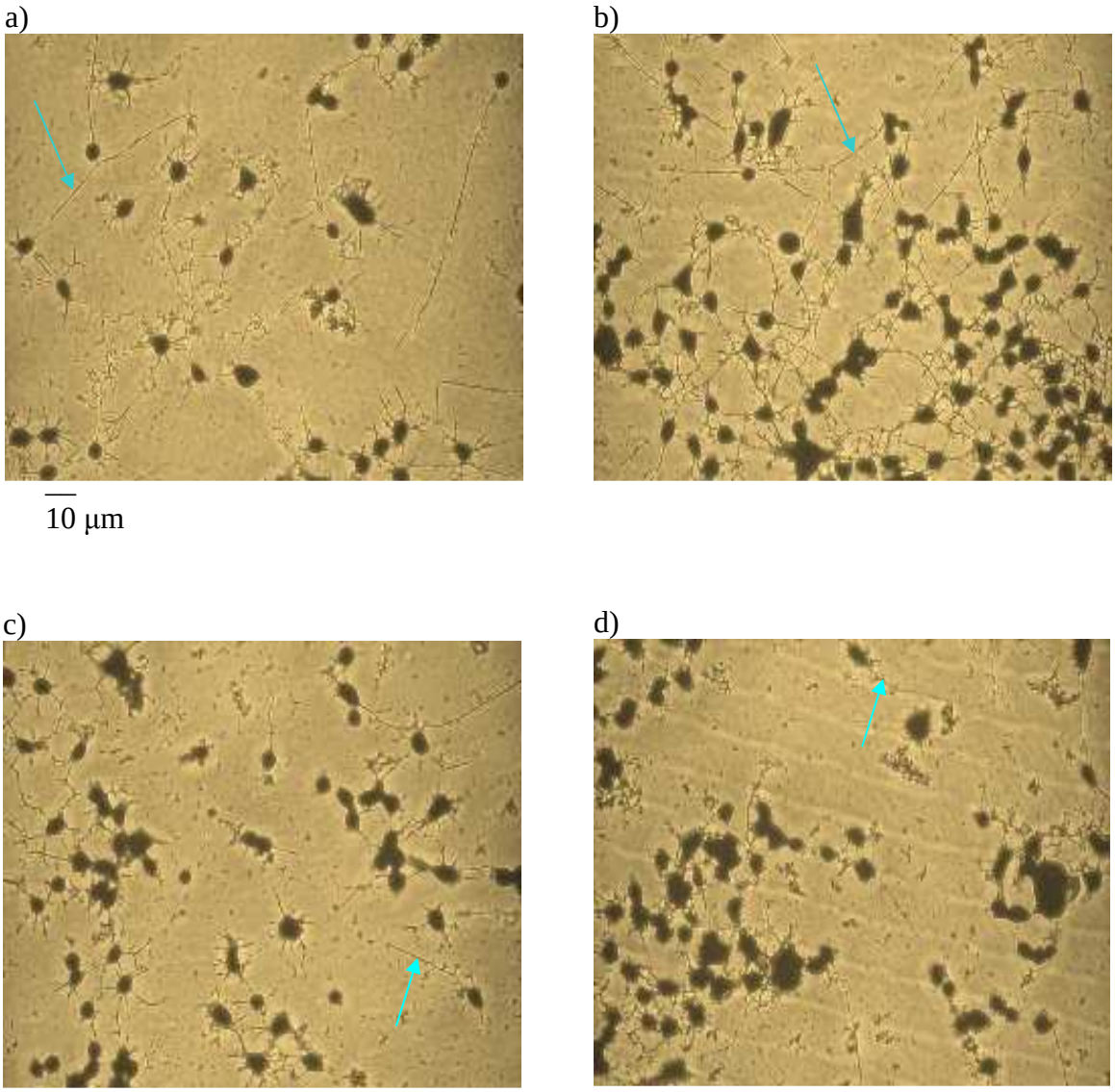

Figure 3.5.4: Effect of thimerosal on differentiated N2a cell morphology

N2a cells were induced to differentiate for 4 (a, c) and 24 (b, d) hours in the presence (c, d) and absence (a, b) of thimerosal. The cells were fixed and stained with Coomassie Brilliant Blue as described in Methods. Blue arrows indicate cellular processes. Images of typical N2a cells were taken at x 200 magnification (n = 4).

The data in figure 3.5.5 shows that exposure to thimerosal had a concentration dependent effect upon neurite production in N2a cells. The average number of neurites per 100 cells after 4 and 24 hours of differentiation was 16 and 22 respectively. After 4 hours of incubation there was no significant inhibition of neurite outgrowth at concentrations below 1 µM thimerosal. Statistical analysis gave a p value of 0.78 for a comparison of the 1 µM data. Exposure to 1 µM thimerosal significantly reduced the number of neurites by 55-60 % after 4 and 24 hours of

incubation. After 24 hours of thimerosal exposure, neurite number was significantly reduced at 0.1 µM by approximately 30 % ($p = 0.049$). Treatment with 10 and 100 µM thimerosal inhibited neurite outgrowth by 90 %. There were no significant changes in neurite number between the 4 and 24 hour exposure times ($p = 0.55$ for 1 µM).

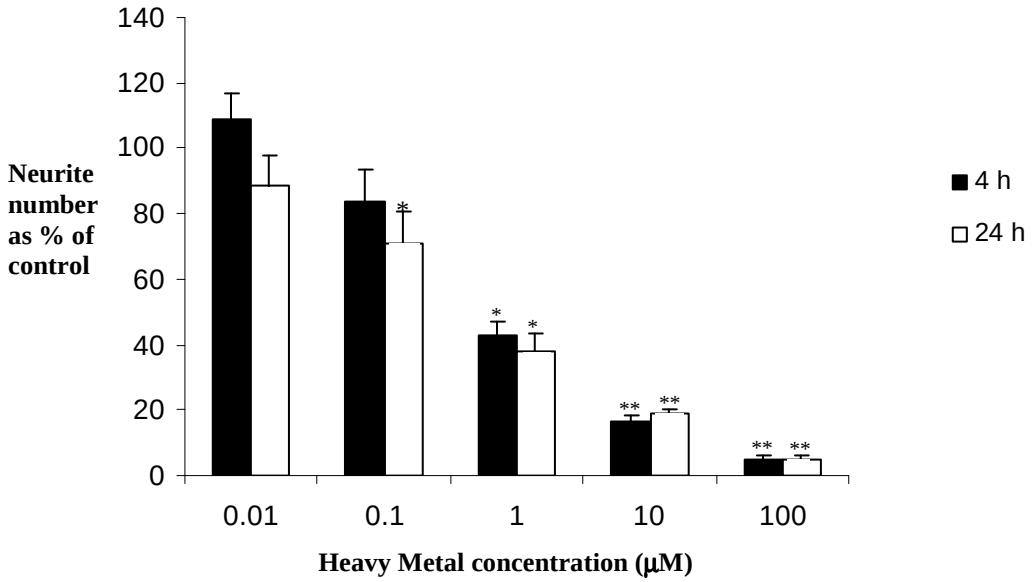

Figure 3.5.5: Effect of thimerosal on neurite outgrowth in differentiated N2a cells

N2a cells were induced to differentiate for 4 and 24 hours in the presence and absence of thimerosal as described in Methods. The Data is expressed as mean percentage of the corresponding control ± SEM (n = 4). Statistical analysis was carried out using 2 way ANOVA. * indicates significant differences from the control, * $p < 0.5$, ** $p < 0.1$.

.

3.6: Effect of methylmercury chloride on MTT reduction and neurite outgrowth

Incubation with methylmercury chloride caused a concentration dependent decrease in MTT reduction after 4, 24 and 48 hours in C6 cells (Figure 3.6.1.a). The typical absorbance value obtained for control cells was 0.453. MeHgCl caused significant decreases ($p<0.01$) in MTT reduction of 80-90 % at 10 and 100 µM but no significant changes below those concentrations. Statistical analysis gave a p value of 0.094 after 48 hours of incubation confirming that the cells ability to reduce MTT was not significantly altered from the control. Analysis of the data using the 2 way ANOVA test showed that there were no significant time differences. Figure 3.1.2.b. shows

MTT reduction in N2a cells; the cells showed no significant changes at concentrations lower than 10 µM after 4 and 24 hours of exposure. After 48 hours exposure, 1 µM MeHgCl caused a significant decrease of 33 % in MTT reduction that was restricted to N2a cells ($p<0.05$). Statistical analysis showed that there was a significant difference in MTT reduction between 4 and 24 time points after exposure to 10 µM ($p = 0.016$).

Control cells differentiated for 4 and 24 hours in the absence of MeHgCl, appeared flattened with short neurites emanating from the ends of the cell (Figure 3.6.2 a – b). After treatment with MeHgCl (Figure 3.1.27 c-d), it appeared that there was a slight reduction in the number of neurites compared to controls.

a)

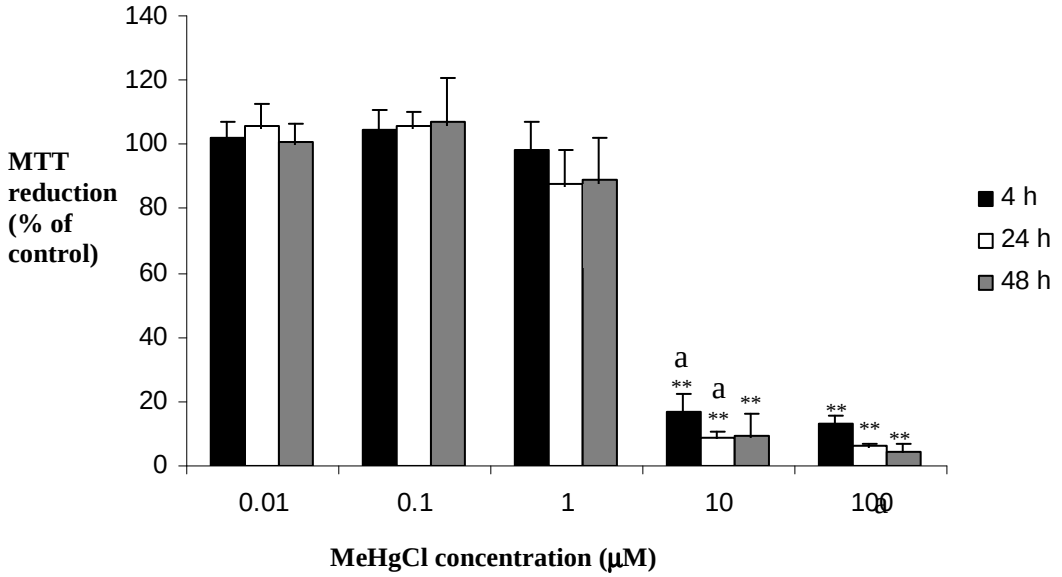

b)

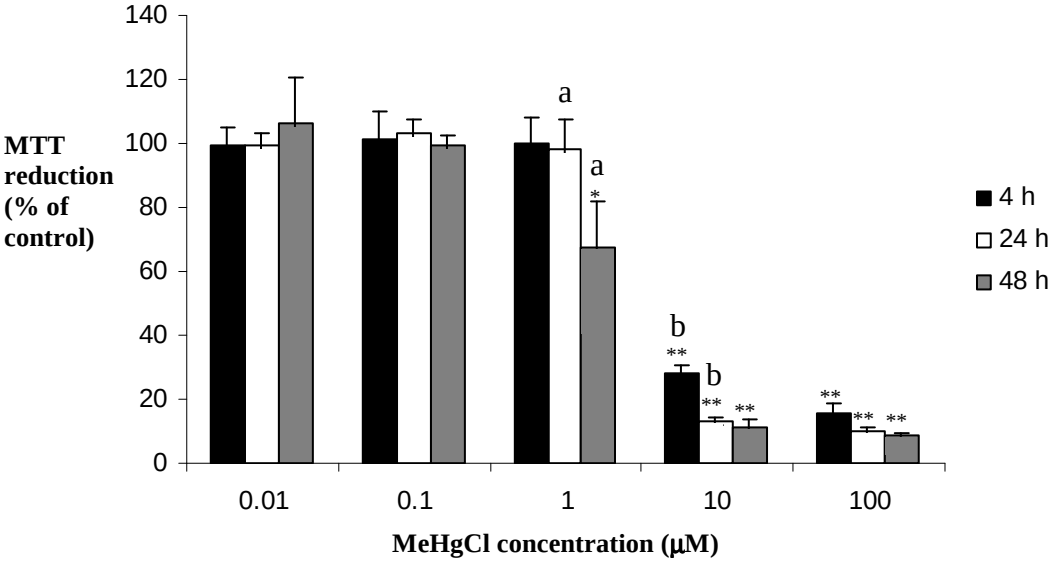

Figure 3.6.1: Effect of methylmercury chloride on MTT reduction in differentiating C6 and N2a cells

C6 (a) and N2a (b) cells were induced to differentiate for 4, 24 and 48 hours in the presence and absence of methylmercury chloride as described in Methods. The Data is expressed as mean percentage of the corresponding control $\pm$ SEM (n = 5). Data was analysed using a 2 way ANOVA. * indicates significant differences from the control, * $p < 0.5$, ** $p < 0.1$, a and b indicates significant differences between the time points.

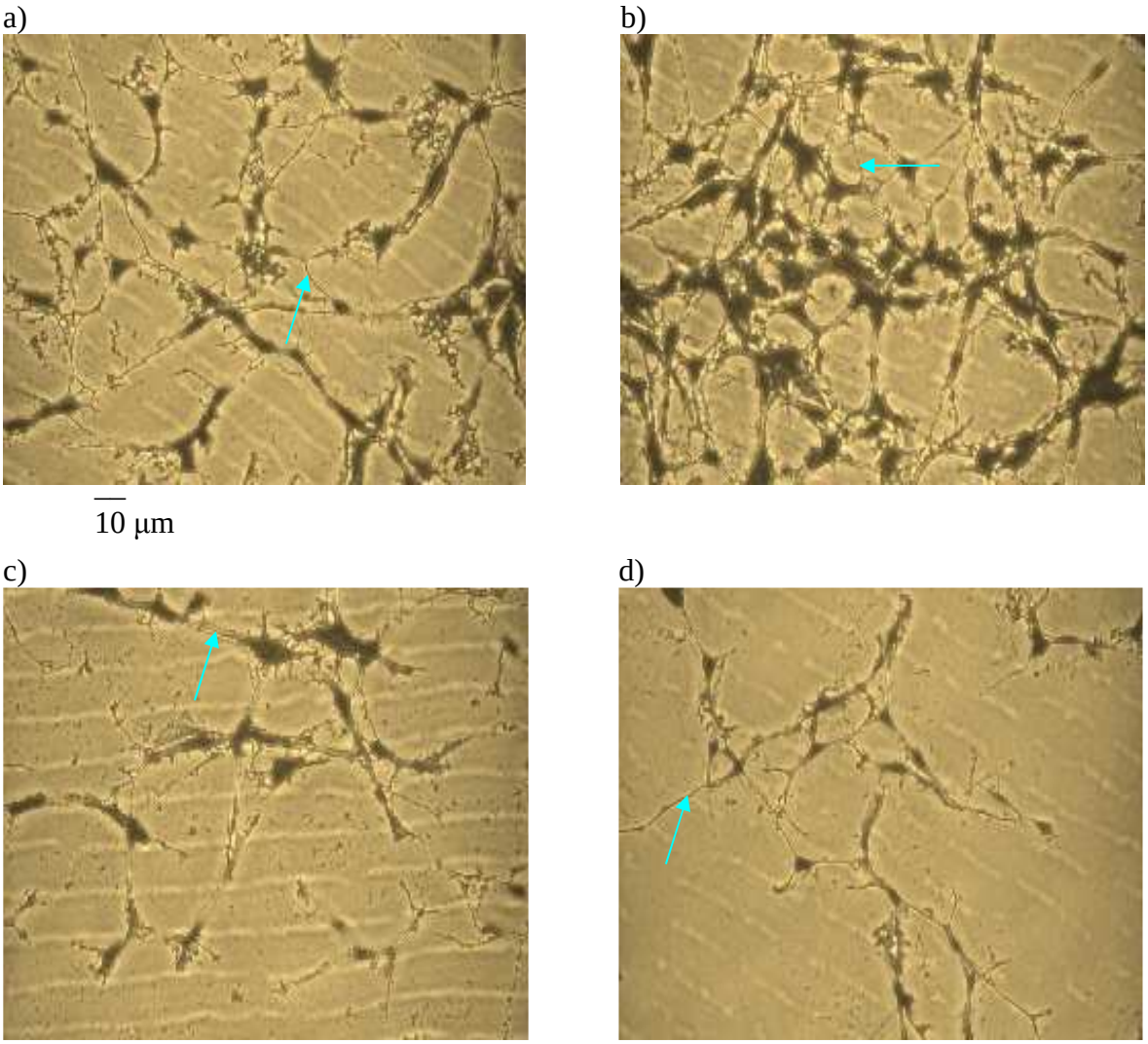

Figure 3.6.2: Effect of methylmercury chloride on differentiated C6 cell morphology

C6 cells were induced to differentiate for 4 (a, c) and 24 (b, d) hours in the presence (c, d) and absence (a, b) of methylmercury chloride. The cells were fixed and stained with Coomassie Brilliant Blue as described in Methods. Blue arrows indicate cellular processes. Images of typical C6 cells were taken at x 200 magnification (n = 4).

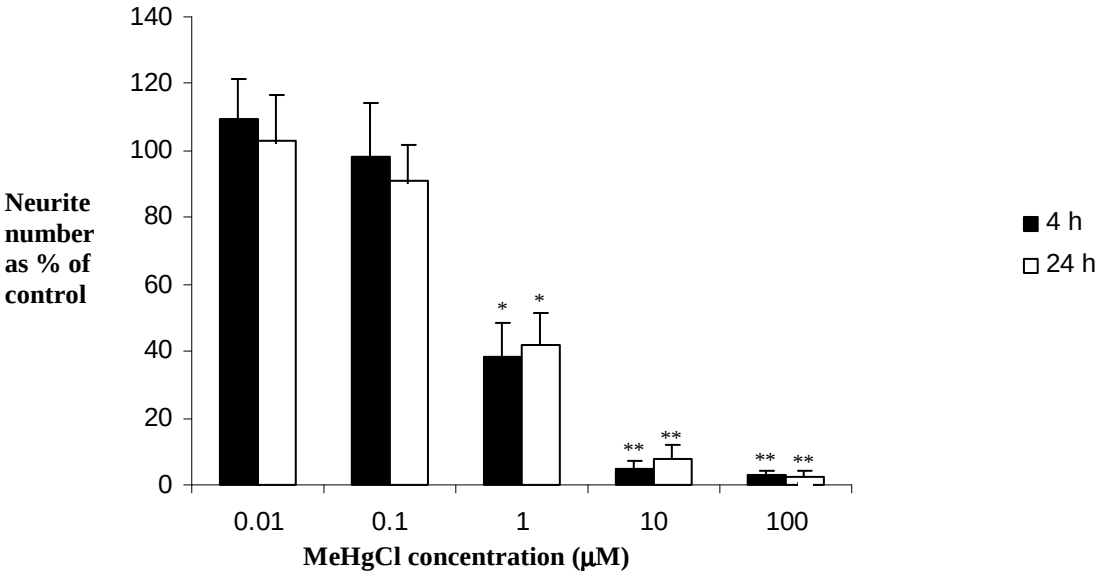

Figure 3.6.3: Effect of methylmercury chloride on neurite outgrowth in differentiating C6 cells

C6 cells were induced to differentiate for 4 and 24 hours in the presence and absence of methylmercury chloride as described in Methods. The Data is expressed as mean percentage of the corresponding control $\pm$ SEM (n = 4). Statistical analysis was carried out using 2 way ANOVA. * indicates significant differences from the control, * $p < 0.5$, ** $p < 0.1$.

Figure 3.6.3 shows that exposure to MeHgCl produces a dose dependent inhibition of neurite outgrowth. The average number of neurites produced by C6 cells was around 19 after 4 hours of differentiation and 23 after 24 hours. MeHgCl displayed no ability to significantly reduce process formation below 1 μM at either time point. Statistical analysis confirmed this with a p value of 0.075 and 0.87 for 4 and 24 hours treatment with 1 μM respectively. Treatment with 1 μM MeHgCl caused a significant ($p<0.05$) reduction in neurite outgrowth of 60-65 %. There was virtually complete inhibition of at least 90 % in process outgrowth following exposure to 10 and 100 μM MeHgCl for 4 and 24 hours. Statistical analysis indicated that there were no significant differences between the 2 incubation times.

N2a cells differentiated for 4 and 24 hours in the absence of MeHgCl were spherical in shape with long axon-like processes extending out from the cell body (Figure 3.6.4

a and b). When exposed to 1 µM MeHgCl, the number of these processes appears reduced when compared to the control cells. There appeared to be a large number of shorter neurites that were not classed as axons, so were not counted (green arrows).

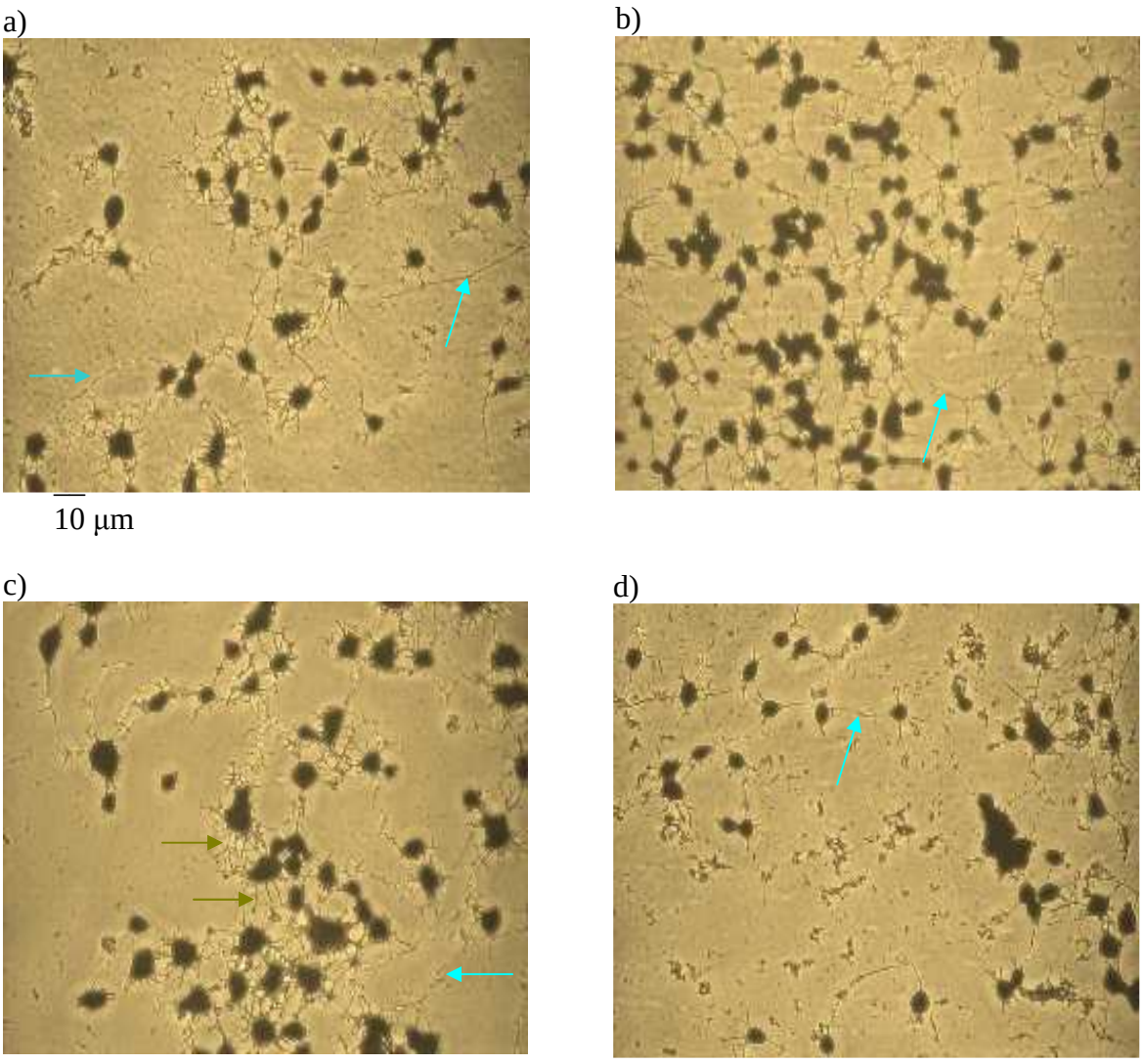

Figure 3.6.4: Effect of methylmercury chloride on differentiated N2a cell morphology

N2a cells were induced to differentiate for 4 (a, c) and 24 (b, d) hours in the presence (c, d) and absence (a, b) of lead chloride. The cells were fixed and stained with Coomassie Brilliant Blue as described in Methods. Blue arrows indicate cellular processes. Images of typical N2a cells were taken at x 200 magnification (n = 4).

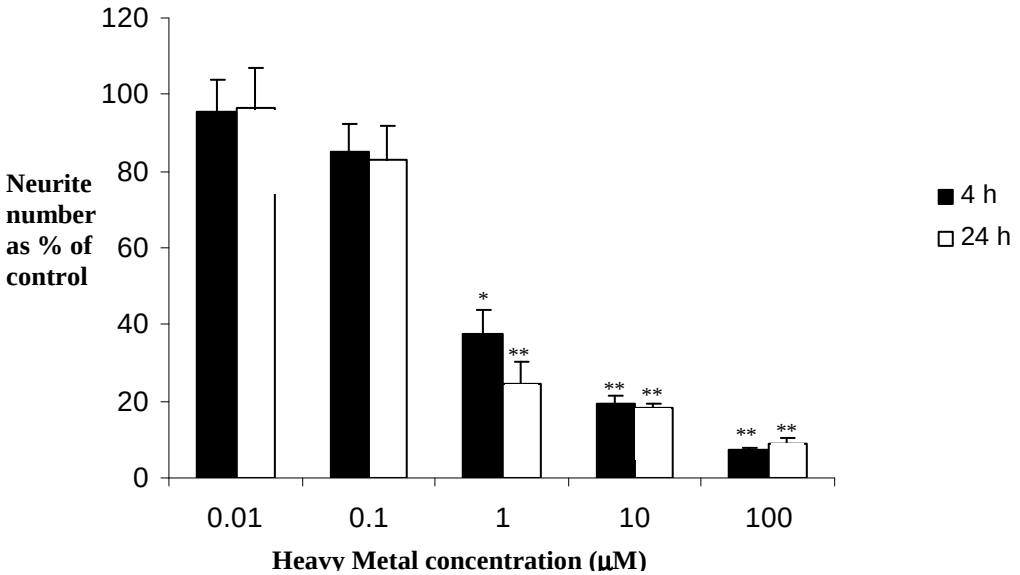

Figure 3.6.5: Effect of methylmercury chloride on neurite outgrowth in N2a cells.

N2a cells were induced to differentiate for 4 and 24 hours in the presence and absence of methylmercury chloride as described in Methods. The Data is expressed as mean percentage of the corresponding control $\pm$ SEM (n = 4). Statistical analysis was carried out using 2 way ANOVA. * indicates significant differences from the control, * $p < 0.5$, ** $p < 0.1$.

Methylmercury chloride exposure induced a concentration dependent reduction in axon number (Figure 3.6.5). After 4 and 24 hours incubation there was no significant reduction in neurite number at MeHgCl concentrations below 1 µM ($p = 0.088$). Exposure to 1 µM MeHgCl caused a 60 % reduction in neurite outgrowth at 4 hours and a 70 % reduction at 24 hours. Statistical analysis showed both reductions to be significant with p values of 0.042 and 0.0034 respectively. The higher concentrations of 10 and 100 µM significantly inhibited neurite outgrowth by 80-90 %. There were no significant differences between the levels of inhibition at the different time points ($p = 0.98$ and 0.72 for 0.01 and 100 µM respectively).

3.7: Dose response curves

All of the dose response curves contained in section 3.7 were created from the MTT reduction assays shown as % of corresponding control in the previous sections of the chapter.

The dose response curves for C6 and N2a cells exposed to concentrations of zinc chloride up to 100 µM indicated that there was no significant effect on MTT reduction (Figure 7.1) (p = 0.35641-0.82984)

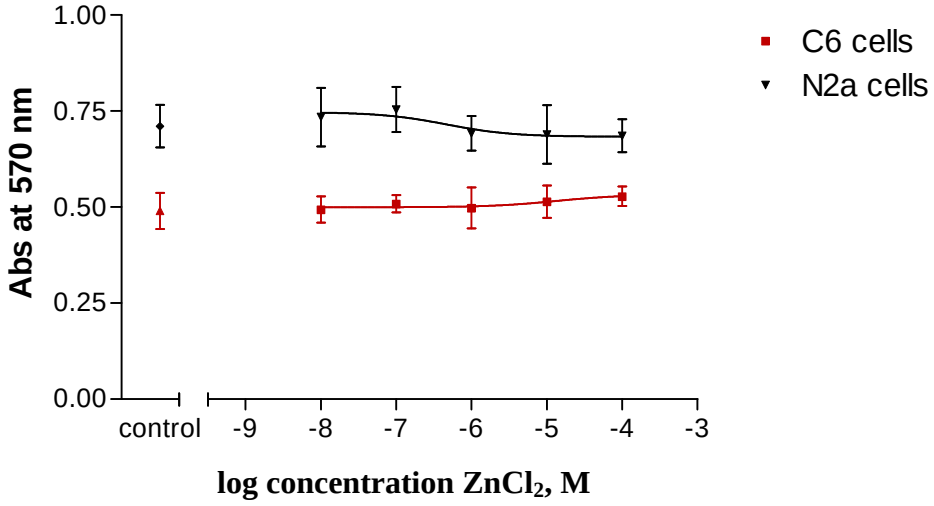

Figure 3.7.1: Dose response curve showing C6 and N2a cells differentiated for 48 hours in the presence and absence of zinc chloride.

N2a and C6 cells were induced to differentiate in the presence and absence of zinc chloride for 48 hours, after which the MTT assay was performed as an assessment of cell viability, as described in Methods. Data is shown as average absorbance + SEM. Statistical test used was the 1 way ANOVA, followed by post hoc Bonferroni's correction for pair wise multiple analysis.

Both cell lines were affected by lead chloride at the same concentration of 10 µM (Figure 3.7.2). MTT reduction increases in an almost identical curve for both cell lines. Statistical analysis using a 1 way ANOVA test indicated that the response seen at 10 and 100 µM were significantly different from the control (p = 0.02343 and 0.01946 respectively). The dose response curve gave an EC50 value of 1.4x10-5 M for C6 cells and 1.1x10-5 M for N2a cells.

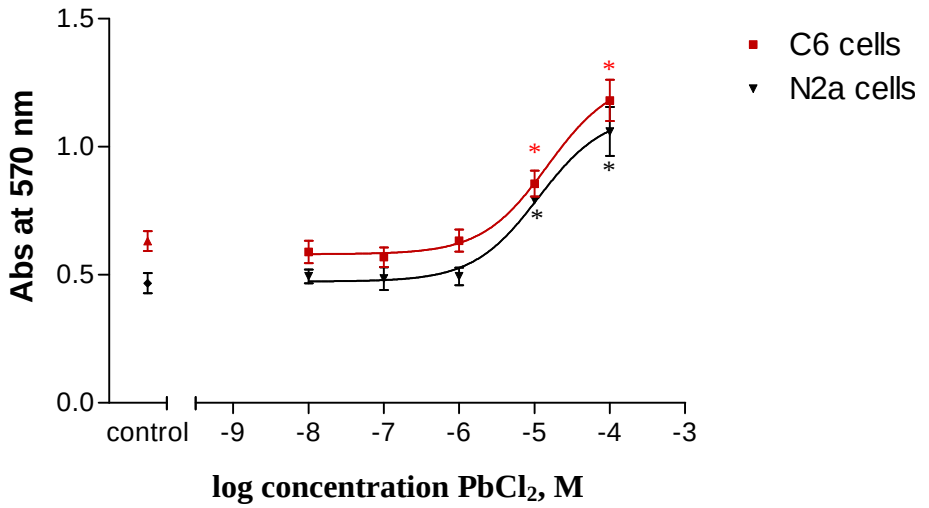

Figure 3.7.2: Dose response curve showing C6 and N2a cells differentiated for 48 hours in the presence and absence of lead chloride.

N2a and C6 cells were induced to differentiate in the presence and absence of lead chloride for 48 hours, after which the MTT assay was performed as an assessment of cell viability, as described in Methods. Data is shown as average absorbance + SEM. Statistical test used was the 1 way ANOVA, followed by post hoc Bonferroni's correction for pair wise multiple analysis (* $p < 0.05$ for C6 cells, * $p < 0.05$ for N2a cells).

The dose response curve for C6 and N2a cells differentiated for 48 hours with cadmium chloride shows that MTT reduction began to decrease significantly at 1 µM in both cell lines (Figure 3.7.3). Statistical analysis indicated that significant decreases occurred at 10 and 100 µM ($p = 0.00895$ and 0.00639 for C6 and N2a cells respectively at 100 µM). The dose response curve gives an EC50 value of 4.6x10-6 in C6 cells and 3.6x10-6 in N2a cells.

The dose response curve in Figure 3.7.4 begins to slope down at log 1 µM for both C6 and N2a cells. Statistical analysis using a 1 way ANOVA indicates that the ability to reduce MTT was not affected significantly until 10 and 100 µM ($p = 0.008760$ and 0.004536 for C6 and N2a cells respectively at 100 µM). The EC50 value in the C6 cell line was 6.6x10-6 and in N2a cells 6.5x10-6.

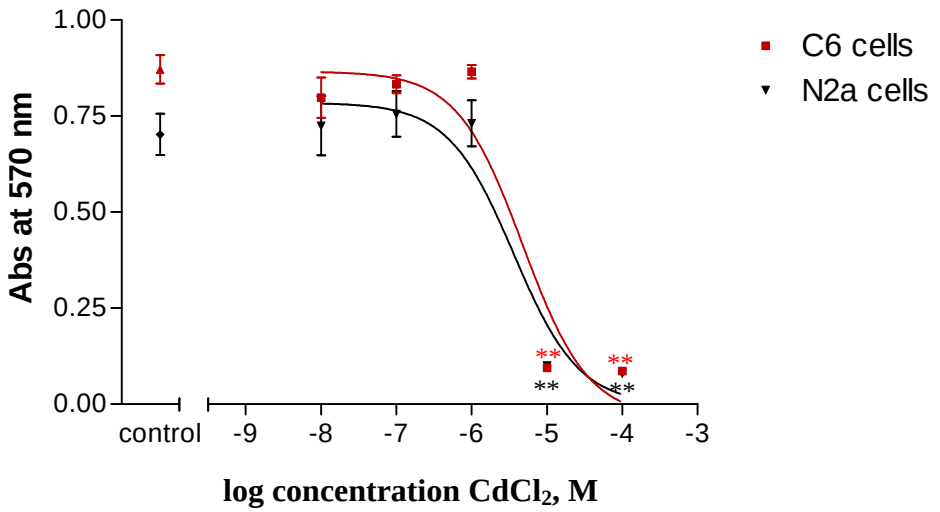

Figure 3.7.3: Dose response curve showing C6 and N2a cells differentiated for 48 hours in the presence and absence of cadmium chloride.

N2a and C6 cells were induced to differentiate in the presence and absence of cadmium chloride for 48 hours, after which the MTT assay was performed as an assessment of cell viability, as described in Methods. Data is shown as average absorbance + SEM. Statistical analysis was carried using a 1 way ANOVA, followed by post hoc Bonferroni's correction for pair wise multiple analysis (** $p < 0.01$ for C6 cells, ** $p < 0.01$ for N2a cells).

The dose response curve for C6 and N2a cells exposed to thimerosal for 48 hours (Figure 7.3.5) begins to decline after 0.1 µM in the N2a cell line. With C6 cells the decline is less steep and occurs in between 0.1 and 1 µM. Statistical analysis using a 1 way ANOVA indicated that in the C6 cell line significant inhibition of MTT reduction did not occur until 10 and 100 µM. In the N2a cells line MTT reduction was significantly inhibited at 1 ($p = 0.0231$ µM). The EC50 value for C6 cells was 3.7x10-6 and for N2a cells 9.9x10-6 M.

The dose response curve in Figure 7.3.6 shows that MeHgCl begins to inhibit the N2a cells ability to reduce MTT between 0.1 and 1 µM. With C6 cells the curve begins to decline at the same range as N2a cells but less steeply. Statistical analysis using a 1 way ANOVA indicates that in the C6 cell line there was significant inhibition of MTT reduction 10 and 100 µM ($p = 0.002458$ and 0.005674 respectively). In the N2a cell line significant inhibition occurred earlier at 1 µM ($p = 0.03464$). The EC50 value for C6 cells was 3.8x10-6 and for N2a cells 1.2x10-6.

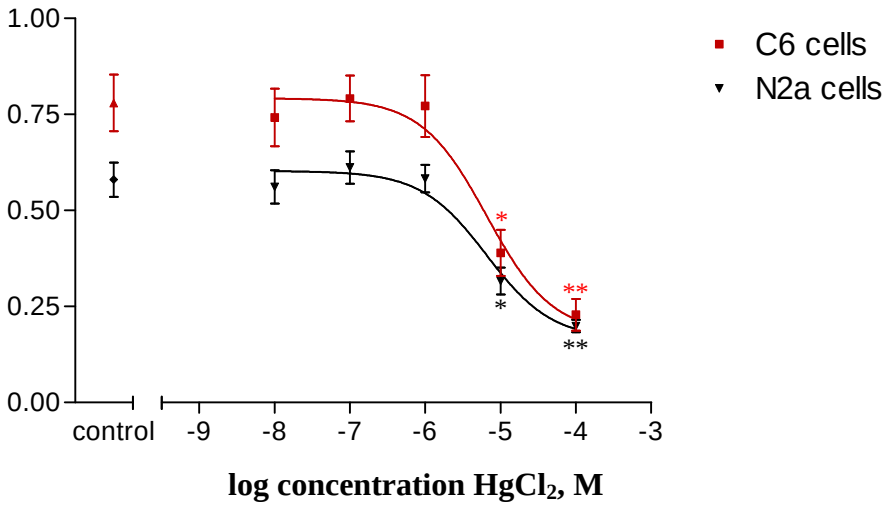

Figure 3.7.4: Dose response curve showing C6 and N2a cells differentiated for 48 hours in the presence and absence of mercury chloride.

N2a and C6 cells were induced to differentiate in the presence and absence of mercury chloride for 48 hours, after which the MTT assay was performed as an assessment of cell viability, as described in Methods. Data is shown as average absorbance + SEM. Statistical analysis was carried using a 1 way ANOVA, followed by post hoc Bonferroni's correction for pair wise multiple analysis (* $p< 0.05$, ** $p< 0.01$ for C6 cells, * $p < 0.05$, ** $p < 0.01$ for N2a cells).

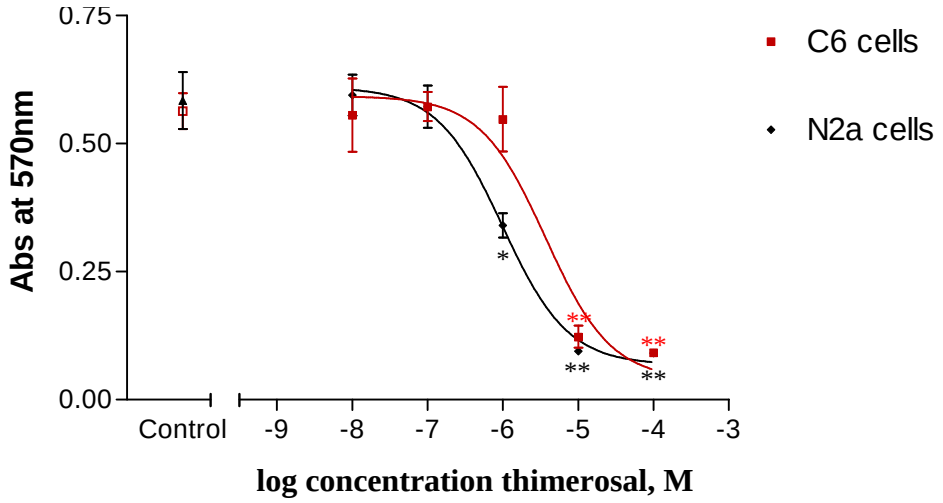

Figure 3.7.5: Dose response curve showing C6 and N2a cells differentiated for 48 hours in the presence and absence of thimerosal.

N2a and C6 cells were induced to differentiate in the presence and absence of thimerosal for 48 hours, after which the MTT assay was performed as an assessment of cell viability, as described in Methods. Data is shown as average absorbance + SEM. Statistical analysis was carried using a 1 way ANOVA, followed by post hoc Bonferroni's correction for pair wise multiple analysis (** $p < 0.01$ for C6 cells, * $p < 0.05$, ** $p < 0.01$ for N2a cells).

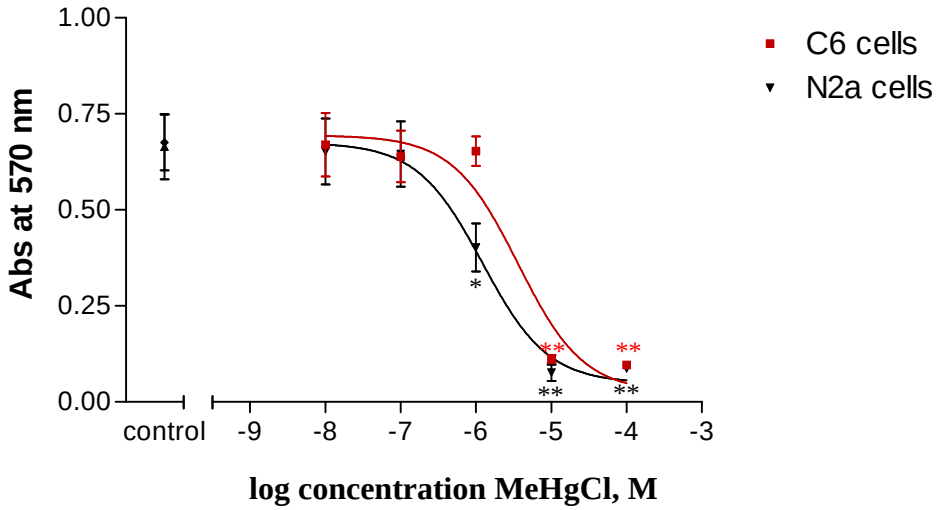

Figure 3.7.6: Dose response curve showing C6 and N2a cells differentiated for 48 hours in the presence and absence of methylmercury chloride.

N2a and C6 cells were induced to differentiate in the presence and absence of methylmercury chloride for 48 hours, after which the MTT assay was performed as an assessment of cell viability, as described in Methods. Data is shown as average absorbance + SEM. Statistical analysis was carried using a 1 way ANOVA, followed by post hoc Bonferroni's correction for pair wise multiple analysis (** $p < 0.01$ for C6 cells, * $p < 0.05$, ** $p < 0.01$ for N2a cells).

3.8: Discussion

This chapter determined the lethal and sub-lethal concentrations of various heavy metal compounds and investigated their effects on the cell morphology of C6 and N2a cell lines. There are no previous studies that have compared the toxicity of such a large number of heavy metal compounds in the same differentiating cell line. However previous studies have investigated smaller groups of compounds or individual metals (Monnet-Tschudi *et al.*, 1996; Braekman *et al.*, 1997; Allen *et al.*, 2001).

The cytotoxicity studies (section 3.1 - 3.6), determined that MeHgCl, thimerosal and cadmium chloride were the most toxic of the heavy metals and that they had the most profound effect on both MTT reduction and neurite outgrowth in both cell lines.

Zinc chloride had no significant effects on MTT reduction or neurite outgrowth in either cell lines at any concentration used (Figure 3.1.1-3.1.5). Zinc is the only one of the heavy metals studied that is essential in the nervous system. Zinc is present in vesicles within excitatory nerve terminals and when released in a calcium dependent manner, can reach concentrations of 100 µM in the extra cellular space (Gee *et al.*, 2002). Synaptically released zinc can then modify the activity of certain proteins such as glutamate and γ-aminobutyric acid (GABA) receptors (Frederickson & Bush, 2001; Mathie *et al.*, 2005). This may be why the toxicity seen with the other metals in this study was not apparent with zinc exposure of up to 100 µM. Our findings are in agreement with those of Park and Koh (1999), who treated mitotic primary cultures of neuronal and glial cells with concentrations of 300 µM zinc chloride before detecting a reduction in cell viability. In their study exposure to 100 µM zinc chloride had no significant effect on cell viability after 8 hours, unfortunately they did not extend the incubation time beyond 8 hours. Hence it is not possible to directly compare their results with the present study after 24 and 48 hours exposure. Park & Koh, (1999) observed no reduction in cell viability after 8 hours, which is consistent with the 4 hour exposure time. Schwartz *et al.*, (2000) found that in the human neuronal SHSY5Y cell line, neurite length remained unaltered in cells exposed to 50 µM zinc chloride. However the study did not use any higher concentrations of zinc to examine whether changes occurred above that concentration. Exposure to 100 µM zinc did not alter cell viability in PC12 cells. Following 24 hours of exposure to 250 µM zinc, cell viability was reduced in mitotic PC12 cells (Watjen, 2001). Thus, the lack of toxicity of zinc chloride in the experiments presented in this thesis is in good agreement with the findings of other workers.

Lead chloride induced significant changes only at the highest concentration of 100 µM (Figures 3.2.1 - 3.2.6). MTT reduction assays showed an increase in the amount of MTT reduced by N2a and C6 cells at all time points (Figure 3.2.1). This increase in the metabolic activity of the cells may be a stress response to reduce lead toxicity. Lead can also have a proliferative effect on cells (Castiglioni, 1993), which would explain the increase in MTT reduction seen in both C6 and N2a cells treated with lead chloride. However, cells viewed with an inverted microscope did not show any evidence of increased proliferation (see Figure 3.2.3 and 3.2.5). Cordova *et al.*, (2004) found that concentrations of lead up to 10 µM had no significant effect on the viability of slices of rat brain when incubated for up to 3 hours. Whilst they did not

use as high a concentration as 100 µM lead. The effects of the lower doses do agree with the findings of the present study. Since the standard error of the mean for the 24 hour exposure to lead chloride (see Figure 3.2.3 and 4) in both cell lines were bigger than the 4 hour exposure which may reflect differences in the batches of cells as the experiments were done at different times. The numbers of neurites were not the same in each individual experiment. Despite the differences in absolute values the trends remained the same.

It required a concentration of Cadmium chloride 10 µM or above to significantly decrease MTT reduction in both C6 and N2a cells (Figure 3.3.1). Watjen, (2001) found that exposure to 15 µM cadmium resulted in decreased cell viability after 24 hours of exposure in PC12 cells, an adrenal chromaffin cell line. This difference in lethal concentration could be due a greater susceptibility of C6 and N2a cells to the toxic effect of cadmium. Cadmium chloride was the only heavy metal that induced any significant effect in neurite outgrowth below 1 µM (see Figure 3.3.5). A concentration of 0.1 µM cadmium chloride reduced neurite outgrowth in N2a cells by 40-50 % after 4 and 24 hours exposure. This reduction was not seen in C6 cells (Figure 3.3.3), indicting that glial cells are less susceptible than N2a cells to the neurite inhibitory effects of cadmium chloride.

Mercury chloride decreased MTT reduction and neurite outgrowth at 10 and 100 µM (Figures 3.4.1 - 3.4.5). Unlike the organic mercury species, mercury chloride did not induce any sub-lethal alterations in neurite outgrowth, as inhibition of neurite number was seen only at concentrations that reduced cell viability. A study by Bonacker *et al.*, (2004) found tubulin assembly to be inhibited by 10 µM mercury chloride in both a cell free system, and in V79 cells microtubule assembly was completely inhibited by treatment with 100 µM mercury chloride. Microtubules comprise part of the cytoskeleton within cells of the CNS and are a major component of the neurites produced by neuronal and glial cells. Thus, this inhibition of tubulin assembly could account for the neurite inhibition seen within this thesis. However, the study by Bonacker *et al.*, (2004) made no mention of any inhibitory effects in the cell system below 100 µM, whereas the data presented in this thesis found neurite number to be reduced by approximately 50 % with 10 µM mercury chloride and 60-70 % with exposure to 100 µM mercury chloride. One possible explanation of this discrepancy is that exposure to 10 µM mercury chloride tends to retard the tubulin subunits within the neurites, rather than the cell body.

Thimerosal and MeHgCl had a similar effect to each other on MTT reduction (Figures 3.5.1 and 3.6.1). Both organic mercury compounds caused a decrease in MTT reduction at 10 and 100 µM in C6 cells and 1, 10 and 100 µM in N2a cells. Sanfeliu *et al.*, (2001) used mitotic cells and found that MeHgCl decreased cell viability at 5 µM in both primary neurons and SHSY5Y neuroblastoma cells and 10 µM in primary glial cells. The viability of glial cells was also reduced by 50 % following 24 hours exposure to 9 µM MeHg (Garg & Chang, 2006). Crespo-López *et al.*, (2006) found a 20 % decrease in the viability of neuroblastoma and glioblastoma cell lines treated with 0.1 and 1 µM MeHg for 24 hours. The present study did not find any significant decrease in MTT reduction with these concentrations, perhaps due to different cell lines used and the fact that they were mitotic during experimentation in the case of Crespo-López et al (2006). The two organic mercury compounds had an inhibitory effect on neurite outgrowth in both cell lines (Figures 3.5.3, 3.5.5, 3.6.3 and 3.6.5) at concentrations not inhibiting the reduction of MTT. This suggests that the changes in morphology observed were sub-lethal events that were occurring before cell death. The reduction in the numbers of neurites may also be caused by changes in the cell volume. Research has shown that heavy metals can cause damage to cell membranes (Herdman *et al.*, 2006), which may allow fluid to enter causing the cells to swell and increase in size causing the neurite to appear shorter. However during examination of cells with a light microscope there did not appear to be any in cell volume when compared to the control.

Comparison of the three mercury compounds using MTT assays and neurite outgrowth shows that the inorganic compound (mercury chloride) is less toxic than the organic compounds (MeHgCl and thimerosal). A number of studies have noted the differences in the toxicity of inorganic and organic mercury (Chetty *et al.*, 1996; Monnet-Tschudi *et al.*, 1996; Allen *et al.*, 2001; Ochi, 2002). However, none of these studies have directly compared the lethal doses of the heavy metals.

Sanfeliu *et al.*, (2001) found that neuronal cells were more sensitive to the effects of MeHgCl using the MTT reduction assay. The research showed that the lowest dose at which cytotoxicity was seen was 5 µM in neuroblastoma cells and 10 µM in astrocytes. The work in the present study has found that exposure to thimerosal and MeHgCl appeared to be more debilitating to N2a cells after 48 hours of incubation with the organic mercury compounds. N2a cells are also more susceptible to the sub-lethal effects of cadmium chloride, as neurite outgrowth in N2a cells was

reduced at concentration 100 times less than the minimum concentration needed to reduce neurite outgrowth in C6 cells. Braekman *et al.,* (1997) compared the toxicity of cadmium chloride, mercury chloride and MeHgCl on an insect cell line exposed to the different heavy metals for 3 hours. MeHgCl was found to be the most toxic of the three metals with sub-lethal concentrations of 2 µM and below. Unlike the current study, Braekman *et al.*, (1997) found cadmium to be the least toxic of the metals tested, with lethal concentrations of 44 µM and above. This is a higher than the lethal concentration determined by the present work. But differences could be explained by the differences in cell lines used, incubation time and the cell viability assay used, as Braekman *et al.,* (1997) used a propidium iodide cell exclusion test. A comparison of cell viability assays indicated that each assay provided slightly different results, making a comparison of toxicity difficult if a different assay was used (Bigl *et al.*, 2007).

The dose response curves contained in section 7.7 used the data obtained from MTT reduction assays and the EC50s are summarised in table 3.1. The re-plotting of the MTT reduction data using log concentrations enabled the EC50 values of the different compounds to be calculated and a comparison to be made. The EC50s clearly demonstrate that N2a cells are more sensitive than C6 cells particularly for the organic mercury compounds.

Heavy Metal	EC50 (M)	
	C6	N2a
Lead chloride	1.5x10-5	1.1x10-5
Cadmium chloride	4.7x10-6	3.6x10-6
Mercury chloride	6.6x10-6	6.5x10-6
Thimerosal	3.7x10-6	9.7x10-7
Methylmercury chloride	3.8x10-6	1.2x10-6

Table 3.1: EC50 derived from dose response curves of MTT reduction.

The EC50 represent 50 % of the metals effective concentration and were calculated by the graph pad prism program used to create the dose response curves.

From the initial cytotoxicity screening studies in this thesis, it was decided that the two organic mercury species thimerosal and MeHgCl would be studied in more detail. Both were highly toxic and in addition thimerosal as a potential source of mercury exposure is relevant and controversial at present due to its presence in vaccinations, the concerns about the health risks that it poses and because very little is known about its potential neurotoxicity.

The aim of the following chapters was to investigate sub-lethal events that preceded cell death. From the MTT reduction assays it was determined that concentrations of 10 µM thimerosal and MeHgCl and above were unsuitable because of the significant reductions in cell viability that they caused. The concentrations used for further work were 1 and 0.1 µM, as they caused no reduction in cell viability at 4 and 24 hours but 1 µM affected on neurite outgrowth after 4 and 24 hours of exposure.

Chapter 4: Effects of organic mercury compounds on the neuronal and glial cell cytoskeleton

Introduction

The previous chapter demonstrated that organic mercury compounds had a detrimental effect upon the production of cellular processes. Major protein components of the processes formed by both neuronal and glial cells are various cytoskeletal proteins. Since changes in neurite length and number were observed in chapter 3, the aim of the work presented in this chapter was to determine whether the reduction in the number of processes was accompanied by molecular changes in the proteins that make up neuronal and glial cell processes.

The cytoskeletal network of the CNS is comprised of microtubules, microfilaments and intermediate filaments (i.e. neurofilaments in neuronal cells and glial fibrillary acidic protein in glial cells). Microtubules are comprised of alternatively arranged α and β tubulin sub-units, organised into protofilaments that form a cylindrical shape that is the microtubule structure (Hargreaves, 1997). Microtubules are dynamic structures that can polymerise and depolymerise; by post-translational modification of the α-tubulin sub-unit, microtubules can become stable and resist depolymerisation (Dhamodharan & Wadsworth, 1995). Post-translational modifications include acetylation or detyrosination. Detyrosination involves the removal of a tyrosine residue from α-tubulin subunit though the action of the enzyme tubulin carboxypeptidase which releases the COOH terminal tyrosine. Detyrosination is a reversible modification and the subunit can be re-tyrosinated as it depolymerises from the microtubule. A tyrosine residue can be added to the same position by tubulin:tyrosine ligase (Sironi *et al.*, 2000). Previous studies have shown that treatment with mercury disturbs microtubule formation and function (Stoiber *et al.*, 2004). Mercury has been shown to possess a high affinity for tubulin sulfhydryl groups (Sager *et al.*, 1983; Vogel *et al.*, 1985; Graff *et al.*, 1997) which may account for the disturbed formation and function of microtubules. Methylmercury can both prevent depolymerisation (Abe *et al.*, 1975) of microtubules and inhibit assembly (Sager, 1998).

The effects of thimerosal and methylmercury chloride on tubulin levels, microtubule organisation and dynamics were investigated by measuring total α-

tubulin, tyrosinated α-tubulin and total β-tubulin, Neuronal cells also contain an intermediate filament network known as neurofilaments (NFs) that is unique to this cell type. NFs confer strength and stability to axon like structures formed by neuronal cells. There are three main forms of the NF chain in animal cells, NFH, NFM and NFL (Yuan *et al.*, 2006). The three forms of NF are distinguished by their molecular weight, which is due to differences in their head and tail domains (Ackerley *et al.*, 2003). This thesis looks at NFH rather than NFM and NFL as NFH is the most extensively phosphorylated form of the NFs and its phosphorylation is associated with axon stability and maturity (Williamson, 1996). NF phosphorylation also regulates transport within the cell, the more extensive the phosphorylation the slower the rate of transport (Yuan *et al.*, 2006). Previous studies have noted the effect of mercury on axon outgrowth but have not looked at the cytoskeletal proteins that make up the axon (Gopal, 2002). Using antibodies that recognise these proteins, this chapter aimed to determine whether organic mercury compounds disrupted the cytoskeletal network within the differentiating cell lines.

Methods

The previous chapter established that concentrations of 0.1 and 1 µM of thimerosal and methylmercury chloride were sub-lethal. The two organic mercury compounds were chosen due to their enhanced toxicity over inorganic mercury and the opportunity to compare the differences in the mechanisms of toxicity that the methyl and ethyl groups confer to the compounds. The cell lines were differentiated in the presence and absence of the organic mercury compounds. After the 4 and 24 hour incubation periods had lapsed the cell extracts were lysed by boiling 0.5 % SDS in TBS (Methods section 2.212). SDS-PAGE followed by western blotting was completed on 6 independent cell lysates for each antibody. SDS-PAGE was used to separate proteins by molecular weight and western blotting was used to probe lysed cell extracts with various antibodies. The antibodies used on western blots created from lysates of both cell lines were B512 (anti-total α-tubulin antibody), T1A2 (anti-tyrosinated α-tubulin antibody) and Tub 1.2 (anti-total β-tubulin antibody). In addition, antibodies against N52 (anti-total NFH antibody), RT97 and SMI34 (anti-phosphorylated NFH antibodies) were used to probe western blots created from N2a cell lysates. These antibodies were chosen due to the high content of cytoskeletal

proteins within the nerve and glial cells and they were all well established within the lab. All antibodies were used at a dilution of 1/1000 in either 3 % BSA or Marvel. The resultant blots were quantified using AIDA software.

The same antibodies were also used for immunofluorescence staining of fixed cells at dilution of 1/200 with 3 % BSA. The secondary antibody was either conjugated with TRITZ which gives a red fluorescence under the microscope or FITZ which was green. Images of the stained cells were obtained using a confocal microscope at x600 magnification. In the results section the number of times the experiment was carried out using separate cell extracts was indicated by the n = x in the figure legend. The data shown is the average densitometric value for 6 western blots created from 6 gels of independent cell extracts. The lane on the blot labelled 0 is the control extract with no added metal. For the thimerosal treated corresponding control sterile distilled water was added at the same volume as the metal in the treated cells and with MeHgCl DMSO was added at the same volume as with the treated cells as the MeHgCl was dissolved in DMSO due to poor solubility in distilled water. Statistical analysis was carried using 2 way ANOVA followed by Bonferroni's post hoc correction for pair wise multiple analysis.

4.1: Effects of organic mercury compounds on the levels and distribution of microtubule protein in differentiated C6 cells

Densitometric analysis of the western blots created from lysed C6 cell extracts in Figure 4.1.1 showed that the levels of B512 reactivity were not significantly altered when compared to the control in cells treated with 0.1 or 1 µM thimerosal or MeHgCl. The average densitometric absorbance for the control cell extract was 0.78359 and the average absorbance for the treated cells was in the range of 0.67849-0.89496 ($p = 0.077 - 0.65$ for both concentrations of both heavy metals). After 24 hours, there was a significant reduction ($p<0.05$) in the reactivity of B512 following exposure of cells to 1 µM concentrations of both thimerosal and methylmercury chloride. A 2 way ANOVA test followed by post hoc Bonferroni's test confirmed significance ($p = 0.0231$ and 0.0364 for 1 µM thimerosal and 1 µM MeHgCl, respectively). Both compounds caused approximately a 75 % reduction in antibody reactivity. Thimerosal alone caused a significant reduction of around 35 % in antibody reactivity at the lower concentration of 0.1 µM. Statistical analysis of the 4

and 24 hour data showed that there were no significant differences between the incubation times with exposure to both concentrations of thimerosal and 1 µM MeHgCl ($p = 0.9323$ for 0.1 µM thimerosal).

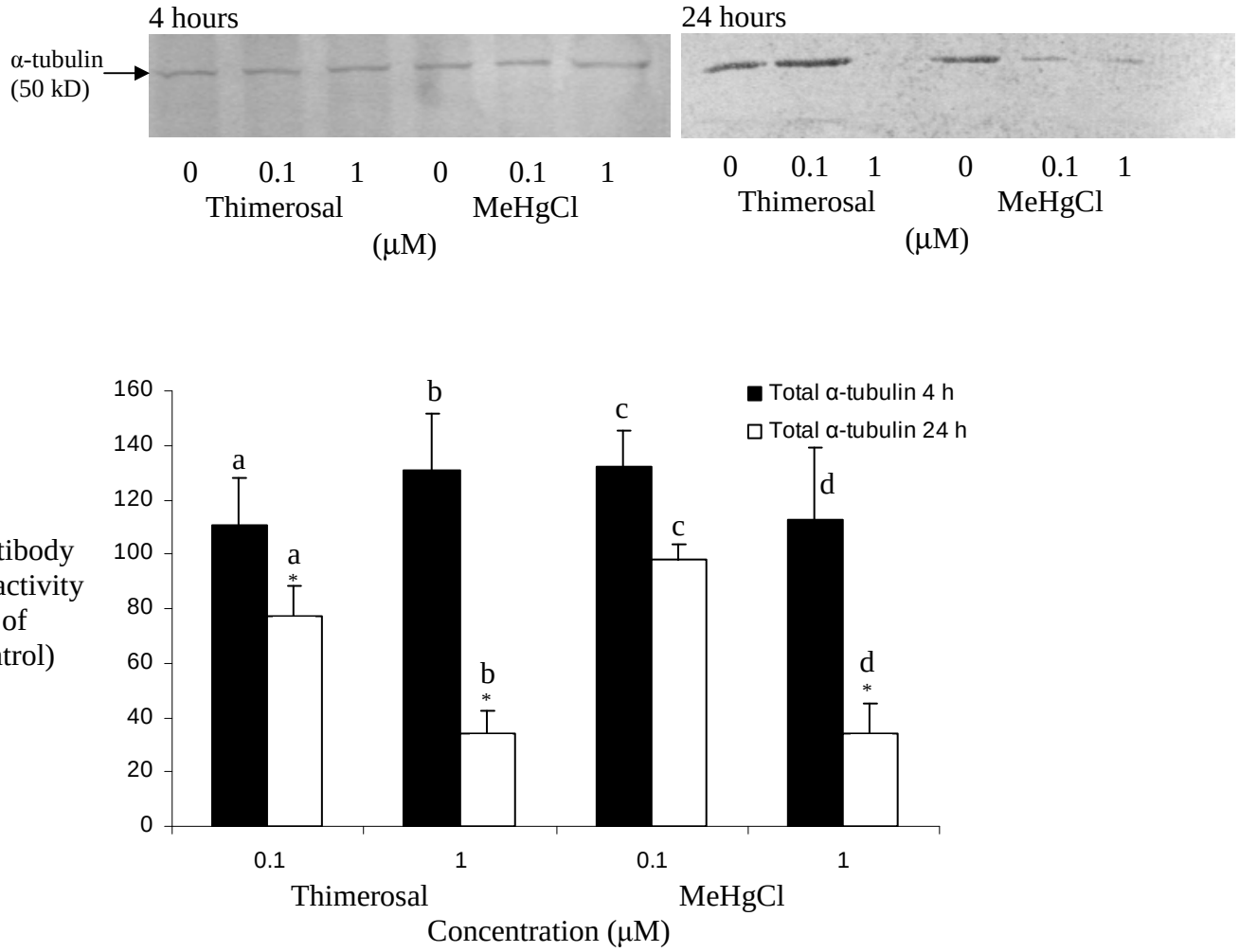

Figure 4.1.1: Western blots of lysates from the differentiated glial C6 cell line following exposure to either thimerosal and methylmercury chloride for 4 or 24 hours. The proteins were visualised using a 1/1000 dilution of the B512 anti- total α-tubulin antibody. Quantification of the antibody reactivity was carried out using AIDA software.

C6 cells were induced to differentiate for 4 and 24 hours in the presence and absence of thimerosal and MeHgCl as indicated. The resultant western blots of cell extracts were then probed with the antibodies indicated. Data represent mean levels of antibody reactivity, expressed as a percentage of difference from the corresponding control $\pm$ SEM ($n = 6$). Untreated cell extracts are indicated on the western blots by 0. Asterisks indicate statistical significance from the control (* p value <0.05). a, b, c and d indicates statistical significance between the 4 and the 24 hour data. Statistical significance was determined using a 2 way ANOVA test, followed by post hoc Bonferroni's correction for pair wise multiple analysis.

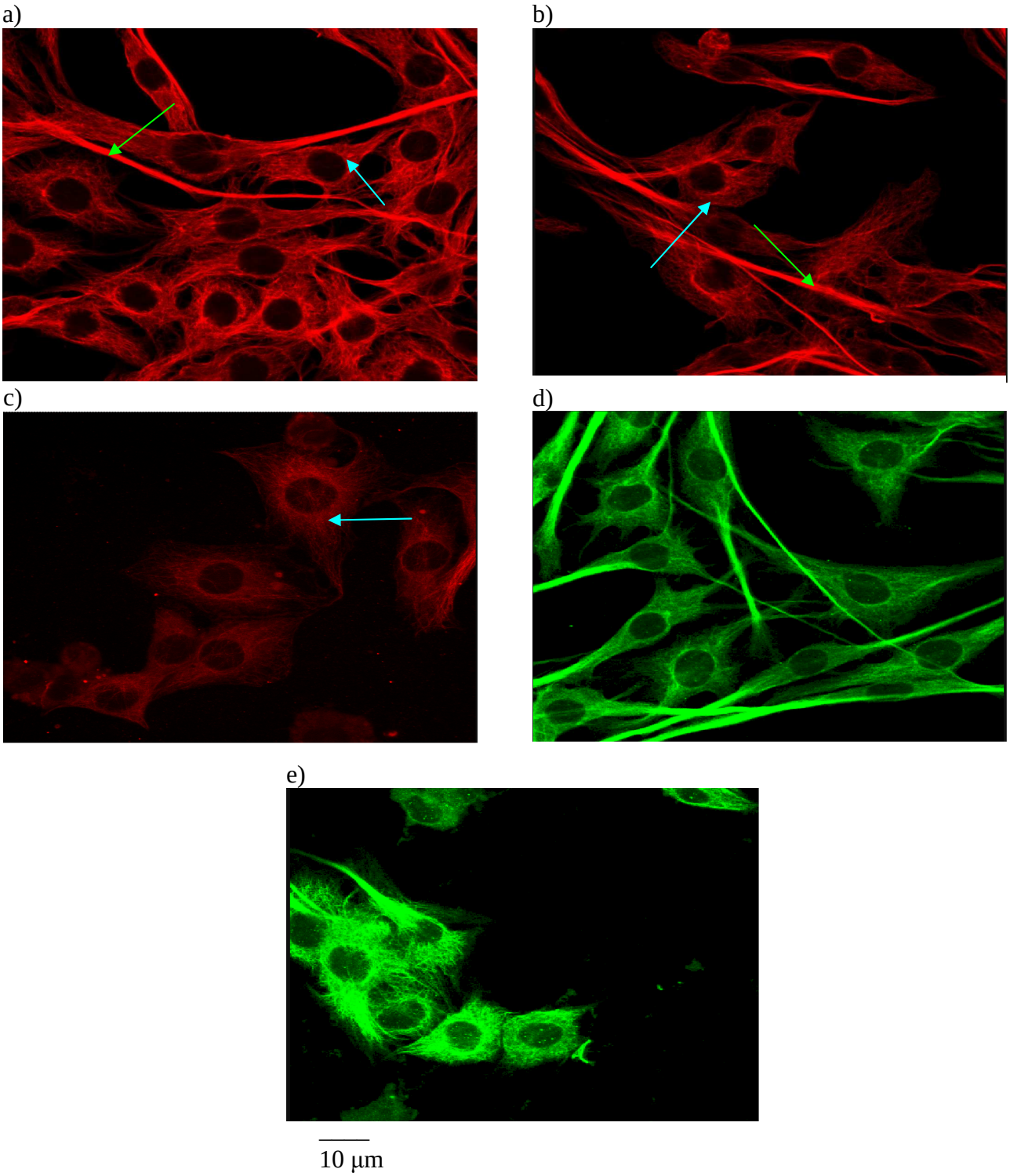

Figure 4.1.2: Immunofluorescence images of C6 cells stained with the anti-total α-tubulin antibody B512

C6 cells were induced to differentiate for 24 hours in the absence (a) or presence (b-e) of thimerosal and MeHgCl, with 0.1 (b) or 1 µM (c) of thimerosal, 0.1 (d) and 1 µM (e) MeHgCl. Cells were then fixed on a slide and stained with B512, an anti-total α-tubulin antibody as described in Methods (n = 3). Green arrows indicate cellular processes and turquoise arrows indicate tubulin networks in the cell body.

Figure 4.1.2 a shows control C6 cells differentiated for 24 hours. The MT network was clearly visible in B512 stained cells and was in organised strands around the cell body, extending in to the cellular processes. In cells that had been exposed to 0.1 µM thimerosal for 24 hours (Figure 4.1.2 b), the MT network was still clearly visible, but it appeared less organised and the staining was less intense. Cellular processes were still brightly stained at this concentration of thimerosal. Cells treated with 1 µM thimerosal exhibited reduced staining with the B512 antibody (Figure 4.1.2. c). Fragmented strands of MTs were still visible in the cell body but the staining was less intense. There were no densely stained processes such as those observed in the control cells. The MT network was less organised when compared to the control in cells exposed to 0.1 µM MeHgCl (Figure 4.1.2. d). Intense staining was still apparent in the processes but in some cells the cytoskeleton was beginning to fragment. Cells exposed to 1 µM MeHgCl were still brightly stained, unlike the cells treated with the same concentration of thimerosal (Figure 4.1.2. e), where there were no stained processes and MT architecture was disrupted by the heavy metal (Figure 4.1.2. c) The difference in the colour of the green fluorescence seen in images d-e is due to the use of a FITZ conjugated secondary antibody. The TRITZ conjugated secondary antibody that gave red fluorescence was no longer available. The secondary antibodies were the same barring their fluorescent conjugate.

The levels reactivity with the anti-tyrosinated α-tubulin antibody was not significantly altered after 4 hours of exposure to either thimerosal or MeHgCl (Figure 4.1.3). The average absorbance for antibody reactivity with the control cell extracts was 0.97332. Statistical analysis confirmed lack of statistical significance ($p = 0.0876$, 0.9654, 0.7654 and 0.8743 for 0.1 and 1 µM of thimerosal and MeHgCl respectively). The average densitometric absorbance for these concentrations was 0.84563 and 0.91145 respectively. After 24 hours of exposure, there was a significant reduction ($p<0.05$) of approximately 40 % in the reactivity of the anti-tyrosinated α-tubulin antibody with cells exposed both concentrations of thimerosal and MeHgCl. ($p = 0.0234$ and 0.0354 for 1 µM thimerosal and MeHgCl respectively). Statistical analysis confirmed that there were significant differences between the 4 and 24 hour data ($p = 0.0124$ to 0.0433).

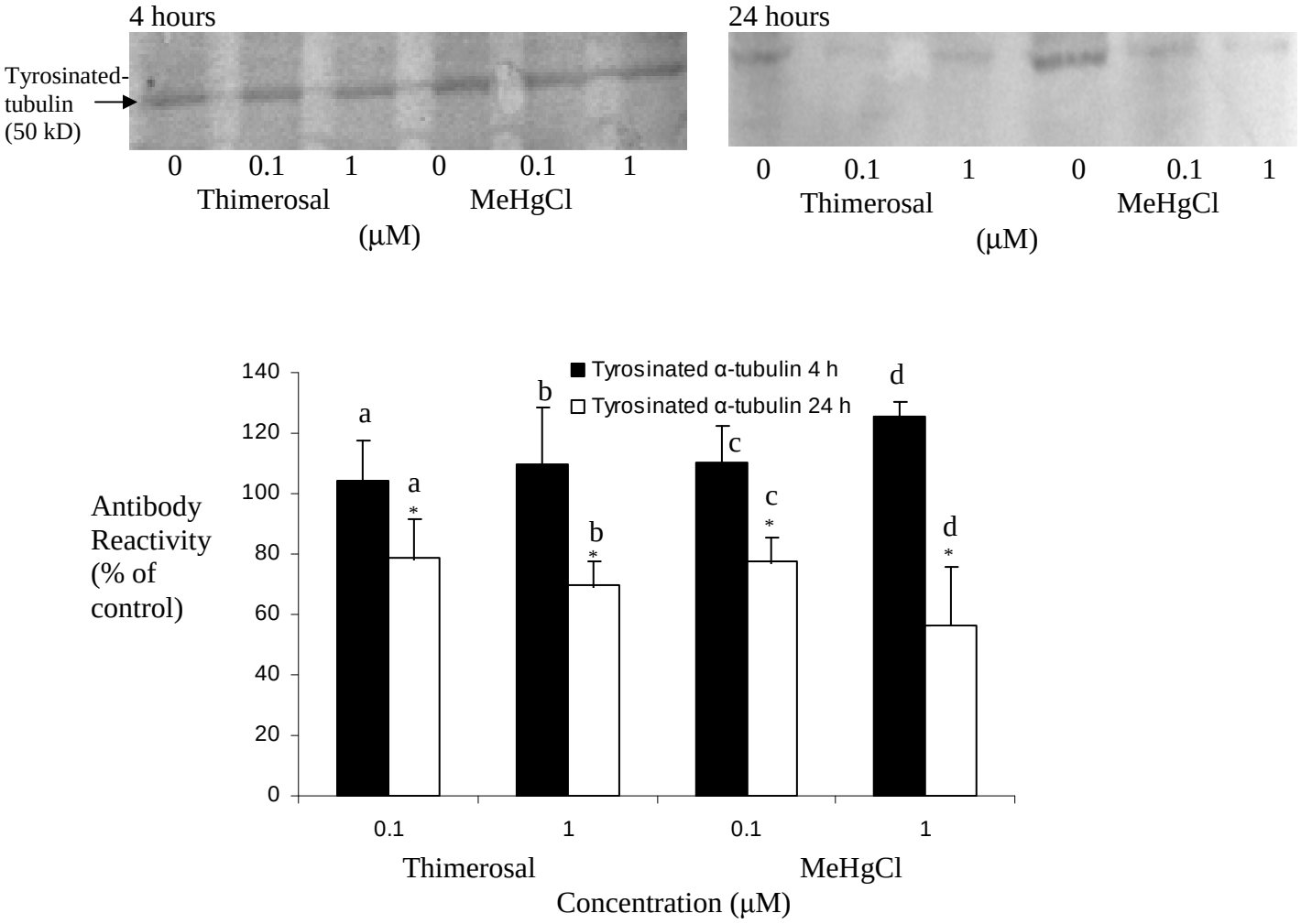

Figure 4.1.3: Western blots of lysates from the differentiated glial C6 cell line following exposure to either thimerosal and methylmercury chloride for 4 or 24 hours. The proteins were visualised using a 1/1000 dilution of the T1A2 anti- tyrosinated α-tubulin antibody. Quantification of the antibody reactivity was carried out using AIDA software.

C6 cells were induced to differentiate for 4 and 24 hours in the presence and absence of thimerosal and MeHgCl as indicated. The resultant Western blots of cell extracts were then probed with monoclonal antibody T1A2. Untreated cell extracts are indicated on the western blots by 0. Data represent mean levels of antibody reactivity, expressed as a percentage of the corresponding control + SEM (n = 6). Asterisks indicate statistical significance from the control (* p value <0.05). a, b, c and d indicates statistical significance between the 4 and the 24 hour data. Statistical significance was determined using a 2 way ANOVA test, followed by post hoc Bonferroni's correction for pair wise multiple analysis.

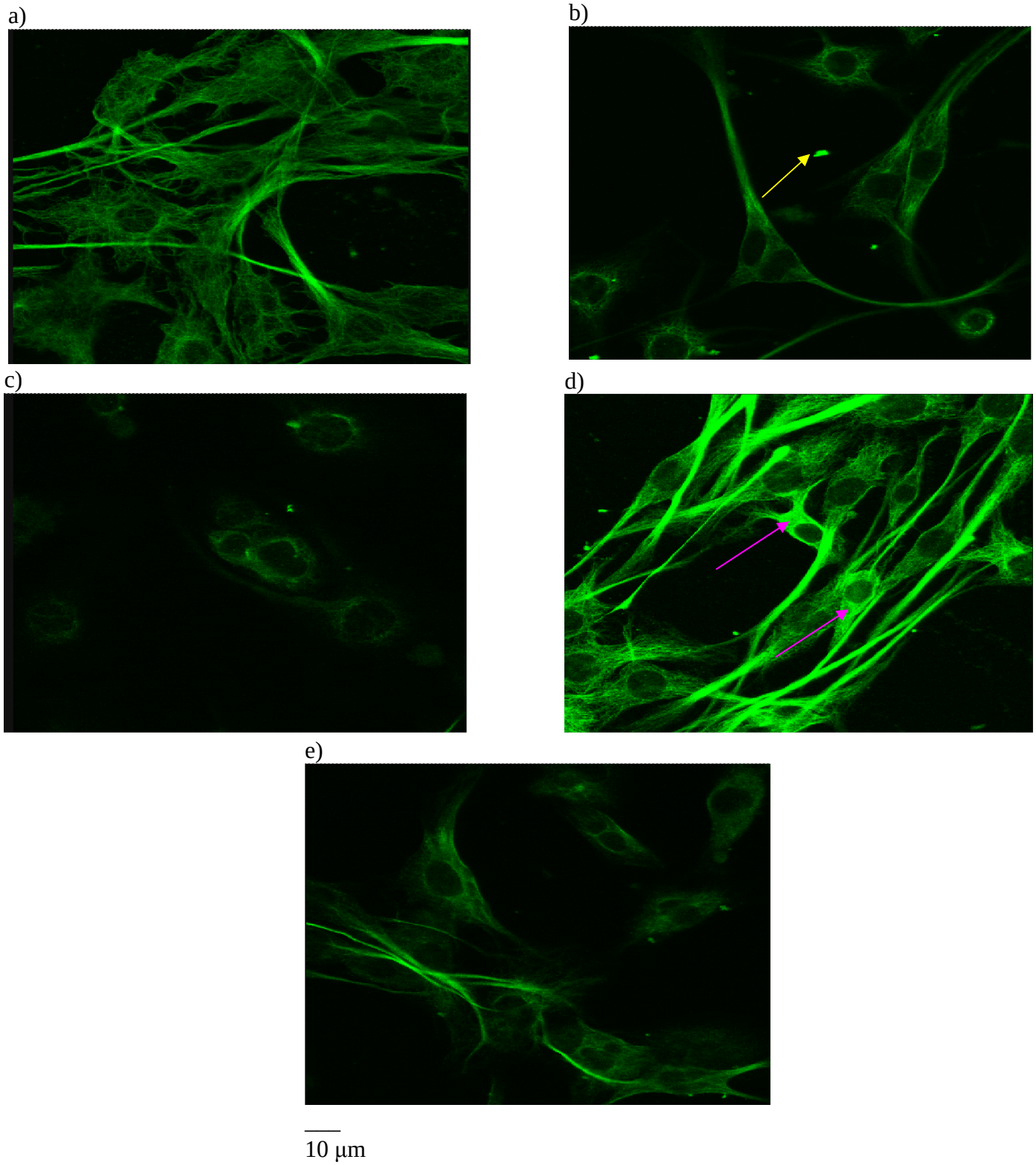

Figure 4.1.4: Immunofluorescence images of C6 cells stained with the anti-tyrosinated α-tubulin antibody T1A2

C6 cells were induced to differentiate for 24 hours in the absence (a) or presense (b-e), of 0.1 µM (b) and 1 µM (c) of thimerosal and 0.1 µM (d) and 1 µM (e) MeHgCl. The cells were stained with T1A2, an anti-tyrosinated α-tubulin antibody as described in Methods (n = 3).

Figure 4.1.4 a shows that control cells differentiated in the absence of thimerosal exhibited intense staining in the processes and the MT network in the cell body. In cells in exposed to 0.1 µM thimerosal (Figure 4.1.4 b), MT staining was less intense than that observed in control. The bright spot in the image (indicated by yellow arrow) is where the fluorescent secondary antibody had aggregated during storage. The secondary antibody was spun in a bench centrifuge but some aggregates remained. Figure 4.1.4 c shows cells treated with 1 µM thimerosal. There were no distinguishable staining processes and the MT network was disrupted. Cells exposed to 0.1 µM MeHgCl (Figure 4.1.4 d) were more intensely stained than control cells. Unlike cells exposed to the same concentration of thimerosal, there was no obvious fragmentation of the cytoskeleton. Certain cells (indicated by pink arrow) had very intense areas of staining within the cell body and the processes were brightly stained. In Figure 4.1.4 e (1 µM MeHgCl) there were no obvious changes in the intensity of the staining with the T1A2 antibody when compared to the control cells. The number of MT networks surrounding the cells was reduced after exposure to 1 µM MeHgCl. However, there did not appear to be the reduction in process staining that is seen with thimerosal. The images are representative of three separate experiments and reflect the trends seen in each individual experiment.

Analysis of Western blots probed with Tub 2.1 indicated that after 4 hours exposure there were no significant changes in the reactivity of the antibody with the C6 cell lysates (Figure 4.1.5). Statistical tests confirmed the lack of significance ($p = 0.2563$ to 0.8769). The average densitometric absorbance for the 4 hour control extracts was 0.77859. After 24 hours exposure to 0.1 µM thimerosal had no effect upon reactivity ($p = 0.7654$) but 1 µM thimerosal decreased antibody binding by approximately 25 %. A 2 way ANOVA, followed by post hoc Bonferroni's test indicated significance ($p = 0.0234$). Both concentrations of MeHgCl significantly decreased antibody reactivity by 30-40 % at this time point. A two way ANOVA test showed that there were statistically significant differences between the 4 and 24 hour data, post hoc Bonferroni's test indicated that the significant differences occurred with exposure to 0.1 µM MeHgCl and both 1 µM thimerosal and MeHgCl ($p = 0.02456$, 0.04653 and 0.01984 respectively).

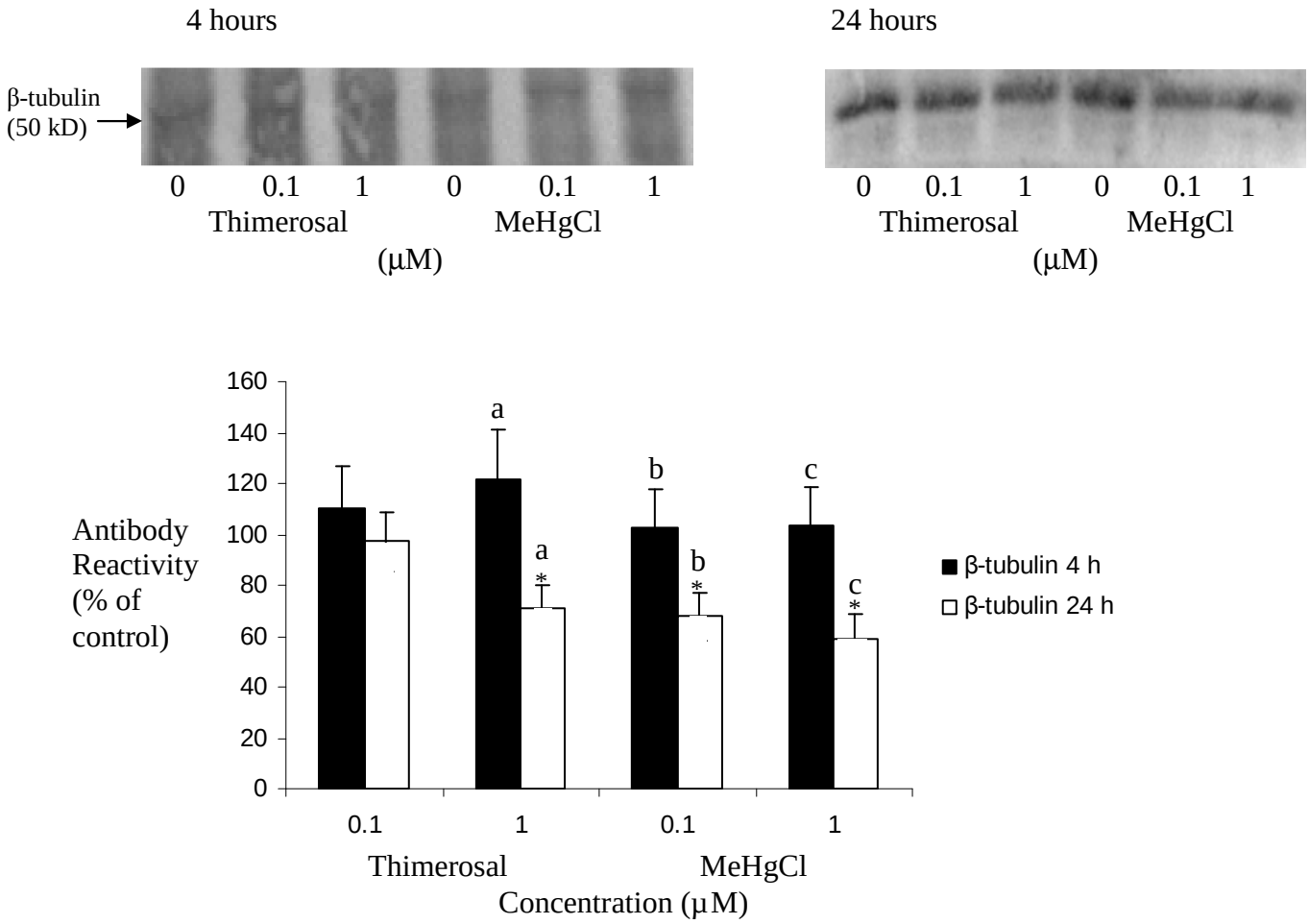

Figure 4.1.5: Western blots of lysates from the differentiated glial C6 cell line following exposure to either thimerosal and methylmercury chloride for 4 or 24 hours. The proteins were visualised using a 1/1000 dilution of the Tub 2.1 anti- total β-tubulin antibody. Quantification of the antibody reactivity was carried out using AIDA software.

C6 cells were induced to differentiate for 4 and 24 hours in the presence and absence of thimerosal and MeHgCl as indicated. The resultant Western blots were then probed with the antibodies indicated. Untreated cell extracts are indicated on the western blots by 0. Data represent mean levels of antibody reactivity, expressed as a percentage of the corresponding control $\pm$ SEM (n = 5). Asterisks indicate statistical significance from the control (* p value <0.05). a, b and c indicates statistical significance between the 4 and the 24 hour data. Statistical significance was determined using a 2 way ANOVA test, followed by post hoc Bonferroni's correction for pair wise multiple analysis.

4.2: Western blot analysis and immunofluorescent staining of microtubule and neurofilament proteins in N2a cells treated with thimerosal and methylmercury chloride

Exposure to 0.1 µM thimerosal had no significant affect upon antibody binding at either 4 or 24 hours ($p = 0.9354$ and 0.3556) (Figure 4.2.1). The average densitometric absorbance for antibody reactivity with control N2a cell extracts was 0.6438. Exposure to 1 µM thimerosal had no effect at 4 hours ($p = 0.4534$) but after 24 hours incubation, antibody reactivity was significantly reduced by approximately 78 % of control values. The average absorbance with this concentration was 0.2148. Neither MeHgCl concentration had an effect upon antibody reactivity at 4 hours (p values 0.45342 and 0.0786) but after 24 hours incubation, 0.1 µM and 1 µM MeHgCl significantly reduced band intensity by 46 % and 67 %, respectively ($p = 0.0442$ and 0.0243). Statistical tests showed that there were significant differences in the effects seen at 4 and 24 hours with both concentrations of MeHgCl and the higher concentration of thimerosal

Figure 4.2.2 (a) shows immunofluorescence staining of control cells differentiated for 24 hours in the absence of thimerosal or MeHgCl. The cells displayed clear tubulin networks around the nucleus of the cell and in some cells, the microtubule organising centre can be visualised as an intense spot located near the nucleus (indicated by the yellow arrows). The axon-like processes were clearly visible and were intensely stained as areas with high levels of tubulin. Figure 4.2.2 (b) shows differentiating N2a cells exposed to 0.1 µM thimerosal. The axons were still visible and brightly stained, as was the microtubule organising centre. In some cells the MT network was losing organisation and spreading out. Figure 4.2.2 (c) shows cells exposed to 1 µM thimerosal. The staining was weak in both the cell body and the neurites. Microtubule organising centres were no longer clearly visible.

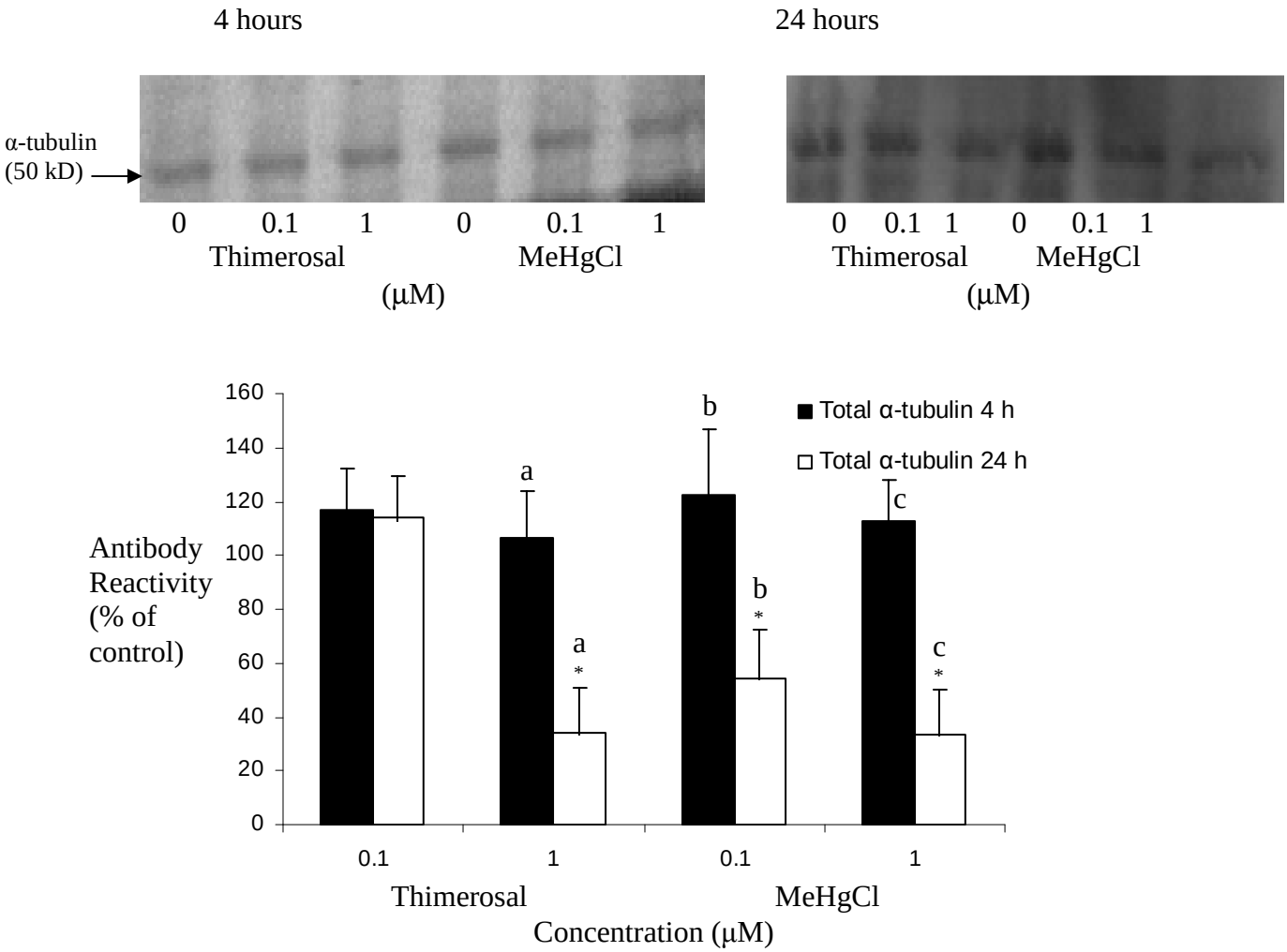

Figure 4.2.1: Western blots of lysates from the differentiated neuronal N2a cell line following exposure to either thimerosal and methylmercury chloride for 4 or 24 hours. The proteins were visualised using a 1/1000 dilution of the B512 anti- total α-tubulin antibody. Quantification of the antibody reactivity was carried out using AIDA software.

N2a cells were induced to differentiate for 4 and 24 hours in the presence and absence of thimerosal and MeHgCl as indicated, then separated by SDS PAGE and Western blotting as described in Methods. Untreated cell extracts are indicated on the western blots by 0. Data represents mean levels of antibody reactivity, expressed as a percentage of the corresponding control $\pm$ SEM (n = 6). Asterisks indicate statistical significance from the control (* p value <0.05). a, b and c indicates statistical significance between the 4 and the 24 hour data. Statistical significance was determined using a 2 way ANOVA test, followed by post hoc Bonferroni's correction for pair wise multiple analysis.

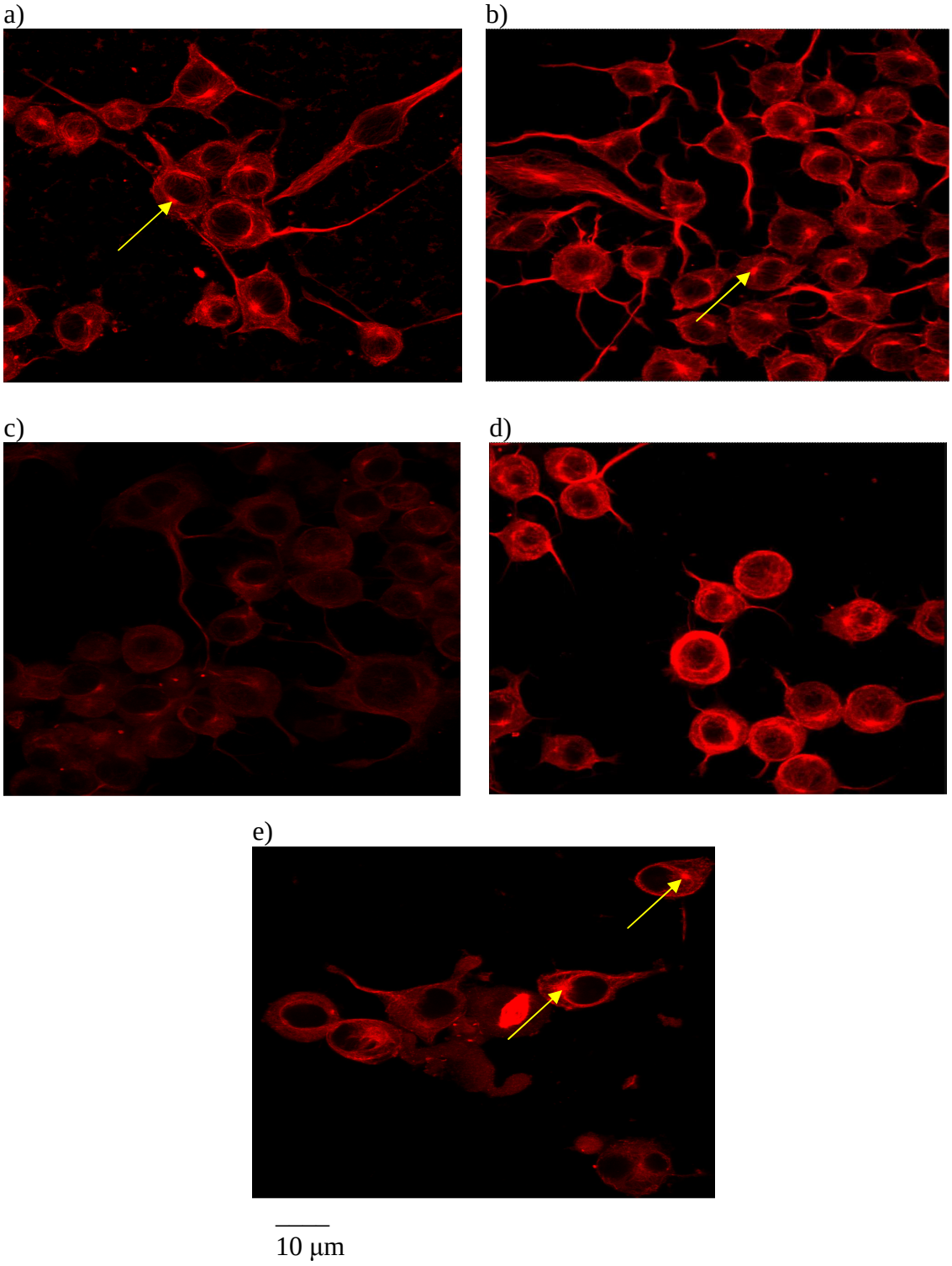

Figure 4.2.2: Immunofluorescence images of N2a cells stained with the anti-total α-tubulin antibody B512

N2a cells were induced to differentiate for 24 hours in the absence (a) or presence (b-e) of 0.1 µM (b) and 1 µM (c) of thimerosal and 0.1 µM (d) and 1 µM (e) MeHgCl. The cells were stained with B512, an anti-total α-tubulin antibody as described in Methods (n = 3).

The cells incubated with 0.1 µM MeHgCl have stunted axon-like processes and the MT network appeared to randomly cover the whole cell (Figure 4.2.2. d). There were visible microtubule organising centres in the image as well as some areas of intense fluorescence, where there appeared to be high levels antibody staining. Cells exposed to 1 µM MeHgCl (Figure 4.2.2. e) have weaker staining than in the control (Figure 2.2.a). There was patchy staining along the axon-like processes and in the cell body, where the MT network staining appeared to have fragmented. There was still some staining of microtubule organising centres in 2 of the cells (indicated by the yellow arrows). The images are representative of three separate experiments and reflect the major trends seen in each one.

Densitometric analysis shown in Figure 4.2.3 shows that 0.1 µM thimerosal had no significant effect upon the reactivity of the anti-tyrosinated α-tubulin antibody at either 4 or 24 hours ($p = 0.0678$ and 0.9756 for 4 and 24 hours respectively). The average absorbance obtained from the densitometry was 0.799342 for the control extracts and 0.482618 for cell lysates exposed to 1 µM thimerosal for 4 hours. Exposure to 1 µM thimerosal caused a significant reduction ($p<0.05$) of 55 % in band intensity at 4 hours and a 46 % reduction after 24 hours. Exposure to 0.1 µM MeHgCl for 4 hours caused a significant reduction of 42- 44 % in antibody reactivity after 4 hours ($p = 0.0445$) and 24 hours ($p = 0.0265$). Statistical analysis of the data obtained from the two incubation times indicated that there were no significant differences between the effects seen at 4 and 24 hours ($p = 0.9756$).

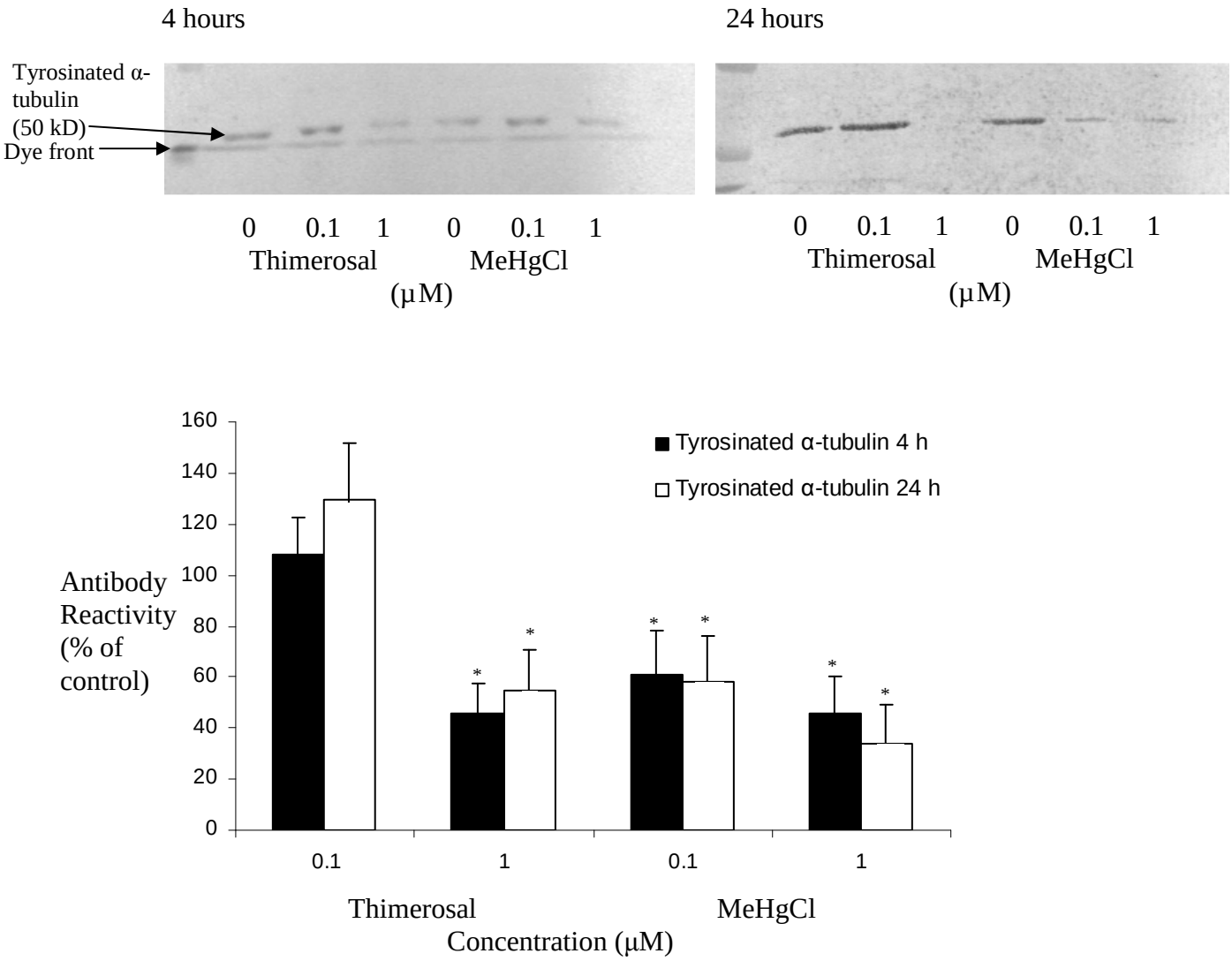

Figure 4.2.3: Western blots of lysates from the differentiated neuronal N2a cell line following exposure to either thimerosal and methylmercury chloride for 4 or 24 hours. The proteins were visualised using a 1/1000 dilution of the T1A2 anti-tyrosinated α-tubulin antibody. Quantification of the antibody reactivity was carried out using AIDA software.

N2a cells were induced to differentiate for 4 and 24 hours in the presence and absence of thimerosal and MeHgCl as indicated, then separated by SDS PAGE and Western blotting as described in Methods. Untreated cell extracts are indicated on the western blots by 0. Data represents mean levels of antibody reactivity, expressed as a percentage of the corresponding control $\pm$ SEM (n = 6). Asterisks indicate statistical significance from the control (* p value <0.05). Statistical significance was determined using a 2 way ANOVA test, followed by post hoc Bonferroni's correction for pair wise multiple analysis.

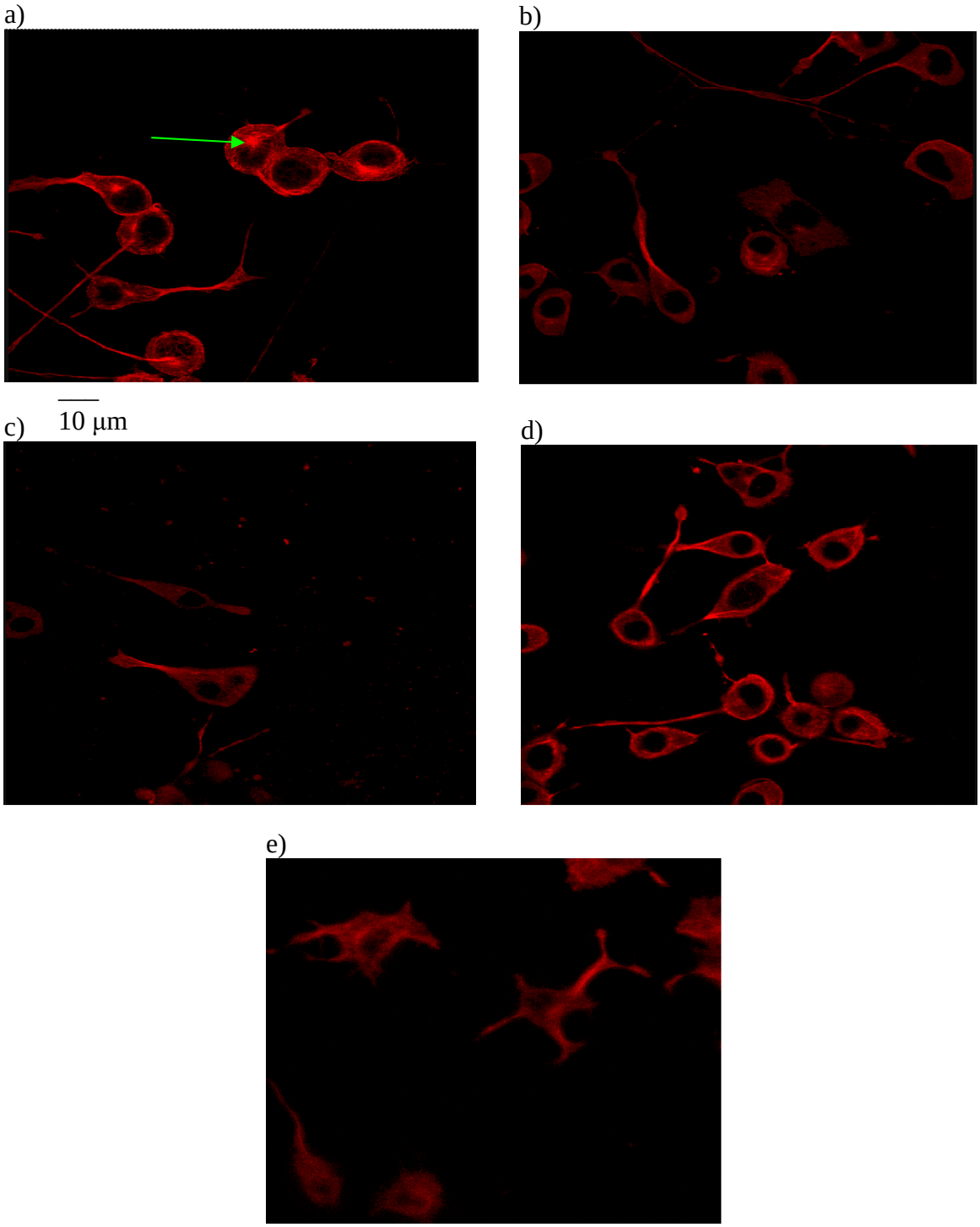

Figure 4.2.4: Immunofluorescence images of N2a cells stained with the anti-tyrosinated α-tubulin antibody T1A2

N2a cells were induced to differentiate for 24 hours in the absence (a) or presence (b-e) of 0.1 µM (b) and 1 µM (c) thimerosal and 0.1 µM (d) and 1 µM (e) MeHgCl. The cells were stained with T1A2, an anti-tyrosinated α-tubulin antibody as described in Methods (n = 3).

Figure 4.2.4 (a-e) shows immunofluorescence staining with the anti-tyrosinated α-tubulin antibody T1A2. The images shown are representative of typical trends obtained from 3 separate experiments. Figure 4.2.2a shows control N2a cells differentiated for 24 hours in the absence of thimerosal or MeHgCl. The cells had clearly stained networks of tyrosinated α-tubulin within the cell body and densely stained long axon-like processes. The microtubule organising centre was clearly visible within the cell (indicated by green arrow). Figure 4.2.4 (b) shows cells treated with 0.1 µM thimerosal. Staining with T1A2 appeared less intense within the axon and the cell body compared to the control. The microtubule organising centre was no longer visible within the cells and the microtubule arrays were less defined. The cells in figure 4.2.4 (c) had been exposed to 1 µM thimerosal for 24 hours. Again, the staining was weaker than that seen in untreated cells (image a). Whilst axon-like processes were still visible they had patchy staining and appeared broken instead of a continuous strand. Cells exposed to 0.1 µM MeHgCl had less visibly stained strands of tyrosinated α-tubulin (Figure 4.2.4. d). The microtubule organising centre was not visible within the cells at this concentration of MeHgCl. The cells in Figure 4.2.4 (e) had been incubated with 1 µM MeHgCl for 24 hours. The tyrosinated α-tubulin network had disintegrated, there were no visible strands. There were some neurites that were weakly stained for tubulin but they were deformed when compared to the untreated cells in image (a).

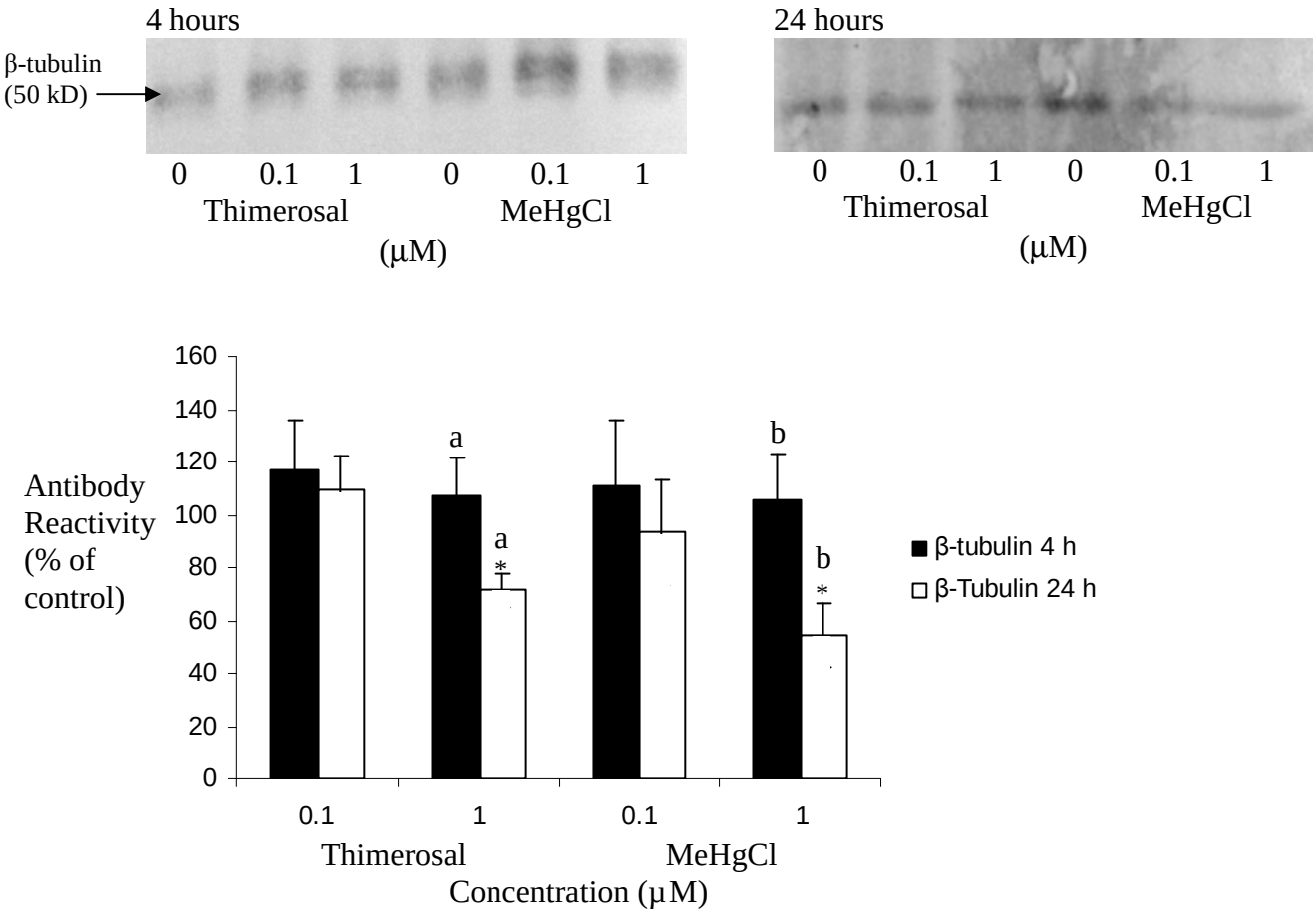

Figure 4.2.5: Western blots of lysates from the differentiated neuronal N2a cell line following exposure to either thimerosal and methylmercury chloride for 4 or 24 hours. The proteins were visualised using a 1/1000 dilution of the Tub2.1 anti-total β-tubulin antibody. Quantification of the antibody reactivity was carried out using AIDA software.

N2a cells were induced to differentiate for 4 and 24 hours in the presence and absence of thimerosal and MeHgCl as indicated, then separated by SDS PAGE and Western blotting as described in Methods. Untreated cell extracts are indicated on the western blots by 0. Data represent mean levels of antibody reactivity, expressed as a percentage of the corresponding control $\pm$ SEM (n = 6). Asterisks indicate statistical significance from the control (* p value <0.05). a, and b ndicates statistical significance between the 4 and the 24 hour data. Statistical significance was determined using a 2 way ANOVA test, followed by post hoc Bonferroni's correction for pair wise multiple analysis.

Figure 4.2.5 shows that after 4 hours there were no significant differences with either concentration of the 2 compounds. Statistical analysis using a 2 way ANOVA test confirmed that there were no significant changes in antibody reactivity when compared to the control ($p = 0.07867$). After 24 hours of exposure to 0.1 μM thimerosal and MeHgCl, there were also no changes in antibody reactivity. Post hoc

Statistical analysis using a two way ANOVA test, followed by Bonferroni's test indicated that there was a significance differences between the effect seen after 4 and 24 hours of exposure to 1 µM of both thimerosal and MeHgCl ($p = 0.032131$and 0.008956 for thimerosal and MeHgCl respectively).

Figure 4.2.6 shows densitometric analysis of western blots probed for total NFH. The average absorbance obtained for the control extracts was 0.59527 and 0.58852 for 4 and 24 hours respectively. The data indicated that after 4 hours incubation time with thimerosal and MeHgCl there was no alteration in the intensity of the bands when compared to the control. A 2 way ANOVA test confirmed the lack of statistical significance from the control ($p = 0.78695$). After 24 hours there was a reduction in the reactivity of the antibody with cells exposed to both thimerosal and MeHgCl. The band intensity was significantly reduced by around 35 % when treated with thimerosal. MeHgCl significantly reduced antibody reactivity by 32 - 40 %. Statistical analysis highlighted significant differences in the data obtained from the 4 and 24 hour exposure times for all concentrations. A comparison of the data obtained from exposure to 1 µM of both thimerosal and MeHgCl ($p = 0.002439$ and 0.004543 respectively).

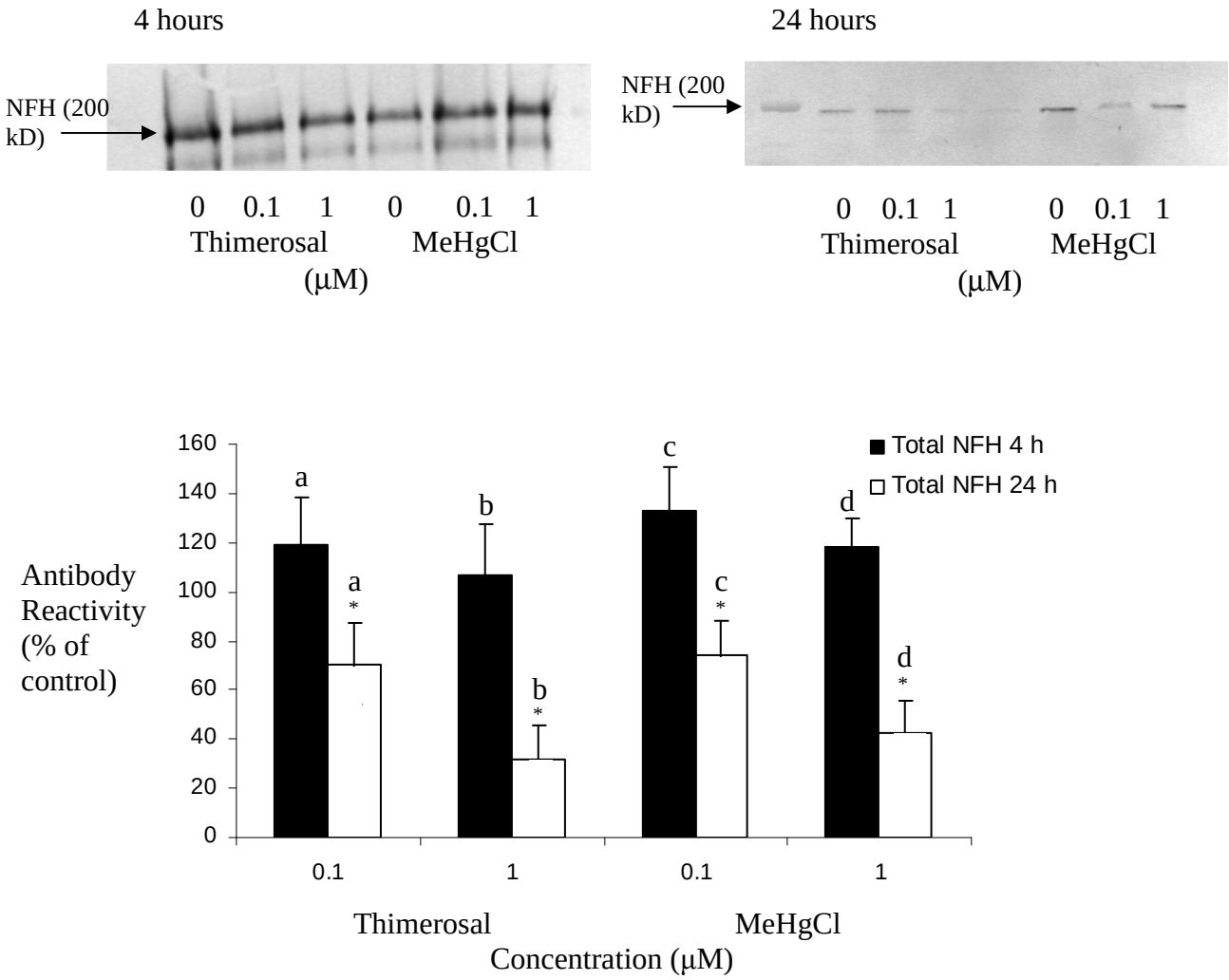

Figure 4.2.6: Western blots of lysates from the differentiated neuronal N2a cell line following exposure to either thimerosal and methylmercury chloride for 4 or 24 hours. The proteins were visualised using a 1/1000 dilution of the N52 anti-total NFH antibody. Quantification of the antibody reactivity was carried out using AIDA software.

N2a cells were induced to differentiate for 4 (a) and 24 (b) hours in the presence and absence of thimerosal and MeHgCl as indicated, then separated by SDS PAGE and Western blotting as described in Methods. Untreated cell extracts are indicated on the western blots by 0. Data represents mean levels of antibody reactivity, expressed as a percentage of the corresponding control + SEM (n = 6). Asterisks indicate statistical significance from the control (* p value <0.05). a, b, c and d indicates statistical significance between the 4 and the 24 hour data. Statistical significance was determined using a 2 way ANOVA test, followed by post hoc Bonferroni's correction for pair wise multiple analysis.

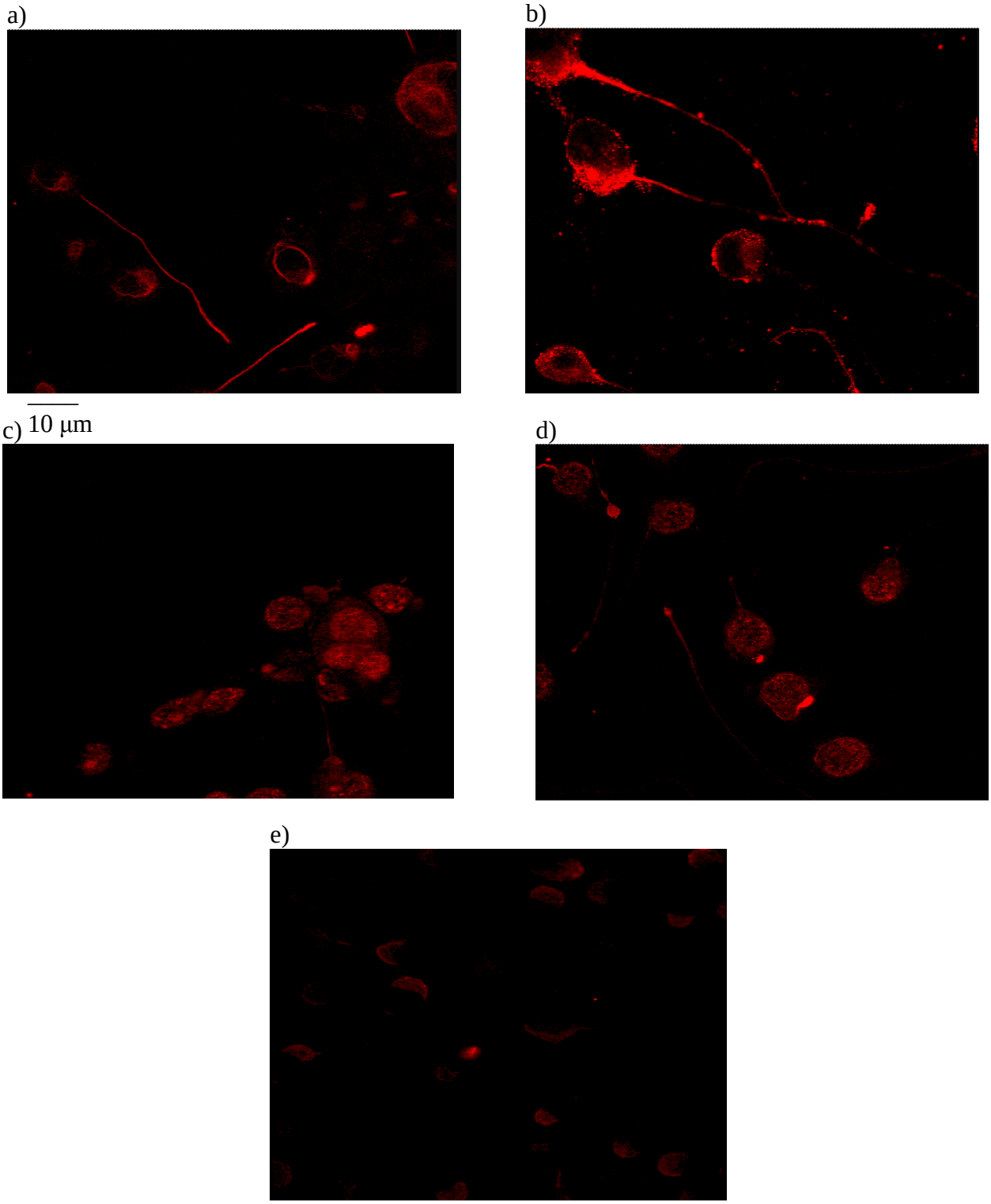

Figure 4.2.7: Immunofluorescence images of N2a cells stained with the anti-total NFH antibody N52

N2a cells were induced to differentiate for 24 hours in the absence (a) or presence (b-e) of 0.1 µM (b) and 1 µM (c) thimerosal and 0.1 µM (d) and 1 µM (e) MeHgCl. The cells were stained with N52, an anti-total NFH antibody as described in Methods (n = 3).

Differentiated control N2a cells stained with an anti-total NFH antibody were heavily stained with the anti-total NFH antibody, as were certain areas within the cell body (Figure 4.2.7. a). After exposure to 0.1 µM thimerosal (Figure 4.2.7 b), intensely stained neurites were still visible but it appeared that the distribution of the staining had changed. The axon staining was fragmented and within the cell body there were areas where the antibody stain was more intense. Exposure to 1 µM thimerosal (Figure 4.2.7 c) reduced the staining within the neurites. The staining within the cells became widespread instead of being localised to certain areas as it was in control cells (a). After 24 hours of exposure to 0.1 µM MeHgCl (Figure 4.2.7 d) axon staining was still visible but they were more weakly stained than in the control cells. Also NFH staining filled the whole of the cell body instead of the discrete areas that were observed in the control cells. Figure 4.2.7 e shows cells treated with 1 µM MeHgCl. The cells were weakly stained and there were no visible axons.

Densitometric analysis in Figure 4.2.8 of western blots prepared from N2a cell extracts and probed with the anti-phosphorylated NFH antibody RT97 showed that band intensity was unaffected by 0.1 µM thimerosal after 4 hours exposure ($p = 0.67534$). The average densitometric absorbance for the control cells after 4 hours of differentiation was 0.720843. Exposure to 1 µM thimerosal and both concentrations of MeHgCl for 4 hours did significantly reduce antibody binding by 60-70 %. Statistical analysis confirmed significance ($p = 0.02562$- 0.04532). Exposure to both compounds for 24 hours significantly reduced antibody reactivity by 20-60 % at both concentrations. A 2 way ANOVA test comparing the 4 and 24 hour data confirmed that there significant differences in the data obtained from the 2 time points. Post hoc Bonferroni's test confirmed that there were significant differences with the 0.1 µM data with both compounds ($p = 0.02243$ and 0.035422 for 0.1 µM thimerosal and MeHgCl respectively).

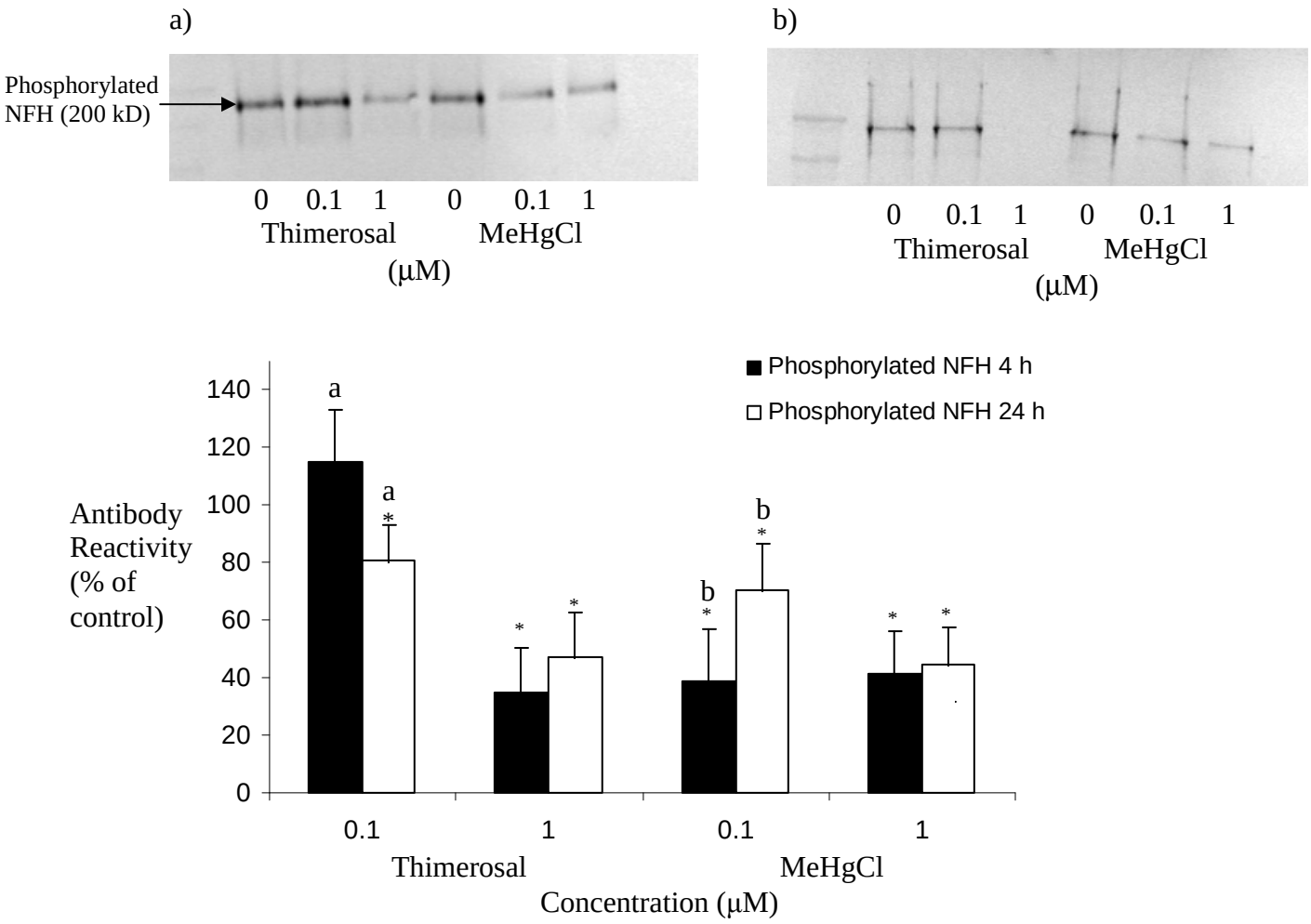

Figure 4.2.8: Western blots of lysates from the differentiated neuronal N2a cell line following exposure to either thimerosal and methylmercury chloride for 4 or 24 hours. The proteins were visualised using a 1/1000 dilution of the RT97 anti-phosphorylated NFH antibody. Quantification of the antibody reactivity was carried out using AIDA software.

N2a cells were induced to differentiate for 4 and 24 hours in the presence and absence of thimerosal and MeHgCl as indicated, then separated by SDS PAGE and Western blotting as described in Methods. Untreated cell extracts are indicated on the western blots by 0. Data represent mean levels of antibody reactivity, expressed as a percentage of the corresponding control $\pm$ SEM (n = 6). Asterisks indicate statistical significance from the control (* p value <0.05). a and b indicates statistical significance between the 4 and the 24 hour data. Statistical significance was determined using a 2 way ANOVA test, followed by post hoc Bonferroni's correction for pair wise multiple analysis.

Figure 4.2.9 (a) shows control cells differentiated for 24 hours in the absence of thimerosal or MeHgCl and stained with RT97. The cells were brightly stained for phosphorylated NFH in certain areas of the cell body and long stained axon-like processes extending from the cell body. Exposure to 0.1 µM thimerosal (Figure 4.2.9 b) strengthened the intensity of the staining in the cell body. At this concentration the cells did not exhibit significant staining in long neurites. There was one extremely stunted outgrowth visible indicated by the yellow arrow. Incubation with 1 µM thimerosal (Figure 4.2.9c) dramatically reduced the visible staining within the cells and prevented staining of the axon-like processes. MeHgCl exposure caused patchy staining within the cell body at 0.1 µM (Figure 4.2.9 d). The cells produced a number of axon-like processes that were brightly stained for phosphorylated NFH and there was also evidence of aggregate staining within the cell body. Figure 4.2.9 e shows cells exposed to 1 µM MeHgCl, which inhibited axon production and staining within the cell body was patchy with areas of intense staining where the antibody has accumulated. The images are representative of the major trends seen with three separate experiments.

The densitometric analysis contained in Figure 2.4.10 shows that 0.1 µM thimerosal had no effect on band intensity at 4 or 24 hours ($p = 0.56748$ and 0.09833 for 4 and 24 hours respectively). However exposure to 1 µM thimerosal caused a significant reduction of approximately 30 % compared to the control at both 4 hours and 24 hours. The average densitometric absorbance obtained for the reactivity of the antibody with control extracts for both 4 and 24 was 0.76851 and 0.89413 respectively. Exposure to 0.1 µM MeHgCl caused approximately a 35-38 % reduction in antibody reactivity. Statistical analysis confirmed significance from the control ($p = 0.04542$ and 0.01784 for 4 and 24 hours respectively). Exposure to 1 µM MeHgCl caused a 30 % reduction in band intensity after 4 hours and a 35 % reduction after 24 hours. A 2 way ANOVA test indicated that there were no significant differences between the 4 and 24 hour data ($p = 0.95674$).

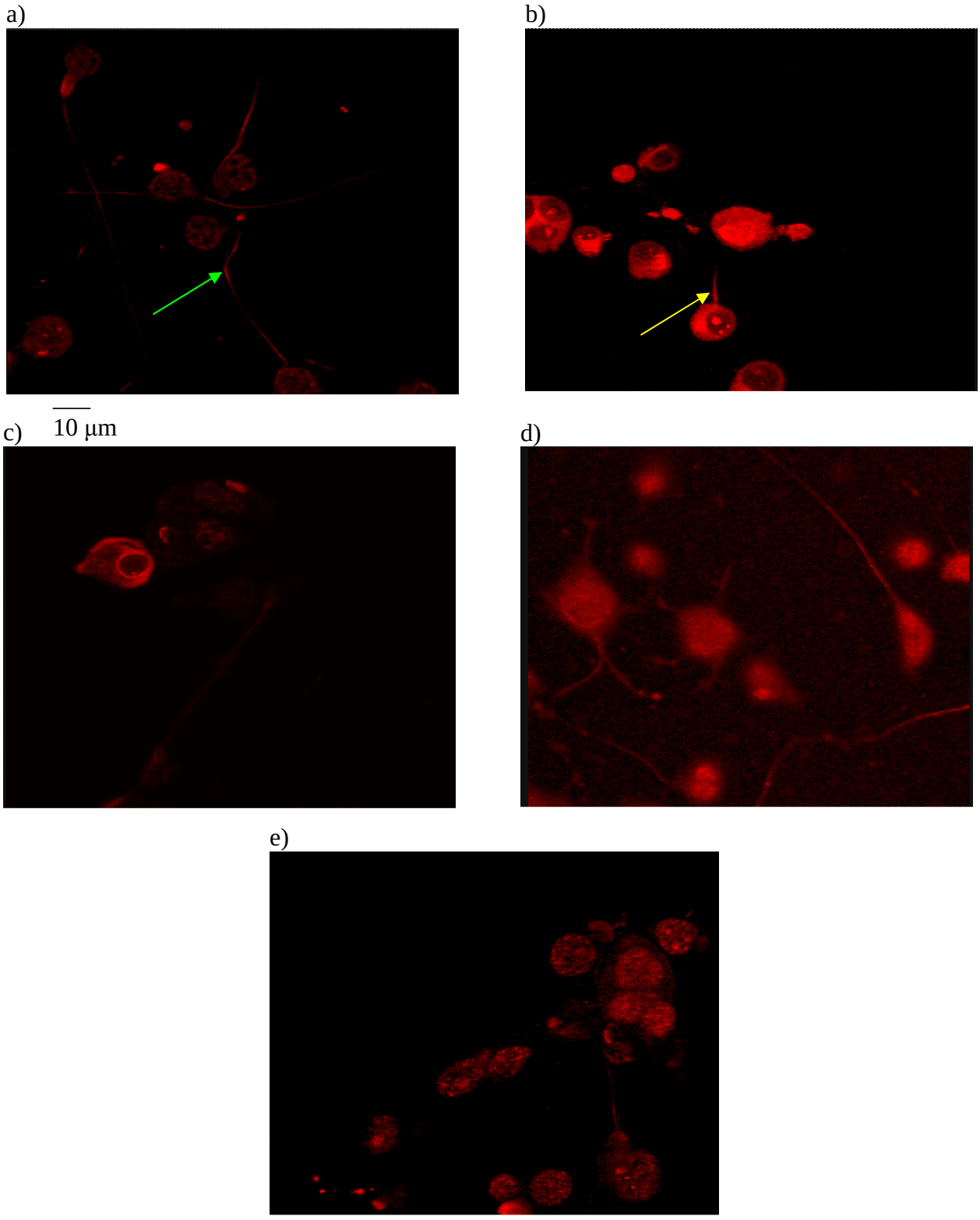

Figure 4.2.9: Immunofluorescence images of N2a cells stained with the anti-phosphorylated NFH antibody RT97

N2a cells were induced to differentiate for 24 hours in the absence (a) or presence (b-e) of 0.1 µM (b) and 1 µM (c) thimerosal and 0.1 µM (d) and 1µM (e) methylmercury chloride. The cells were stained with RT97, an anti-phosphorylated NFH antibody as described in Methods (n = 3).

Figure 4.2.11 (a) shows N2a cells differentiated in the absence of thimerosal or MeHgCl. The cells were brightly stained with SMI 34 in both the cell body and within the long neurites. The image showed a number of long axon-like processes (indicated by green arrows) that had a greater intensity of staining than the majority of the cell bodies. There were also visible patches of very brightly stained areas within the cell body, highlighting areas that have a greater level of phosphorylated NFH (indicated by blue arrows). The cells in Figure 4.2.11 (b) were exposed to 0.1 µM thimerosal for 24 hours. There was less neurite staining in Figure 4.2.11 (b) when compared to the control Figure 4.2.11 (a). The cell body also had more intense spots of fluorescence spread over the whole of the cell body instead of the patches seen in Figure 4.2.11 (a). Figure 4.2.11 (c) shows cells exposed to 1 µM thimerosal for 24 hours. There was only 1 visibly stained short neurite and there were a number of weakly stained cells that appeared to be fragmenting. In addition there were some intensely stained cells. Figure 4.2.11 (d) shows cells exposed to 0.1 µM MeHgCl for 24 hours. The axon-like processes in this image were malformed with clumps of fluorescence along the length of axon-like process. Within the cell body there were small areas of intense staining distinct from those in cells exposed to 0.1 µM thimerosal. Figure 4.2.11 (e) shows cells exposed to 1 µM MeHgCl for 24 hours. There were no visible neurites and the cells were weakly stained barring some bright areas.

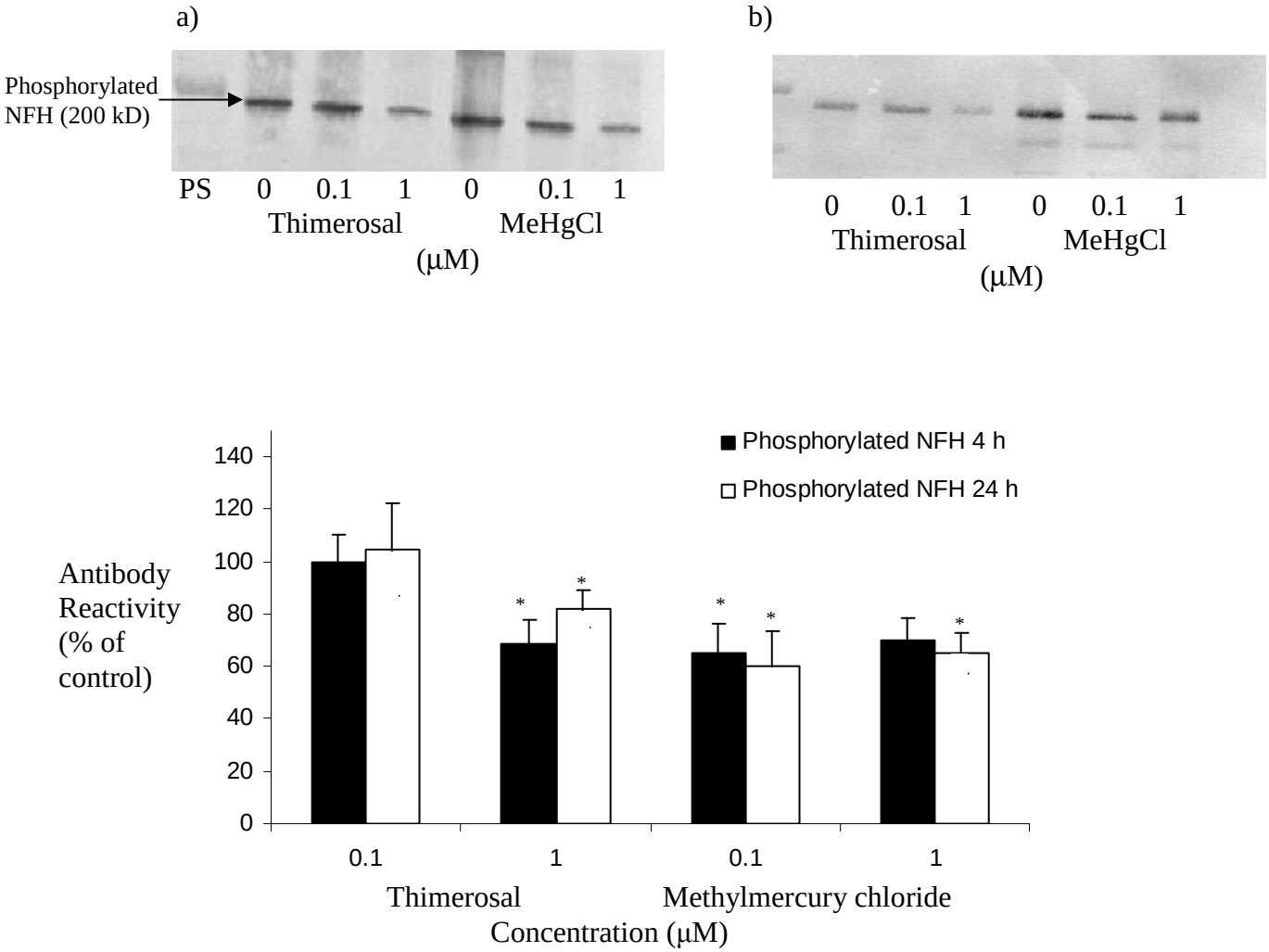

Figure 4.2.10: Western blots of lysates from the differentiated neuronal N2a cell line following exposure to either thimerosal and methylmercury chloride for 4 or 24 hours. The proteins were visualised using a 1/1000 dilution of the SMI 34 anti-phosphorylated NFH antibody. Quantification of the antibody reactivity was carried out using AIDA software.

N2a cells were induced to differentiate for 4 and 24 hours in the presence and absence of thimerosal and MeHgCl as indicated, then separated by SDS PAGE and Western blotting as described in Methods. Untreated cell extracts are indicated on the western blots by 0 and PS indicates the protein standards. Data represents mean levels of antibody reactivity, expressed as a percentage of the corresponding control $\pm$ SEM (n = 6). Asterisks indicate statistical significance of difference from the control (* p value <0.05). Statistical analysis was carried out using a 2 way ANOVA test, followed by post hoc Bonferroni's correction for pair wise multiple analysis.

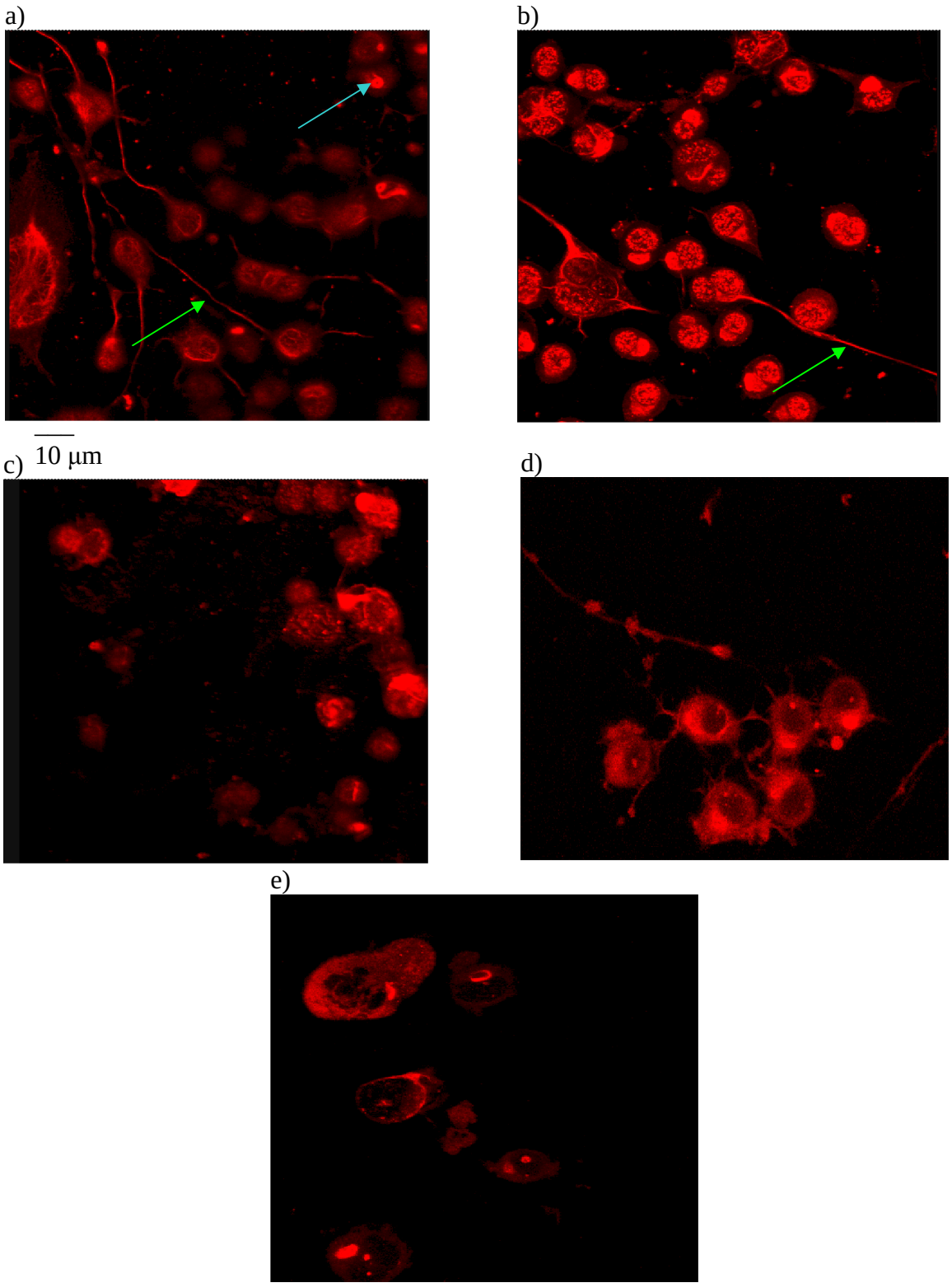

Figure 4.2.11: Immunofluorescence images of N2a cells stained with the anti-phosphorylated NFH antibody SMI 34

N2a cells were induced to differentiate for 24 hours in the absence (a) or presence (b-e) of 0.1 µM (b) and 1 µM (c) thimerosal and 0.1 µM (d) and 1 µM (e) methylmercury chloride. The cells were stained with SMI 34, an anti-phosphorylated NFH antibody as described in Methods (n = 3).

4.3 Discussion

The reduction in neurite outgrowth caused by exposure to the organic mercury compounds, thimerosal and MeHgCl indicated that these two compounds had a detrimental effect upon the production of cellular processes by some unknown mechanism (Chapter 3). This chapter aimed to determine whether this unknown mechanism of inhibition was due to the ability of thimerosal and MeHgCl to interfere with cytoskeletal proteins, a major component of both the processes produced by C6 cells and N2a cells.

Previous studies have determined that incubation with 5 µM MeHgCl for 3 hours causes the complete disappearance of microtubules in mouse glioma cells and rat pheochromocytoma cells (Miura & Imura, 1989; Miura *et al.*, 1999). Experiments in this chapter determined that lower concentrations of 0.1 and 1 µM of both MeHgCl and thimerosal caused disruption of the microtubule network in N2a and C6 cells without its complete disintegration.

Western blots of C6 cells probed with antibodies against total α-tubulin and tyrosinated α-tubulin have shown that after 4 hours there was no change in the levels of total α-tubulin (see Figure 4.1.1 (a) and 4.1.2), or tyrosinated α-tubulin (see Figure and 4.1.5). After exposing C6 cells to the organic mercury compounds for 24 hours western blot analysis indicated that there was a reduction in the levels of both total (see Figure 4.1.1 (b) and 4.1.2) and tyrosinated α-tubulin (see Figures 4.1.4 (b) and 4.1.5.). Normally the levels of total α-tubulin would not change as the tubulin subunits are constantly being replenished to keep the pool of unpolymerised tubulin the same. However polymerisation of MTs does not occur if the levels of free tubulin drops too low (Hargreaves, 1997). The observed decrease in reactivity with antibodies against both total (B512) and tyrosinated (T1A2) α-tubulin indicated that there may be proteolytic degradation or reduced synthesis of tubulin at the later time point.

Confocal microscope images of cells incubated with anti-total α-tubulin, anti tyrosinated α-tubulin and the appropriate secondary antibody with a fluorescent label (see Figures 4.1.3 and 4.1.6) confirmed the disintegration of microtubules. The microtubule arrays within the cells treated with thimerosal and methylmercury chloride appear very different from the controls. In untreated cells the microtubule network was clearly visible within the cell body and the processes extending out from it. When exposed to thimerosal or methylmercury chloride there were less defined and

organised microtubule arrays. The disruption of the MT network became more marked as the concentration of the compound increased. In C6 cells, the levels of both tyrosinated α-tubulin and total α-tubulin were reduced after exposure to the organic mercury compounds. It would appear that tyrosinated MTs were more susceptible to thimerosal, as the disruption of tyrosinated tubulin seemed more apparent in the confocal images shown in Figure 4.1.6 (b and c). An independent study by Sager *et al.*, (1983) found similar disruption of the microtubule network after 22 hours of exposure to 0.2 µM MeHg in fibroblast cells. Unfortunately, in the work presented in this thesis, confocal images could only be obtained after 24 hours of differentiation. The cells differentiated more slowly on the slides used for confocal imaging and after the 4 hour time point very few processes had developed.

The levels of β-tubulin remained unchanged from the control levels at 4 hours. As with α-tubulin, the levels of reactivity with the anti-β-tubulin antibody decreased after 24 hours of exposure to both concentrations of MeHgCl and 1 µM thimerosal (Figure 4.2.5). The levels of β-tubulin should remain unchanged as β-tubulin subunits are constantly synthesised to keep the pool of unpolymerised tubulin consistent. Thus the reduction in the levels of total β-tubulin at 24 hours may be caused by a proteolytic event that is targeting the microtubule network or the organic mercury compounds are affecting tubulin synthesis. Reactivity with the anti-β-tubulin antibody TUB 2.1 was less sensitive to thimerosal and MeHgCl exposure than that of the anti-α tubulin antibodies used in this thesis as less reduction in reactivity was observed with the β-tubulin at 24 hours. The difference antibody reactivity could indicate sensitivity differences in the two sub-units or it could reflect a less sensitive anti-β-tubulin antibody as the background on the anti-β-tubulin blots was higher. Reactivity with the Tub 2.1 antibody was not as clear as the anti-α-tubulin antibody B512.

As with C6 cells, total α and β-tubulin levels in N2a cells were not significantly altered after 4 hours exposure to both organic mercury compounds. However, tyrosinated α-tubulin levels were significantly reduced when cells were treated with 1 µM thimerosal and both concentrations of MeHgCl. The detyrosination of the α-tubulin subunit, along with various other post-translational modifications, is a mechanism by which microtubules resist depolymerisation and achieve stability. Tyrosinated tubulin is associated with labile microtubules (Graff *et al.*, 1997) and the

changes in tubulin tyrosination may indicate that the mercury compounds affect microtubule dynamics at the earlier time point. A change in the tyrosination state of α-tubulin has also been recognised in an animal model (Ishida *et al.*, 1997). These workers found that the levels of tyrosinated α-tubulin were reduced in rats exposed to 10 mg/kg methylmercury per day. The observation that the tyrosination state of microtubules remained unaltered in the glial cell line at 4 hours, indicates that altered tubulin tyrosination may represent an early neuronal specific marker for toxicity. Confocal images of N2a cells stained for total and tyrosinated α-tubulin confirmed the reduction of tubulin levels determined by western blot analysis (Figure 4.2.12). (Hunter & Brown, 2000) also found that 2 hours exposure to 1 µM MeHgCl almost completely disrupted the α-tubulin network in mouse neuronal P19 cells.

Tyrosinated α-tubulin is more sensitive to the effects of the heavy metals than total α-tubulin (see Figure 4.2.15). Cells treated with 0.1 µM thimerosal have weaker staining within the axons and the cell bodies. Some of the axonal microtubule were fragmented, an effect that was not highlighted by the total α-tubulin antibody. Tyrosinated microtubules have been found to be the most susceptible form of MTs to the effects of MeHgCl (Graff *et al.*, 1993; Graff *et al.*, 1997). For example, exposure to 2 µM MeHgCl for 1 hour caused an almost complete disruption of tyrosinated MTs, while detyrosinated microtubules were less affected. The difference in incubation conditions probably accounts for the higher concentration needed to disrupt microtubules than which was determined by this investigation. However, the detrimental effect of MeHgCl upon the microtubule network was noted in both investigations.

In N2a cells the levels of β-tubulin remained unaffected after 4 hours of exposure to both concentrations of thimerosal and MeHgCl (Figure 4.2.10). After 24 hours β-tubulin levels were not significantly altered by exposure to 0.1 µM thimerosal or MeHgCl but they were significantly reduced by the higher concentrations of both organic mercury compounds (Figure 4.2.10). The levels of α and β-tubulin should be equal as they have equal distribution within the microtubule structure. However densitometric analysis of western blots probed with anti-α and β-tubulin antibodies indicated that the two sub-units were not reduced to the same extent by MeHgCl treatment. The α-tubulin sub-unit was more susceptible to MeHgCl or thimerosal

exposure. The difference between α and β-tubulin could be caused by the differences in the sub-units' sensitivities or the lesser reactivity of the β-tubulin antibody.

Wasteneys *et al.*, (1988) found that treatment with MeHg for up to 2 hours caused a time and concentration dependant disassembly of MTs in embryonal carcinoma cells. Using immunofluorescence they discovered that concentrations of 0.1 μM had no effect on microtubules. Exposure to 1 μM caused what they classed as slight disruption; in that the staining pattern observed was less intense than with untreated cells. Western blots using anti-total α and β-tubulin antibodies did not agree with this finding, as only tyrosinated α-tubulin was affected after 4 hours. However, as the study by Wasteneys *et al.*, (1988) used immunofluorescence staining, it is possible that despite the slight disruption in staining of the microtubule network, the absolute levels of tubulin were unaltered.

Heavy Metal Concentration (μM)	N2a cells		C6 Cells	
	4 hours	24 hours	4 hours	24 hours
0.1 μM Thimerosal	1:1	1:1	1:1	1:1
1 μM Thimerosal	0.4:1	1.6:1	0.8:1	2:1
0.1 μM MeHgCl	0.5:1	1:1	0.8:1	0.8:1
1 μM MeHgCl	0.4:1	1:1	1:1	1.5:1

Table 4.1: Table of α-tubulin tyrosination to total α-tubulin ratios for N2a and C6 cell lysates.

Table 4.1 shows the ratio of tyrosinated α-tubulin to total α-tubulin in N2a and C6 cell extracts treated with thimerosal and MeHgCl for 4 and 24 hours. The ratios were obtained from the densitometric data contained in chapter 4. The tyrosination ratios were calculated for each individual extract using the equation:

$$\frac{\%\text{ relative to control tyrosinated α-tubulin}}{\%\text{ relative to control total α-tubulin}}$$

The ratios were then averaged for each metal concentration and time point. The ratios enable a direct quantifiable comparison to be made about the changes in the levels of tyrosination.

The ratio of tyrosination confirms that at 4 hours reduced levels of tyrosinated α-tubulin is restricted to N2a cells at the higher thimerosal concentration and both concentrations of MeHgCl. After 24 hours the higher concentrations of both

compounds actually increased the ratio of tyrosinated α-tubulin to total α-tubulin in C6 cells. Western blotting showed that levels of total α-tubulin were reduced. In N2a cells there is no difference in the ratio with 0.1 µM thimerosal exposure and both concentrations of MeHgCl but with 1 µM thimerosal the ratio shows that levels of tyrosinated α-tubulin is higher than total α-tubulin. This may highlight a difference in the way thimerosal disrupts the microtubule network in the cell lines.

In addition to microtubules, N2a cells also contain the neuron specific class of intermediate filaments called neurofilaments (NFs). The neurofilament heavy chain (NFH) is the most phosphorylated of the three NFs and is important in the stabilisation and growth of the axon.

Heavy Metal Concentration (µM)	4 hours	24 hours
0.1 µM Thimerosal	1:1	1:1
1 µM Thimerosal	0.4:1	1.5:1
0.1 µM MeHgCl	0.3:1	1:1
1 µM MeHgCl	0.3:1	1:1

4.2: Table of NF-H phosphorylation to total NF-H ratios for N2a cell lysates

Table 4.2 shows the ratio of phosphorylated NFH to total NFH in N2a extracts treated with thimerosal and MeHgCl for 4 and 24 hours. The ratios were obtained from the densitometric data contained in chapter 4. The ratios were calculated for each individual extract using the equation:

$$\frac{\%\text{ relative to control Phosphorylated NFH}}{\%\text{ relative to corresponding control total NFH}}$$

The ratios were then averaged for each metal concentration and time point. The ratios enable a direct quantifiable comparison to be made about the changes in the levels of NFH phosphorylation.

The ratio of Phosphorylated NFH to total NFH confirms that with exposure to organic mercury compounds the level of phosphorylated NFH was either less than or equal to total NFH. Only exposure to 1 µM thimerosal actually gave a ratio where phosphorylated NFH was greater than total NFH, indicted that the effect on NFs was dependant upon the type and concentration of the metal.

The levels of total NFH remains unaltered after 4 hours of incubation with thimerosal and MeHgCl (Figure 4.2.10), which in agreement with the study by Funchal *et al.,* (2006). The levels of phosphorylated NFH (Figures 4.2.13, and 4.2.16) were significantly reduced after 4 hours of incubation with 1 µM thimerosal and exposure to MeHgCl significantly reduced levels of phosphorylated NFH at both 0.1 and 1 µM. Two different neurofilament antibodies were used and gave a virtually identical result. The two phosphorylated NF-H antibodies (RT97 and SMI34) recognise different epitopes on the NFH chain, but both indicated a change in NFH stability. The phosphorylation of NFH is associated with the maturity and stability of the axon (Williamson, 1996). Since the axon has little protein synthesis machinery, these NF are synthesized in the cell bodies and preassembled as insoluble hetero-oligomers and/or short filaments they are transported into and through axons by axonal transport. As stable synapses are established during postnatal development, neurofilaments accumulate in axons, which are accompanied by extensive phosphorylation on the carboxyl terminal tail domains of both NFH and NFM subunits and increased radial growth of axons. Phosphorylation at serine residues of multiple KSP repeat motifs along these tail domains is mediated by several proline-directed protein kinases (Roy *et al.,* 2000). The reduction NFH phosphorylation is indicative of the breakdown of NFH stability and thus axon stability. After 24 hours exposure to thimerosal and MeHgCl the levels of total NFH were reduced with both compounds and at both concentrations. As with tubulin, it seems that proteolysis is occurring after 24 hours of exposure time and, as both NF-H and tubulin are affected by this event, it appears that it may be targeting the cytoskeleton in general.

Confocal images of cells stained with anti-total and phosphorylated NF-H antibodies confirm that the cytoskeletal protein becomes more degraded as the concentration of thimerosal and MeHgCl increases. Braekman *et al.,* (1997) found that 2 µM MeHg altered the length of axons after 3 hours of incubation. Presumably the axon shortening would have been accompanied by a change in NF levels but since the study only used a light microscope to view cell morphology this could not be confirmed. The slightly lower concentration found to affect neurite outgrowth in the present study could be due to a longer incubation time and the different cell line used.

The cytoskeleton of both N2a and C6 cells are equally vulnerable to the effects of the organic mercury compounds used after 24 hours of exposure. After just 4 hours of thimerosal and MeHgCl treatment the integrity of the neuronal and glial

cell cytoskeleton was compromised but there were no significant changes in the tyrosination of α-tubulin in C6 cells. This indicates that glial cells may be slightly more resistant than N2a cells or that the mechanism of organic mercury compound toxicity may be different in glial cells. Sager & Syversen, (1984) looked at the effects of MeHg on microtubule disassembly in neuronal, glial and fibroblast cells and found no differences in the MT staining of the three cells types at concentrations of 5 µM. At lower concentrations of 1 µM the MT network of the neuronal cell was more sensitive. Kim *et al.*, (2002) found that exposure to 20 µM thimerosal for 1 hour produced changes in the cytoskeleton. Images of cells stained for f-actin showed reduced levels of actin fibres in serum starved HeLa cells, indicting that the disruption of the cytoskeleton occurs in all three of the major network types, NFs, microtubules and microfilaments.

The regulation of cytoskeletal proteins is controlled by various signalling pathways. The next stage in the investigation into thimerosal and methylmercury was to determine what effect the compounds had upon the MAPK signalling pathways. ERK1/2 is known to regulate the cell cycle and JNK and P38 are important in stress responses (Robinson & Cobb, 1997). Furthermore, ERK1/2 has a role in neurite outgrowth and neurofilament phosphorylation (Veeranna *et al.*, 1998), both of which have been shown to be altered during exposure to organic mercury compounds.

Chapter 5: Effects of organic mercury compounds on cell signalling pathways in differentiating N2a and C6 cells

Introduction

Previous chapters demonstrated that sub-lethal concentrations of both thimerosal and MeHgCl had an inhibitory effect on neurite formation. Chapter 4 indicated that the inhibition was associated with disruption of microtubules and neurofilaments. Due to the changes highlighted by western blotting and immunofluorescence staining, it was decided to investigate cellular signalling mechanisms that are known to be linked with the cytoskeleton.

The cytoskeletal protein α-tubulin comprises 450 amino acid residues. The sequence contains areas abundant in serine and threonine residues targeted by activated ERK1/2. The COOH region of 66 residues are devoid of asparagine, glutamine, threonine, cysteine, proline, and isoleucine, and the last 40 positions have 47 % acidic side chains, 16 glutamic and three aspartic, rendering this segment one of the most acidic part of the protein (Ponstingl *et al.*, 1981). The NFH protein contains a region that has repeats of the motif lysine-serine-proline (KSP repeats). It is in this KSP region that the filament is phosphorylated by various kinases including ERK1/2 (Ackerley *et al.*, 2003).

The mitogen-activated protein kinase signalling cascades have roles in various cellular functions. They are serine/threonine kinases that are ubiquitous enzymes of signalling pathways. They are activated via reversible phosphorylation and are vital in connecting cell surface receptors to intracellular targets (Kaminska, 2005). The MAPK family consists of three main groups, the extra cellular signal related protein kinase (ERK 1/2), the stress activated protein kinases (SAPK) p38, and the SAPK, c-jun N-terminal kinases (JNK). Each MAPK is activated by a specific mitogen activated protein kinase kinase (MAPKK), MEK1/2 activates ERK1/2. ERK1/2 has roles in cell cycle progression (Robinson & Cobb, 1997) and cytoskeletal organisation (Reszka *et al.*, 1995). The ERK1/2 signalling pathway is also known to be important in neurite outgrowth and NFH phosphorylation (Veeranna *et al.*, 1998), whereas JNK and p38 are stress activated kinases (Wang *et al.*, 1998). Activated ERK1/2 targets cytoskeletal proteins for phosphorylation such as NFs and Tau. ERK also

phosphorylates m-calpain at Ser50 both *in vitro* and *in vivo* even in the absence of millimolar concentrations of Ca^{2+} (Glading *et al.*, 2001).

Previous studies have shown that heavy metals can affect the MAPK signalling pathway. Exposure to mercury has been to shown to both increase the activation of JNK (Matsuoka *et al.*, 1999) and not alter the activation of the pathway (Barnes & Kircher, 2005). Mercury exposure has been shown to increase ERK activation initially after 2.5 minutes of exposure to methylmercury then cause levels to decrease (Parran *et al.*, 2004).

Activated ERK1/2 targets serine and threonine residues for phosphorylation so it was of interest to the investigation to determine whether changes in ERK1/2 activation were accompanied by changes in substrate phosphorylation levels in the neuronal and glial cell lines. It was anticipated that that these blots may highlight changes in protein phosphorylation in addition to the decreases seen in NFH phosphorylation, which could then be investigated in more depth.

Methods

N2a and C6 cells were differentiated for 4 and 24 hours in 0.1 and 1 µM thimerosal and MeHgCl. Each incubation time had a separate control of differentiated cells untreated with the organic mercury compounds (Methods section 2.2.10). The cells were extracted in boiling 0.5 % SDS in TBS and lysed by a further 5 minutes of boiling. Lysed cell extracts were diluted in x2 concentrated Laemmli electrophoresis sample buffer (see Methods section 2.2.12 for detail) and loaded on to 10 % acrylamide gel at a protein concentration of 30 µM.

Levels of total ERK1/2, phosphorylated ERK, total JNK and phosphorylated JNK were investigated using western blots of N2a and C6 cell lysates probed with antibodies against total ERK1/2 (K-23), phosphorylated ERK (E-4), total JNK (D-2) and phosphorylated JNK (G-7). All antibodies were well established in the lab as effective with the cell lines used. In addition, the levels of phosphorylated serine and threonine levels were also investigated by western blotting analysis. Antibodies raised against phosphorylated serine (PSR-45) and phosphorylated threonine (PTR-8) were used to probe the western blots to determine whether the levels of the phosphorylation states indicate other protein kinase substrates were altered. All secondary antibodies were tested for non specific binding using a non primary control western blot. The resultant western blots were then probed with the antibodies indicated and the reactive

bands were scanned densitometrically using AIDA software. Each experiment was repeated at least 5 times with separate cell extracts. The number of times the experiment was carried out on individual cell extracts was indicated in the figure legend by n = x. Data represent mean levels of antibody reactivity, expressed as a percentage of the corresponding control $\pm$ SEM. Statistical test used was initially a 2 way ANOVA to highlight significance differences in dose and time data sets. Post hoc Bonferroni's correction for pair wise analysis was used to establish significance between individual doses and times. Asterisks indicate statistical significance of differences from the control (* p value <0.05). The data shown is the average densitometric value for 6 western blots created from 5 gels of independent cell extracts. The lane on the blot labelled 0 is the control extract with no added metal. For the thimerosal treated corresponding control sterile distilled water was added at the same volume as the metal in the treated cells and with MeHgCl DMSO was added at the same volume as with the treated cells as the MeHgCl was dissolved in DMSO due to poor solubility in distilled water.

5.1: The effect of thimerosal and methylmercury chloride on the levels and activation of ERK1/2 in C6 cells

The densitometric analysis in figure 5.1.1 confirmed that, after 4 hours of incubation with thimerosal and MeHgCl there was no change in the anti-total ERK1/2 antibody reactivity with C6 cell lysates. The average densitometric absorbance obtained from the control was 0.823034 for cell lysates probed with ERK1/2 and 0.827393 for phosphorylated ERK1/2. Statistical analysis using a 2 way ANOVA test and post hoc Bonferroni's test confirmed that there were no significant changes when compared the control (p ranged from 0.06944-0.4180). However, there was a 45-65 % increase in the reactivity of the anti-phosphorylated ERK antibody with cells exposed to 0.1 and 1 µM thimerosal respectively. A 2 way ANOVA confirmed that the increase was statistically significant (p = 0.04678 and 0.02990 for 0.1 and 1 µM respectively). In contrast exposure to MeHgCl significantly decreased antibody reactivity by approximately 25-30 % (p<0.05). Statistical analysis confirmed that there were significant differences between the effects seen at 4 hours and those seen after 24 hours (Figure 5.1.2) of incubation.

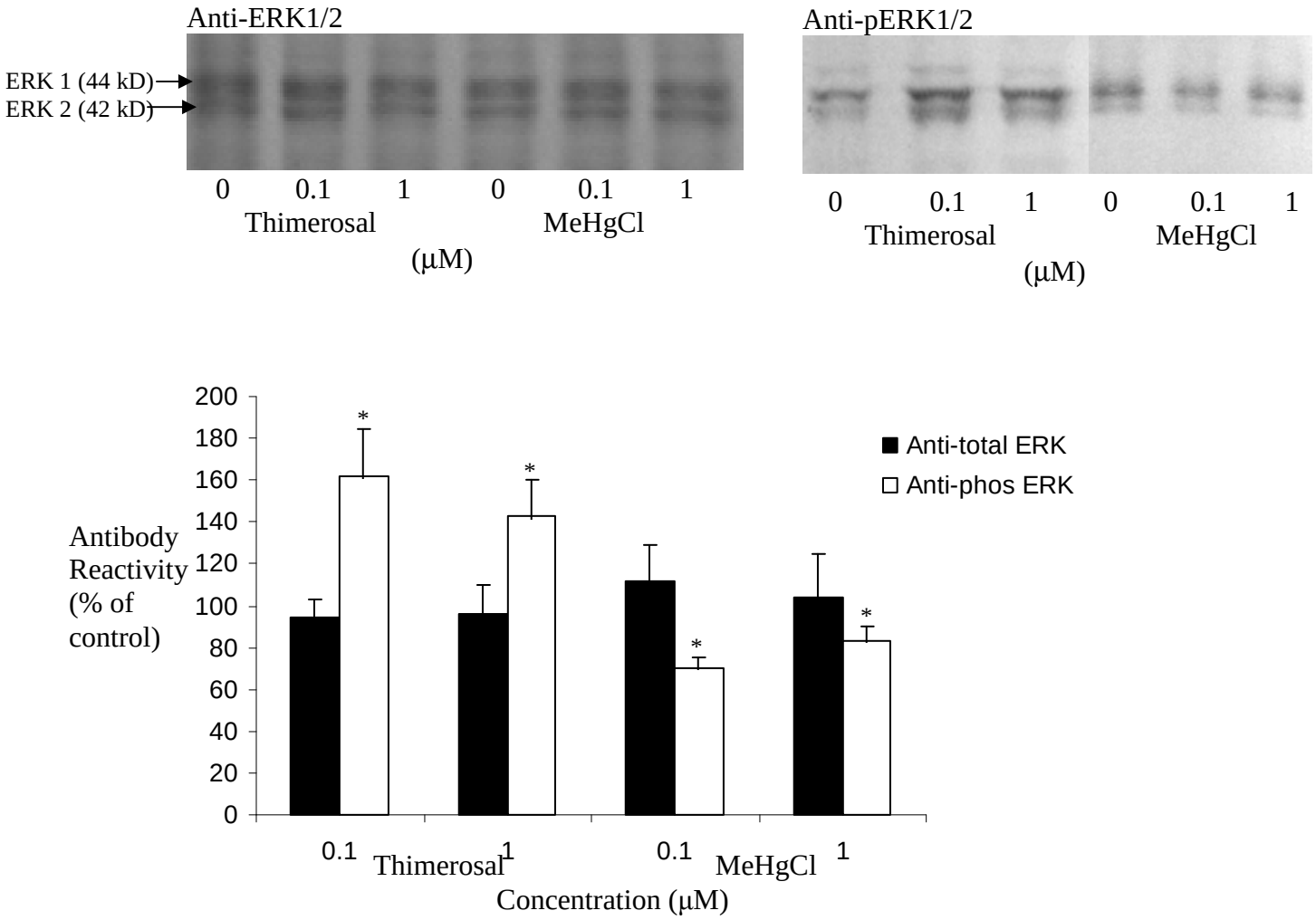

Figure 5.1.1: Western blots and densitometric analysis of lysed C6 cell extracts exposed to thimerosal and MeHgCl for 4 hours. The proteins were visualised with a 1/1000 dilution of an anti-ERK1/2 and phosphorylated ERK1/2 antibody and compared with the corresponding control that was untreated with the organic mercury compounds.

C6 cells were induced to differentiate for 4 hours in the presence and absence of thimerosal and MeHgCl as indicated, then separated by SDS PAGE and western blotting as described in Methods section 2.2.10-12. Data represent mean levels of antibody reactivity, expressed as a percentage of the corresponding control $\pm$ SEM (n = 6). Asterisks indicate statistical significance of differences from the control (* p value <0.05). Statistical significance was determined using a 2 way ANOVA test, followed by post hoc Bonferroni's correction for pair wise multiple analysis.

After 24 hours of exposure to thimerosal and MeHgCl there was no significant ($p<0.05$) change in the reactivity of the anti- ERK1/2 antibody with C6 cell lysates (Figure 5.1.2). The average control absorbance obtained from densitometry of the phosphorylated ERK western blots was 0.946631 and for extracts exposed to 0.1 µM thimerosal 0.543821. After 24 hours the reactivity of the anti-phosphorylated ERK antibody was significantly reduced by 45-50 % with exposure to thimerosal. Statistical analysis confirmed the difference from the control as significant ($p = 0.03414$). Exposure to 0.1 µM and 1 µM MeHgCl significantly reduced ($p< 0.05$) the binding of the anti-phosphorylated ERK antibody by around 38 % and 40 %, respectively. A statistical comparison of the 4 (Figure 5.1.1) and 24 hour data indicated that there was a significant time componant in the reactivity of the phosphorylated ERK1/2 antibody with exposure to both concentrations of thimerosal ($p = 0.03428$ and 0.02369 for 0.1 and 1 µM respectively), but not with exposure to MeHgCl.

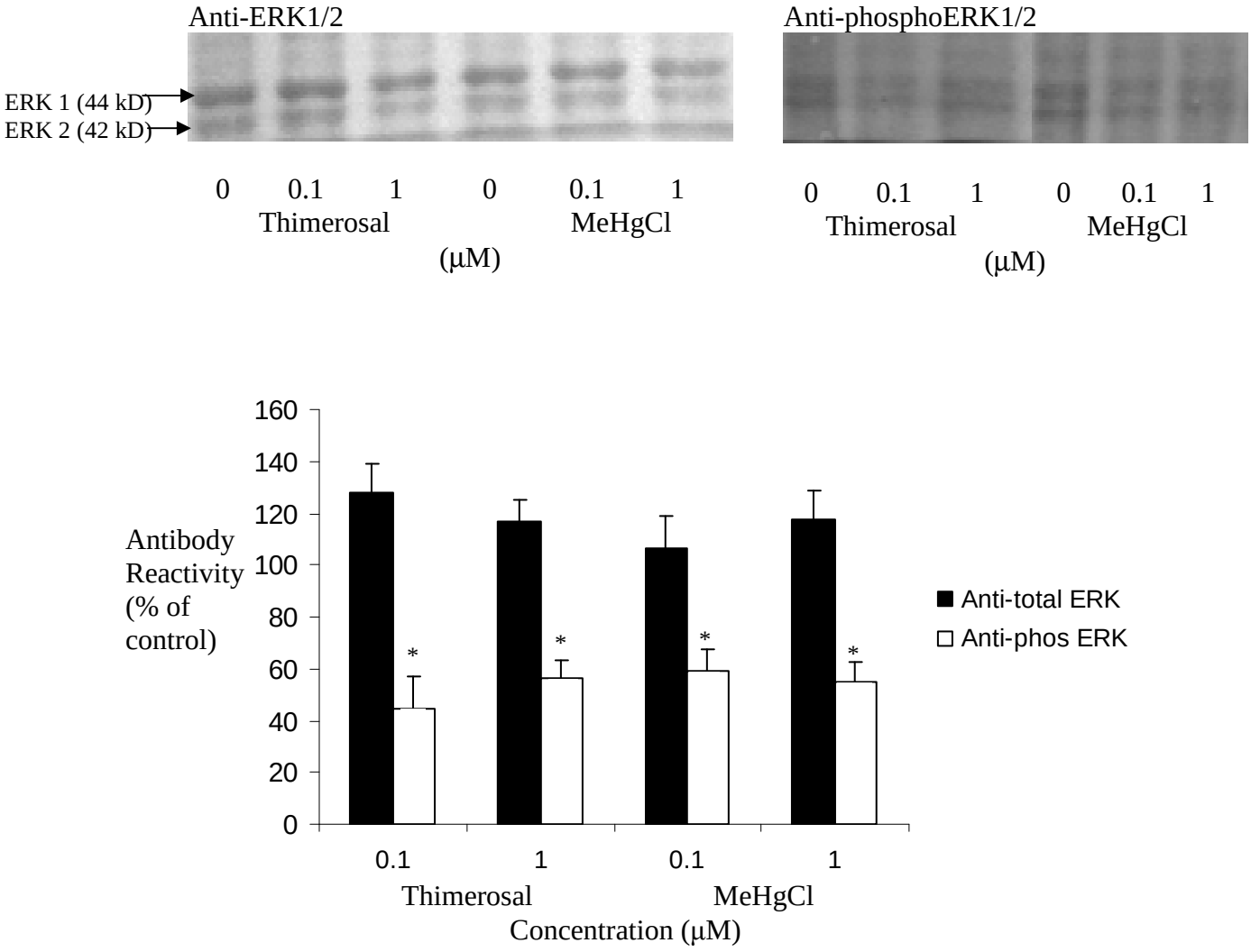

Figure 5.1.2: Western blots and densitometric analysis of lysed C6 cell extracts exposed to thimerosal and MeHgCl for 24 hours. The proteins were visualised with a 1/1000 dilution of an anti-ERK1/2 and phosphorylated ERK1/2 antibody and compared with the corresponding control that was untreated with the organic mercury compounds.

C6 cells were induced to differentiate for 24 hours in the presence and absence of thimerosal and MeHgCl as indicated, then separated by SDS PAGE and western blotting as described in Methods section 2.2-10-12. Data represent mean levels of antibody reactivity, expressed as a percentage of the corresponding control $\pm$ SEM (n = 6). Asterisks indicate statistical significance of differences from the control (* p value <0.05). Statistical significance was determined using a 2 way ANOVA test, followed by post hoc Bonferroni's correction for pair wise multiple analysis.

5.2: The effect of thimerosal and methylmercury chloride on ERK and phosphorylated ERK in N2a cells

After 4 hours there were no significant changes in the levels of bound anti-ERK1/2 antibody to the N2a cell lysates with either thimerosal or MeHgCl (Figure 5.2.1). Statistical analysis using a 2 way ANOVA and post hoc Bonferroni's test showed p to be in the range of 0.05446-0.92251. The average densitometric absorbance obtained for cells extracts probed with the anti-ERK1/2 antibody was 0.729491 at 4 hours and 0.945816 with the western blot of the 24 hour differentiated cells. By contrast, exposure to both concentrations of thimerosal and MeHgCl caused approximately a 40 % decrease in the reactivity of the anti-phosphorylated ERK antibody, which was statistically significant ($p = 0.015529$-0.043316).

Figure 5.2.2 shows that after 24 hours there were no significant changes in the levels of bound anti-total ERK1/2 antibody to the N2a cell lysates treated with either thimerosal or MeHgCl ($p = 0.744719$).. Densitometric analysis of the western blots gave an average absorbance of 0.773096 for the control cells reacted with the anti-phosphorylated ERK1/2 antibody and 0.438926 for extracts exposed to 0.1 µM thimerosal. After 24 hours exposure to 0.1 µM thimerosal the anti-phosphorylated ERK reactivity was significantly reduced by 45 % ($p = 0.003425$). Exposure to 1 µM thimerosal caused also caused around a 48 % decrease in antibody reactivity. Exposure to MeHgCl significantly reduced the intensity of the anti-phosphorylated ERK antibody by 38-50 % ($p = 0.03528$ and 0.26281 for 0.1 and 1 µM respectively). A statistical comparison of the 4 and 24 hour data showed that there were significant differences between both compounds and concentrations ($p = 0.19567$-0.38461).

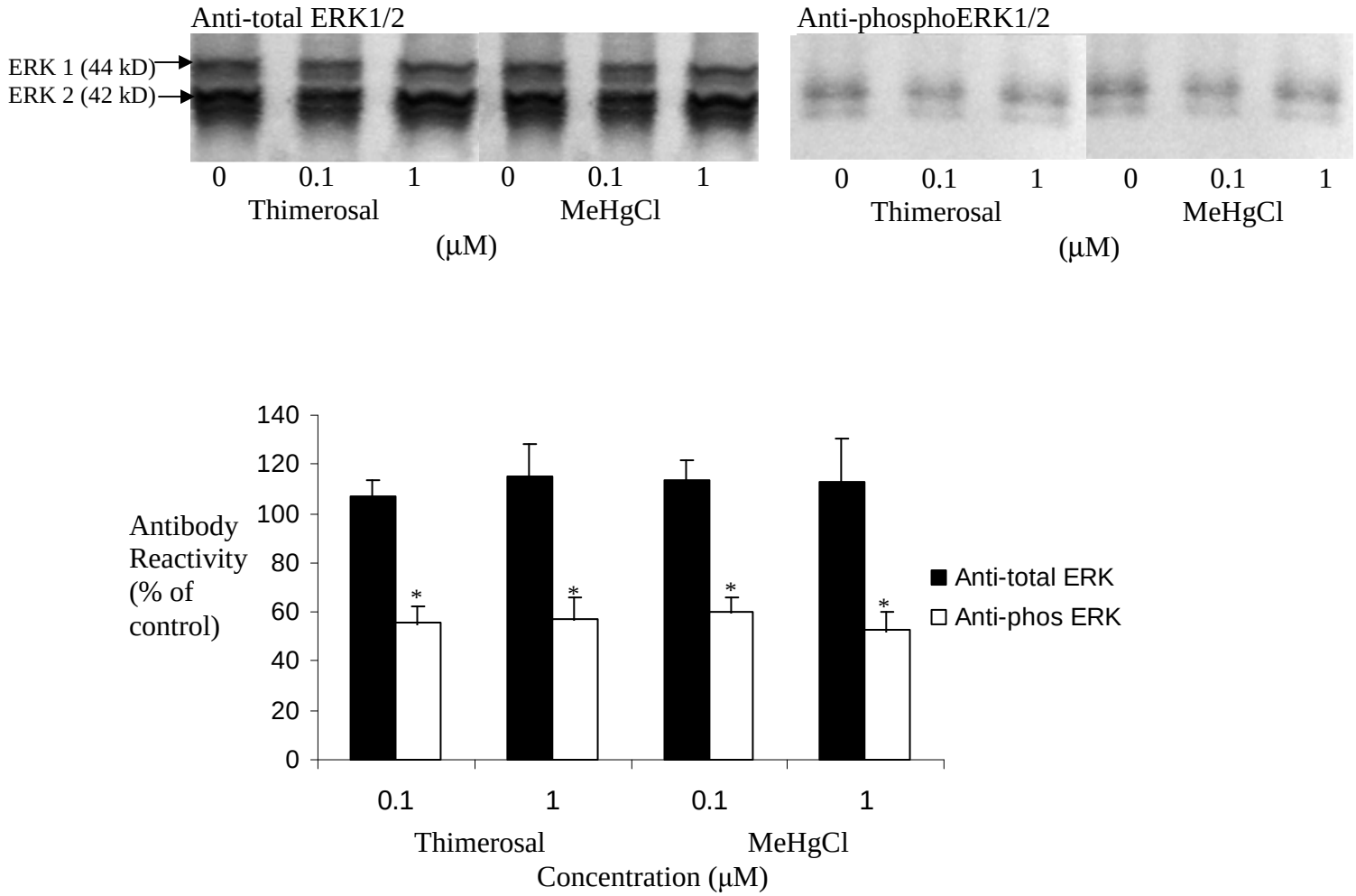

Figure 5.2.1: Western blots and densitometric analysis of lysed N2a cell extracts exposed to thimerosal and MeHgCl for 4 hours. The proteins were visualised with a 1/1000 dilution of an anti-ERK1/2 and phosphorylated ERK1/2 antibody and compared with the corresponding control that was untreated with the organic mercury compounds.

N2a cells were induced to differentiate for 4 hours in the presence and absence of thimerosal and MeHgCl as indicated, then separated by SDS PAGE and western blotting as described in Methods section 2.2.10-12. Data represents mean levels of antibody reactivity, expressed as a percentage of the corresponding control $\pm$ SEM (n = 5). Asterisks indicate statistical significance of difference from the control (* p value <0.05). Statistical significance was determined using a 2 way ANOVA test, followed by post hoc Bonferroni's correction for pair wise multiple analysis.

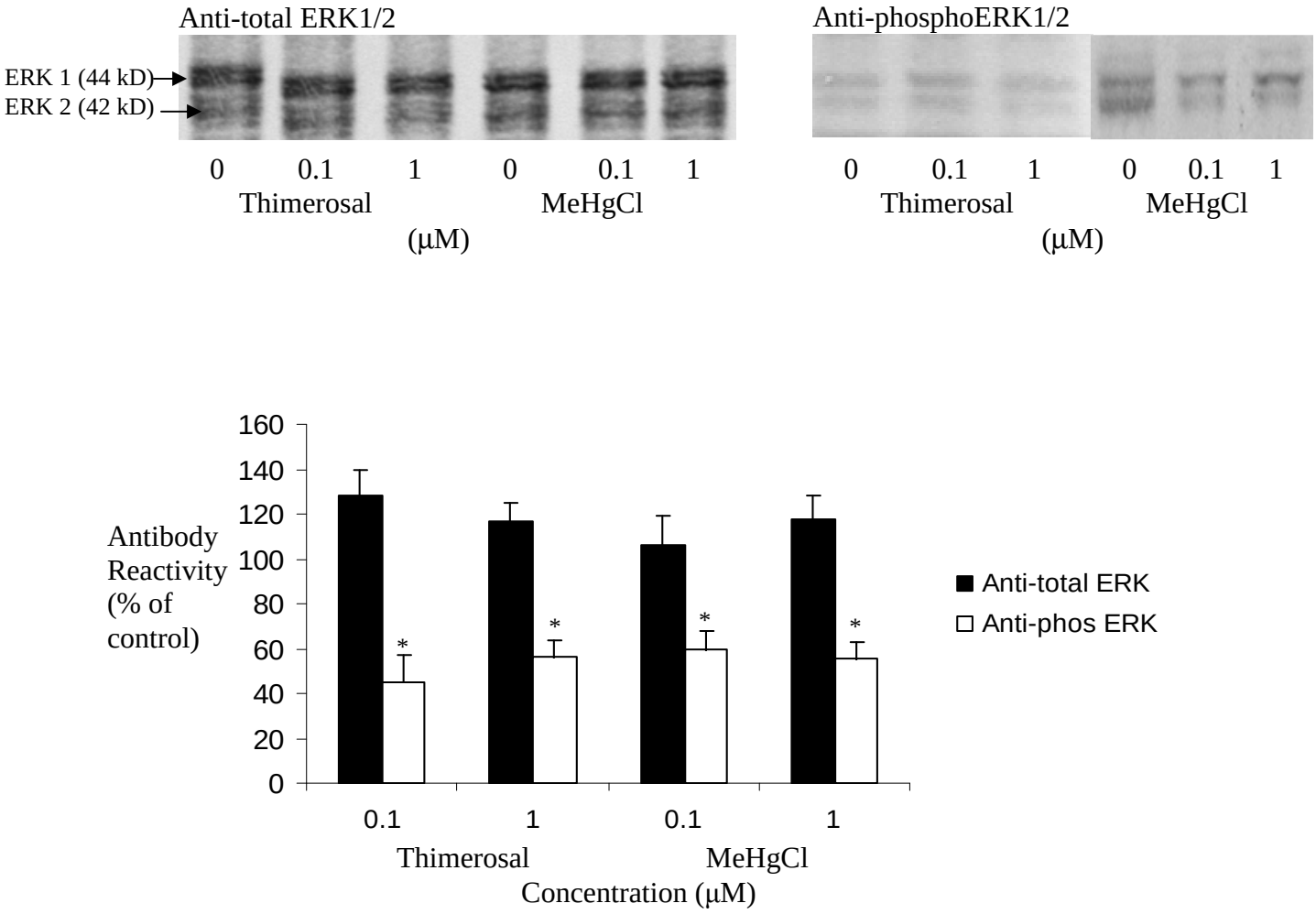

Figure 5.2.2: Western blots and densitometric analysis of lysed N2a cell extracts exposed to thimerosal and MeHgCl for 24 hours. The proteins were visualised with a 1/1000 dilution of an anti-ERK1/2 and phosphorylated ERK1/2 antibody and compared with the corresponding control that was untreated with the organic mercury compounds.

N2a cells were induced to differentiate for 24 hours in the presence and absence of thimerosal and MeHgCl as indicated, then separated by SDS PAGE and western blotting as described in Methods section 2.2.10-12. Data represents mean levels of antibody reactivity, expressed as a percentage of the corresponding control $\pm$ SEM (n = 5). Asterisks indicate statistical significance of difference from the control (* p value <0.05). Statistical significance was determined using a 2 way ANOVA test, followed by post hoc Bonferroni's correction for pair wise multiple analysis.

5.3: Effects of thimerosal and methylmercury chloride on the levels of phosphorylation in serine and threonine residues

Figure 5.3.1 shows that there was a complex pattern of reactivity reflecting the multitude of proteins with serine residues that could potentially be phosphorylated by activated ERK. The cell extracts exposed to 1 µM thimerosal appears to have caused a reduction in antibody reactivity. However statistical analysis did not highlight the reduction as significant ($p = 0.06692$ and 0.14826 for 4 and 24 hours respectively). There were changes in the pattern of reactivity of the phosphorylated serine antibody with C6 cells differentiated for 4 and 24 hours. After 24 hours of differentiation the highest molecular weight band of 230 kD evident in the 4 hour incubation was no longer visible the highest molecular weight protein was 100 kD. The 80 kD band visible at 4 hours was not evident after 24 hours of incubation and there were bands of 74 and 60 kD that were not there after 4 hours. However, there were no obvious or consistent differences in reactivity between the control and the organic mercury treated cells for individual time points or treatments. The pattern was considered too complex to perform detailed quantitative analysis.

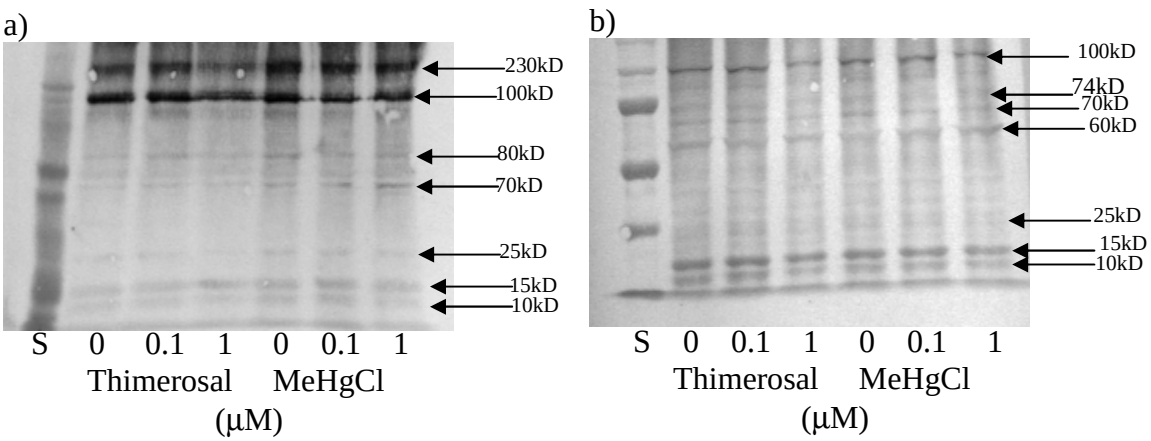

Figure 5.3.1: Western blots of lysates from the differentiated glial C6 cell line following exposure to either thimerosal and methylmercury chloride for 4 or 24 hours. The proteins were visualised using a 1/1000 dilution of the PSR-45 anti-phosphorylated serine antibody. Quantification of the antibody reactivity was carried out using AIDA software.

C6 cells were induced to differentiate for 4 (a) and 24 (b) hours in the presence and absence of thimerosal and MeHgCl as indicated and extracts were separated by SDS PAGE and western blotted as described in Methods section 2.2.12. The blots were probed with an anti-phosphorylated serine residue antibody. Molecular weight markers are in lane S.

Heavy metal concentration (μM)	Molecular weight of band (kD)				
	230	100	80	70	25
0.1μM thimerosal	99±25.1	99±19.2	105±23.1	124±24.9	104±18.5
1 μM thimerosal	78±27.1	89±14.1	104±22.4	99±18.9	98±24.3
0.1 μM MeHgCl	137±12.6	96±29.2	113±17.5	123±15.3	96±19.8
1 μM MeHgCl	94±23.0	103±26.7	83±32.3	105±31.7	107±14.0

Table 5.3.1: Densitometric analysis of the effects of thimerosal and MeHgCl on the levels of phosphorylated serine in C6 cells differentiated for 4 hours.

C6 cells were induced to differentiate for 24 hours in the presence and absence of thimerosal and methylmercury chloride, then separated by SDS PAGE and western blotting as described in Methods section 2.2.10-12. Data represents mean levels of antibody reactivity, expressed as a percentage of the corresponding control ± SEM.

Heavy metal concentration (µM)	Molecular weight of band (kD)						
	100	74	70	60	25	15	10
0.1µM thimerosal	103±18.0	104±23.5	98±19.0	123±33.3	126±12.3	105±23.6	108±29.6
1 µM thimerosal	123±13.1	86±18.2	97±21.1	105±17.6	135±18.6	103±12.4	97±30.3
0.1 µM MeHgCl	106±28.4	123±31.8	104±30.1	87±19.1	95±18.5	114±22.5	122±17.9
1 µM MeHgCl	98±21.2	104±12.6	123±10.9	139±20.1	98±18.9	103±24.1	110±19.1

Table 5.3.2: Densitometric analysis of the effects of thimerosal and MeHgCl on the levels of phosphorylated serine in C6 cells differentiated for 24 hours

C6 cells were induced to differentiate for 4 hours in the presence and absence of thimerosal and methylmercury chloride, then separated by SDS PAGE and western blotting as described in Methods section 2.2.10-12. Data represents mean levels of antibody reactivity, expressed as a percentage of the corresponding control ± SEM.

Tables 5.3.1 and 2 shows that there was no change in band intensity at any molecular weight with C6 cell extracts incubated with the organic mercury compound for 4 and 24 hours ($p = 0.0798$ and 0.5621 for 4 and 24 hours respectively).

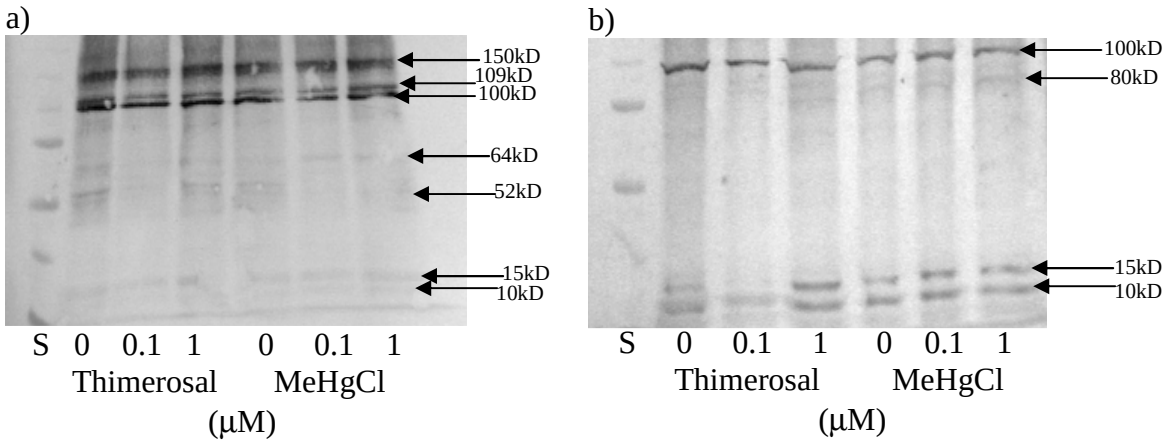

Figure 5.3.2: Western blots of lysates from the differentiated glial C6 cell line following exposure to either thimerosal and methylmercury chloride for 4 or 24 hours. The proteins were visualised using a 1/1000 dilution of the PTR-8 anti-phosphorylated threonine antibody. Quantification of the antibody reactivity was carried out using AIDA software.

C6 cells were induced to differentiate for 4 and 24 hours in the presence and absence of thimerosal and MeHgCl as indicated and extracts were separated by SDS PAGE and western blotted as described in Methods section 2.2.12. The blots were probed with an anti-phosphorylated threonine antibody for 4 hours (a) and 24 hours (b). Molecular weight markers are in lane S.

Figure 5.3.2 shows that, as with the phosphorylated serine antibody, probing the western blot with an anti-phosphorylated threonine antibody produced a very complicated pattern of reactivity. After incubating the C6 cells with thimerosal and MeHgCl for 4 hours, there were no statistically significant changes reactivity of the antibody. The pattern of reactivity became less complex after 24 hours of treatment with the organic mercury compounds. Some of the bands visible at 4 hours incubation were no longer visible after 24 hours, the 52, 64, 109 and 150 kD bands were all absent from the western blot of the 24 hours cell lysates. There were no significant changes in the levels of reactivity after 4 or 24 hours of exposure with either compound. As with the phosphorylated serine western blot, quantification was only carried out on the major bands.

Heavy metal concentration (µM)	Molecular weight of band (kD)						
	150	109	100	64	52	15	10
0.1µM thimerosal	91±17.6	87±19.7	108±11.9	89±24.8	92±12.4	129±18.3	134±14.3
1 µM thimerosal	124±28.4	94±12.6	86±34.2	96±27.5	83±18.7	123±22.8	103±27.7
0.1 µM MeHgCl	103±19.1	91±20.6	97±25.3	95±19.1	89±19.6	105±31.6	118±13.8
1 µM MeHgCl	109±28.4	97±13.9	95±16.9	116±29.3	95±29.1	103±21.9	95±25.9

Table 5.3.3: Densitometric analysis of the effects of thimerosal and MeHgCl on the levels of phosphorylated threonine in C6 cells differentiated for 4 hours.

C6 cells were induced to differentiate for 4 hours in the presence and absence of thimerosal and methylmercury chloride, then separated by SDS PAGE and western blotting as described in Methods section 2.2.10-12. Data represents mean levels of antibody reactivity, expressed as a percentage of the corresponding control ± SEM (n = 5).

Heavy metal concentration (µM)	Molecular weight of band (kD)			
	100	64	15	10
0.1µM thimerosal	94±29.9	89±22.2	87±18.1	108±30.3
1 µM thimerosal	102±26.2	104±17.2	98±18.5	133±28.6
0.1 µM MeHgCl	107±15.1	98±22.8	102±17.1	113±30.3
1 µM MeHgCl	115±25.8	86±19.8	98±28.6	119±27.1

Table 5.3.4: Densitometric analysis of the effects of thimerosal and MeHgCl on the levels of phosphorylated threonine in C6 cells differentiated for 24 hours

C6 cells were induced to differentiate for 24 hours in the presence and absence of thimerosal and methylmercury chloride, then separated by SDS PAGE and western blotting as described in Methods section 2.2.10-12. Data represents mean levels of antibody reactivity, expressed as a percentage of the corresponding control ± SEM (n = 5).

Tables 5.3.3 and 4 shows that there was no statistically significant change in band intensity at any molecular weight with C6 cell extracts incubated with the organic

mercury compound for 4 and 24 hours (p = 06887 and 0.9735 for 4 and 24 hours respectively).

Figure 5.3.3 shows that after 4 (a) and 24 (b) hours of differentiation in the absence and presence of the organic mercury compounds, the anti-phosphorylated serine antibody reacted with numerous proteins of varying molecular weight. The pattern of reactivity did not alter after treatment with either thimerosal or MeHgCl after 4 or 24 hours of exposure. Statistical analysis of the densitometric data showed that neither 4 nor 24 hours of exposure caused significant changes from the control (p = 0.518329 and 0.802471 for 4 and 24 hours respectively). However the molecular weight of the proteins recognised by the antibody changed with the different differentiation times (Table 3.3.3-4). After 24 hours of differentiation the bands seen at 200 and 50 kD after 4 hours of differentiation were no longer visible. There were bands visible at 79 and 55 kD that were not seen with the western blot created from cell extracts differentiated for 4 hours. As with C6 cells the pattern of reactivity was considered to complex to perform detailed quantification.

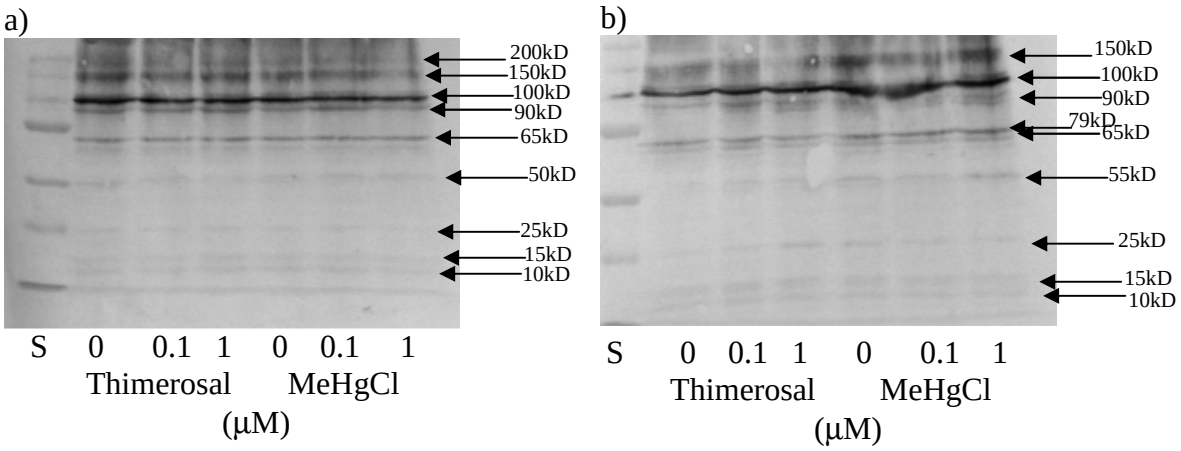

Figure 5.3.3: Western blots of lysates from the differentiated neuronal N2a cell line following exposure to either thimerosal and methylmercury chloride for 4 or 24 hours. The proteins were visualised using a 1/1000 dilution of the PSR-45 anti-phosphorylated serine antibody. Quantification of the antibody reactivity was carried out using AIDA software.

N2a cells were induced to differentiate for 4 (a) and 24 (b) hours in the presence and absence of thimerosal and methylmercury chloride and extracts were separated by SDS PAGE and western blotted as described in Methods section 2.2.12. The blots were probed with an anti-phosphorylated serine residue antibody. Molecular weight markers are in lane S.

Heavy metal concentration (µM)	Molecular weight of band (kD)								
	200	150	100	90	65	50	25	15	10
0.1µM thimerosal	96±16.4	96±14.02	112±14.2	98±12.9	104±18.8	124±20.9	103±17.8	103±11.5	75±14.3
1 µM thimerosal	110±11.7	104±16.9	86±14.4	95±22.2	97±16.1	95±18.2	124±14.7	87±28.1	87±18.5
0.1 µM MeHgCl	91±18.4	108±15.9	104±29.2	106±14.1	111±14.3	103±23.0	104±14.6	94±18.8	96±16.9
1 µM MeHgCl	86±13.2	94±29.2	112±37.6	114±33.7	109±26.4	92±14.6	115±21.5	74±12.6	104±20.7

Table 5.3.5: Densitometric analysis of the effects of thimerosal and MeHgCl on the levels of phosphorylated serine in N2a cells differentiated for 4 hours

N2a cells were induced to differentiate for 4 hours in the presence and absence of thimerosal and methylmercury chloride, then separated by SDS PAGE and western blotting as described in Methods section 2.2.10-12. Data represents mean levels of antibody reactivity, expressed as a percentage of the corresponding control ± SEM (n = 5).

Heavy metal concentration (µM)	Molecular weight of band (kD)								
	150	100	90	79	65	55	25	15	10
0.1µM thimerosal	104±22.2	104±15.5	88±16.2	109±18.2	92±18.3	105±31.3	117±28.2	102±27.3	102±12.8
1 µM thimerosal	102±12.0	89±15.2	97±15.6	123±12.1	102±21.2	117±18.9	104±21.3	113±16.2	109±19.6
0.1 µM MeHgCl	115±21.8	78±19.5	103±12.3	98±16.4	114±28.5	99±41.6	122±35.9	98±29.4	93±10.7
1 µM MeHgCl	92±24.2	108±16.6	120±13.6	88±17.0	122±20.5	90±22.2	97±17.6	87±35.5	112±9.3

Table 5.3.6: Densitometric analysis of the effects of thimerosal and MeHgCl on the levels of phosphorylated threonine in N2a cells differentiated for 24 hours

N2a cells were induced to differentiate for 24 hours in the presence and absence of thimerosal and methylmercury chloride, then separated by SDS PAGE and western blotting as described in Methods section 2.2.10-12. Data represents mean levels of antibody reactivity, expressed as a percentage of the corresponding control ± SEM (n = 5).

Tables 5.3.5 and 6 shows that there is no change in antibody reactivity with C6 cell lysates incubated with thimerosal and MeHgCl for 4 and 24 hours (p = 0.0688 and 0.1358 for 4 and 24 hours respectively).

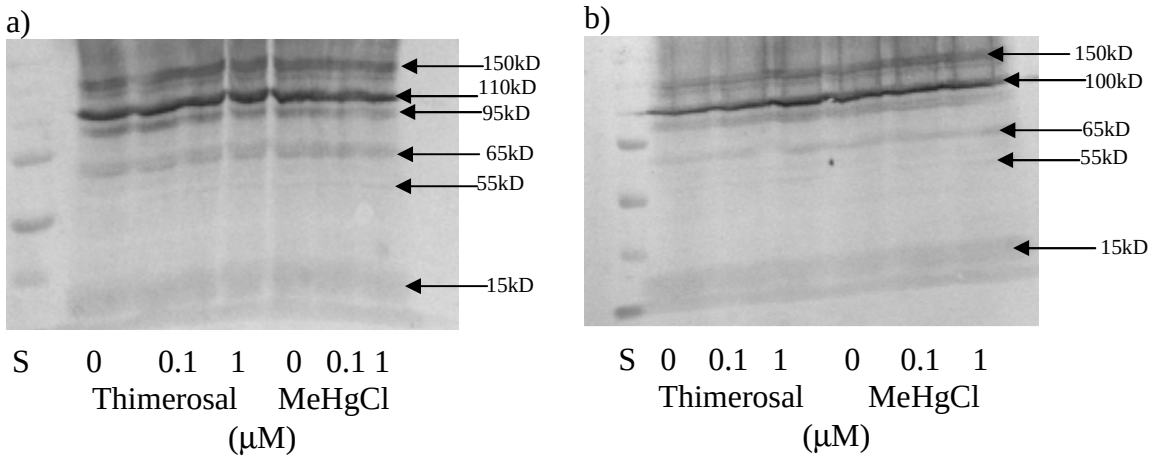

Figure 5.3.4: Western blots of lysates from the differentiated neuronal N2a cell line following exposure to either thimerosal and methylmercury chloride for 4 or 24 hours. The proteins were visualised using a 1/1000 dilution of the PTR-8 anti-phosphorylated threonine antibody. Quantification of the antibody reactivity was carried out using AIDA software.

N2a cells were induced to differentiate for 4 (a) and 24 (b) hours in the presence and absence of thimerosal and MeHgCl as indicated, and the extracts were separated by SDS PAGE and western blotted as described in Methods section 2.2.12. The blots were probed with an anti-phosphorylated threonine residue antibody. Molecular weight markers are in lane S

Figure 5.3.4 indicates that that the reactivity of the anti-phosphorylated threonine antibody did not alter when cell extracts were exposed to either thimerosal or MeHgCl. As with the anti-phosphorylated serine antibody, the pattern of reactivity appeared to change with the different differentiation times. The numbers of proteins recognised by this antibody were not as numerous as with the anti-phosphorylated serine antibody, but the pattern of reactivity was still fairly complex. There no significant reduction in antibody reactivity with exposure to the organic mercury compounds. Unlike the phosphorylated serine antibody the molecular weights of the phosphorylated proteins did not appear to change with the incubation times. The images show evidence of a number of bands that were considered too faint to obtain accurate quantification.

Heavy metal concentration (µM)	Molecular weight of band (kD)				
	100	64	52	15	10
0.1µM thimerosal	101±23.1	110±18.6	98±16.3	94±15.5	102±16.6
1 µM thimerosal	108±18.3	98±23.4	96±19.5	96±18.5	118±16.3
0.1 µM MeHgCl	117±19.3	103±13.6	89±17.4	108±22.1	98±18.9
1 µM MeHgCl	95±20.3	129±10.8	111±9.3	116±20.6	105±21.1

Table 5.3.7: Densitometric analysis of the effects of thimerosal and methylmercury chloride on the levels of phosphorylated threonine in N2a cells differentiated for 4 hours

N2a cells were induced to differentiate for 4 hours in the presence and absence of thimerosal and methylmercury chloride, then separated by SDS PAGE and western blotting as described in Methods section 2.2.10-12. Data represents mean levels of antibody reactivity, expressed as a percentage of the corresponding control ± SEM (n = 5).

Heavy metal concentration (µM)	Molecular weight of band (kD)				
	100	64	52	15	10
0.1µM thimerosal	101±23.1	110±18.6	98±16.3	94±15.5	102±16.6
1 µM thimerosal	108±18.3	98±23.4	96±19.5	96±18.5	118±16.3
0.1 µM MeHgCl	117±19.3	103±13.6	89±17.4	108±22.1	98±18.9
1 µM MeHgCl	95±20.3	129±10.8	111±9.3	116±20.6	105±21.1

Table 5.3.8: Densitometric analysis of the effects of thimerosal and methylmercury chloride on the levels of phosphorylated threonine in N2a cells differentiated for 24 hours

N2a cells were induced to differentiate for 24 hours in the presence and absence of thimerosal and methylmercury chloride, then separated by SDS PAGE and western blotting as described in Methods section 2.2.10-12. Data represents mean levels of antibody reactivity, expressed as a percentage of the corresponding control ± SEM (n = 5).

Tables 5.3.7 and 8 show that there was no change in band intensity at any molecular weight with N2a cell extracts incubated with the organic mercury compound for 4 and 24 hours ($p = 0.4526$ and 0.7206 for 4 and 24 hours respectively).

5.5: Discussion

One possible signalling cascade that is involved in both cytoskeletal organisation and cell death is the MAPK pathway. ERK has been shown to phosphorylate cytoskeletal proteins such as NFH (Veeranna *et al.*, 1998; Perron & Bixby, 1999; Pant *et al.*, 2000) and Tau (Robinson & Cobb, 1997). Tau is a MAP, which confers stability to microtubules by binding along the length of the structure. The data in chapter 5 shows that the activation of ERK was inhibited by the organic mercury compounds thimerosal and MeHgCl, whilst levels of total ERK1/2 were unaffected.

Until recently it was thought that ERK activation opposed cell death whilst JNK and p38 activated it (Subramaniam & Unsicker, 2006). However, it has been discovered that ERK may also have a death-promoting role in neuronal cells under various conditions, such as glutamate-induced cell death and ROS-induced death (Chin *et al.*, 2004). In this study ERK activation (phosphorylation) increased after 4 hours exposure of differentiating C6 cells to both thimerosal concentrations and decreased with MeHgCl exposure, indicating a different mechanism of toxicity for the organic mercury compounds (Figures 5.1.1(b) and 5.1.2). It could be that cells exposed to MeHgCl are beginning the apoptotic process, as it has been noted that in many conditions leading to apoptosis, ERK activity is suppressed (Wang *et al.*, 1998). However, MTT reduction assays in chapter 3 did not find any evidence of decreased cell viability or changes in cell morphology with the lower concentration of 0.1 µM. Another possibility is that the transient increase in ERK activation, as seen with thimerosal exposure occurred earlier in C6 cells exposed to MeHgCl and would not be detected at 4 hours. Work carried out by Parran *et al.*, (2004) showed that ERK activation and inhibition changes throughout the course of mercury exposure, thus the pattern of ERK inhibition could be different for the two compounds. Further work needs to be carried out on apoptotic markers such as caspase activation to clarify this. The increase in ERK activation seen with thimerosal could also be indicative of cellular damage as ERK has been found to be activated in certain stressful conditions, such as insult from ROS (Robinson & Cobb, 1997; Wang *et al.*, 1998). Previous studies have shown that mercury exposure does increase levels of ROS in cells (Burlando *et al.*, 1997; Dare *et al.*, 2000), which may account for this increase. MTT reduction assays in chapter 3 did not find cell viability to be decreased, so it is

unlikely that ERK activation has a death promoting role in this instance. The rate constant for ERK phosphorylation is $0.75s^{-1}$ and the maximal rate for ERK dephosphorylation is 10^{-9}-10^{-6} M^{s-1} (Maly *et al.*, 2004). As organic mercury compounds inhibit ERK activation it would be expected that they would decrease the rates of phosphorylation and dephosphorylation.

Heavy Metal Concentration (μM)	N2a cells		C6 Cells	
	4 hours	24 hours	4 hours	24 hours
0.1 μM Thimerosal	0.5:1	0.5:1	1.7:1	0.4:1
1 μM Thimerosal	0.5:1	0.46:1	1.5:1	0.5:1
0.1 μM MeHgCl	0.52:1	0.5:1	0.6:1	0.55:1
1 μM MeHgCl	0.46:1	0.5:1	0.8:1	0.56:1

Table 5.9: Ratios of phosphorylated ERK to total ERK in C6 and N2a cells.

Table 5.9 shows the ratio of phosphorylated ERK1/2 to total ERK1/2 in N2a and C6 cell extracts treated with thimerosal and MeHgCl for 4 and 24 hours. The ratios were obtained from the densitometric data contained in chapter 5. The ratios were calculated for each individual extract using the equation:

$$\frac{\%\text{ relative to control Phosphorylated ERK1/2}}{\%\text{ relative to control total ERK1/2}}$$

The ratios were then averaged for each metal concentration and time point. The ratios enable a direct quantifiable comparison to be made about the changes in the levels of phosphorylation.

The ratios show that apart from 4 hour thimerosal treatment in C6 cells, exposure to organic mercury compounds causes the levels of phosphorylated ERK to decrease in comparison to the levels of total ERK. This confirms the western blots and Quantiscan data. This decrease in the activity of ERK1/2 corresponds to the decrease in NFH phosphorylation seen in chapter 4.

Exposing N2a cells to MeHgCl for 4 hours had a similar effect of inhibiting ERK phosphorylation as was seen with C6 cells at the same time point (see Figure 5.2.1 b and 5.2.2). ERK activation decreased with both concentrations of MeHgCl. However, both concentrations of thimerosal caused a decrease in activated ERK in N2a cells as opposed to the increase in the levels of phosphorylated ERK seen with the same concentration and time point in C6 cells. This perhaps highlights a possible

difference in the toxicity of thimerosal in the two cell types, either at the level of sensitivity in the cell lines or differences in the time course of response in the actual mechanism of toxicity in the two cell lines.

After 24 hours of exposure in C6 cells the levels of activated ERK remained reduced with both concentrations of MeHgCl. Both concentrations caused a reduction in activation in contrast to the transient increase seen at 4 hours. After 24 hours levels of activated ERK were decreased with both concentrations of thimerosal and MeHgCl in N2a cells (see Figure 5.2.3 (b) and 5.2.4). Thus, in the neuronal cell line ERK inhibition was a sustained event. Parran *et al.*, (2004) looked at ERK activation in PC12 cells and found that total ERK remained at control levels throughout treatment with mercury for 1 hour, the present study indicated that the levels of total ERK remained unchanged at both 4 and 24 hours in both cell lines, with both concentrations of the organic mercury compounds.

Generally ERK signalling was inhibited by the addition of organic mercury compounds; there was only a transient increase in C6 cells at the 4 hour time point. Sustained ERK activation is known to be essential for the promotion of neurite outgrowth and stabilisation, as is NFH phosphorylation (Veeranna *et al.*, 1998). Decreased ERK activity coincides with a decrease in NFH phosphorylation (see chapter 4), which occurs during neurite outgrowth. A relative decrease in the reactivity with the anti-phosphorylated ERK antibody may mean decreased activation, but it is not conclusive evidence in itself. However, similarly altered phosphorylation of a known substrate (also known to be important in neurite outgrowth), is supporting evidence of an effect on the ERK1/2 signalling cascade. A similar study using 2.5 µM phenyl saligenin phosphate (PSP) found ERK activation to be increased during exposure to the organophosphate in N2a cells. This increased activation in the signalling pathway was accompanied by an increase in the phosphorylation of NFH (Hargreaves *et al.*, 2006). Thus, PSP had the opposite effect on NFH phosphorylation and ERK1/2 signalling to the organic mercury compounds used in the present study.

Cordova *et al.*, (2004) found that inhibiting ERK activation protected cells from lead induced cell death. Hence the inhibition of ERK activation seen in this study could be a protective mechanism employed by the cells.

In contrast to the study by Cordova *et al.*, (2004) other investigations have shown that the activation of ERK can also confer a survival advantage to cells (Xia *et al.*, 1995; Guyton *et al.*, 1996; Wang *et al.*, 1998). Thus the activation of ERK at 4

hours might give the glial cells a survival advantage in response to thimerosal that is not possible after the longer exposure time. It would of interest for further work if a larger range of concentrations and more incubation times between time 0 and 4 hours were used to monitor the activation or suppression of the ERK1/2 pathway.

Ziemba *et al.*, (2006) found ERK activation was prevented in T-cells by the failure of Ras to become properly activated after exposure to non-lethal concentrations of mercury. An investigation into the effect of MeHg on protein kinase C (PKC) activity showed that exposure to organic and inorganic mercury inhibited PKC activity in purified extracts from rat brain (Rajanna *et al.*, 1995). PKC is involved in a G-protein mediated pathway to ERK activation. PKC becomes activated by a G-protein and phosphorylates the Raf kinase inhibitory protein (RKIP) causing it to disassociate from Raf allowing ERK signalling to occur (Werry *et al.*, 2005). If mercury disrupts PKC in the N2a and C6 cells lines it may cause the inhibition of ERK1/2 signalling pathway seen in this thesis. Parran *et al.*, (2004) found levels of phosphorylated ERK to be reduced in differentiated PC12 cells after 2.5 minutes of exposure to 0.1-0.3 µM MeHgCl, then activation of ERK increased rapidly and peaked at 5 minutes before falling, indicating that MeHgCl treatment produces earlier transient signalling events. The time course did not exceed 1 hour so it can not be determined whether the activity of ERK would continue to fall to levels below the control as with the N2a cells in the present study.

Studies into the effects of other heavy metals on ERK activation indicate that responses are varied. Exposure to 300 µM zinc elevated levels of phosphorylated ERK in a mixed culture of neuronal and glial cells for up to 8 hours (Park & Koh, 1999). A separate study attributed this increase in ERK activity to damaged caused by ROS (Seo *et al.*, 2001). Exposure to mercury caused no alteration in the activation of ERK but caused an increase in the levels of activated p38, highlighting the difference in toxicity between the organic and the inorganic mercury species (Kim & Sharma, 2005). Cadmium can both inhibit and activate the ERK pathway depending on the concentration. Low levels of cadmium inhibit ERK activation, whilst high concentrations activate ERK signalling (Pulido & Parrish, 2003).

Activated ERK phosphorylates a variety of different substrates such as NFH (Veeranna *et al.*, 1998), Tau and calpain (Subramaniam & Unsicker, 2006). ERK targets serine and threonine residues for phosphorylation. Western blots of C6 cell lysates probed for phosphorylated serine and threonine residues (Figures 5.3.1 and

5.3.2) show no changes in the gross levels of phosphorylated serine or threonine with either concentration of thimerosal or MeHgCl. This is to be expected if there was an inhibition in ERK activity as with MeHgCl. However ERK activity increased in C6 cells after 4 hours incubation with both concentrations of thimerosal, but the increase does not correspond to a rise in substrate levels as would be expected. It is possible that the affected proteins were in too low abundance to be detected by the antibody. As with C6 cells there were no alterations in the levels of phosphorylated serine and threonine residues in N2a cells (Figures 5.3.3 and 5.3.4). This result suggests that the change in substrate phosphorylation involves a lower abundance protein that shows lower specificity for the anti-phosphoserine and threonine antibodies. As the numbers of phosphorylated proteins within cells is so high it was unlikely that the western blots would pick up the proteins such as NFH that are targeted by ERK1/2. However an attempt was considered to be worth while on the off chance that it presented any interesting data. Future investigations could involve the use of 2D gels to provide better separation of proteins.

Attempts to investigate the effect of organic mercury compounds on the JNK pathway are shown in the appendix. Unfortunately the reactivity of the antibody was rather poor under the conditions used in this project. Further work needs to be carried out to optimise the procedures for this antibody. However, Quantiscan analysis was completed on the western blots and indicated that there was an increase in JNK activation with both concentrations of the organic mercury compounds, but reactivity was to low to allow for a confident conclusion (see appendix).

Investigations into the effect of organic mercury compounds on the p38 pathway were unsuccessful despite numerous attempts. There antibody displayed very low reactivity with both C6 and N2a cell lysates.

Chapter 6: The effect of thimerosal and methylmercury chloride on the organisation of the cell and calpain activity

Introduction

It has been shown in previous chapters that the cytoskeletal organisation of C6 and N2a cells was disturbed following exposure to thimerosal and MeHgCl. Given that the endomembrane system, which is dependent on MT integrity (Waterman-Storer & Salmon, 1998), houses intracellular Ca^{2+} stores; it was of interest to this investigation to determine whether the organisation of cell organelles were affected by the exposure to organic mercury compounds. Using a bodipy labelled probe to recognise the endoplasmic reticulum (ER) and an antibody against a Golgi apparatus protein called GRASP 65, confocal microscopy was carried out to visualise any disruptions caused by the mercury compounds.

Both the ER and the Golgi apparatus depend upon MTs for their positioning within a cell and MT based motors such as kinesin and dynein are involved in membrane trafficking (Presley *et al.*, 1997). The Golgi apparatus of mammalian cells is organised into stacks of cisternae. Each stack contains an average of 4–8 cisternae, and about 40–80 such stacks are attached to each other and anchored in the pericentriolar region. When mammalian cells enter mitosis, the pericentriolar stacks of Golgi cisternae undergo extensive fragmentation, and the fragments are dispersed throughout the cytosol. This process is mediated by mitogen-activated protein kinase kinase 1 (MEK1). GRASP 65 (Golgi reassembly stacking protein of 65 kDa) is a Golgi associated protein that is required for mitotic Golgi fragmentation (Sutterlin *et al.*, 2002).

Changes in intracellular calcium concentrations disrupt calcium dependent signalling mechanisms and enzyme activity. The ryanodine receptor mediates the release of calcium from ER stores and is activated by raised levels of cytosolic calcium of around 100 µM in a process known as Ca^{2+} induced Ca^{2+} release (Fabiato, 1985). The ER is an important organelle in the maintenance of calcium homeostasis in both neuronal and glial cells. Previous work has shown that disrupting the ER hinders the cells ability to maintain intracellular concentrations (Doutheil *et al.*, 1997; Lee *et al.*, 2006). Calcium is removed from the intracellular matrix by a variety of mechanisms. These include SERCA; an energy dependent pump that sequesters

calcium within the ER. SERCA is important in the regulation of intracellular calcium as research has shown that overexpression of SERCA decreases the time period of a calcium wave (Falcke *et al.*, 2003). Thapsigargin is a plant derivative that binds to SERCA; using fluorescently labelled bodipy thapsigargin and bodipy ryanodine allowed the capture of images showing the distribution of SERCA and ryanodine receptors within cells. In this chapter experiments were carried to determine whether the addition of thimerosal or MeHgCl changed the distribution of the ryanodine receptors and SERCA within differentiating C6 and N2a cells.

One possible consequence of raised intracellular calcium levels is the activation of calpains. Calpains are calcium activated enzymes that are known to target cytoskeletal proteins (Huang & Wang, 2001). There are two main forms of calpains in vertebrate cells; calpain 1 and 2 and they are distinguished by their calcium requirements for activation. Calpain 1 requires concentrations of 5-50 µM and calpain 2 requires concentrations of 200-1000 µM for activation (Wang, 2000). Calpains are known to be involved in the formation of processes and cells adhesion, they are also known to degrade various MAPs. MAPs are important in the stabilisation of MTs and their degradation by calpain may have an adverse affect on MT stability (Sorimachi *et al.*, 1997). Due to the degradation of the cytoskeletal network seen in chapter 4, it was of interest to the study to determine if the addition of the organic mercury compounds affected the activation of calpain 1, as changes in activity may indicate a possible role for calpain in organic mercury induced disruption of the cytoskeleton.

Methods

The concentrations of thimerosal and MeHgCl used for the western blotting and confocal microscopy in this chapter were the same as previous chapters 0.1 and 1 µM. Cells were seeded into an 8 well chamber slide (see Methods section 2.2.14-15), there were 2 wells for the control and each concentration of the organic mercury compounds (0.1 and 1 µM). Each experiment was repeated a minimum of 3 times and the images contained in the chapter represent what was seen in each individual experiment. All antibodies and probes were diluted in 3 % BSA (see Methods for detail). The calpain 1 antibody (sc-7530) was used at a dilution of 1/1000 and the secondary anti-goat antibody was used at 1/2000. The dilution factor for the anti-golgi antibody was 1/200; Bodipy thapsigargin was diluted to 10 µM and the final

concentration of Bodipy ryanodine was 1 µM. Each experiment was completed in triplicate using different batches of cells.

For the calpain assay the cells were seeded at the normal density in T25 flasks and then extracted in the homogenisation buffer described in the methods section with a cell scraper. The cell suspension was kept on ice to minimise enzyme activity and sonicated for 5 minutes. A mini-Lowry protein estimation was carried out on the sonicates so that the activity could be corrected for protein concentration. The lane on the blots labelled 0 is the control extract with no added metal. For the thimerosal treated corresponding control sterile distilled water was added at the same volume as the metal in the treated cells and with MeHgCl DMSO was added at the same volume as with the treated cells as the MeHgCl was dissolved in DMSO due to poor solubility in distilled water.

Figure 6.1 (a) shows control cells differentiated for 24 hours without the addition of heavy metals. The probe bodipy thapsigargin stained cell bodies and outgrowths in a punctate manner. The brightest staining was located around the nucleus of the cell, where the highest concentration of ER would be expected. Figure 6.1 (b) shows cells differentiated for 24 hours in the presence of 0.1 µM thimerosal. The cells exhibited a relatively diffuse staining pattern. In some cells the bright area of staining circling the nucleus was no longer visible, although the processes were still visibly stained at this concentration. The cells exposed to 1 µM thimerosal for 24 hours (figure 6.1 c), exhibited very intense punctate staining and little or no staining of neurites. The perinuclear organisation was no longer visible. Figure 6.1 (d) shows cells exposed to 0.1 µM MeHgCl. There was little difference between the cells in this image and those treated with the same concentration of thimerosal. The cells still had stained processes and the bright area around the nucleus was either less intense or had become disrupted. Cells exposed to 1 µM MeHgCl for 24 hours, no longer displayed visibly stained processes, but the nuclei were more discernable than in the image of cells treated with the same concentration of thimerosal. The images are representative of 3 separate experiments and reflect the major trends seen in each one.

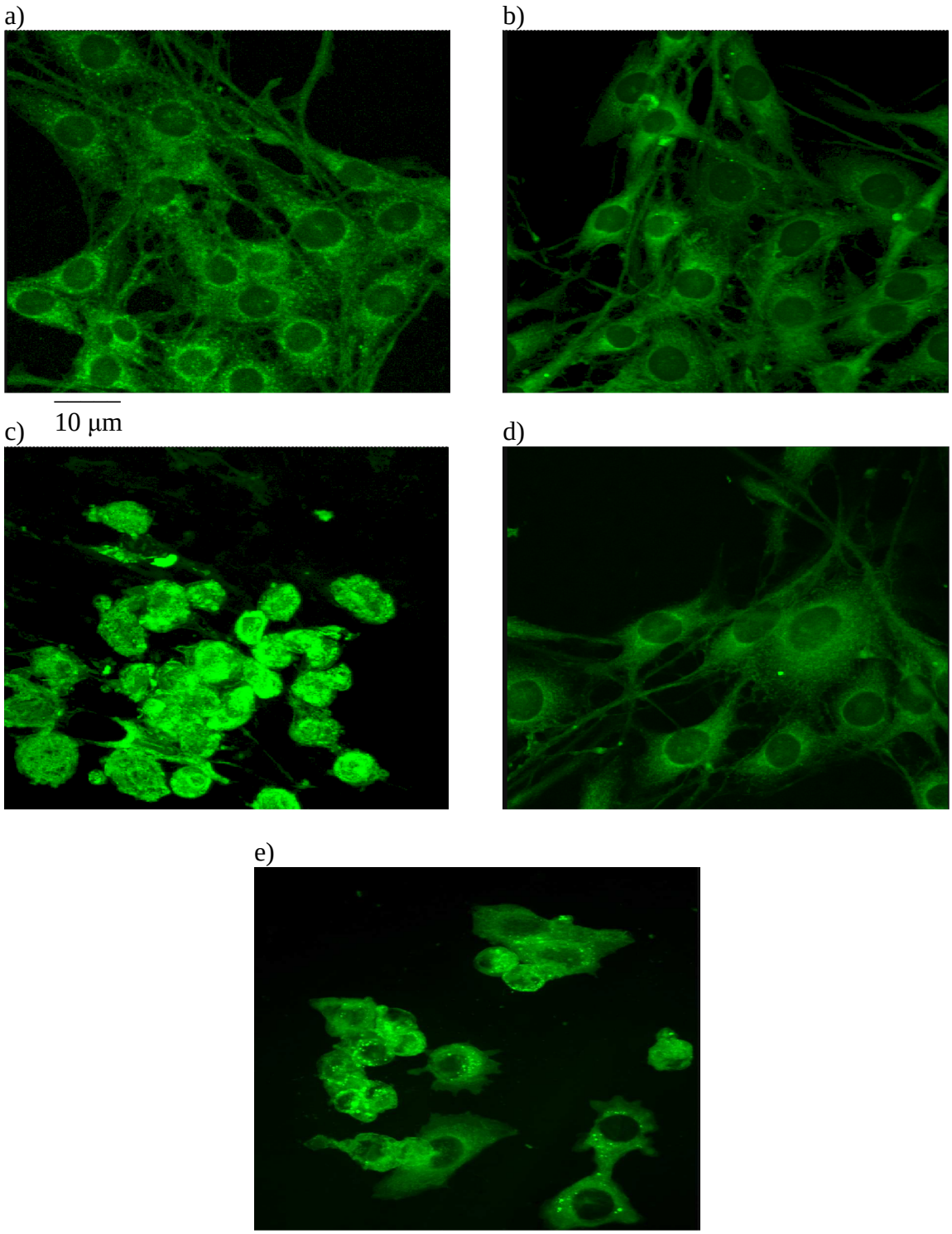

Figure 6.1: The effect of thimerosal and MeHgCl on the distribution of SERCA in C6 cells

C6 cells were induced to differentiate for 24 hours in the absence of thimerosal (a), with 0.1 (b) and 1 μM (c) of thimerosal and 0.1 (d) and 1 μM (e) methylmercury chloride. The cells were stained with bodipy thapsigargin, which binds to SERCA as described in Methods section 2.2.15 (n = 3).

Figure 6.2 (a) shows N2a cells differentiated for 24 hours in the absence of thimerosal and MeHgCl. The cells were stained in neurite outgrowths but the strongest of the staining was observed on one side of the nucleus. Bodipy thapsigargin appeared to have stained N2a cells in a less punctate manner than that observed in C6 cells. Figure 6.2 (b) shows cells exposed to 0.1 µM thimerosal for 24 hours. The cells were stained more weakly with the bodipy thapsigargin but the most intense staining was still localised around the nucleus of the cell but still detectable in neurites. Cells exposed to 1 µM thimerosal for 24 hours, exhibited no visible neurite staining and the staining within the cell body was punctate and relatively disperse. Figure 6.2 (d) shows cells incubated with 0.1 µM MeHgCl for 24 hours. The cells were weakly stained in comparison to the control cell, but still exhibited fluorescent staining in cell bodies and neurites. In the vast majority of cells, the strongest staining was still around the nucleus, but in one cell the bodipy thapsigargin covered the whole cell.

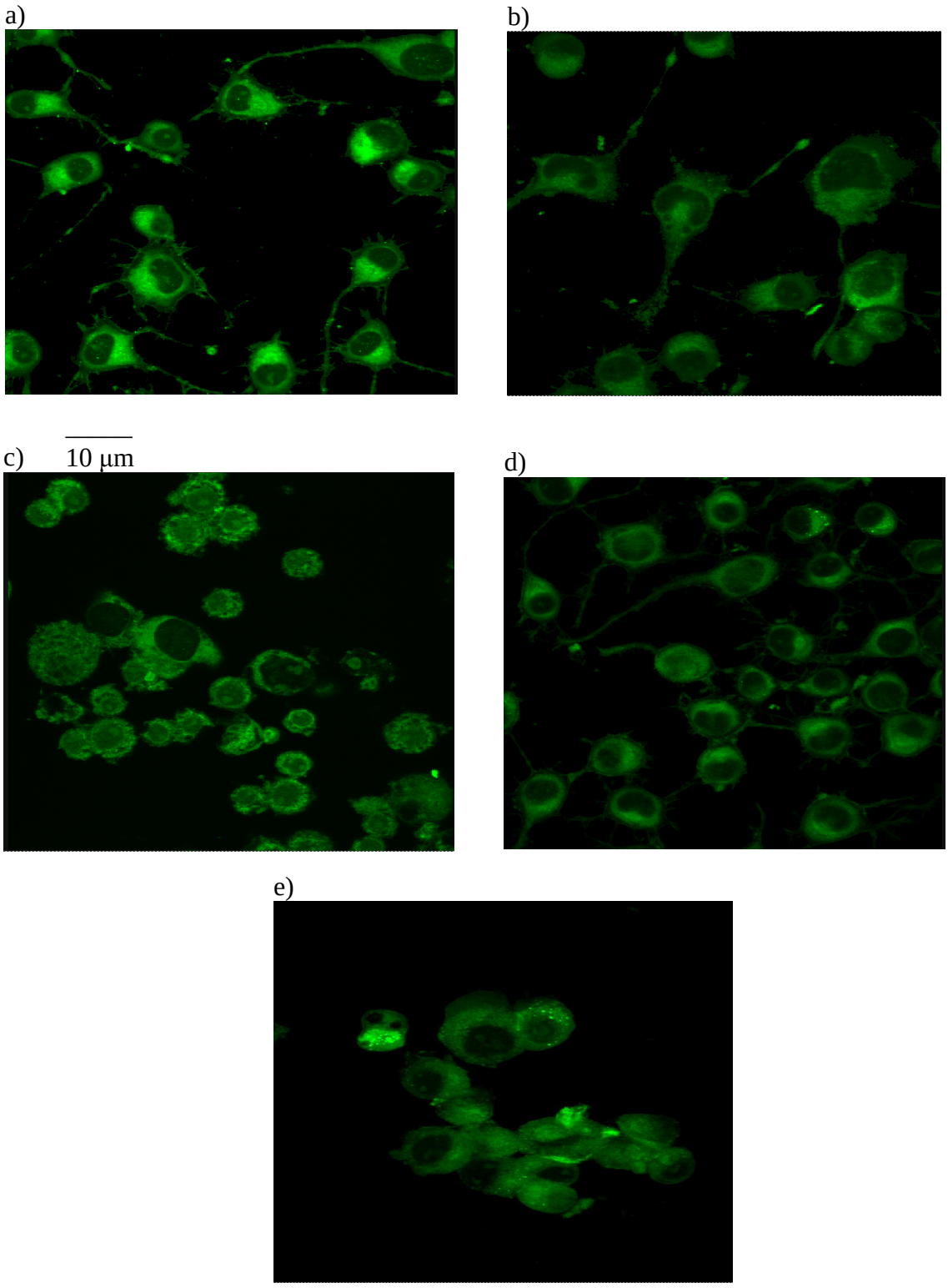

Figure 6.2: The effect of thimerosal and MeHgCl on the distribution of SERCA in N2a cells

N2a cells were induced to differentiate for 24 hours in the absence of thimerosal (a), with 0.1 (b) and 1 μM (c) of thimerosal and 0.1 (d) and 1 μM (e) methylmercury chloride. The cells were stained with bodipy thapsigargin, which binds to SERCA as described in Methods section 2.2.15 (n = 3).

In figure 6.2 (e) the cells have been treated with 1 µM MeHgCl for 24 hours and like the cells exposed to the same concentration of thimerosal, there was no visible neurite staining and staining in the cell body was more diffuse than in the control. The images shown are representative of three separate experiments and reflect the changes seen in each one.

Figure 6.3 (a) shows that bodipy ryanodine staining of C6 cells differentiated for 24 hours without the addition of thimerosal or MeHgCl was detected throughout the cell body and extended into the processes in a punctate manner. In cells exposed to 0.1 µM thimerosal for 24 hours (figure 6.3 (b)), the staining did not appear as intense as with the control cells but the distribution of the ryanodine receptor staining was similar to that of untreated cells. The cells in figure 6.3 (c) have been exposed to 1 µM thimerosal for 24 hours. At this concentration there were very few weakly stained processes and the distribution of the ryanodine receptor within the cell body had changed when compared to control cells. There was no longer a defined nucleus due to the disperse staining pattern. The punctate staining visible within control cell was no longer evident. Cells exposed to 0.1 µM MeHgCl for 24 hours show that there is little difference from the control apart from the intensity of the staining. The cells in figure 6.3 (e) have been exposed to 1 µM MeHgCl for 24 hours. There were no visible processes in the image and the nucleus was not as clearly defined as with control cells. The images shown are representative of three separate experiments and reflect the major changes seen in each individual experiment.

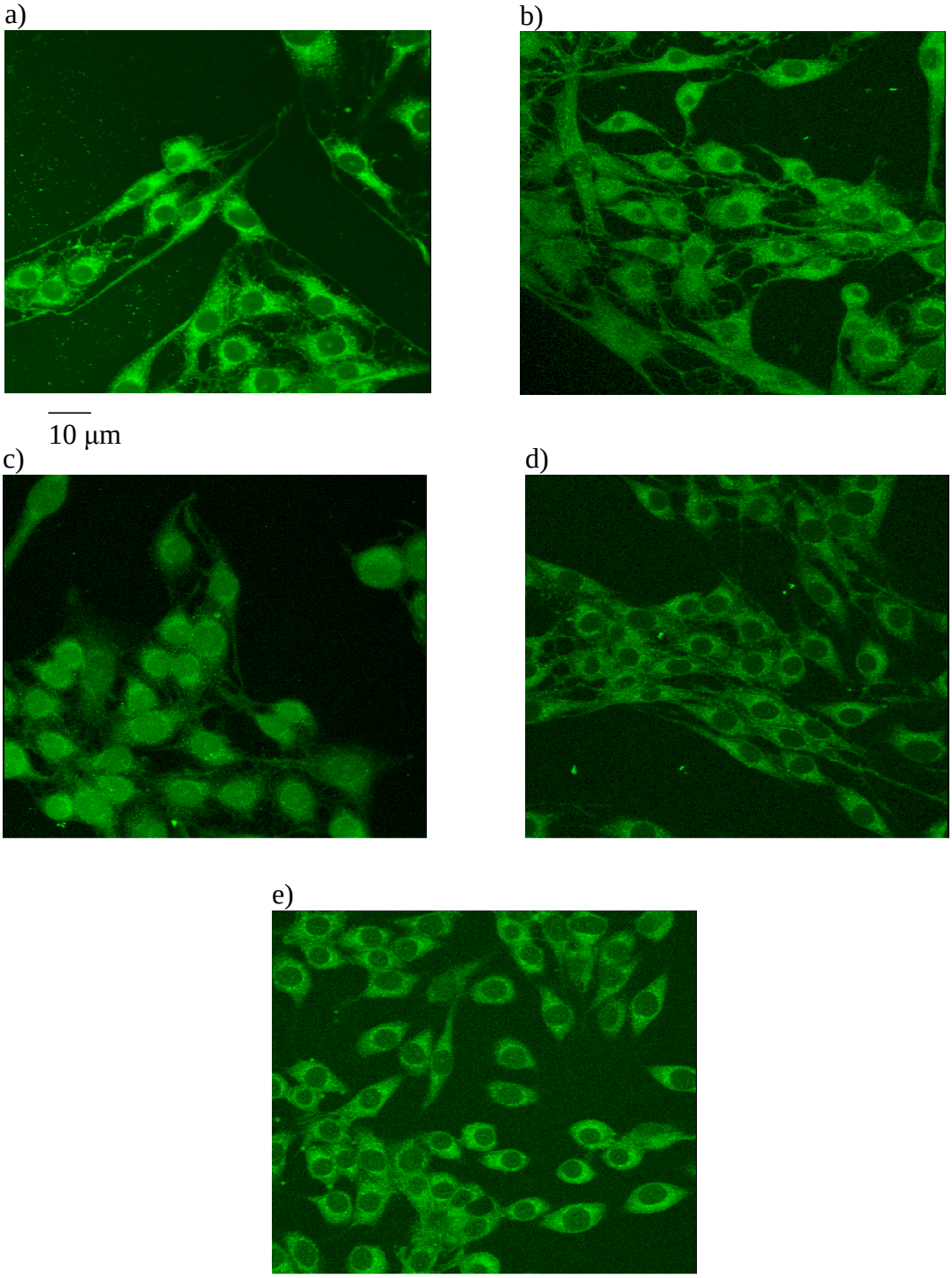

Figure 6.3: The effect of thimerosal and methylmercury chloride on the distribution of ryanodine receptors in C6 cells

C6 cells were induced to differentiate for 24 hours in the absence (a) and presence (b-e) of 0.1 µM (b) and 1 µM (c) of thimerosal and 0.1 µM (d) and 1 µM (e) MeHgCl. The cells were stained with bodipy ryanodine, which binds to ryanodine receptors as described in Methods section 2.2.15 (n = 3).

Figure 6.4 (a) shows that N2a cells differentiated for 24 hours without thimerosal or MeHgCl exhibited ryanodine receptor staining in the cell body with the greatest intensity around the nucleus, and also staining within the neurites. The staining pattern appeared punctate. The cells in figure 6.4 (b) have been exposed to 0.1 µM thimerosal for 24 hours. The cells in the image did not appear different from the control. The neurites were still visible and the pattern of staining within the cell body appeared unaltered from the control cells. Figure 6.4 (c) shows cells incubated with 1 µM thimerosal for 24 hours. The cells had no visibly stained neurites and the staining pattern was different from the control in that there was a disperse distribution of staining such that the nucleus was no longer discernable. Figure 6.4 (d) did not appear radically different from the control cells, there was still a visible nucleus within the cell body and the staining was quite granular. However in agreement with neurite outgrowth in chapter 3, neurites were generally more stunted but the pattern of staining was similar to controls. Cells incubated with 1 µM MeHgCl for 24 hours (figure 6.4 (e)), displayed very few visibly stained axons and they were extremely stunted. There did appear to be a redistribution of ryanodine receptor staining with this concentration in that there appeared to be an accumulation of the receptor staining on the edge of the nucleus. The images shown are representative of three separate experiments and reflect the changes seen in each one.

Figure 6.5 (a) shows C6 cells differentiated for 24 hours in the absence of thimerosal and MeHgCl. The cells had been incubated with an ER tracker. The distribution of the ER in C6 cells appeared to be cell wide. Figure 6.5 (b) shows N2a cells differentiated for 24 hours without the addition of heavy metals. ER staining was localised to the area surrounding the nucleus and to a lesser extent, in neurites. When the cells were differentiated in the presence of the organic mercury compounds the fluorescence staining was too weak to be captured on digital image. Staining with the ER tracker was attempted on three separate occasions and each time staining only occurred in the control cells without the presence of thimerosal and MeHgCl.

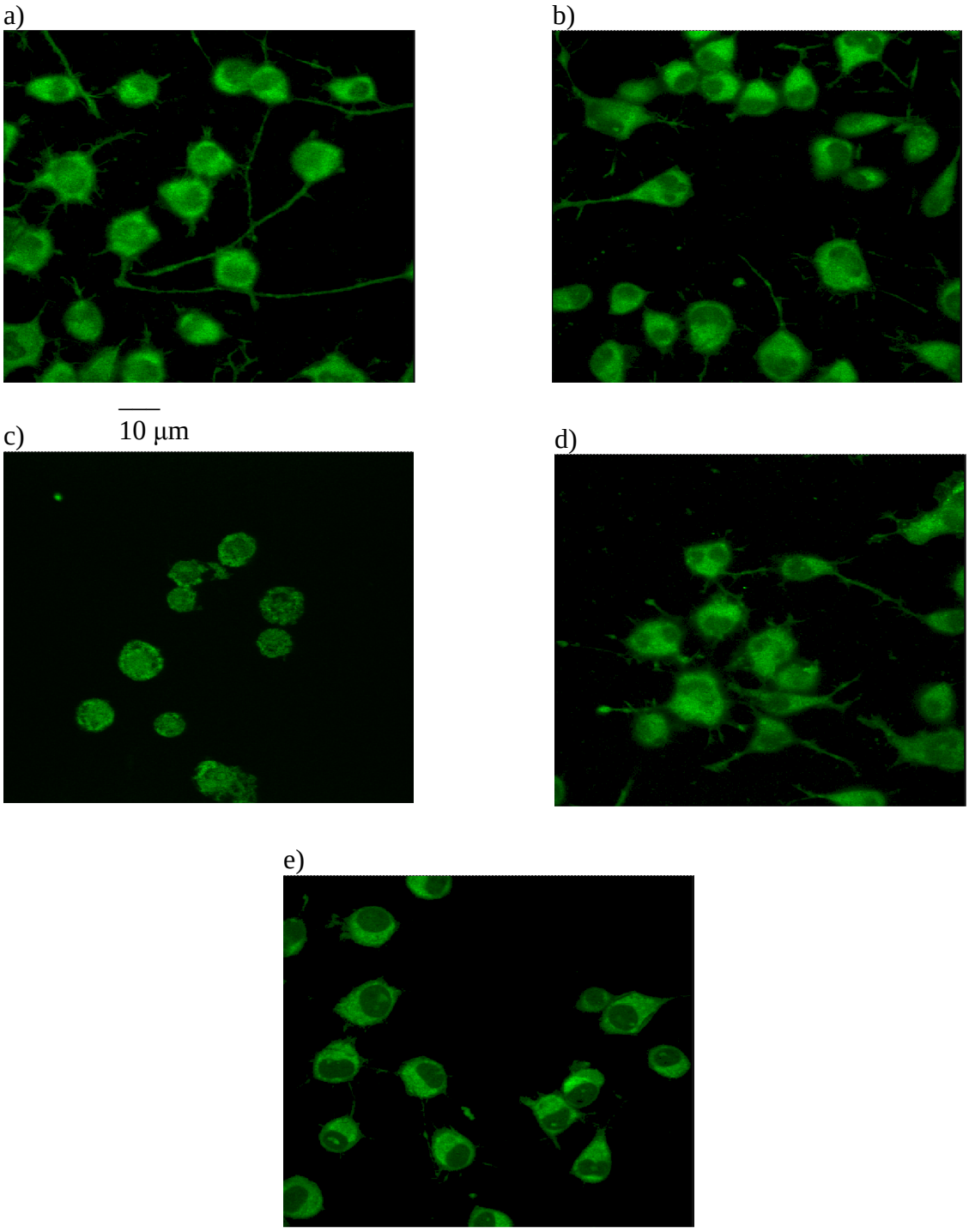

Figure 6.4: The effect of thimerosal and methylmercury chloride on the distribution of ryanodine receptors in N2a cells

N2a cells were induced to differentiate for 24 hours in the absence (a) and presence (b-e) of 0.1 µM (b) and 1 µM (c) of thimerosal and 0.1 µM (d) and 1 µM (e) MeHgCl. The cells were stained with bodipy ryanodine, which binds to ryanodine receptors as described in Methods section 2.2.15 (n = 3).

a)

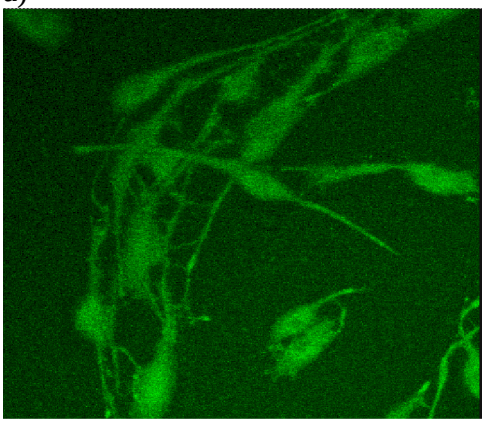

b)

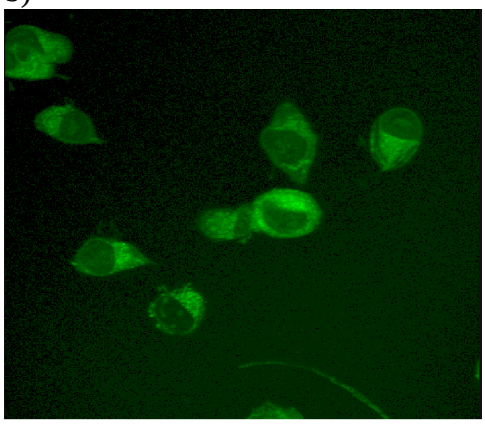

10 µm

Figure 6.5: The distribution of ER in C6 and N2a cells untreated with organic mercury compounds.

N2a and C6 cells were induced to differentiate for 24 hours in the absence of thimerosal and methylmercury chloride. Cells were then stained with ER tracker and fixed with ice cold methanol as described in Methods section 2.2.15 (n = 3).

Figure 6.6 (a) shows control C6 cells differentiated for 24 hours in the absence of thimerosal and MeHgCl. The anti-Golgi apparatus antibody was punctate throughout the cell body and was particularly intense in the cell processes. The widespread staining pattern indicated that the antibody had reacted with other cellular components as well as the Golgi apparatus. Figure 6.6 (b) shows cells exposed to 0.1 µM thimerosal for 24 hours. Treatment did not appear to cause disruption when compared to the control. In cells incubated with 1 µM thimerosal for 24 hours (figure 6.6 (c)), the organisation of the cell appeared different to that of the control. With the higher concentration there appeared to be minor disruption in the cell body staining. Figure 6.6 (d) shows cells exposed to 0.1 µM MeHgCl for 24 hours. There did not appear to be any radical changes to the antibody staining, but there does seem to be a slight disruption in the cell body staining. Figure 6.6 (e) shows cell incubated with 1 µM MeHgCl for 24 hours. The organisation of the cells appeared very different from the control. The cells contained some intensely stained areas indicating a breakdown in cellular organisation. The images shown are representative of three separate experiments and reflect the changes seen in each one.

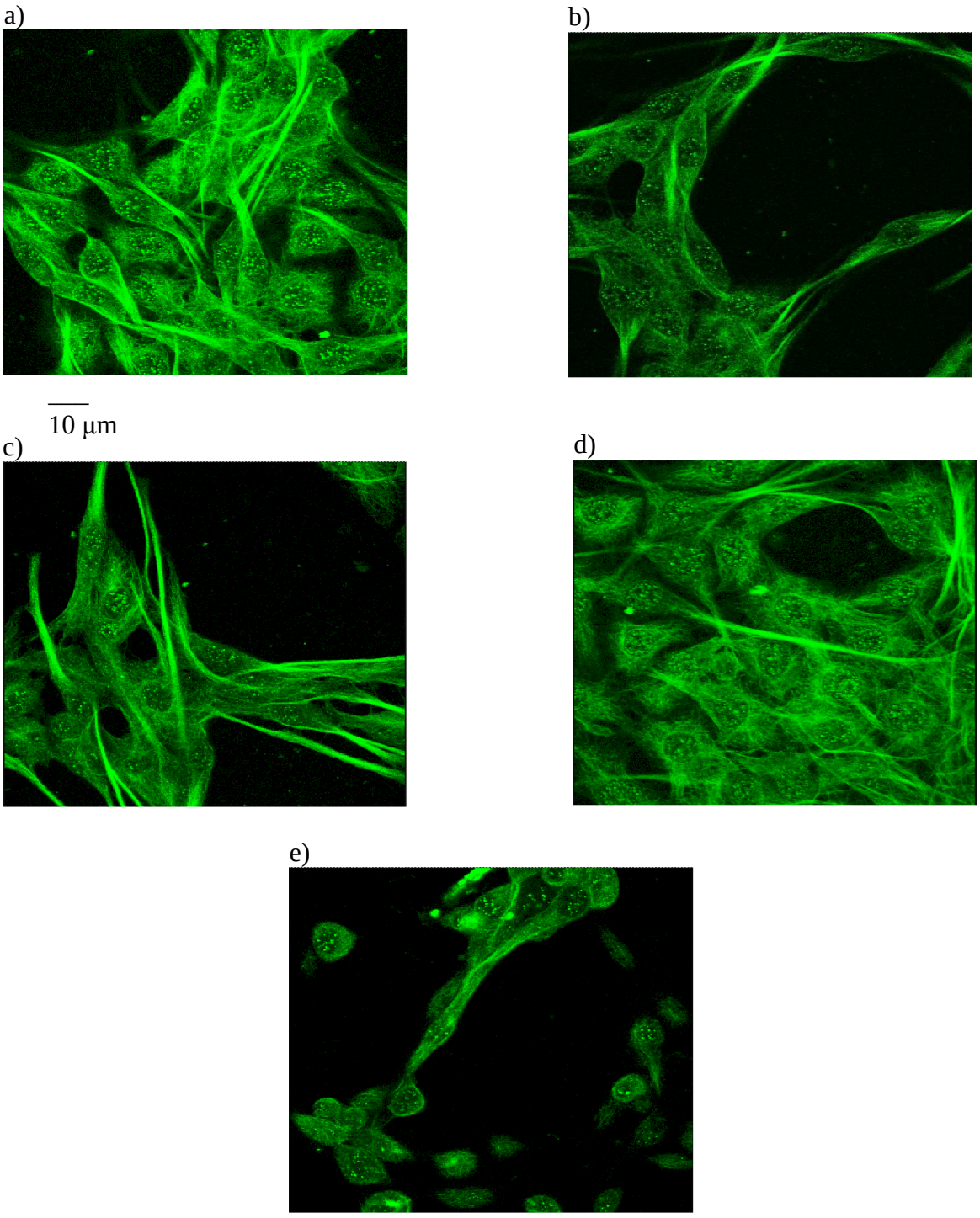

Figure 6.6: The effect of thimerosal and methylmercury chloride on antibody staining of the Golgi apparatus in differentiating C6 cells

C6 cells were induced to differentiate for 24 hours in the absence (a) and presence (b-e) of 0.1 µM (b) and 1 µM (c) of thimerosal and 0.1 µM (d) and 1 µM (e) MeHgCl. The cells were stained with N-20, an anti-Golgi apparatus antibody as described in Methods section 2.2.15 (n = 3).

Figure 6.7 (a) shows control N2a cells differentiated for 24 hours in the absence of thimerosal and MeHgCl. Anti-Golgi apparatus antibody staining was distributed around the cell body, with an intense perinuclear spot and into the neurites. The antibody may be binding to other proteins apart from the GRASP 65 protein in the Golgi apparatus membrane as normally the organelle would be located near the nucleus and would not cover the whole cell as the binding of this antibody suggests. Figure 6.7 (b) shows cells exposed to 0.1 µM thimerosal for 24 hours. The distribution of the Golgi apparatus and other proteins being detected by the antibody had altered with the addition of thimerosal. The area of staining had become much more disperse than control staining. There was still visible staining within the axon-like processes. Figure 6.7 (c) shows cells treated with 1 µM thimerosal for 24 hours. Here the cells showed a different staining pattern from the control. Staining was more punctate and disperse throughout the cell body and no neurite staining was observed. The cells in figure 6.7 (d) have been exposed to 0.1 µM MeHgCl for 24 hours. As with the same concentration of thimerosal, the staining was more punctate and disperse in a proportion of cells and neurite staining, though present was less intense. Figure 6.7 (e) shows cells incubated with 1 µM MeHgCl for 24 hours. There was no visible neurite staining in this image and the staining within the cell body was much weaker than that seen in the control. The images shown are representative of three separate experiments and reflect the major trends seen in each individual experiment.

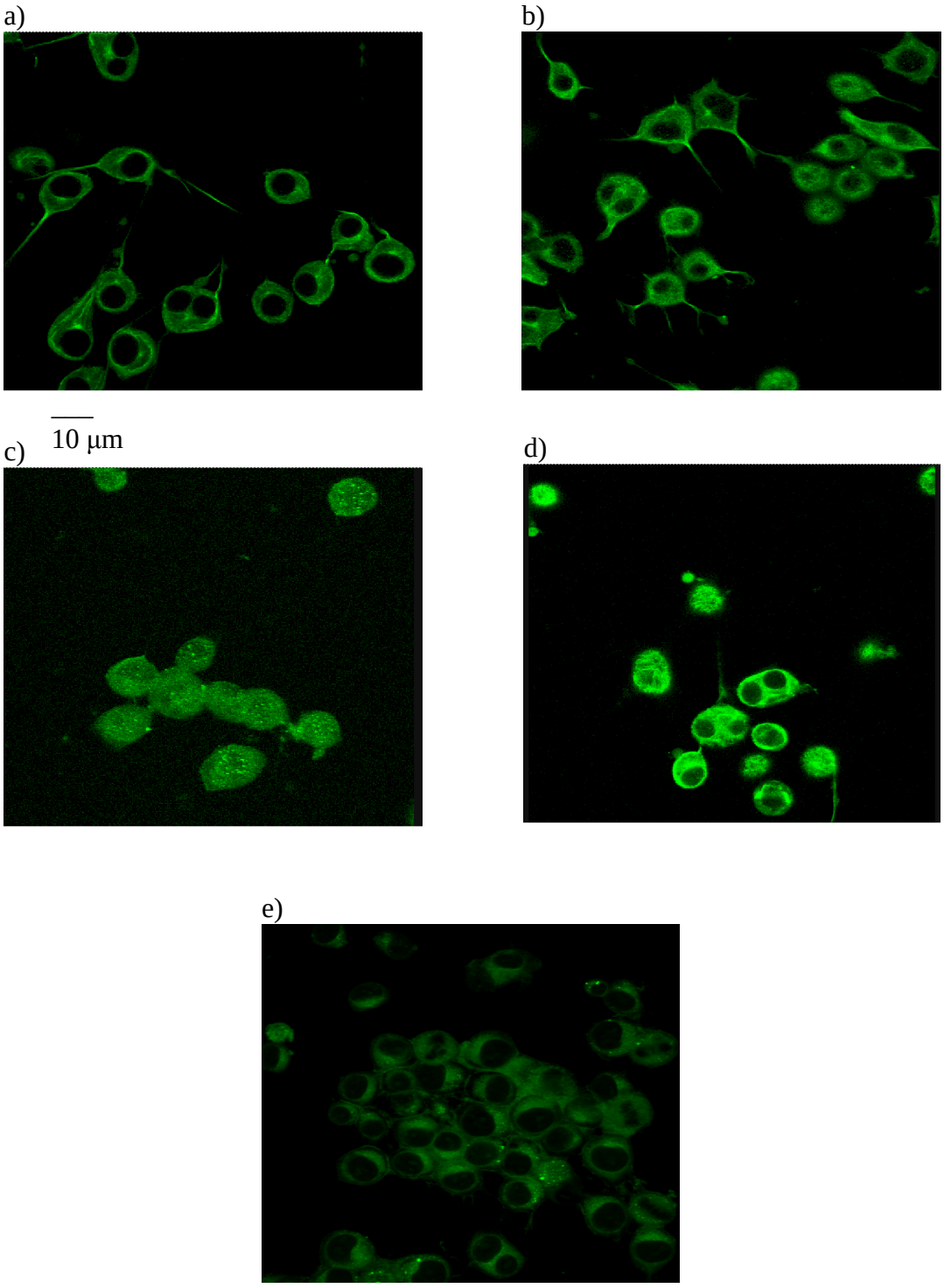

Figure 6.7: The effect of thimerosal and methylmercury chloride on the antibody staining of the Golgi apparatus in N2a cells

N2a cells were induced to differentiate for 24 hours in the absence (a) and presence (b-e) of 0.1 µM (b) and 1 µM (c) of thimerosal and 0.1 µM (d) and 1 µM (e) MeHgCl. The cells were stained with N-20, an anti-Golgi apparatus antibody as described in Methods section 2.2.15 (n = 3).

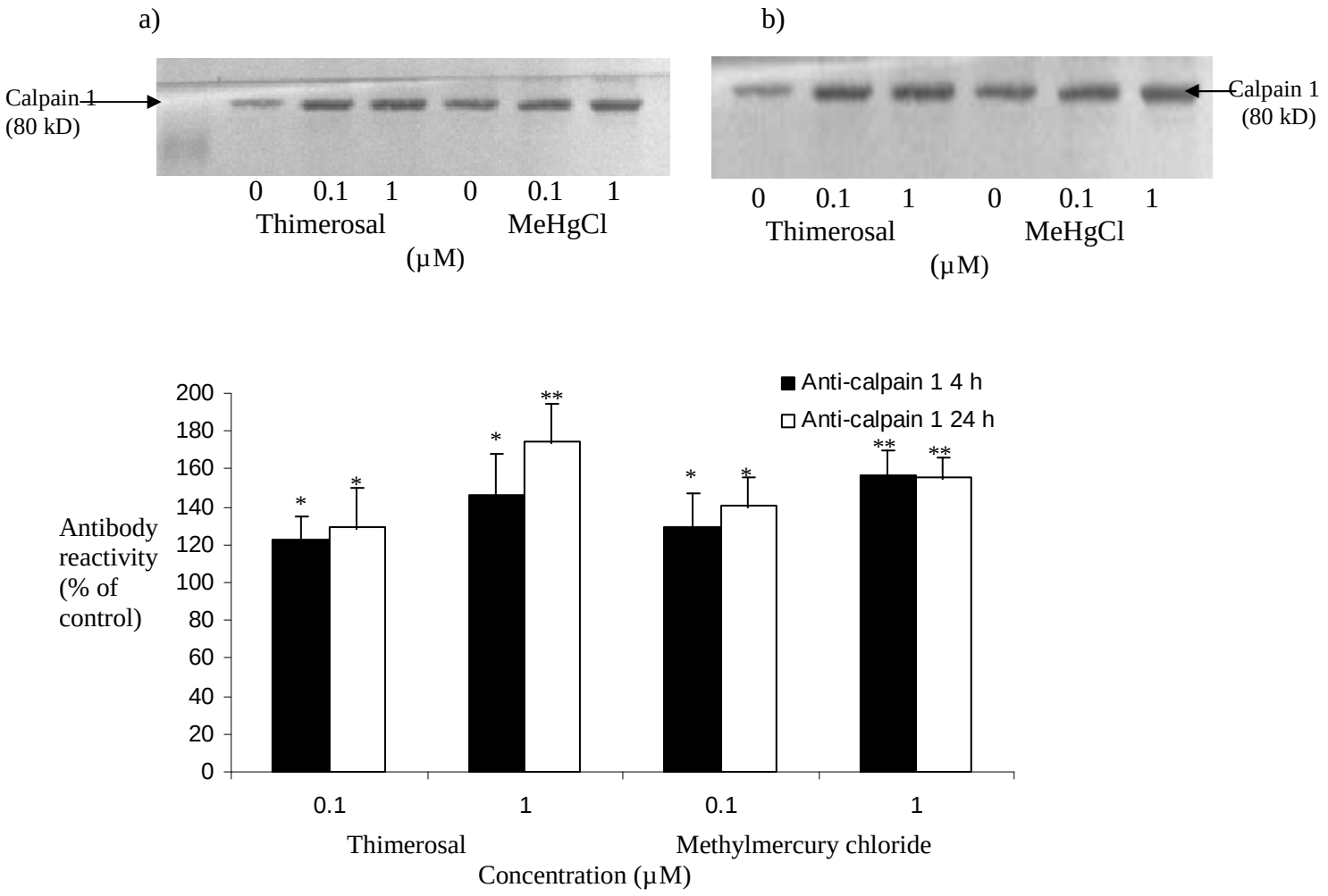

Figure 6.8: The effect of thimerosal and methylmercury chloride on the levels of calpain 1 in C6 cells

C6 cells were induced to differentiate for 4 and 24 hours in the presence and absence of thimerosal and MeHgCl, then separated by SDS PAGE and western blotting as described in Methods section 2.2.10-12. Data represents mean levels of antibody reactivity, expressed as a percentage of the corresponding control ± SEM (n = 5). Asterisks indicated statistical significance of differences from the control (*$p<0.05$, **$p<0.001$). The 2 way ANOVA test was used for statistical analysis, followed by post hoc Bonferroni's correction for pair wise multiple analysis.

Figure 6.8 shows that at both 4 and 24 hours, both concentrations of thimerosal and MeHgCl significantly increased the reactivity of the anti-calpain 1 antibody with C6 cell lysates. The average densitometric absorbance from control cell lysates probed with anti-calpain 1 antibody was 0.95823 for 4 hour extracts and 0.93795 for 24 hours. After 4 hours incubation with thimerosal antibody reactivity was increased by around 23 % - 46 % when compared to the reactivity of the control extracts. Statistical analysis using a 2 way ANOVA test indicated that there was a significant difference

in the 4 hour data (p = 0.02439). Post hoc tests confirmed that the 0.1 and 1 µM concentrations were significantly different from the control (p = 0.03281 and 0.004562 for 0.1 and 1 µM respectively). Exposure to 0.1 µM and 1 µM MeHgCl increased antibody reactivity by 19 - 57 %. Statistical analysis of the data confirmed significance (p = 0.04332 for 0.1 µM and 0.00674 for 1 µM). After 24 hours of exposure, thimerosal significantly increased band intensity by 29 %- 75 %. Twenty four hours exposure to 0.1 µM and 1 µM MeHgCl increased the reactivity of the anti-calpain antibody by 21 % and 56 % (p range of 0.00253-0.00643). The 2 way ANOVA test indicated a significant difference in the 4 and 24 hour data (p = 0.04543), the post hoc Bonferroni's test confirmed that the data obtained from exposure to 1 µM thimerosal was significantly different but a comparison of the other concentrations did not highlight any significant differences between the two incubation times.

Figure 6.9 shows that at both 4 and 24 hours, both concentrations of thimerosal and MeHgCl significantly increased the reactivity of the anti-calpain 1 antibody with N2a cell lysates. After 4 hours incubation with 0.1 µM thimerosal antibody reactivity was increased by around 33 %. Exposure to 1 µM caused a significant 62 % increase in band intensity when compared to the control. Exposure to 0.1 µM and 1 µM MeHgCl increased antibody reactivity by 24 % and 75 % respectively. Statistical analysis using a 2 way ANOVA test indicated significance differences (p = 0.04786 for the 4 hour data set). A post hoc Bonferroni's test confirmed that all both concentrations of both compounds were significantly different from the control with p ranging from 0.04859-0.00348. After 24 hours of exposure 0.1 µM thimerosal increased band intensity by 38 % and 1 µM caused a 67 % increase in antibody reactivity. Exposure to 0.1 µM and 1 µM MeHgCl for 24 hours increased the reactivity of the anti-calpain antibody by 40 % (p = 0.002435) and 80 % (p = 0.008987) respectively. Statistical analysis using a 2 way ANOVA did not highlight any significant differences between the 4 and 24 hour data, (p = 0.07865).

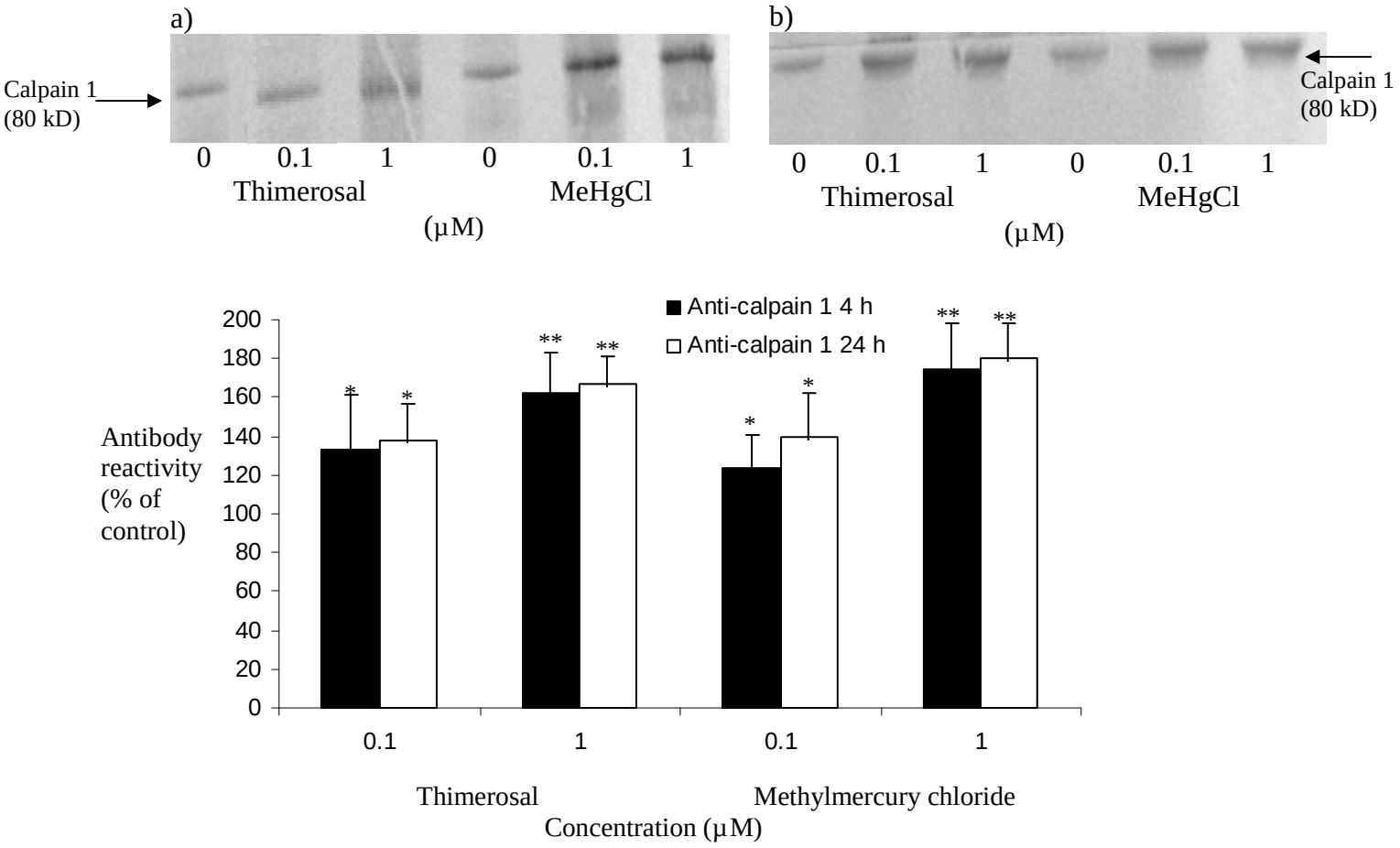

Figure 6.9: The effect of thimerosal and methylmercury chloride on the levels of calpain 1 in N2a cells

N2a cells were induced to differentiate for 4 and 24 hours in the presence and absence of thimerosal and MeHgCl, then separated by SDS PAGE and western blotting as described in Methods section 2.2.10-12. Data represents mean levels of antibody reactivity, expressed as a percentage of the corresponding control $\pm$ SEM (n = 5). Asterisks indicated statistical significance of differences from the corresponding control (*$p<0.05$, **$p<0.01$). The 2 way ANOVA test was used for statistical analysis, followed by post hoc Bonferroni's correction for pair wise multiple analysis.

a)

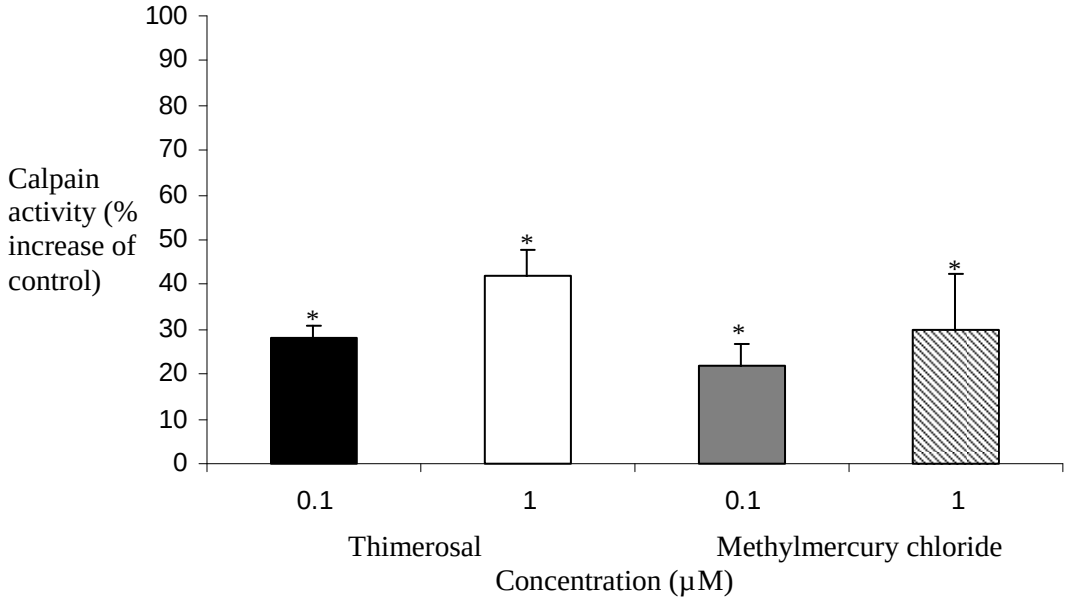

b)

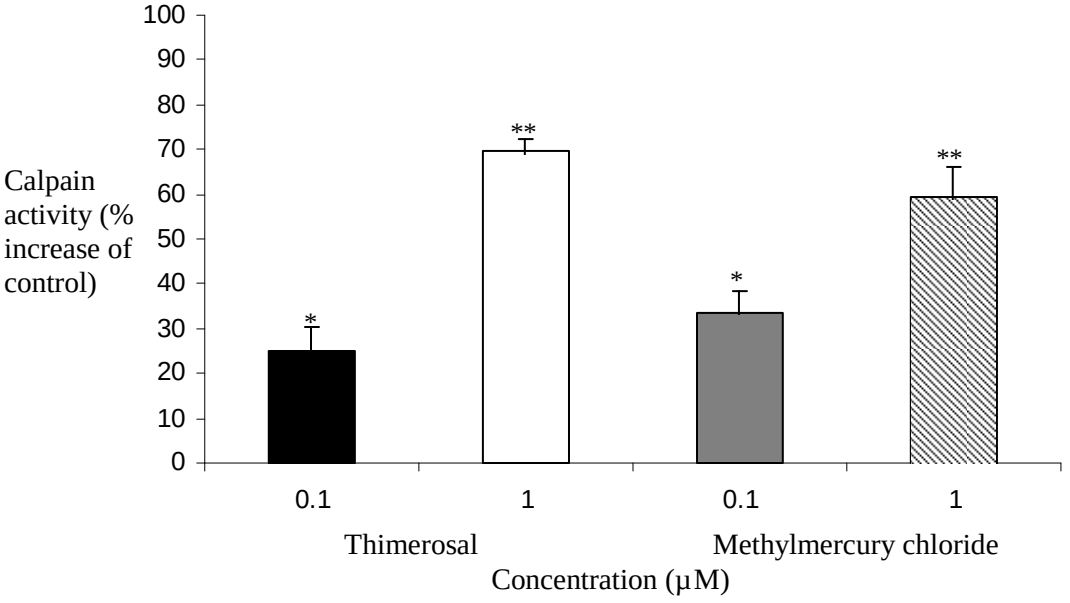

Figure 6.10: The effect of thimerosal and methylmercury chloride on the activity of calpain in differentiating C6 cells

C6 cells were induced to differentiate for 4 (a) and 24 (b) hours in the presence and absence of thimerosal and MeHgCl as indicated. Cells were lysed by sonication and the extracts were used to measure calpain activity as described in Methods section 2.2.16. Data represents mean levels of calpain activity expressed as a percentage of the corresponding control $\pm$ SEM (n = 4). Asterisks indicate statistical significance of difference from the control (*$p<0.05$). The 2 way ANOVA test was used for statistical analysis, followed by post hoc Bonferroni's correction for pair wise multiple analysis.

Figure 6.10 indicates that there was a concentration dependent increase in calpain activity compared to the controls in sonicated C6 cell extracts differentiated in the presence of thimerosal and MeHgCl for both 4 and 24 hours. Activity increased by approximately 25-43 % in cells exposed to both concentrations of the organic mercury compounds after 4 hours (Figure 6.10 a). Statistical analysis confirmed significance with p ranging from 0.01639-0.3629. Actual activity in absorbance change/mg protein/hour was 14.5 and 18.6 for 0.1 and 1 µM thimerosal and 16.8 and 22.3 for MeHgCl. After 24 hours (Figure 6.10 b) the activity of calpains was greater with a 70 % increase with exposure to the higher concentrations of the mercury compounds and around a 24-35 % increase in activity with the lower concentration of 0.1 µM. Statistical analysis using a 2 way ANOVA confirmed that there was a significant difference from the control ($p = 0.02441$). Post hoc Bonferroni's test indicated that both concentrations and both compounds were significantly different from the control ($p = 0.02329$, 0.00119, 0.01163, and 0.00803 for 0.1, 1 µM thimerosal and 0.1, 1 µM MeHgCl respectively). Actual enzyme activity expressed as change in absorbance/mg protein/hour was 25.2 and 89.7 for 0.1 and 1 µM thimerosal and 21.2 and 83.1 for MeHgCl. Statistical analysis also confirmed significant differences in the effects seen with the different incubation times ($p < 0.05$).

Figure 6.11 (a) shows that after 4 hours incubation both concentrations of thimerosal and MeHgCl significantly increased calpain activity ($p<0.05$) by 25-36 %. A 2 way ANOVA ($p = 0.03471$), indicting that there were significant differences within the 4 hour treatment. Further analysis using post hoc Bonferroni's test confirmed that both concentrations of thimerosal and MeHgCl were significantly different from the control. Actual enzyme activity expressed as change in absorbance/mg protein/hour was 19.6 and 21.4 after exposure to 0.1 and 1 µM thimerosal and 20.9 and 24.8 for MeHgCl. After 24 hours (Figure 6.11 b) treatment with 0.1 µM of both compounds increased activity by 25-30 % ($p = 0.04931$ and 0.02798 for thimerosal and MeHgCl respectively). Exposure to 1 µM thimerosal and MeHgCl significantly increased calpain activity by approximately 60-70 %. Actual enzyme activity expressed as change in absorbance/mg protein/hour was 28.7 and 97.6 following exposure to 0.1 and 1 µM thimerosal and 22.3 and 88.4 for MeHgCl.

a)

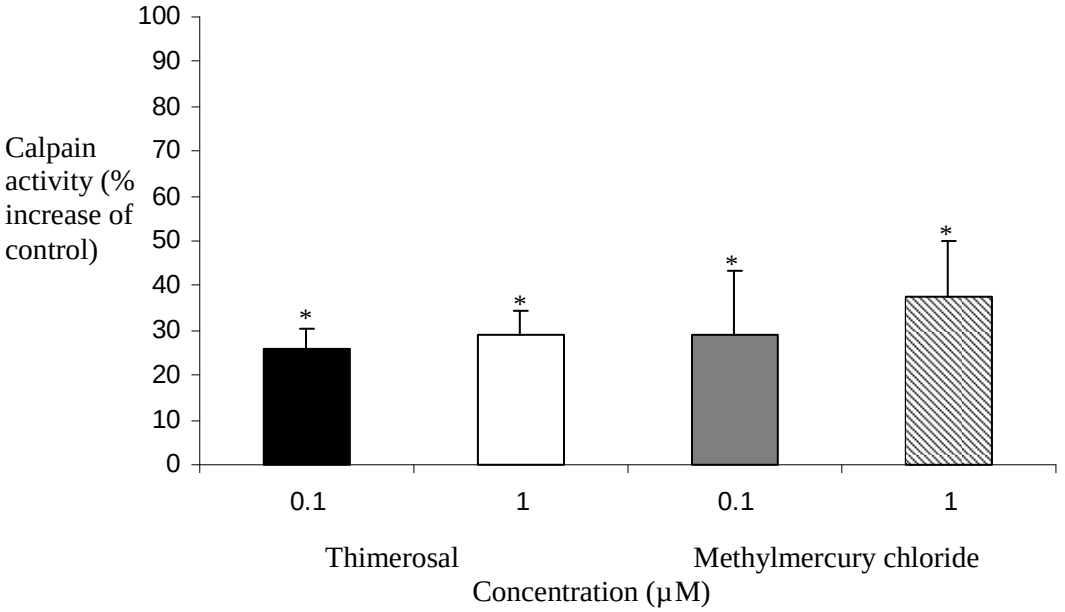

b)

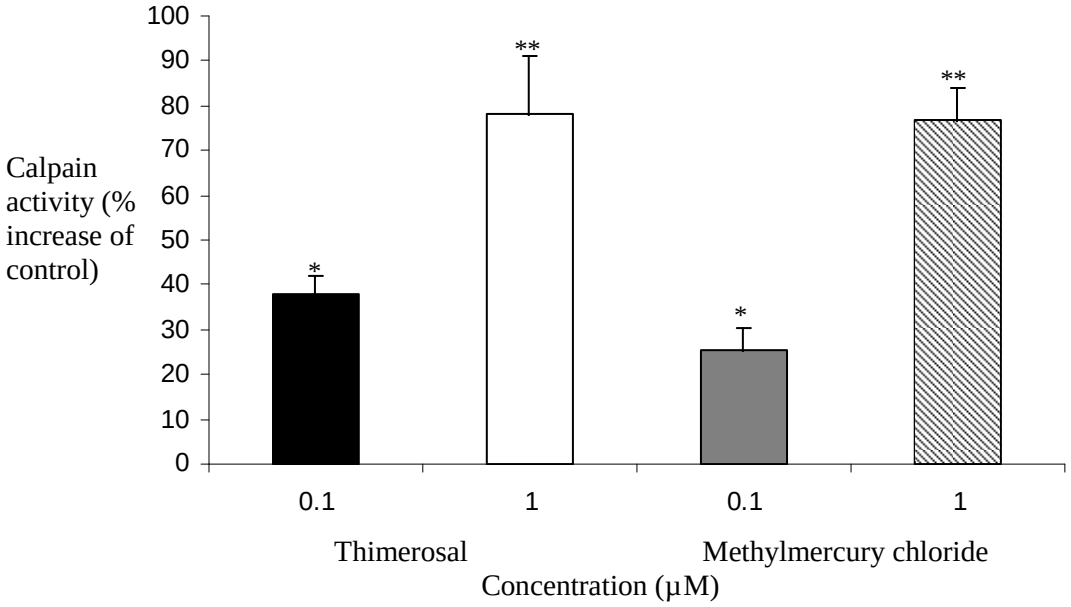

Figure 6.11: The affect of thimerosal and methylmercury chloride on the activity of calpain in N2a cells

N2a cells were induced to differentiate for 4 (a) and 24 (b) hours in the presence and absence of thimerosal and methylmercury chloride. Cells were lysed via sonication and the extracts were used to measure calpain activity as described in Methods section 2.2.16. Data represents mean levels of calpain activity expressed as a percentage of the corresponding control $\pm$ SEM (n = 5). Asterisks indicate statistical significance (*$p<0.05$). The 2 way ANOVA test was used for statistical analysis, followed by post hoc Bonferroni's correction for pair wise multiple analysis.

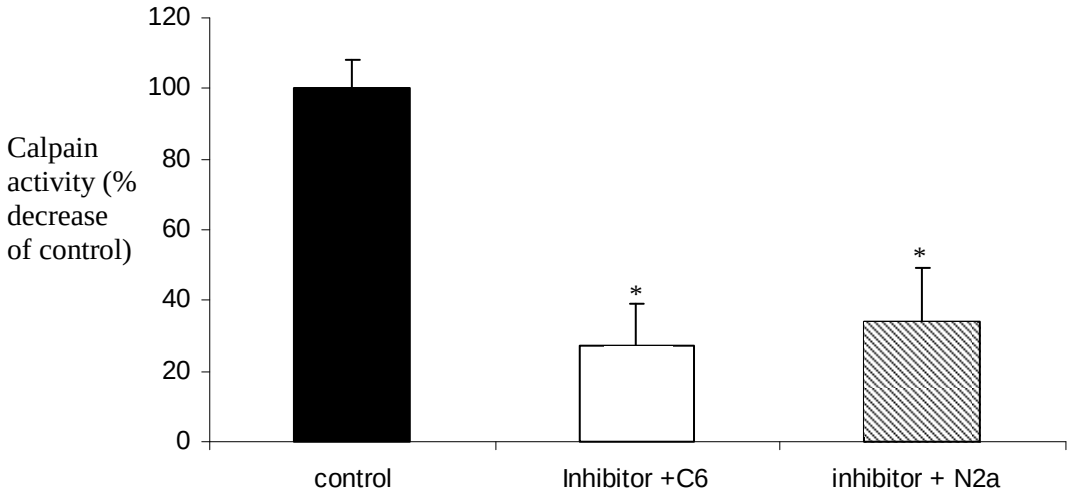

Figure 6.12: The affect of a calpain inhibitor on calpain activation in N2a and C6 cells

C6 and N2a cells were induced to differentiate for 24 hours in the absence of thimerosal and MeHgCl. Cells were lysed via sonication and the extracts were used to measure calpain activity with a calpain inhibitor added as described in Methods section 2.2.16. Data represents mean levels of calpain activity expressed as a percentage of the corresponding control $\pm$ SEM (n = 4). Asterisks indicate statistical significance of differences from the corresponding control (*$p<0.05$). The 2 way ANOVA test was used for statistical analysis, followed by post hoc Bonferroni's correction for pair wise multiple analysis.

Figure 6.12 shows the effect that a calpain inhibitor had on the activity of calpains 1 and 2 in N2a and C6 cells. Calpain activity was significantly reduced in both cell lines by the addition of the inhibitor. In C6 cells activity was reduced by 70 % and in N2a cells activity was reduced by 63 %. Statistical analysis confirmed significance ($p = 0.016296$ and 0.27193 for C6 and N2a cells respectively). Actual enzyme activity expressed as absorbance change/protein/hour was 27.

Chapter 6 Discussion

The aim of chapter 6 was to determine whether thimerosal and MeHgCl had any effect upon cellular organisation and calpain activation. Previous studies have noted that both thimerosal and MeHgCl increase intracellular calcium concentrations (Leonhardt *et al.*, 1996; Burlando *et al.*, 1997; Elferink, 1999; Marchi *et al.*, 2000). The previous chapter has already demonstrated that ERK activation is either elevated or inhibited during exposure to the organic mercury compounds. The ERK signalling cascade can be activated by elevations in intracellular calcium (Subramaniam & Unsicker, 2006). PKC activity is known to be inhibited by the addition of mercury (Rajanna *et al.*, 1995). The inositol triphosphate receptor is sensitised by thimerosal treatment, leading to unregulated release of calcium from the ER (Bootman *et al.*, 1992; Hilly *et al.*, 1993; Sayers *et al.*, 1993; Thrower *et al.*, 1996). Other important calcium dependent enzymes within the cell are the calpains. The regulation of theses enzymes are control by calcium concentrations and calpain inhibitors. Calpain has also been identified as a downstream target of ERK (Subramaniam & Unsicker, 2006).

SERCA is responsible for the removal of calcium from the cell cytoplasm into the ER for storage. The results in this chapter suggest that exposure to thimerosal and MeHgCl affects the distribution of SERCA in C6 cells (see figures 6.1 (a-e)). Bodipy thapsigargin staining showed that both thimerosal and MeHgCl affected the organisation of SERCA in a concentration dependant manner. The change in organisation observed was consistent with a major disruption in the endomembrane and that of the MT network (observed in chapter 4), on which the ER is dependent for its organisation (Waterman-Storer & Salmon, 1998). Heavy metals such as the two organic mercury compounds chosen for further investigation in this study have a high affinity for sulphydryl groups. By attacking proteins within the calcium pump the cell would be unable to sequester calcium, leading to sustained elevations in the calcium concentration. Sayers *et al.*, (1993) found that calcium uptake was inhibited by the addition of thimerosal in a concentration dependant manner. At 2 µM calcium uptake was completely halted. The study hypothesised that the inhibition could be due to the metals high affinity for sulphydryl groups on SERCA.

The redistribution of SERCA was less apparent in N2a cells exposed to the lower concentration of both thimerosal and MeHgCl, but major distribution was

apparent at 1 µM of both organic mercury compounds, suggesting that major changes in the organisation of the endomembrane system occurred in the neuronal cell line as well. SERCA within N2a cells appear to be less susceptible than within C6 cells as the lower concentrations of the organic mercury compounds produced a more noticeable change on the distribution in the C6 cell line. The Kd of SERCA is between 0.136-0.164 µM (Falcke *et al.*, 2003).

Staining for the ryanodine receptor produced images very similar in appearance to SERCA staining, which is unsurprising as both probes recognise pumps and channels on the ER (compare Figures 3.3 and 6.4 with Figures 6.1 and 6.2). The lower concentration of each compound caused minor changes in the staining pattern compared to controls, whereas major disruption to punctate disperse distribution mainly in the cell bodies was observed at the higher concentration. This is consistent with a major distribution of the ER network housing both SERCA and ryanodine receptors. Changes in the distribution or conformation of the ryanodine receptor could lead to sustained calcium release or complete inhibition of calcium release. Micromolar concentrations of thimerosal have been shown to stimulate calcium release from ER stores via the ryanodine receptor by altering the receptors affinity (Abramson *et al.*, 1995). The ryanodine receptor has a quarterfoil shape with a pore in the centre, thought to be the channel for calcium movement. The pore is blocked by a mass thought to be the method of channel regulation (Zucchi & Ronca-Testoni, 1997). The Kd for the ryanodine receptor is 9.6 nm (Pessah *et al.*, 1986).

As with C6 cells fluorescent staining for the ryanodine receptor (see Figure 6.4) in N2a cells indicated major disruption in the distribution of the ryanodine receptor at the higher concentration of the heavy metals, which taken together with the SERCA staining points to a disruption of the endomenbrane system. The exact mechanism by which heavy metals cause the opening of the ryanodine receptor is not yet known but previous work has shown that the addition of an SH reducing compound such as dithiothreitol or glutathione prevents the calcium release caused by mercurial compounds (Brunder *et al.*, 1988). Indicating that damage to the proteins within the channel is important. It could be that the calcium influx seen with the addition of mercury compounds bypasses the receptor completely as other studies have indicated that although the target of the metals was SH groups. Those SH groups were within the membrane rather than the receptor. Either by binding directly to the

SH group or by causing oxidation mercury caused the membrane of the SR to become more permeable to calcium (Abramson *et al.*, 1983).

Both SERCA and the ryanodine receptor are located on the ER, so by using an ER tracker it could be determined if the disruption in the SERCA and the ryanodine receptor was coupled with a disruption in the ER. The fact that ER staining could only be seen in control cells is consistent with the possibility that the ER network was disperse or damaged in organic mercury treated cells. However the possibility that the presence of the heavy metal in the cell culture medium rendered the tracker ineffective can not be ruled out. The ER stain in C6 cells covers the cells (see figure 6.7 a); while in N2a cells the majority of the staining is in the cell body and less intensely in neurites. This would be expected as ER is generally distributed through out the cell.

Inhibition of calcium release via the ryanodine receptor provided minor relief from calcium rises, indicating that the receptor may play a small role in the inhibition of calcium homeostasis caused by MeHg (Bearrs *et al.*, 2001). The changes seen in the distribution of the SERCA and the ryanodine receptor may be down to the heavy metals affinity for thiol groups within proteins or non-specific lipid peroxidation (Limke *et al.*, 2004)

The antibody used to stain for the Golgi apparatus was not as specific as hoped. The huge target area for the antibody indicates that the antibody binds to other proteins, in addition to GRASP 65 with the Golgi membrane or that the Golgi protein GRASP 65 is also a component of Golgi vesicles and the enzyme track them throughout the cells. Despite its non-specificity the antibody is additional conformation of cellular reorganisation. There was evidence of redistribution at the higher concentrations of the organic mercury compounds in both the neuronal and glial cell lines.

Calpains have various targets within the cell and the apparent degradation of tubulin and NFH staining observed in chapter 4 could be due to increased activity of calpains. The Kd for calpain 1 is 240 nm (Guttmann *et al.*, 1997). In both differentiating cell lines calpain activity was significantly increased with both concentrations of thimerosal and MeHgCl at both 4 and 24 hours (see Figure 6.12 a and b). The calpain assay detected both calpain 1 or 2, so the specific calpain responsible could not be determined by assay alone. However, western blotting using an anti-calpain 1 antibody showed that levels of activated calpain 1 significantly

increased in both cell lines after exposure to both organic mercury compounds. (Figures 6.9 and Figure 6.11). The predominant calpain in the CNS is calpain 1 which explains why the anti-calpain 2 antibody did not react with either C6 or N2a cells. The increased activation of calpain corresponds to decreased levels of tubulin and NFH, indicating that degradation by calpain may be at least partly responsible for the changes in the levels of NFH and tubulin seen at the 24 hour time point in chapter 4. The addition of a calpain inhibitor to cell sonicates reduced activity by 65-70 % in both cell lines (figure 6.14), indicating that the majority of the activity being measured by the assay was down to calpains. However the possibility that other proteases were affected can not be ruled out. Proteases such as pronase which is activated by calcium concentrations of 5-10 mM and has a Kd value of $2.99x10^{-7}$ M (Kramer *et al.*, 1979) and metalloproteases such MP-112 which becomes activated by calcium concentrations ranging from 25-100 µM (Nelson & Siman, 1989). ADAMT13 cleaves Von Willebrand units and is activated by 4.8 µM calcium and has a dissociation constant of 15nM with the Von Willebrand units (Anderson *et al.*, 2006). The metalloproteases would become activated before calpain 1 and may also contribute to the degradation of the cytoskeleton in conjunction with calpain 1. Calpain 1 would be activated before pronase and the calcium concentration needed for the activation of pronase would be unlikely to occur within cells of the CNS. The activation of lipases such as phospholipase C (PLC) may also contribute to cellular degradation. PLC activity increases at calcium concentrations of 29-160 nM (Renard *et al.*) and has a dissociation constant of 100-200 µM for lipids (James *et al.*, 1995). Phospholipase A_2s (PLA_2s) specifically hydrolyse the sn-2 fatty acid acyl bond of phospholipids, producing a free fatty acid and a lyso-phospholipid. The dissociation constant for calcium is 2 mM and the lipase requires 0.25 mM of calcium for activation (Lathrop & Biltonen, 1992).

Sakaue *et al.*, (2005) measured the cleavage of calpain substrates tau and α-fodrin in neuronal cells. It was found that the cleavage products increased at 0.3 µM MeHg, pointing to an increase in calpain activity. 0.3 µM is in between the two concentrations used in this thesis. The study by Sakaue *et al.*, (2005) did not use lower concentrations.

Zhang *et al.*, (2003) found that calpain 1 was increased in rats exposed to 10 mg/kg MeHg per day. It increased gradually during the 7 days of treatment and did not decrease until 3 days after the last dose. Addition of a calpain inhibitor reduced

activity by 65 %, once again confirming that the majority of the activity was down to calpains. Western blots were attempted to look at levels of calpain 2 in both cell line but were unsuccessful. It could be that there was insufficient substrate concentration for the antibody to detect as calpain 1 is the most prominent form of calpain in the CNS (Subramaniam & Unsicker, 2006).

In summary the results presented in this chapter support the degradation of the cytoskeleton seen in chapter 4, in that sub-lethal concentrations of thimerosal and MeHgCl induce major reorganisation of the architecture of the cell. The increased activation of calpain 1 and possibly other proteases may have been responsible for the decreased levels of tubulin and NFH observed following 24 hour exposure of differentiating cells to the mercury compounds.

Chapter 7: General Discussion

Heavy metals are extremely toxic compounds that cause numerous health problems and although widespread cases of poison heavy metal poisoning are rare in modern society, individuals remain at risk through the consumption of contaminated food (Atchison, 2005), exposure through the work place (Papanikolaou *et al.*, 2005) and cigarette smoke (Waisberg *et al.*, 2003). The symptoms of heavy metals can affect various organs within the body including the kidney, central nervous system and liver (Rajanna *et al.*, 1995). At a cellular level heavy metals are thought to produce their effect via several different mechanisms, such as the formation of free radicals (Yee & Choi, 1996; Dare *et al.*, 2000), interaction with the cytoskeleton (Graff *et al.*, 1997; Miura *et al.*, 1999) and the disruption of calcium homeostasis (McNulty & Taylor, 1999; Marchi *et al.*, 2000).

Various researchers have shown that heavy metal exposure affects the CNS in both adults and in children (Kim *et al.*, 2000; Castoldi *et al.*, 2001). The developing CNS is extremely susceptible to heavy metal toxicity, probably due to the intense proliferation and differentiation that occurs during the formation of a mature CNS (Bertossi *et al.*, 2004). Children are at risk from developmental problems when exposed to concentrations as low as 0.1 μM of lead and mercury (Crumpton *et al.*, 2001; Heidemann *et al.*, 2001). Both lead and mercury can also cross the placental barrier and impair foetal development (Miura & Imura, 1989; Papanikolaou *et al.*, 2005).

The aim of the study was to initially investigate the relative toxicity of several heavy metals before selection for further study. Following the determination of non-lethal concentrations, the sub-lethal effects of thimerosal and methylmercury chloride on differentiating neuronal and glial cells was investigated.

7.1: Cytotoxicity and cell differentiation assays

Cytotoxicity studies were carried out on the 6 different metals to determine their sub-lethal concentrations and neurite inhibitory concentrations. The investigation showed that zinc had no effect upon MTT reduction or neurite outgrowth. This is perhaps not surprising, as zinc is the second most prevalent metal in the body, and can reach concentrations in excess of 100 μM during synaptic transmission. Previous

studies used very high concentrations of zinc before an effect was noted (Park & Koh, 1999; Watjen, 2001). Exposure to lead resulted in increased MTT reduction and reduced neurite number at 100 µM but had no effect at lower concentrations. A study using brain slices found no affect on the viability of the brain tissue at concentrations of up to 10 µM (Cordova *et al.*, 2004), which agrees with the findings in this thesis using cell lines. MTT reduction assays and neurite counts highlighted the difference in the toxicity of inorganic and organic mercury compounds. Inorganic mercury was shown to be less toxic to the cell line than the organic mercury species. This difference in toxicity may be related to the organic properties of thimerosal and methylmercury chloride, as they more readily penetrate cell membranes. Cadmium was the only compound that caused a significant reduction in neurite outgrowth after 4 hours of exposure to 0.1 µM indicating that it was the most toxic of the compounds investigated.

MTT reduction and neurite outgrowth assays showed that, superficially, the two organic mercury compounds had a similar level of toxicity. Further investigation into the biochemical and molecular effects would determine whether the similarity continued. Initial studies also highlighted the higher sensitivity of the neuronal cell line compared to differentiating glial cells. After 48 hours, MTT reduction was depressed only in N2a cells incubated with 1 µM MeHgCl. The lower sensitivity of the C6 cells may reflect the fact that *in vivo* glial cells are thought to protect the central nervous system from the trace amounts of heavy metals that are found normally, since they have higher levels of metallothioniens and anti-oxidants, thus enabling them to deal with metals more efficiently than neurons (Castiglioni & Qian, 2001).

7.2: Cytoskeletal studies

Total and tyrosinated α-tubulin levels remained unchanged after 4 hours in C6 cells, in contrast to N2a cell which displayed decreased levels of tyrosinated α-tubulin indicates an interesting difference in the response of the two cell types to organic mercury exposure. Hence, the fall in tubulin tyrosination may be a neuron specific marker for the toxicity of organic mercury compounds. Tyrosinated α-tubulin sub-units are enriched in labile microtubules, thus the change in tubulin levels may

indicate that both thimerosal and MeHgCl affect microtubule dynamics in the N2a cell line. The decreased tyrosination seen in N2a cells may indicate that organic mercury compounds have an inhibitory effect on the enzyme responsible for detyrosination of the α-tubulin subunit. Alternatively tubulin-tyrosine ligase, which adds tyrosine to the c terminus of tubulin, could be inhibited by organic mercury compounds. Hence the net effect of thimerosal and MeHgCl on tubulin tyrosination would depend on the degree to which the addition or removal steps are inhibited. It may be of interest to measure the activity of tyrosine carboxypeptidase after exposure to MeHgCl and thimerosal to determine if the changes in tubulin tyrosination are due to the heavy metals affecting the enzyme activity rather than directly interacting with the tubulin subunit. After 24 hours exposure there was an overall reduction in both total and tyrosinated tubulin in both cell lines, indicating that thimerosal and MeHgCl causes some proteolytic degradation or reduced synthesis of tubulin subunits. As microtubules are composed of obligate heterodimers of α and β subunits, the levels of each one should remain equal. The consistent reduction in reactivity with anti α and β-tubulin antibodies after 24 h exposure indicates a reduction in the levels of tubulin compared to controls. This could be due to decreased expression of tubulin genes and/or increased turnover (i.e. proteolysis) of both subunits in mercury compound-treated cells compared to controls. Immunofluorescence imaging confirmed that the organic mercury compounds caused major disruption in the MT network in comparison to controls.

The reduction in the levels of phosphorylated NFH that occurred after 4 hours of exposure to the compounds may indicate a change in neurofilament organisation or its interaction with other macromolecules in the axon, as the phosphorylation of neurofilaments is known to be associated with axon stability and maturity (Williamson, 1996). This was further confirmed by the observation of similar patterns of reactivity to SMI 34 a different anti-NFH antibody. The smaller changes observed with SMI 34 reactivity may reflect specificity differences between the two antibodies. The reduction of phosphorylated NFH levels was accompanied by a reduction in the levels of phosphorylated ERK1/2. ERK1/2 is one of the kinases responsible for the phosphorylation of NFH, so its mirrored decrease adds further evidence to the argument that organic mercury compounds cause hypophosphorylation of NFH. A similar study using organophosphates found NFH phosphorylation to be increased in N2a cells exposed to PSP but neurite outgrowth was also inhibited (Hargreaves *et al.*,

2006), indicating that the levels and alterations in the phosphorylation state of NFH are useful markers of neurotoxicity, although not specific for any one compound.

The observed decreases in reactivity with all anti-NFH antibodies after 24 hours exposure to both thimerosal and MeHgCl indicated that there may be a reduction in the overall levels of NFH at this time point. This could be due to reduced synthesis or increased turnover of NFH. This reorganisation of the cytoskeleton may affect ERK activation if its association with the cytoskeleton were disrupted; this could potentially be examined using anti-ERK in dual fluorescence staining with either anti-tubulin or anti-NFH antibodies. It has been shown that cytoskeletal proteins such as actin modulate the plasma membrane Ca^{2+} pump (PMCAs) via direct binding to the enzyme (Vanagas *et al.*, 2007). Evidence in this thesis suggests that mercury compounds disrupt the cytoskeleton, which may in turn impair cellular ability to maintain calcium homeostasis

7.3: Cell signalling studies

In C6 cells there was transient ERK activation at 4 hours with both concentrations of thimerosal and decreases with both concentrations of MeHgCl, suggesting either a different mechanism of toxicity for the two compounds or differences in the timing of the mechanisms in these cell lines. The possibility that an increase occurred earlier in MeHgCl treated cells can not be ruled out, as activation has been described within minutes in PC12 cells (Parran *et al.*, 2004). After 24 hours the levels of activated ERK fell with both concentrations of thimerosal and MeHgCl.

In N2a cells ERK activity decreased on exposure to both concentrations of the mercury compounds, the initial increase seen with C6 cells was not evident in neuronal cells. It may be that a transient increase in ERK1/2 phosphorylation occurred earlier in the neuronal cell line. ERK activity remained suppressed at both 4 and 24 hours. NF-H is a substrate of ERK 1 / 2 during axon development and ERK activation is known to play a central role in axonal outgrowth (Jin *et al.*, 2002). ERK plays a role in NFH phosphorylation, an event that was also suppressed by thimerosal and MeHgCl. Thus the decrease in ERK activity may be responsible for the reduction in NFH phosphorylation, and contribute to the degradation of the microtubule network. As ERK activation is now known to have a duel role in cell survival (Subramaniam & Unsicker, 2006), further investigation would be needed to determine if the changes in

activity are protective or the beginning of cell death. One way to investigate this would be to perform experiments in the presence of ERK inhibitors, such as ERK activation inhibitors 1 ($SteMEK1_{13}$) and 2 ($MTP_{TAT}G\text{-}MEK1_{13}$). Both inhibitors are cell permeable and prevent the activation of the ERK pathway by inhibiting the phosphorylation of MEK1/2; the upstream activator of ERK1/2. As over-activation of ERK is also associated with inhibition of neurite outgrowth the optimum concentration for the inhibitors in the two cell lines used in this thesis must be elucidated initially. Indeed, the finding of increased activation in the case of organophosphate toxicity (Hargreaves *et al.*, 2006) does suggest that there is a very fine balance between the activation state of ERK 1/2 and the phosphorylation of key substrates of importance to neurite outgrowth such as neurofilaments. The majority of ERK in cells are bound the cytoskeleton indicating a role closely associated with the cytoskeletal organisation (Robinson & Cobb, 1997). Thus, the deviations from normal activity in MeHgCl and thimerosal treated cells may be associated with the disruption of the tubulin network. The exact mechanism by which organic mercury compounds alter ERK activity is still not clear. It could be due to the disruption of the cytoskeleton but it may also involve changes in the upstream activators of ERK1/2 such as MEK. Future work could look at upstream regulators of the ERK cascade, using antibodies against MEK and phosphorylated MEK.

ERK targets serine and threonine residues on substrate proteins when activated. Western blotting analysis with anti-phospho-serine and anti-phospho-threonine antibodies suggested that neither target showed altered phosphorylation when compared to the control in either cell line. However, it is likely that the antibodies have only revealed the target proteins of highest abundance, which may not necessarily be the key targets in terms of sub-lethal toxicity. Future studies could use 2-D gel electrophoresis which would be more likely to reveal depression in the phosphorylation of minor proteins than the currant studies. ERK is just one of many protein kinases and phosphatase that regulate the phosphorylation of thousands of proteins within the cell. Although western blotting analysis suggested that JNK activity increased in both cell lines, the level of reactivity was very close to background and it would therefore be advisable to repeat this work in order to improve the signal to noise ration.

7.4: Ca^{2+} homeostasis and calpain activity

Changes in calcium homeostasis are known to play a role in the toxicity of the two organic mercury compounds. Calcium is also known to be an upstream regulator of the ERK signalling pathway (Subramaniam & Unsicker, 2006), which has been shown to be inhibited by the addition of organic mercury compounds. Calcium can act as either an inhibitor or activator of the ERK1/2 signalling pathway. Other important targets of ERK1/2 are calpains 1 and 2. Activated ERK phosphorylates calpain 2 at Ser50 even in the absence of milimolar calcium concentrations (Glading *et al.*, 2001)

Confocal microscopy studies showed that thimerosal and MeHgCl exposure alter the distribution of SERCA within both neuronal and glial cells. Changes in either the distribution or the configuration of this energy dependent pump, could lead to sustained elevations in calcium concentrations within the cell (Sayers *et al.*, 1993) found that 2 µM thimerosal exposure inhibited calcium uptake completely, via the interaction with sulphydryl groups in SERCA. The distribution of the ryanodine receptor was also affected by the organic mercury compounds. The ryanodine receptor is responsible for the release of calcium from ER stores and any changes in its distribution could lead to unregulated release and further disruption to calcium homeostasis (Abramson *et al.*, 1995). The change in the positioning of both SERCA and the ryanodine receptor indicates that there may be disruption of the ER within the cell, which houses these two Ca^{2+} regulatory proteins. However, the ER tracker dye used in the present work was not detectable in MeHgCl and thimerosal treated cells, this may indicate dispersal of the tubular network in treated cells but further staining, for example with anti-ER protein antibodies could give a more conclusive result.

The disperse pattern of staining seen with the anti-Golgi apparatus antibody could be due to the antibody recognising a membrane protein that is also part of the Golgi vesicles used for transport round the cell. Though not specific for Golgi apparatus-like structures within the cells, the staining pattern with the anti-Golgi apparatus antibody did further supported the view that disruption of the endomembrane system occurred, at least at the higher concentrations of both compounds. Furthermore, since ER distribution is known to be dependent on the integrity of the microtubule network (Waterman-Storer & Salmon, 1998), this indicates that the major disruption of MTs seen in immunofluorescence staining

analysis would be expected to cause major ER disruption, as ER tubules depend upon MTs for localisation via association along the length of the MT or by binding to the tip of the MT (Waterman-Storer & Salmon, 1998).

Calpain activity increased in neuronal and glial cells with both concentrations of the organic mercury compounds at both 4 and 24 hours. The increase in activity is a strong indication that calcium concentrations are elevated in both cell lines, as the calpains are calcium dependent enzymes (Sorimachi *et al.*, 1997). Furthermore, as the calpains are known to target cytoskeletal proteins, the increased activity may in part explain the degradation seen in the levels of both NFH and tubulin following 4 and 24 hours exposure to MeHgCl and thimerosal. Previous studies have shown that increases in intracellular calcium causes a reduction in the phosphorylation of ERK1/2 (Millar *et al.*, 2007), which further supports the argument that organic mercury compounds causes increases in intracellular calcium as ERK1/2 phosphorylation was seen to be decreased in this thesis.

In conclusion, this thesis has achieved most of the aims set out at the beginning of the work. Figure 7.1 gives an overview of the effects of thimerosal and MeHgCl had upon neuronal and glial cells.

- The sub-lethal and neurite inhibitory concentrations have been identified for the 6 heavy metals chosen at the beginning of the project.

Sub-lethal neurite outgrowth inhibitory concentrations of MeHgCl and thimerosal are associated with:

- Inhibition of neurite outgrowth, accompanied by changes in the levels, distribution and posttranslational modification of tubulin in C6 and N2a cells and NFH in N2a cells.

- Alteration of the cell signalling pathways associated with the control of the cytoskeleton. ERK activity was inhibited in both cell lines after 24 hours.

- Measurement of calcium homeostasis was attempted but a suitable environment for the determination of intracellular calcium concentrations could not be established within the limited time scale. It has been shown that organic mercury compounds caused an increase in levels and activity of calpain in N2a and C6 cells after exposure to 4 and 24 hours of both concentrations of thimerosal and MeHgCl, which suggests that calcium levels are increased by thimerosal and MeHgCl.

- Addition of organic mercury compounds altered distribution of SERCA and ryanodine receptors in both cell lines. The anti-GRASP 65 antibody was further conformation of the disruption of the cells architecture.

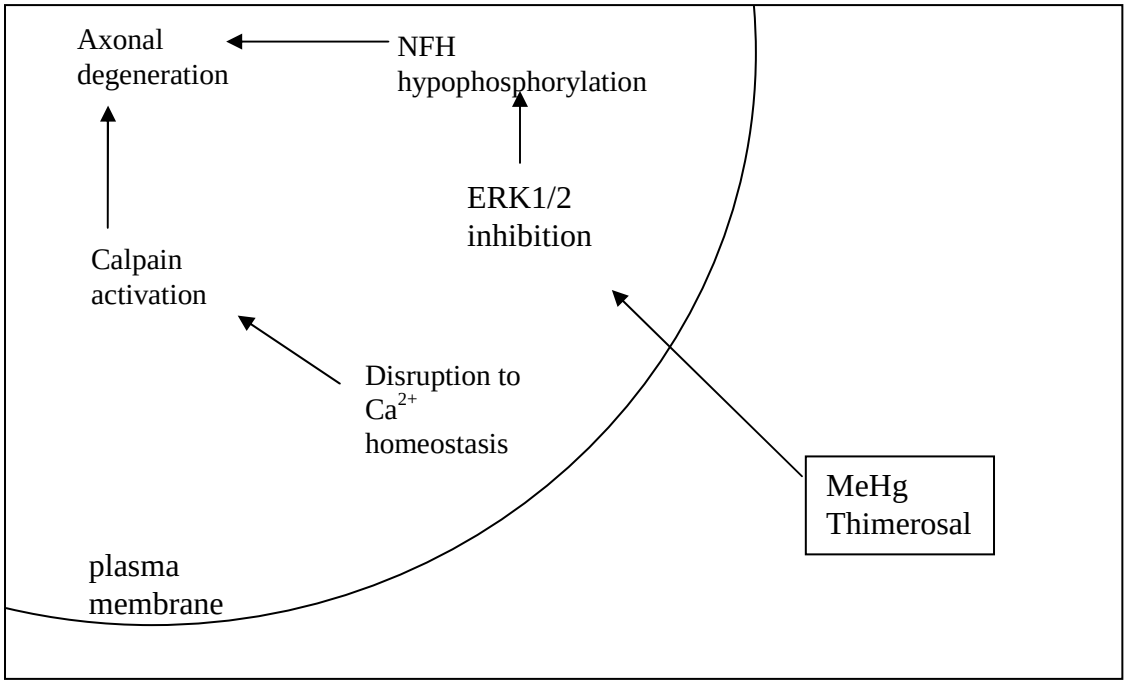

Figure 7.1: Summary diagram of some of the possible routes by which an organic mercury compound may exert its toxic effect.

Figure 7.1 summarises a possible route of toxicity uncovered by the work in this thesis for organic mercury compounds. Once inside the cell, thimerosal and MeHgCl causes inhibition of the ERK1/2 signalling pathway, leading to hypophosphorylation of NFs and the reduction of axon outgrowth in neuronal cells. Organic mercury compounds have also been shown to increase the activity of calcium dependant enzymes called calpains. Calpains are generally activated by raises in calcium concentrations but they have also been shown to become activated through phosphorylation by ERK1/2. The inhibition of ERK1/2 indicates that the intracellular calcium concentration rose sufficiently to activate calpain 1. The activity of the calpain may be responsible for the degradation of the cytoskeleton seen in both neuronal and glial cells.

7.5: FUTURE WORK

With hindsight it would have been of use to measure the concentration of free metal within the media in order to establish how much of the compound had bound to organic matter within the media. It would have also been of interest to the thesis if the concentration of metal had been measured within the cell lysates after the different incubation times to determine how much of the compound added to the media actually entered the cell. The concentrations could be determined using an atomic absorption spectrophotometer equipped with a HGA-300 graphite furnace and calibrated with known metal concentrations. Whilst information on the actual amount taken up is lacking, organic mercury compounds elicit a variety of responses in N2a and C6 cells.

The confocal microscopy work on the cytoskeleton in chapter 4 would be further enhanced by electron microscope images of the cells to view cytoskeletal changes in more detail. The same antibodies would be used for visualisation of the neuronal and glial cell cytoskeleton. The cause of the reduction could be investigated to identify whether it is a result of the inhibition of the enzyme that detyrosinates α-tubulin. The activity of the enzyme tubulin carboxypeptidase can be measured by assay developed by (Sironi *et al.*, 2000) that uses [$_{14}$C] labelled tubulin as a substrate for the enzyme. The assay would use purified tubulin from the cell lysates obtained from centrifugation at 100,000 g for 60 minutes at 2-4^{o}C.

In chapter 4 this study looked at tyrosination; one form of post-translational modification for tubulin sub-units. Experiments showed that the addition of organic mercury compounds caused the levels of tyrosination to fall. However detyrosination of MTs is only one way that the MT network is stabilised. Acetylation of α-tubulin is another form of post-translational modification and future studies could determine if it responded in the way as tyrosinated α-tubulin to the organic mercury compounds using the same techniques of western blotting and immunofluorescence but with an anti-acetylated tubulin antibody.

Future work is required on the measurement of intracellular calcium concentrations. Initial experiments were unsuccessful in measuring calcium changes using fura-2 in a spectrofluorimeter. There was a low signal to noise ratio, which prevented accurate determination of changes in calcium concentrations in the fluorimeter. Intracellular calcium concentrations steadily increased even in the control

cells, indicating that the cells were not in a suitable environment. Further experiments are needed to determine a suitable medium that allows the cells to survive in non-stressed state that does not interfere with calcium measurements. Once the cells are stabilised under these conditions experiments to determine the instantaneous effect that the addition of thimerosal and MeHgCl to the cells had upon calcium mobilisation could be carried out, as well as looking at calcium changes within cells pre-treated with the organic mercury compounds. Using calcium free medium would determine whether calcium was mobilised from intracellular stores or from outside the cell. SERCA pump inhibiters such as thapsigargin, which binds to irreversible to SERCA causing inactivation would determine the importance of intracellular calcium stores to the rises in calcium concentrations.

The work on calcium receptors and SERCA could be expanded by looking at the distribution of IP_3 receptors in the cell lines, using an anti-IP3 receptor antibody (C-20).

Studies of the changes in cellular organisation in chapter 6 need to be expanded to other organelles such as the mitochondria which are important intracellular calcium stores (Dietmer *et al.*, 1998). MeHg is known to affect mitochondrial calcium release and uptake leading to the induction of apoptosis (Levesque *et al.*, 1988). Using the Mitosox Red mitochondrial superoxide indicator, would elucidate the effect of the organic mercury compounds on the organisation of organelles within the cell. In addition it may also indicate if the mitochondrial calcium store is partly responsible for the rises in intracellular calcium, which have been found to accompany exposure to thimerosal and MeHg (Abramson *et al.*, 1983; Bearrs *et al.*, 2001).

Western blotting analysis and calpain activity assays have shown an increase in the levels of calpain I and its activity in MeHgCl and thimerosal treated cells. It would therefore be of interest to add membrane-permeable calpain inhibitors to living cells incubated with the organic mercury compounds to determine whether calpain inhibition provides any protection from the toxic effects of these agents. Using the established antibodies used throughout this thesis, western blotting and confocal microscope may highlight any protective effects that the calpain inhibitors had upon the degradation of the cytoskeleton.

Chapter 5 indicated that ERK1/2 signalling was inhibited by the addition of organic mercury compounds. Western blots with cell lysates prepared under the same conditions as in this study may be used to look at the levels and activation of the

upstream activators of ERK1/2 such as MEK. The importance of the changes ERK1/2 signalling can be expanded upon by using cell permeable ERK inhibitors prior to either the lysing of the cells for western blotting or fixing for immunofluorescence.

REFERENCES

ABRAMSON, J. J., ZABLE, A. C., FAVERO, T. G. & SALAMA, G. (1995). Thimerosal interacts with the Ca2+ release channel ryanodine receptor fron the sarcoplasmic reticulum. *The Journal of Biological Chemistry* **270,** 29644-29647.

ACKERLEY, S., THORNHILL, P., GRIERSON, A. J., BROWNLEES, J., ANDERTON, B. H., LEIGH, P. N., SHAW, C. E. & MILLER, C. C. J. (2003). Neurofilament heavy chain side arm phosphorylation regulates axonal transport of neurofilaments. *The Journal of Cell Biology* **161,** 489-495.

ALLEN, J. W., MUTKUS, L. A. & ASCHNER, M. (2001). Mercuric chloride, but not methylmercury, inhibits glutamine synthetase activity in primary cultures of cortical astrocytes. *Brain Research* **891,** 148-157.

ALLEN, J. W., SHANKER, G., TAN, K. H. & ASCHNER, M. (2002). The consequences of methylmercury exposure on interactive functions between astrocytes and neurons. *Neurotoxicology* **23,** 755-759.

ANDRIEUX, A., SALIN, P. A., VERNET, M., KUJALA, P., BARATIER, J., GORY-FAURÉ, S., BOSC, C., POINTU, H., PROIETTO, D., SCHWEITZER, A., DENARIER, E., KLUMPERMAN, J. & JOB, D. (2002). The suppression of brain cold-stable microtubules in mice induces synaptic defects associated with neuroleptic-sensitive behavioral disorders. *Genes and Development* **16,** 2350-2364.

ASCHNER, M. (1996). Astrocytes as modulators of mercury induced neurotoxicity. *Neurotoxicology* **17,** 663-670.

ATCHISON, W., D. (2005). Is chemical neurotransmission altered specifically during methylmercury-induced cerebellar dysfunction? *Trends in Pharmacological Sciences* **26,** 549-557.

ATCHISON, W. D. & HARE, M. F. (1994). Mechanisms of methylmercury-induced neurotoxicity. *FASEB J* **8,** 622-629.

BALDWIN, D. R. & MARSHALL, W. J. (1999). Heavy metal poisoning and its laboratory investigation. *Annals of Clinical Biochemistry* **36,** 267-300.

BALL, L. K., BALL, R. & PRATT, R. D. (2001). An assessment of thimerosal use in childhood vaccines. *Pediatrics* **107,** 1147-1154.

BARNES, D. M. & KIRCHER, E. A. (2005). Effects of mercuric chloride on glucose transport in 3T3-L1-adipocytes. *Toxicology in Vitro* **19,** 207-214.

BARRES, B. A. & BARDE, Y. A. (2000). Neuronal and glial cell biology. *Current opinion in neurobiology* **10,** 642-648.

BEARRS, J. J., LIMKE, T. L. & ATCHISON, W. D. (2001). Methylmercury (MeHg) causes calcium release from smooth endoplasmic reticulum

(SER) inositol-1,4,5-triphosphate receptors in rat cerebellar granule neurons. *The Toxicologist* **60,** 184.

BEZZI, P. & VOLTERRA, A. (2001). A neuron-glia signalling network in the active brain. *Current opinion in neurobiology* **11,** 387-394.

BIGL, K., SCHMITT, A., MEINERS, I., MUNCH, G. & ARENDT, T. (2007). Comparison of the results of the CellTiter Blue, the tetrazolium (3-[4,5-dimethylthioazol-2-yl]-2,5-diphenyl tetrazolium bromide), and the lactate dehydrogenase assay applied in brain cells after exposure to advanced glycation endproducts. *Toxicology in Vitro* **21,** 962-971.

BLAXILL, M. F., LYN REDWOOD & BERNARD, S. (2004). Thimerosal and autism? A plausible hypothesis that should not be dismissed. *Medical Hypotheses* **62,** 788-794.

BONACKER, D., STOIBER, T., WANG, M., BOHM, K. J., PROTS, I., UNGER, E., THIER, R., BOLT, H. M. & DEGEN, G. H. (2004). Genotoxicity of inorganic mercury salts based on disturbed microtubule function. *Archives of Toxicology* **78,** 575-583.

BOOTMAN, M. D., TAYLOR, C. W. & BERRIDGE, M. J. (1992). The thiol reagent thimerosal evokes Ca^{2+} spikes in HeLa cells by sensitizing the inositol 1,4,5-triphosphate receptor. *The Journal of Biological Chemistry* **267,** 25113-25119.

BOUTON, C. M. L. S., HOSSAIN, M. A., FRELIN, L. P., LATERRA, J. & PEVSNER, J. (2001). Microarray analysis of differential gene expression in lead-exposed astrocytes. *Toxicology and Applied Pharmacology* **176,** 34-53.

BRAEKMAN, B., SIMOENS, C., RZEZNIK, U. & RAES, H. (1997). Effect of sublethal doses of cadmium, inorgainic mercury and methylmercury on the cell morphology of an insect cell line (*Aedes albopictus*, C6/36). *Cell Biology International* **21,** 823-832.

BRAY, T. M. & BETTGER, W. J. (1990). The physiological role of zinc as and antioxidant. *Free radical Biology & Medicine* **8,** 281-291.

BRESSLER, J., KIM, K., CHAKRABORTI, T. & GOLDSTEIN, G. (1999). Molecular Mechanisms of Lead Neurotoxicity. *Neurochemical Research* **24,** 595-600.

BUNKER, J. M., WILSON, L., JORDAN, M. A. & FEINSTEIN, S. C. (2004). Modulation of microtubule dynamics by Tau in living cells: Implications for development and neurodegeneration. *Molecular Biology of the Cell* **15,** 2720-2728.

BURLANDO, B., A., V., PERTICA, M., MANCINELLI, G., MARCHI, B. & ORUNESU, M. (1997a). Effects of Hg^{2+} on Ca^{2+} dynamics in the scallop sarcoplasmic reticulum (*Pecten jacobaeus*): Protective role of glutathione. *Comparative Biochemistry and Physiology* **116C,** 77-83.

BURLANDO, B., VIARENGO, A., PERTICA, M., PONZANO, E. & ORUNESU, M. (1997b). Effects of free oxygen radicals on Ca2+ release mechanisms in the sarcoplasmic reticulum of Scallop (Pecten jacobaeus) abductor muscle. *Cell Calcium* **22,** 83-90.

CALLAWAY, K., RAINEY, M. A. & DALBY, K. N. (2005). Quantifying ERK2-protein interactions by fluorescence anisotropy: PEA-15 inhibits ERK2 by blocking the binding of DEJL domains. *Biochimica et Biophysica Acta* **1754,** 316-323.

CANESI, L., CIACCI, C. & GALLO, G. (2000). Hg2+and Cu 2+ interfere with agonist-mediated Ca2+ signalling in isolated in isolated Mytilus digestive gland cells. *Aquatic Toxicology* **49,** 1-11.

CASTIGLIONI, E. T. (1993). Cell culture models for lead toxicity in neuronal and glial cells. *Neurotoxicology* **14,** 513-536.

CASTIGLIONI, E. T., GUERRI, C., ASCHNER, M., MATSUSHIMA, G. K., P., O. C. J. & STREIT, W. J. (2001). Roles of Glia in Developmental Neurotoxicity: Session VI Summary and Research needs. *Neurotoxicology* **22,** 567-573.

CASTIGLIONI, E. T. & QIAN, Y. (2001). Astroglia as metal depots: Molecular mechanisms for metal accumulation, storage and release. *Neurotoxicology* **22,** 577-592.

CASTOLDI, A. F., COCCINI, T., CECCATELLI, S. & MANZO, L. (2001). Neurotoxicity and molecular effects of methylmercury. *Brain Research Bulletin* **55,** 197-203.

CHANG, L. & KARIN, M. (2001). Mammalian MAP kinase signalling cascades. *Nature* **410,** 37-40.

CHETTY, C. S., RAJANNA, S., HALL, E., YALLAPRAGADA, P. R. & RAJANNA, B. (1996). In vitro and in vivo effects of lead, methylmercury and mercury on inositol 1,4,5-triphosphate and 1,3,4,5-tetrakisphosphate receptor bindings in rat brain. *toxicology letters* **87,** 11-17.

COOKSON, M. R., MEAD, C., AUSTWICK, S. M. & PENTREATH, V. W. (1995). Use of MTT assay for estimating toxicity in primary astrocytes and C6 glioma cell cultures. *Toxicology in Vitro* **9,** 39-48.

COOKSON, M. R. & PENTREATH, V. W. (1996). Protective roles of glutathione in the toxicity of mercury and cadmium compounds to C6 glioma cells. *Toxicology in Vitro* **10,** 257-264.

CORDOVA, F. M., RODRIGUES, A. S., GIACOMELLI, M. B. O., OLIVEIRA, C. S., POSSER, T., DUNKLEY, P. R. & LEAL, R. B. (2004). Lead stimulates ERK1/2 and P38 MAPK phosphorylation in the hippocampus of immature rats. *Brain Research* **998,** 65-73.

COUNTER, S. A. & BUCHANAN, L. H. (2004). Mercury exposure in children: a review. *Toxicology and Applied Pharmacology* **198,** 209-230.

CRESPO-LÓPEZ, M. E., LIMA DE SÁ, A., HERCULANO, A. M., BURBANO, R. R. & MARTINS DO NASCIMENTO, J. L. (2006). Methylmercury genotoxicity: A novel effect in human
cell lines of the central nervous system. *Environment International* **In press**.

CRUMPTON, T., ATKINS, D. S., ZAWIA, N. H. & BARONE JR, S. (2001). Lead Exposure in Pheochromocytoma (PC12) Cells Alters Neural Differentiation and Sp1 DNA-Binding. *Neurotoxicology* **22,** 49-62.

DARE, E., GOTZ, M. E., ZHIVTOVSKY, B., MANZO, L. & CECCATELLI, S. (2000). Antioxidants J811 and 17?-Estradiol protect cerebellar granule cells from Methylmercury-induced apoptotic cell death. *Journal of Neuroscience Research* **62,** 557-565.

DEITMER, J. W., VERKHRASTSKY, A. & LOHR, C. (1998). Calcium signalling in glial cells. *Cell Calcium* **24,** 405-416.

DHAMODHARAN, R. & WADSWORTH, P. (1995). Modulation of microtubule dynamic instability in vivo by brain microtubule associated proteins. *Journal of Cell Science* **108,** 1679-1689.

DIETMER, J. W., VERKHRATSKY, A. J. & LOHR, C. (1998). Calcium signalling in Glial cells. *Cell Calcium* **24,** 405-416.

DRZEWIECKA, A. W., WYCZÓ KOWSKA, J. & DASTYCH, J. (2005). c-Jun N-terminal kinase is Involved in mercuric ions-mediated interleukin-4 secretion in mast cells. *International Archives of Allergy and Immunology* **136,** 181-190.

EDMONDSON, J. M., ARMSTRONG, L. S. & MARTINEZ, A. O. (1988). A rapid and simple MTT-based spectrophotometric assay for determining drug sensitivity in monolayer cultures. *Methods In Cell Science* **11**.

ELFERINK, J. G. R. (1999). Thimerosal a versatile sulfhydryl reagent, calcium mobilizer, and cell function-modulating agent. *General Pharmacology* **33,** 1-6.

ERDAHL, W. L., CHAPMAN, C. J., TAYLOR, R. J. & PFEIFFER, D. R. (2000). Ionomycin, a carboxylic acid ionophore, transports Pb^{2+} with high selectivity. *The Journal of Biological Chemistry* **275,** 7071-7079.

FINKELSTEIN, Y., MARKOWITZ, M. E. & ROSEN, J. F. (1998). Low-level lead-induced neurotoxicity in children: an update on central nervous system effects. *Brain Research Reviews* **27,** 168-176.

FLASKOS, J., MCLEAN, W. G., FOWLER, M. J. & HARGREAVES, A. J. (1998). Tricresyl phosphate inhibits the formation of axon-like processes and disrubts neurofilaments in cultured in cultured mouse N2a and Rat PC12 cells. *Neuroscience Letters* **242,** 101-104.

FOULKES, E. C. (2000). Transport of toxic heavy metals across cell membranes. *Proceedings of the Society for Experimental Biology and Medicine* **223,** 234-240.

FOWLER, M. J., FLASKOS, J., MCLEAN, W. M. & HARGREAVES, A. J. (2001). Effects of neuropathic and non-neuropathic isomers of tricresyl phosphate and their microsomal activation on the production of axon-like processes by differentiating mouse neuroblastoma cells. *Journal of Neurochemistry* **76,** 671-678.

FRAGA, C. G. (2005). Relevence, essentiality and toxicity of trace elements in human health. *Molecular Aspects of Medicine* **26,** 235-244.

FREDERICKSON, C. J. & BUSH, A. I. (2001). Synaptically released zinc: Physiological functions and pathological effects. *Biometals* **14,** 353-366.

FUNCHAL, C., MORETTO, M. B., VIVIAN, L., ZENI, G., ROCHA, J. B. T. & PESSOA-PUREUR, R. (2006). Diphenyl ditelluride- and methylmercury-induced hyperphosphorilation of the high molecular weight neurofilament subunit is prevented by organoselenium compounds in cerebral cortex of young rats. *Toxicology* **222,** 143-153.

GARG, T. K. & CHANG, J. Y. (2006). Methylmercury causes oxidative stress and cytotoxicity in microglia: Attenuation by 15-deoxy-delta 12, 14-Prostaglandin J2. *Journal of Neuroimmunology* **171,** 17-28.

GATTI, R., BELLETTI, S., UGGERI, J., VETTORI, M. V., MUTTI, A., SCANDROGLIO, R. & ORLANDINI, G. (2004). Methylmercury cytotoxicity in PC12 cells is mediated by primary glutathione depletion independent of excess reactive oxygen species generation. *Toxicology* **204,** 175-185.

GEE, K. R., ZHOU, Z. L., TON-THAT, D., SENSI, S. L. & WEISS, J. H. (2002). Measuring zinc in living cells. A new generation of sensitive and selective fluorescent probes. *Cell Calcium* **31,** 245-251.

GITLER, D. & SPIRA, M. E. (1998). Real time imaging of calcium-induced localised proteolytic activity after axotomy and its relation to growth cone formation. *Neuron* **20,** 1123-1135.

GLADING, A., UBERALL, F., KEYSE, S. M., LAUFFENBURGER, D. A. & WELLS, A. (2001). Membrane proximal ERK signalling is required for M-calpain activation downstream of epidermal growth factor receptor signalling. *Journal of Biological Chemistry* **276,** 23341-23348.

GOPAL, K. V. (2002). Neurotoxic effects of mercury on auditory cortex networks growing on microelectrode arrays: a preliminary analysis. *Neurotoxicology and teratology* **5526,** 1-8.

GRAFF, R. D., FALCONER, M. M., BROWN, D. L. & REUHL, K. R. (1997). Altered sensitivity of posttranslationally modified microtubules to Methylmercury in differentiating embryonal carcinoma-derived neurons. *Toxicology and Applied Pharmacology* **144,** 215-224.

GRAFF, R. D., PHILBERT, M. A., LOWNDES, H. E. & REUHL, K. R. (1993). The effect of glutathione depletion on methylmercury induced microtubule disassembly in cultured embryonal carcinoma cells. *Toxicology and Applied Pharmacology* **120,** 20-28.

GRANDJEAN, P., WEIHE, P. & NIELSON, J. B. (1994). Significance of intrauterine and postnatal exposures. *Clinical Chemistry* **40,** 1935-2000.

GUNDERSEN, G. G. & BULINSKI, J. C. (1986). Microtubule arrays in differentiated cells contain elevated levels of post-translationally modified forms of tubulin. *European Journal of Cell Biology* **42,** 288-294.

GURER, H. & ERCAL, N. (2000). Can antioxidants be beneficial in the treatment of lead poisoning. *Free Radical Biology and Medicine* **29,** 927-945.

GUYTON, K. Z., LUI, Y., GOROSPE, M., XU, Q. & HOLBROOK, N. J. (1996). Activation of mitogen-activated protein kinases by H2O2. Role in cell survival following oxident injury. *Journal of Biological Chemistry* **271,** 4138-4142.

HABEEBU, S. S., LUI, J. & KLAASSEN, C. D. (1998). Cadmium-induced apoptosis in mouse liver. *Toxicology and Applied Pharmacology* **149,** 203-209.

HAFFKE, S. C. & SEEDS, N. W. (1975). Neuroblastoma, the *E.Coli* of neurobiology. *Life Science* **16,** 1649-1658.

HARE, M. F., MCGINNIS, K. M. & ATCHISON, W. D. (1993). Methylmercury increases intracellular concentrations of Ca2+ and heavy metals in NG108-15 cells. *Journal of Pharmacology and Experimental Therapeutics* **266,** 1626-1635.

HARGREAVES, A. J. (1997). The cytoskeleton as a target in cell toxicity. *Advances in Molecular and Cell Biology* **20,** 119-144.

HARGREAVES, A. J., FOWLER, M. J., SACHANA, M., FLASKOS, J., COUTTS, I. C., GLYNN, P., HARRIS, W. & MCLEAN, W. G. (2006). Inhibition of neurite outgrowth in differentiating mouse N2a neuroblastoma cells by phenyl saligenin phosphate: Effects on MAP kinase (ERK 1/2) activation, neurofilament heavy chain phosphorylation and neuropathy target esterase activity. *Biochemical Pharmacology* **71,** 1240-1247.

HEIDEMANN, S. R., LAMOUREUX, P. & ATCHISON, W. D. (2001). Inhibition of Axonal Morphogenesis by Nonlethal, Submicromolar Concentrations of Methylmercury. *Toxicology and Applied Pharmocology* **174,** 49-59.

HERDMAN, M. L., MARCELO, A., HUANG, Y., NILES, R. M., DHAR, S. & KININGHAM, K. K. (2006). Thimerosal induces apoptosis in a neuroblastoma model via the cJun N-terminal kinase pathway. *Toxicological Science* **92,** 246-253.

HIDALGO, J., GARCIA, A., OLIVA, A. M., GIRALT, M., GASULL, T., GONZALEZ, B., MILNEROWICZ, H., WOOD, A. & BREMNER, I. (2000). Effect of zinc, copper and glucocorticoids on metallothionein levels of cultured neurons and astrocytes from rat brain. *Journal of Neural Transmission* **107,** 321-329.

HILLY, M., PIETRI-ROUXEL, F., COQUIL, J., GUY, M. & MAUGER, J. (1993). Thiol reagents increase the affinity of the inositol1,4,5-triphosphate receptor. *The Journal of Biological Chemistry* **268,** 16488-16494.

HINKLE, P. M. & OSBORNE, M. E. (1994). Cadmium toxicity in rat pheochromocytoma cells: Studies on the mechanism of uptake. *Toxicology and Applied Pharmacology* **124,** 91-98.

HIRSCH, D. D. & STORK, P. J. S. (1997). Mitogen-activated protein kinase phosphotases inactivate stress-activated protein kinase pathways *in vivo*. *The Journal of Biological Chemistry* **272,** 4568-4575.

HSU, P. C. & GUO, Y. L. (2002). Antioxidants nutrients and lead toxicity. *Toxicology* **180,** 33-44.

HUANG, Y. & WANG, K. K. W. (2001). The calpain family and human disease. *Trends in Molecular Medicine* **7,** 355-362.

HUNTER, A. M. & BROWN, D. L. (2000). Effects of microtubule associated protein (MAP) expression on methylmercury-induced microtubule disassembly. *Toxicology and Applied Pharmacology* **166,** 203-213.

HUSEMAN, C. A., VARMA, M. M. & ANGLE, C. R. (1992). Neuroendocrine effects of toxic and low blood lead levels in children. *Pediatrics* **90,** 186-189.

ISHIDA, Y., ICHIMURA, H., SUMI, H., HORIGOME, T. & OMATA, S. (1997). Methylmercury alters the tyrosination status of tubulin in the brains of acutely intoxicated rats. *Toxicology* **122,** 171-181.

JACOBSON, J. L. (2001). Contending with Contradictory Data in a Risk Assessment Context: The Case of Methylmercury. *Neurotoxicology* **22,** 667-675.

JIN, K., MAO, X. O., ZHU, Y. & GREENBERG, D. A. (2002). MEK and ERK protect hypoxic cortical neurons via phosphorylation of Bad. *Journal of Neurochemistry* **80,** 119-125.

KAMINSKA, B. (2005). MAPK signalling pathways as molecular targets for anti-inflammatory therapy-from molecular mechanisms to therapeutic benefits. *Biochimica et Biophysica Acta*.

KAUFMAN, A. S. (2001). Do low levels of lead produce IQ loss in children: A careful examination of the literature. *Archives of Clinical Neuropsychology* **16,** 303-341.

KEILBAUGH, S. A., PRUSOFF, W. H. & SIMPSON, M. V. (1991). Rapid communication the PC12 cell as a model for studies of the mechanism of induction of peripheral neuropathy by anti-Hiv-1 dideoxynucleoside analogs. *Biochemical Pharmacology* **42,** 5-8.

KHORCHID, A. & IKURA, M. (2002). How calpain is activated by calcium. *Nature Structural Biology* **9,** 239241.

KIM, A. H., SHELINE, C. T., TIAN, M., HIGASHI, T., MCMAHON, R. J., COUSINS, R. J. & CHOI, D. W. (2000). L-type Ca2+ channel-mediated Zn2+ toxicity and modulation by ZnT in PC12 cells. *Brain Research* **886,** 99-107.

KIM, E., KIM, J. H., KIM, H. S., RYU, S. H. & SUH, P. (2002). Thimerosal stimulates focal adhesion kinase and cytoskeletal changes by redox modulation. *Biochimica et Biophysica Acta* **1593,** 9-15.

KIM, S. H. & SHARMA, R. P. (2005). Mercury alters endotoxin-induced inflammatory cytokine expression in liver: differential roles of p38 and extracellular signal-related mitogen-activated protein kinases. *Immunopharmacology and Immunotoxicology* **27,** 123-135.

KLEBE, R. J. & RUDDLE, F. H. (1967). Neuroblastoma, cell culture analysis of a differentiating system. *Cell Biology* **165,** 65a.

KNEZEVIC, I., GRIFFITHS, E., REIGEL, F. & DOBBELAER, R. (2004). Thiomersal in vaccines: A regulatory perspective WHO consultation, Geneva, 15-16 april 2002. *Vaccine* **22,** 1836-1841.

KORNACK, D. R. & GIGER, R. J. (2005). Probing Microtubules + TIPS: regulation of axon branching. *Current opinion in neurobiology* **15,** 1-9.

KOSTYUK, P. G. & VERKHRASTSKY, A. N. (1995). Calcium Signalling in the Nervous system. *John Wiley & Sons;* **Chichester**.

KRUH, J. (1982). Effects of sodium butyrate, a new pharmacological agent, on cells in culture. *Molecular and Cell Biochemistry* **42,** 65-82.

KUMAR, S., WEINGARTEN, D. P., CALLAHAN, J. W., SACHAR, K. & DE VELLIS, J. (1984). Regulation of mRNAs for three enzymes in the glial cell model C6 cell line. *Journal of Neurochemistry* **43,** 1455-1463.

KUNIMOTO, M. & SUZUKI, T. (1997). Migration of granule neurons in cerebellar organotypic cultures is impaired by methylmercury. *Neuroscience Letters* **226,** 183-186.

LAEMMLI, U. K. (1970). Cleavage of structural proteins during the assembly of the head of bacteriophage T4. *Nature* **227,** 680-685.

LAU, A. T. Y., ZHANG, J. & CHIU, J. F. (2006). Acquired tolerence in cadmium-adapted lung epithelial cells: Roles of the c-Jun N-terminal kinase signalling pathway and basel level of metallothionein. *Toxicology and Applied Pharmacology*.

LEONHARDT, R., PEKEL, M., PLATT, B., HAAS, H. L. & BUSSELBERG, D. (1996). Voltage- activated calcium channel currents of rat DRG neurons are reduced by mercuric chloride (HgCl2) and methylmercury (CH3HgCl). *Neurotoxicology* **17,** 85-92.

LERMIOGLU, F. & BERNARD, A. (1998). Effect of calmodulin-inhibitors and verapamil on the nephrotoxicity of cadmium in rat. *toxicology letters* **95,** 9-13.

LEVESQUE, P. C., ATCHISON, W. D. & . (1988). Effect of alteration of nerve terminal Ca^{2+} regulation on increased spontaneous quantal release of acetylcholine by methyl mercury. *Toxicology and Applied Pharmacology* **94,** 55-65.

LI, W., ZHAO, Y. & CHOU, I. N. (1993). Alterations in cytoskeletal protein sulfhydryls and cellular glutathione in cultured cells exposed to cadmium and nickle ions. *Toxicology* **77,** 65-79.

LIMKE, T. L., HEIDEMANN, S. R. & ATCHISON, W. D. (2004). Disruption of Intraneuronal Divalent Cation Regulation by Methylmercury: Are Specific Targets Involved in Altered Neuronal Development and Cytotoxicity in Methylmercury Poisoning? *Neurotoxicology* **25,** 741-760.

LOIKKANEN, J. J., NAARALA, J. & SAVOLAINEN, K. M. (1998). Modification of glutamate-induced oxidative stress by lead: The role of extracellular calcium. *Free radical Biology & Medicine* **24,** 277-384.

LOPEZ, E., ARCE, C., OSET-GASQUE, M. J., CANADAS, S. & GONZALEZ, M. P. (2006). Cadmium induces reactive oxygen species generation and lipid peroxidation in cortical neurons in culture. *Free radical Biology & Medicine* **40,** 940-951.

LOWRY, O. H., ROSENBROUGH, N. J., FARR, A. L. & RANDALL, R. J. (1951). Protein measurement with the folin phenol reagent. *Journal of Biological Chemistry* **258,** 13722-13726.

LUTSENKO, S. & KAPLAN, J. H. (1995). Organisation of P-type ATPases: significance of structural diversity. *Biochemistry* **34,** 15607-15613.

MANCA, D., RICARD, A. C., TROTTIER, B. & CHEVALIER, G. (1991). Studies on lipid peroxidation in rat tissues following administration of low and moderate doses of cadmium chloride. *Toxicology* **67,** 303-323.

MARCHI, B., BURLANDO, B. & VIARENGO, A. (2000). Interference of heavy metal cations with fluorescent Ca2+ probes does not affect Ca2+ measurements in living cells. *Cell Calcium* **28,** 225-231.

MARET, W. & SANDSTEAD, H. J. (2006). Zinc requirements and the risks and benefits of zinc supplementation. *Journal of Trace Elements in Medicine and Biology* **20,** 3-18.

MASON, A. Z. & NOTT, J. A. (1981). The role of intracellular biomineralised granules in the regulation and detoxification of metalsin gastropodswith special reference to the marine prosobranch *Littorina littorea*. *Journal of Histochemistry and cytochemistry* **28,** 1301-1311.

MATHIE, A., SUTTON, G. L., CLARKE, C. E. & VEALE, E. L. (2005). Zinc and copper: Pharmacological probes and endogenous modulators of neuronal excitability. *Pharmacology and Therapeutics*.

MATSUOKA, M., WISPRIYONO, B., IRYO, Y. & IGISU, H. (1999). Mercury Chloride Activates c-Jun N-Terminal Kinase and Induces c-jun Expression in LLC-PK1 Cells. *Toxicological Sciences* **53,** 361-368.

MAZZOLINI, M., TRAVERSO, S. & MARCHETTI, C. (2001). Multiple pathways of Pb^{2+} permeation in rat cerebellar granule neurones. *Journal of Neurochemistry* **79,** 407-416.

MCNULTY, T. J. & TAYLOR, C. W. (1999). Extracellular heavy-metal ions stimulate Ca^{2+} mobilization in hepatocytes. *Biochemical Journal* **339,** 555-561.

MIKE, A., PEREIRA, E. F. R. & ALBUQUERQUE, E. X. (2000). Ca2+-sensitive inhibition by Pb2+ of 7-containing nicotinic acetylcholine receptors in hippocampal neurons. *Brain Research* **873,** 112-123.

MILAEVA, E. R. (2006). The role of radical reactions in organomercurials impact on lipid peroxidation. *Journal of Inorganic Biochemistry* **100,** 905-915.

MILLAR, T. M., PHAN, V. & TIBBLES, L. A. (2007). ROS generation in endothelial hypoxia and reoxygenation stimulates MAP kinase signaling and kinase-dependent neutrophil recruitment. *Free radical Biology & Medicine* **42,** 1165-1177.

MIURA, K. & IMURA, N. (1989). Mechanisms of cytotoxicity of methylmercury with special reference to microtubule disruption. *Biological Trace Element Research* **21,** 313-316.

MIURA, K., KOIDE, N., HIMENO, S., NAKAGAWA, I. & IMURA, N. (1999). The involvement of microtubular disruption in Methylmercury-induced apoptosis in neuronal and nonneuronal cell lines. *Toxicology and Applied Pharmocology* **160,** 279-288.

MONNET-TSCHUDI, F., ZURICH, M. G. & HONEGGER, P. (1996). Comparison of the developmental effects of two mercury compounds on glial cells and neurons in aggregate cultures of rat telencephalon. *Brain Research* **741,** 52-59.

MOREIRA, E., G, , VASSILIEFF, I. & VASSILIEFF, V. S. (2001). . Developmental lead exposure: behavioural alterations in the long and short term. *Neurotoxicology and teratology* **23,** 489-495.

MORI, S., WATANABE, W. & SHIGETA, S. (1995). A colorimetric LDH assay for the titration of infectivity and the evaluation of anti-viral activity against ortho- and paramyxoviruses. *Tohoku Journal of Experimental Medicine* **177,** 315-325.

MOSMANN, T. (1983). Rapid colorimetric assay for cellular growth and survival:application to proliferation and cytotoxicity assays. *Journal of Immunological Methods* **65,** 55-63.

MYERS, G. J., DAVIDSON, P. W., COX, C., SHAMLAYE, C., CERNICHIARI, E. & CLARKSON, T. W. (2000). Twenty seven years studying the human neurotoxicity of methylmercury exposure. *Environmental Research* **Sect A 83,** 275-285.

NAROTZKY, R. & BONDAREFF, W. (1974). Biogenic amines in cultured neuroblastoma cells. *Journal of Cell Biology* **69,** 64-70.

NISHIO, H., NEZASA, K-I., HIRANO, J., NAKATA, Y. (1996). Effects of thimerosal, an organic sulphhydryl modifying agent, on serotonin transport activity into rabbit blood platelets. *Neurochemistry International* **29,** 391-396.

NIXON, R. A. (2003). The calpains in aging and aging-related diseases. *Ageing Research Reviews* **2,** 407-418.

OCHI, T. (2002). Methylmercury, but not inorganic mercury, causes abnormality of centrosome integrity (multiple foci of γ–tubulin), micropolar spindles and multinucleated cells without mirotubule disruption in cultured chinese hamster V79 cells. *Toxicology* **175,** 111-121.

PANT, H. C., VEERANNA & GRANT, P. (2000). Regulation of axonal neurofilament phosphorylation. *Current Topics in Cellular Regulation* **36,** 133-150.

PAPANIKOLAOU, N. C., HATZIDAKI, E. G., S, B., TZANAKAKIS, G. N. & TSATSAKIS, A. M. (2005). Lead toxicity update. A brief review. *Medical Science Monit* **11,** 329-336.

PARK, J. A. & KOH, J. Y. (1999). Induction of a immediate early gene erg-1 by zinc through extracellular signal-related kinase activation in cortical culture: its role in zinc-induced neuronal death. *Journal of Neurochemistry* **73,** 450-456.

PARRAN, D. K., S, B. J. & MUNDY, W. R. (2004). Methylmercury inhibits TrkA signalling through the ERK 1/2 cascade after NGF stimulation of PC12 cells. *Developmental Brain Research* **149,** 53-61.

PERRON, J. C. & BIXBY, J. L. (1999). Distinct neurite outgrowth signalling pathways converge on ERK activation. *Molecular Cell Neuroscience* **13,** 362-378.

PETZOLD, A. (2005). Neurofilament phosphoforms: Surrogate markers for axonal injury, degeneration and loss. *Journal of the Neurological Sciences* **233,** 183-198.

PRASAD, K. N. & SINHA, P. K. (1976). Biochemical differentiation of neuroblastoma cells. *In Vitro* **12,** 125-132.

PULIDO, M. D. & PARRISH, A. R. (2003). Metal-induced apoptosis: mechanisms. *Mutation Research* **533,** 227-241.

RAJANNA, B., CHETTY, C. S., RAJANNA, S., HALL, E., FAIL, S. & YALLAPRAGADA, P. R. (1995). Modulation of protein kinase C by heavy metals. *toxicology letters* **81,** 197-203.

RAUNIO, S. & TAHTI, H. (2000). Glutamate and calcium uptake in astrocytes after acute lead exposure. *Chemosphere* **44,** 355-359.

REDWOOD, L. B., S. BROWN, D. (2001). Predicted mercury concentrations in hair from infant immunizations: Cause for concern. *Neurotoxicology* **22,** 691-697.

RESZKA, A. A., SEGER, R., DILTZ, C. D., KREBS, E. G. & FISCHER, E. H. (1995). Association of mitogen-activated protein kinase with the microtubule cytoskeleton. *Proceedings of the Natural Academy of Science* **92,** 8881-8885.

REVERTER, D., SORIMACHI, H. & BODE, W. (2001). The Structure of Calcium-Free Human m-Calpain Implications for Calcium Activation and Function. *Trends in Cardiovascular Medicine* **11,** 222-229.

ROBINSON, M. J. & COBB, M. H. (1997). Mitogen-activated protein kinase pathways. *Current opinion in cell biology* **9,** 180-186.

ROSS, G. M., SHAMOVSKY, I. L., LAWRANCE, G., SOLC, M., DOSTALER, S. M., JIMMO, S. L., WEAVER, D. F. & RIOPELLE, R. J. (1997). Zinc alters confomation and inhibits biological activities of nerve growth factor and related neurotrophins. *Nature Medicine* **3,** 872-878.

ROY, S., COFFEE, P., SMITH, G., LIEM, R., BRADY, S. T. & BLACK, M. M. (2000). Neurofilaments are transported rapidly but intermittently in axons: implications for slow axonal transport. *Journal of Neuroscience* **20,** 6849–6861.

SACHANA, M., FLASKOS, J., ALEXAKI, E., GLYNN, P. & HARGREAVES, A. J. (2001). The toxicity of chlorpyrifos towards differentiating mouse N2a neuroblastoma cells. *Toxicology in Vitro* **15,** 369-372.

SACHANA, M., FLASKOS, J., ALEXAKI, E. & HARGREAVES, A. J. (2003). Inhibition of neurite outgrowth in N2a cells by leptophos and carbaryl: effects on neurofilament heavy chain, GAP-43 and HSP-70. *Toxicology in Vitro* **17,** 115-120.

SAGER, P. R., DOHERTY, R. A. & OLMSTED, J. B. (1983). Interaction of methylmercury with microtubules in cultured cells and in vitro. *Experimental Cell Research* **146,** 127-137.

SAGER, P. R. & SYVERSEN, T. (1984). Differential responses to methylmercury exposure and recovery in neuroblastoma and glioma and fibroblasts. *Experimental Neurology* **85,** 371-382.

SAINO, T., MATSUURA, M. & SATOH, Y. I. (2002). Application of real-time confocal microscopy to intracellular calcium ion dynamics in rat arterioles. *Histochemistry and Cell Biology* **117,** 295-305.

SAKAUE, M., OKAZAKI, M. & HARA, S. (2005). Very low levels of methylmercury induce cell death of cultured rat cerebellar neurons via calpain activation. *Toxicology* **213,** 97-106.

SANDSTEAD, H. H. (1993). Zinc requirements, the recommended dietary allowance and the reference dose. *Scandanavian Journal of Work and Environmental Health* **19,** 128-131.

SANFELIU, C., SEBASTIA, J. & KIM, S. U. (2001). Methylmercury Neurotoxicity in cultures of human neurons, astrocytes, neuroblastoma cells. *Neurotoxicology* **22,** 317-327.

SAYERS, L. G., BROWN, G. R., MICHELL, R. H. & MICHELANGELI, F. (1993). The effects of thimerosal on calcium uptake and inositol 1,4,5-triphosphate induced calcium release in cerbellar microsomes. *Biochemical Journal* **289,** 883-887.

SCEMES, E. (2001). Components of Astrocytic intracellular Calcium signalling. *Molecular Neurobiology* **22,** 167-179.

SCHWARTZ, P. J., GROTE, S. K., STEPHENS, K. L. & ADLER, E. M. (2000). Zinc elevates neuropeptide Y levels in rat pheochromocytoma cells by a mechanism independent of L-channel mediated inhibition of release. *Brain Research* **877,** 12-22.

SEO, S. R., CHONG, S. A., LEE, S., SUNG, J. Y., AHN, Y. S., CHUNG, K. C. & SEO, J. T. (2001). Zn2+-induced ERK activation mediated by reactive oxygen species causes cell death in differentiated PC12 cells. *Journal of Neurochemistry* **78,** 600-610.

SILBERGELD, E. K. (2003). Facilitative mechanisms of lead as a carcinogen. *Mutation Research* **533,** 121-133.

SORIMACHI, H., ISHIURA, S. & SUZUKI, K. (1997). Structure and physiological functions of calpains. *Biochemical Journal* **328,** 721-732.

STAESSEN, J. A., BULPITT, C. & FAGARD, R. (1994). Hypertension caused by low-level lead exposure: myth or fact. *Journal of Cardivascular risk* **1**.

STOHS, S. J. & BAGCHI, D. (1995). Oxidative mechanisms in the toxicity of metal ions. *Free radical Biology & Medicine* **18,** 321-336.

SUBRAMANIAM, S. & UNSICKER, K. (2006). Extracellular signal-regulated kinase as an inducer of non-apoptotic neuronal death. *Neuroscience* **138,** 1055-1065.

TAKEDA, A., HIRATE, M., TAMANO, H. & OKU, N. (2003). Zinc movement in the brain under kainate-induced seizures. *Epilepsy Research* **54,** 123-129.

TAKUMA, K., BABA, A. & MATSUDA, T. (2004). Astrocyte apoptosis: implications for neuroprotection. *Progress in Neurobiology* **72,** 111-127.

TAMM, C., DUCKWORTH, J., HERMANSON, O. & CECCATELLI, S. (2006). High susceptibility of neural stem cells to methylmercury toxicity: effects on cell survival and neuronal differentiation. *Journal of Neurochemistry* **97,** 69-78.

TAN, M. & PARKIN, J. E. (2000). Route of decomposition of thiomersal (thimerosal). *International Journal of Pharmaceutics* **208,** 23-34.

THROWER, E. C., DUCLOHIER, H., LEA, E. J. A., MOLLE, G. & DAWSON, A. P. (1996). The inositol 1,4,5-triphosphate-gated Ca^{2+} channel: effect of the protein thiol reagent thimerosal on channel activity. *Biochemical Journal* **318,** 61-66.

TLEUGABULOVA, D., PEREZ, I. G. (1996). Reverse-phase high performance liquid chromatographic study of thimerosal stability in Cuban recombinant hepatitis B vaccine. *Journal of Chromatography* **729;,** 219-227.

TONNER, L. E. & HEIMAN, A., S. (1997). Lead may affect glucocorticoid signal transduction in cultured hepatoma cells through inhibition of protein kinase C. *Toxicology* **119,** 155-166.

TOSCANO, C. D. & GUILARTE, T. R. (2005). Lead neurotoxicity: From exposure to molecular effects. *Brain Research Reviews* **49,** 529-554.

TOWBIN, H., STAEHELIN, T. & GORDEN, J. (1979). Electrophoretic transfer of proteins from polyacrylamide gels to nitrocellulose sheets: Procedure and some applications. *Proceedings of the Natural Academy of Science* **76,** 4350-4354.

TURAN, B., FLISS, H. & DESILETS, M. (1997). Oxidants increase intracellular free Zn^{2+} concentration in rabbit ventricular myocytes. *American Journal of Physiology* **272,** H2095-H2106.

UCHA-ISHIBASHI, T., OYAMA, Y., NAKAO, H., UMEBAYASHI, C., NISHIZAKI, Y., TAKTSUISHI, T., IWASE, K., MURAO, K. & SEO, H. (2004). Effect of thimerosal, a preservative in vaccines, on intrcellular Ca^{2+} concentrations of rat cerebellar neurons. *Toxicology* **195,** 77-84.

VANAGAS, L., ROSSI, R. C., CARIDE, A. J., FILOTEO, A. G., STREHLER, E. E. & ROSSI, J. P. F. C. (2007). Plasma membrane calcium pump activity is affected by the membrane protein concentration: Evidence for the involvement of the actin cytoskeleton. *Biochimica et Biophysica Acta*.

VAN'T VEEN, A. J. (2001). Vaccines without thiomersal Why so necessary, why so long coming? *Drugs* **61,** 565-572.

VEERANNA, AMIN, N. D., AHN, N. G., JAFFE, H., WINTERS, C. J. & GRANT, P. (1998). Mitogen activated protein kinases (ERK1/2) phosphorylate Lys-Ser-Pro (KSP) repeats in neurofilament proteins NFH and NFM. *Journal of Neuroscience* **18,** 4008-4021.

WAISBERG, M., JOSEPH, P., HALE, B. & BEYERSMANN, D. (2003). Molecular and cellular mechanisms of cadmium carcinogenesis. *Toxicology* **192,** 95-117.

WALL, M. J. (2005). Short-term synaptic plasticity during development of rat mossy fibre to granule cell synapses. *European Journal of Neuroscience* **21,** 2149-2158.

WANG, K. K. W. (2000). Calpain and caspase: can you tell the difference? *Trends in Neuroscience* **23,** 20-26.

WANG, X., MARTINDALE, J. L., LIU, Y. & HOLBROOK, N. J. (1998). The cellular response to oxidative stress: influences of mitogen-activated protein kinase signalling pathways on cell survival. *Biochemical Journal* **333,** 291-300.

WANG, Z., LUI, Y. & CUI, Y. (2005). Pathways to caspase activation. *Cell Biology International* **29,** 489-496.

WASTENEYS, G., CADRIN, M., REUHL, K. R. & BROWN, D. L. (1988). The effects of methylmercury on the cytoskeleton of murine embryonal carcinoma cells. *Cell Biology and Toxicology* **4,** 41-60.

WATERMAN-STORER, C. M. & SALMON, E. D. (1998). Endoplasmic reticulum membrane tubules are distributed by microtubules in living cells using three distinct mechanisms. *Current Biology* **8,** 798-806.

WATJEN, W., BENTERS, J., HAASE, H., SCHWEDE, F., JASTORFF, B., BEYERSMANN, D. (2001). Zn2+ and Cd2+ increase the cyclic GMP level in PC12 cells by inhibition of the cyclic nucleotide phosphodiesterase. *Toxicology* **157,** 167-175.

WAYMIRE, J. C., WEINER, N. & PRASAD, K. N. (1972). Regulation of tyrosine hydroxylase activity in cultured mouse neuroblastoma cells, elevation induced by analoques of adenosine 3',5'-cyclic monophosphate. *Proceedings of the Natural Academy of Science* **69,** 2241-2245.

WEISS, J. H., SENSI, S. L. & KOH, J. Y. (2000). Zn^{2+} : a novel ionic mediator of neural injury in brain disease. *Trends in Pharmacological Sciences* **21,** 395-401.

WERRY, T. D., SEXTON, P. M. & CHRISTOPOULOS, A. (2005). Ins and outs of seven-transmembrane receptor signalling to ERK. *Trends in Endocrinology and Metabolism* **16,** 26-33.

WIKTOREK, M., SABALA, P., CZARNY, M. & BARANSKA, J. (1996). Phosphatidylserine synthesis in glioma C6 cell is inhibited by Ca^{2+} depletion from the endoplasmic reticulum: Effects of 2,5-Di-tert-butylhydroquinone and thimerosal. *Biochemical and Biophysical Research Communications* **224,** 645-650.

WILLIAMSON, T. L., MARSZALEK, J. R., VECHIO, J. D., BRUIJN, L. J., LEE, M. K., XU, Z., BROWN, R. H., CLEVELAND, D. W. (1996). Neurofilaments, radial growth of axons, and mechanisms of motor neuron disease. *Cold Spring Harbor Symposium. Quantitative Biology* **61,** 709-723.

XIA, Z., DICKENS, M., RAINGEAUD, J., DAVIS, R. J. & GREENBERG, M. E. (1995). Opposing effects of ERK and JNK-p38 MAP kinases on apoptosis. *Science* **270,** 1326-1331.

YAO, C. P., ALLEN, J. W., CONKLIN, D. R. & ASCHNER, M. (1999). Transfection and overexpression of metallothionein-I in neonatal rat primary astrocyte cultures and in astrocytoma cells increases their resistance to methylmercury-induced cytotoxicity. *Brain Research* **818,** 414–420.

YEE, S. & CHOI, B. H. (1996.). Oxidative stress in neurotoxic effects of methylmercury poisoning. *Neurotoxicology* **17,** 17-26.

YUAN, A., NIXON, R. A. & RAOA, M. V. (2006). Deleting the phosphorylated tail domain of the neurofilament heavy subunit does not alter neurofilament transport rate in vivo. *Neuroscience Letters* **393,** 264-268.

ZAHIR, F., RIZWI, S. J., HAQB, S. K. & KHANB, R. H. (2005). Low dose mercury toxicity and human health. *Environmental Toxicology and Pharmacology* **20,** 351–360.

ZHANG, J., MIYAMOTO, K., HASHIOKA, S., HAO, H., MURAO, K., SAIDO, T. & NAKANISHI, H. (2003). Activation of μ–calpain in developing cortical neurons following methylmercury treatment. *Developmental Brain Research* **142**.

ZIEMBA, S. E., MATTINGLY, R. R., MCCABE, M. J. J. & ROSENSPIRE, A. J. (2006). Inorganic mercury inhibits the activation of LAT in T-cell receptor-mediated signal transduction. *Toxicological Sciences* **89,** 145-153.

Appendix

A.1: The effect of thimerosal and methylmercury chloride on the levels of JNK and phosphorylated JNK in C6 cells

Figure A.1.1: The effect of thimerosal and methylmercury chloride on the levels of total JNK and phosphorylated in 4 hour differentiated C6 cells

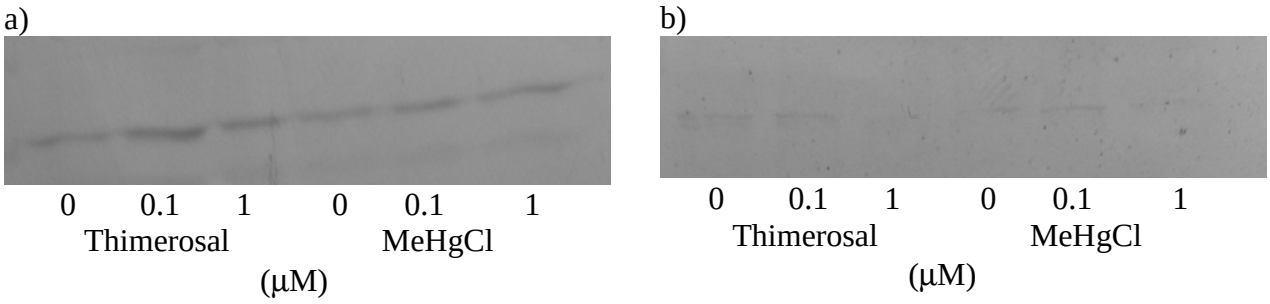

C6 cells were induced to differentiate for 4 hours in the presence and absence of thimerosal and methylmercury chloride and extracts were separated by SDS PAGE and western blotted as described in Methods. The blots were probed with anti-total JNK (a) and phosphorylated JNK (b) antibodies.

Figure A.1.1 shows that there was no apparent change in the reactivity of the total JNK antibody after 4 hours of exposure to thimerosal and MeHgCl. After 4 hours it seems that there is a slight increase in the reactivity of the phosphorylated JNK antibody with 0.1 μM of thimerosal and MeHgCl but a decrease in antibody reactivity with 1 μM thimerosal and MeHgCl.

Figure A.1.2: Densitometric analysis of the effects of thimerosal and methylmercury chloride on total and phosphorylated JNK

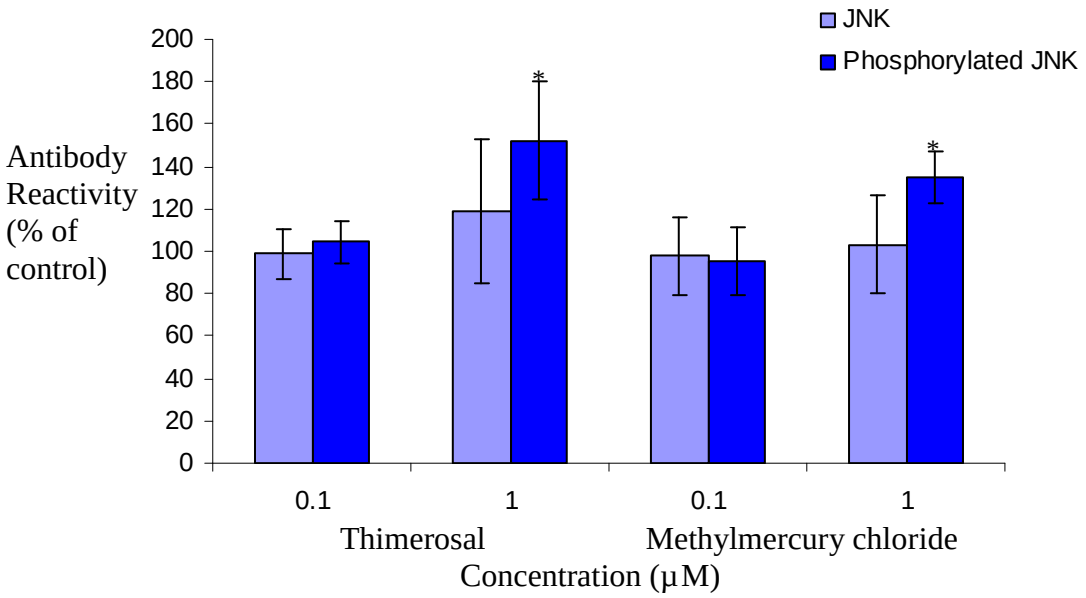

C6 cells were induced to differentiate for 4 hours in the presence and absence of thimerosal and methylmercury chloride, then separated by SDS PAGE and western blotting as described in Methods. The resultant western blots were then probed with the antibodies indicated and the reactive bands were scanned densitometrically using Quantiscan software. Data represents mean levels of antibody reactivity, expressed as a percentage of the corresponding control $\pm$ SEM. Asterisks indicate statistical significance (* p value <0.05).

Figure A.1.2 shows that the reactivity of the anti-total JNK antibody was not significantly altered ($p<0.05$) with C6 cell extracts that had been exposed to either concentration of thimerosal or MeHgCl. However the reactivity of the anti-phosphorylated JNK antibody was significantly increased by around 45 % with cell lysates exposed to 1 µM thimerosal and 40% with 1 µM MeHgCl. 0.1 µM of both heavy metals caused no significant alterations in the anti-phosphorylated JNK antibody reactivity.

Figure A.1.3: The effect of thimerosal and methylmercury chloride on the levels of total JNK and phosphorylated JNK in 24 hour differentiated C6 cells

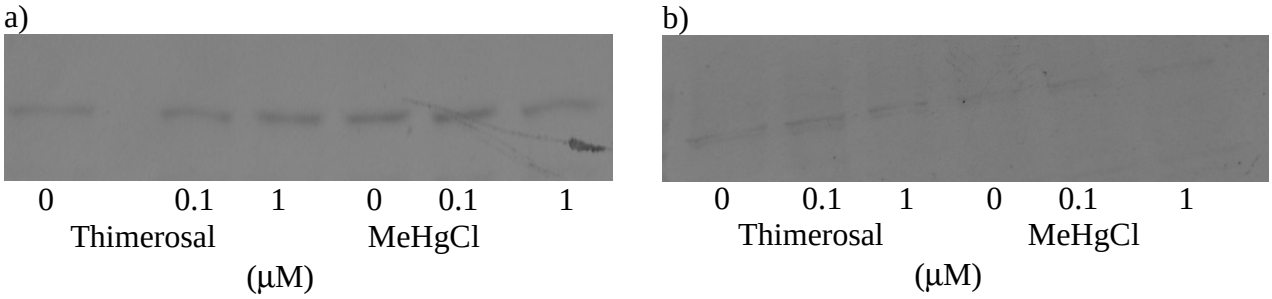

C6 cells were induced to differentiate for 24 hours in the presence and absence of thimerosal and methylmercury chloride and extracts were separated by SDS PAGE and western blotted as described in Methods. The blots were probed with anti-total JNK (a) and phosphorylated JNK (b) antibodies.

Figure A.1.3 shows that there was no apparent change in the reactivity of the total JNK antibody after 24 hours of exposure to thimerosal and MeHgCl. After 24 hours of exposure to both concentrations of thimerosal it appears that the reactivity of the phosphorylated JNK antibody increases. There is no obvious change in the reactivity of the phosphorylated JNK antibody with either concentration of MeHgCl.

Figure A.1.4: Densitometric analysis of the effects of thimerosal and methylmercury chloride on total and phosphorylated JNK

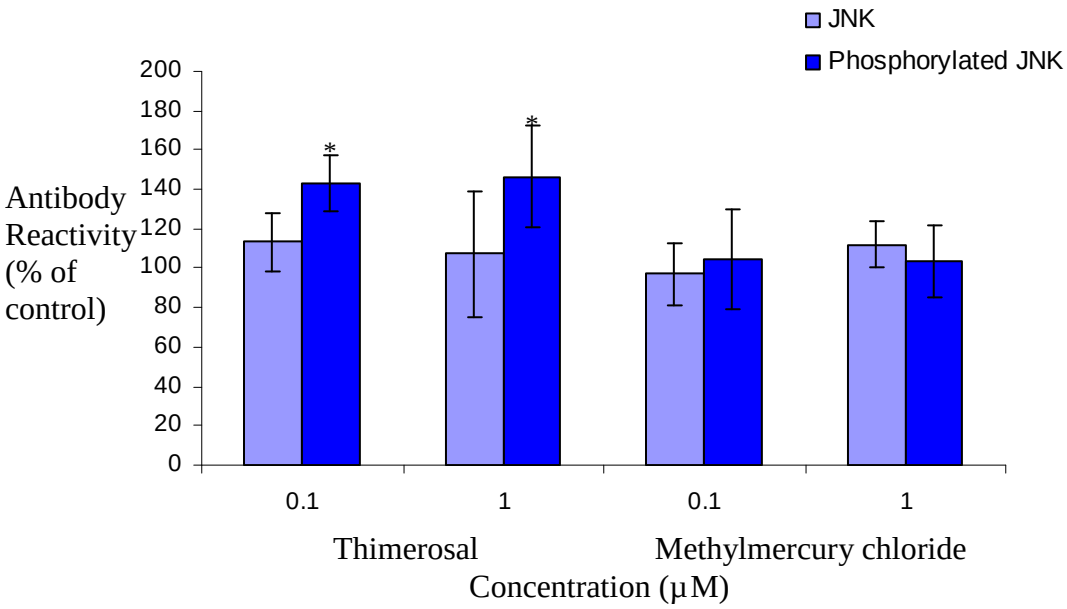

C6 cells were induced to differentiate for 24 hours in the presence and absence of thimerosal and methylmercury chloride, then separated by SDS PAGE and western blotting as described in Methods. The resultant western blots were then probed with the antibodies indicated and the reactive bands were scanned densitometrically using Quantiscan software. Data represents mean levels of antibody reactivity, expressed as a percentage of the corresponding control $\pm$ SEM. Asterisks indicate statistical significance (* p value <0.05).

Figure A.1.4 shows that the reactivity of the anti-total JNK antibody was not significantly altered ($p<0.05$) with C6 cell extracts that had been exposed to either concentration of thimerosal or MeHgCl for 24 hours. The reactivity of the anti-phosphorylated JNK antibody was also unaffected in cell lysates exposed to both concentrations of MeHgCl. In cell extracts exposed to 0.1 µM thimerosal, there was a statistically significant 40 % increase in the binding of the antibody and a 48% increase with 1 µM thimerosal.

A.2: The effect of thimerosal and methylmercury chloride on the levels of total JNK and phosphorylated JNK in differentiated N2a cells

Figure A.2.1: The effect of thimerosal and methylmercury chloride on the levels of total JNK and phosphorylated JNK in 4 hour differentiated N2a cells

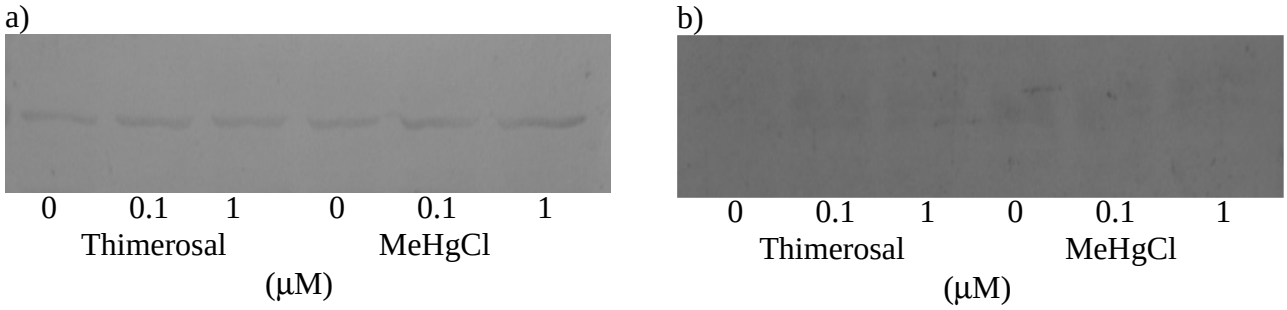

N2a cells were induced to differentiate for 4 hours in the presence and absence of thimerosal and methylmercury chloride and extracts were separated by SDS PAGE and western blotted as described in Methods. The blots were probed with anti-total JNK (a) and phosphorylated JNK (b) antibodies**.**

Figure A.2.1 shows that there was no apparent change in the reactivity of the total JNK antibody after 4 hours of exposure to thimerosal and MeHgCl. The reactivity of the phosphorylated JNK antibody appears to increase with both concentrations of thimerosal and decrease when exposed to both 0.1 and 1 μM MeHgCl.

Figure A.2.2: Densitometric analysis of the effects of thimerosal and methylmercury chloride on total and phosphorylated JNK

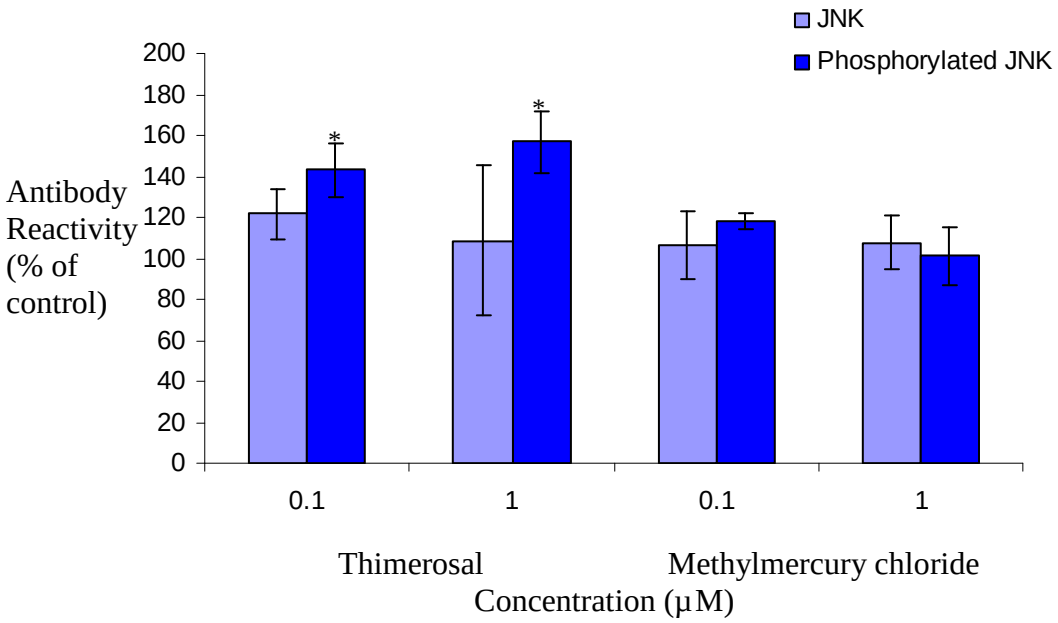

N2a cells were induced to differentiate for 24 hours in the presence and absence of thimerosal and methylmercury chloride, then separated by SDS PAGE and western blotting as described in Methods. The resultant western blots were then probed with the antibodies indicated and the reactive bands were scanned densitometrically using Quantiscan software. Data represents mean levels of antibody reactivity, expressed as a percentage of the corresponding control $\pm$ SEM. Asterisks indicate statistical significance (* p value <0.05)

Figure A.2.2 shows that the reactivity of the anti-total JNK antibody was not significantly altered ($p<0.05$) with N2a cell extracts that had been exposed to either concentration of thimerosal or MeHgCl for 4 hours. The binding of the anti-phosphorylated JNK antibody was not affected in N2a cells exposed to either concentration of MeHgCl. But exposure to 0.1 µM thimerosal caused a significant increase of around 40 %. Exposure to 1 µM thimerosal increased the reactivity of the anti-phosphorylated JNK antibody by 58 %.

Figure A.2.3: The effect of thimerosal and methylmercury chloride on the levels of total JNK and phosphorylated JNK in 24 hour differentiated N2a cells

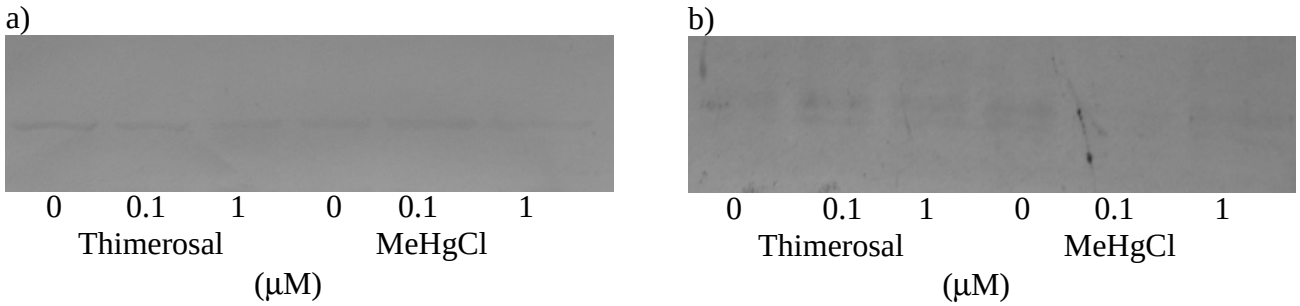

N2a cells were induced to differentiate for 4 hours in the presence and absence of thimerosal and methylmercury chloride and extracts were separated by SDS PAGE and western blotted as described in Methods. The blots were probed with anti-total JNK (a) and phosphorylated JNK (b) antibodies**.**

Figure A.2.3 shows that there was no apparent change in the reactivity of the total JNK antibody after 24 hours of exposure to thimerosal and MeHgCl. Image b indicates that as with the 4 hour exposure the reactivity of the phosphorylated JNK antibody increases with cell lysates incubated with both 0.1 and 1 μM thimerosal and decreases with both concentrations of MeHgCl.

Figure A.2.4: Densitometric analysis of the effects of thimerosal and methylmercury chloride on total and phosphorylated JNK

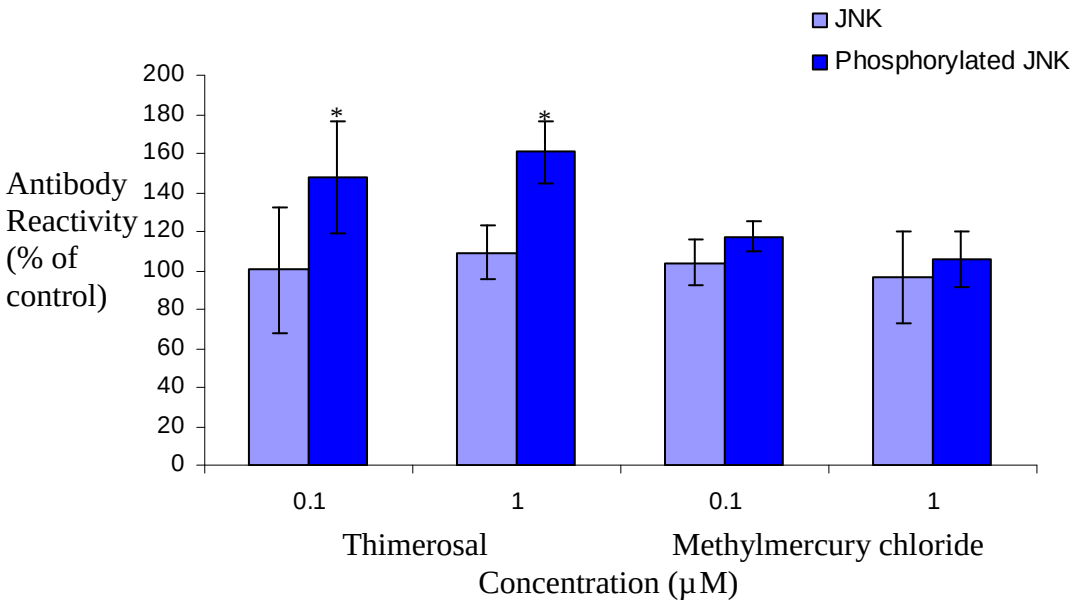

N2a cells were induced to differentiate for 24 hours in the presence and absence of thimerosal and methylmercury chloride, then separated by SDS PAGE and western blotting as described in Methods. The resultant western blots were then probed with the antibodies indicated and the reactive bands were scanned densitometrically using Quantiscan software. Data represents mean levels of antibody reactivity, expressed as a percentage of the corresponding control $\pm$ SEM. Asterisks indicate statistical significance (* p value <0.05).

Figure A.2.4 shows that the reactivity of the anti-total JNK antibody was not significantly altered ($p<0.05$) with N2a cell extracts that had been exposed to either concentration of thimerosal or MeHgCl for 24 hours. Reactivity of the anti-phosphorylated JNK antibody remained unaltered when compared to the control in N2a cell lysates exposed to 0.1 and 1 µM MeHgCl. Antibody binding was significantly increased by 50 % with cell extracts exposed to 0.1 µM and 60 % with cells exposed to 1 µM.